

MODELING AND EVALUATION OF REAL-TIME CONTROLLED GREEN INFRASTRUCTURE

By

Seth Petersen Bryant

Thesis

Submitted to Department of Civil and Environmental Engineering

College of Engineering

Villanova University

In partial fulfillment of the requirements for the degree of

MASTER OF SCIENCE

In

Civil and Environmental Engineering

August, 2017

Villanova Pennsylvania

Copyright @ 2017 Seth Petersen Bryant

All Rights Reserved

STATEMENT BY AUTHOR

This thesis has been submitted in partial fulfillment of requirements for an advanced degree at the Villanova University.

Brief quotations from this thesis are allowable without special permission, provided that accurate acknowledgment of source is made. Requests for permission for extended quotation from or reproduction of this manuscript in whole or in part may be granted by the head of the major department or the Associate Dean for Graduate Studies and Research of the College of Engineering when in his or her judgment the proposed use of the material is in the interests of scholarship. In all other instances, however, permission must be obtained from the author.

ACKNOWLEDGMENTS

I would like to thank my advisor, Dr. Bridget Wadzuk, for her guidance throughout this project and throughout my five years at Villanova. I would also like to thank the entire Civil and Environmental Engineering department for their dedication and commitment to their students, I couldn't have asked for a better undergraduate and graduate experience from them.

Thank you to Conor and Jerry for your help over the past year, especially for doing all the hard work in setting up the sites. I also owe thanks to Jamie and everyone at Opti for dealing with our many requests, you have been a great partner to work with throughout this project.

This research was funded by the National Science Foundation under Grant Number 13-587, thank you for support and for making this project possible.

Lastly, thank you to all the other VUSP graduate students for making graduate school so enjoyable, my family and friends for their support, and especially to my parents for all their support and guidance over the years.

Table of Contents

ACKNOWLEDGMENTS	4
Table of Contents	5
List of Tables	9
List of Figures.....	10
NOMENCLATURE.....	16
ABSTRACT.....	17
CHAPTER 1: INTRODUCTION.....	18
1.1 Literature Review	19
1.2 Site Overviews.....	23
1.2.1 CEER Green and Gray Roof.....	24
1.2.2 Treatment Train.....	28
1.2.3 Continuous Monitoring and Adaptive Control	31
CHAPTER 2: FORECAST RELIABILITY	33
2.1 Introduction.....	33
2.3 Methodology.....	37
2.3.1: Retention Model Setup	37
2.3.2: Detention Model Setup	39
2.3.3: Forecast Based Controls	40
2.3.4: Rain Check Controls	43
2.3.5: Model Runs for Forecast Analysis.....	46
2.4 Results	48
2.4.1 Forecast Accuracy for Simple Retention Model.....	48
2.4.2 Forecast Reliability as a Rain Check:	56
2.4.3 Probability of Precipitation Sensitivity	59
2.5 Conclusion	66

2.5.1 Summary of Findings.....	66
2.5.2 Design Recommendations.....	67
2.5.3 Future Work	68
CHAPTER 3: INTEGRATION OF PUBLICALLY AVAILABLE CLIMATE DATA	69
3.1 Introduction.....	69
3.2 Literature Review	70
3.2.1 PDSI.....	70
3.2.2 SPEI	71
3.2.3 SMAP Satellite.....	72
3.3 Methodology	73
3.4 Results	76
3.4.1 Monthly PDSI	76
3.4.2 Modified Weekly PDSI.....	78
3.4.3 SPEI	82
3.4.4 SMAP Satellite.....	88
3.5 Conclusion	97
CHAPTER 4: MODELING OF REAL-TIME CONTROLLED SYSTEMS.....	102
4.1 Introduction.....	102
4.2 Literature Review	102
4.3.1 Site Overview.....	104
4.3.2 Data Acquisition	105
4.3.4 Green Roof Model Calibration	114
4.3.5 Real-Time Control Model Development	118
4.3.6: Sensitivity Analysis Setup	121
4.4 Results	124
4.4.1 Baseline Model Results.....	124

4.4.2 Soil Moisture Threshold Sensitivity Analysis.....	133
4.4.3: Drainage Area Sensitivity Analysis	138
4.4.4: Probability of Precipitation Threshold Sensitivity Analysis	144
4.5 Conclusion	149
4.5.1 Design Recommendations.....	150
4.5.2 Future Work	152
CHAPTER 5: PERFORMANCE OF REAL-TIME CONTROLLED SYSTEMS.....	154
5.1 Introduction.....	154
5.2 Literature Review	155
5.3 Methodology	156
5.3.1 Project Description.....	156
5.3.3 Sediment Grain Size Analysis.....	160
5.4 Green Roof Results	162
5.4.1 CEER Green Roof Performance	162
5.4.2 Controlled Cistern	165
5.5 Treatment Train Results	167
5.5.1 Treatment Train Storm Capture	167
5.5.2 Infiltration Capacity of Treatment Train.....	171
5.5.3 Particle Size Analysis.....	174
5.5.4 Potential Factors for Sediment Results	177
5.5.5 General Performance Notes	178
5.5 Conclusion	182
6 CONCLUSIONS	185
6.1 Forecast Uncertainty	185
6.2 Integration of Climate Indices.....	186
6.3 Analysis of Villanova Smart Stormwater Systems	187

6.4 Future Work.....	189
REFERENCES.....	191
APPENDIX.....	195

List of Tables

Table 2.1: Forecast Input Data Sources for Forecast Analysis Model Runs	47
Table 2.2: Simple RTC Retention Performance with Real and Perfect Forecasts.....	49
Table 2.3: Typical Overflow Volumes for Retention Model Simulation	53
Table 2.4: Simple RTC Detention Performance with Real and Perfect Forecasts	54
Table 2.5: Wet Weather Outflow of RTC Modeled System with a 2 Hour Rain Delay Drawdown	57
Table 2.6: Wet Weather Outflow of RTC Modeled System with a 6 Hour Rain Delay Drawdown	57
Table 4.1: Input Values for Soil Moisture Threshold Sensitivity Analysis	122
Table 4.2: Sensitivity Analysis Inputs for Variations in Gray Roof Drainage Area	123
Table 4.3: Performance Metrics for Modeled RTC and Passive Green Roofs	131
Table 4.4: Performance Metrics for Modeled and Passive Green Roofs (Including Passive Gray Roof)	132
Table 5.1: Green Roof and Treatment Train Site Instrumentation	159
Table 5.2: Green Roof Rain Events with Overflow	163
Table 5.3: Storm Statistics for Major Rainfall Events at Treatment Train	169
Table 5.4: Changes in Mean Particle Size in Treatment Train, February to May 2017	176

List of Figures

Figure 1.1: CEER Green Roof Construction	24
Figure 1.2: Geotextile and Drainage Layer of CEER Green Roof	25
Figure 1.3: Sample Cumulative Potential ET, Actual ET, and Rainfall for CEER Green Roof ..	26
Figure 1.4: Drainage Area and Cistern Added to CEER Green Roof System with RTC Retrofit	27
Figure 1.5: Overview of CEER Green Roof in May, 2017	28
Figure 1.6: Overview of Treatment Train.....	29
Figure 1.7: Graf Carat-S Rainwater Tanks	30
Figure 1.8: Treatment Train Infiltration Trench	30
Figure 2.1: Retention Model Conceptualization	38
Figure 2.2: Detention Model Conceptualization.....	39
Figure 2.3: Forecast Inputs in the SWMM5 GUI	41
Figure 2.4: Sample Control Curve for Forecast Inflow Volume at 50% of Tank Capacity	42
Figure 2.5: Extreme Event Check in SWMM GUI.....	43
Figure 2.6: Rain Check Setup in SWMM5 GUI.....	44
Figure 2.7: Example Rain Check Storage Response to Storms in Series	45
Figure 2.8: Rain Events in Long-Term Simulation	48
Figure 2.9: Forecast Inaccuracy – Storm Event Not Predicted.....	50
Figure 2.10: Forecast Inaccuracy – Storm Volume Underestimated.....	51
Figure 2.11: Forecast Inaccuracy – Storm Volume Overestimated.....	52
Figure 2.12: Storm on 5/21/2016, Comparison of RTC Detention with Real and Perfect Forecasts	55
Figure 2.13: Overflow Cases Caused by Forecast Inaccuracy	58
Figure 2.14: Tank Storage Depths for POP Sensitivity Analysis, May 2016	60

Figure 2.15: Wet Weather Outflow Hours for Changes in POP Threshold of RTC Retention System.....	61
Figure 2.16: Total Overflow Hours for Changes in POP Threshold of RTC Retention System..	62
Figure 2.17: Retention Times for Changes in POP Threshold of RTC Retention System.....	64
Figure 2.18: Comparison of Wet Weather Outflow and Retention Time for POP Sensitivity Analysis.....	65
Figure 3.1: Historic Record of Rainfall at Villanova BTI (May 2012 to December 2015).....	74
Figure 3.2: Historic Rainfall at Philadelphia International Airport (1950 to 2016)	75
Figure 3.3: Monthly Comparison of Rainfall and PDSI at Villanova University	76
Figure 3.4: Monthly Comparison of Average Temperature and PDSI at Villanova University ..	77
Figure 3.5: Weekly PDSI and Rainfall Comparison.....	78
Figure 3.6: Weekly PDSI and Average Temperature Comparison.....	79
Figure 3.7: Average Weekly Temperature for PDSI Values Indicating Dryer than Typical Conditions	80
Figure 3.8: PDSI and Weekly Temperature Comparison for Dry Conditions with 95% Confidence Limits.....	81
Figure 3.9: SPEI and Monthly Rainfall Comparison for Philadelphia, PA	83
Figure 3.10: Confidence Limits on Monthly Rainfall Predicated on SPEI	84
Figure 3.11: Comparison of Monthly Rainfall to SPEIs of Varying Computation Time Steps ...	85
Figure 3.12: Monthly Average of Daily High Temperatures and SPEI Comparison	87
Figure 3.13: Monthly Average of Daily Low Temperature and SPEI Comparison	87
Figure 3.14: Comparison of SMAP Predicted Soil Moisture and On-Site Measured Soil Moisture	90
Figure 3.15: Average Difference in Soil Moisture Readings between SMAP and BTI Measurements with 95% Confidence Limits	91
Figure 3.16: Sample Storm Response by SMAP Satellite.....	92

Figure 3.17: Time Series Results of SMAP and On-Site Soil Moisture Readings.....	93
Figure 3.18: Recent Rainfall Comparison to SMAP Soil Moisture Readings.....	95
Figure 3.19: Rainfall in Past 2 Weeks and SMAP Comparison, 95% Confidence Limits	96
Figure 3.20: Green Roof SPEI Based Irrigation Multiplier	100
Figure 4.1: Study Site Overview.....	104
Figure 4.2: Rainfall Events in Long-Term Continuous Simulation.....	106
Figure 4.3: Daily Temperatures used for SWMM Climate File	107
Figure 4.4: Green Roof Model in SWMM GUI	108
Figure 4.5: Original Estimate for Green Roof Storage Curve	110
Figure 4.6: Final Storage Curve for CEER Green Roof Model.....	111
Figure 4.7: Daily Modeled and Measured Evapotranspiration.....	112
Figure 4.8: Measured and Modeled Cumulative Evapotranspiration for CEER Green Roof	113
Figure 4.9: Model Calibration Run for Storm of $P = 1.82$ Inches	114
Figure 4.10: Model Validation Run for Storm of $P = 3.40$ Inches	115
Figure 4.11: Sample Soil Moisture Data from CEER Green Roof.....	116
Figure 4.12: Average Measured and Modeled Soil Moisture Volume on CEER Green Roof... ..	117
Figure 4.13: CEER Gray Roof and Cistern in SWMM GUI	119
Figure 4.14: CEER Gray Roof and Cistern	119
Figure 4.15: Sample Time-Series Results of RTC Green Roof Model for May, 2016	125
Figure 4.16: Rainfall and Outflow from Passive and RTC Green Roof Models	126
Figure 4.17: Cumulative Rainfall, Overflow, and ET from Passive Green Roof.....	128
Figure 4.18: Cumulative Rainfall, Overflow, and ET from RTC Green Roof	129
Figure 4.19: Sample Comparison of Green Roof Storage Volumes for RTC and Passive Systems	130
Figure 4.20: Total Inflow and Outflow to Modeled Green Roof System for Varied Soil Moisture Thresholds.....	134

Figure 4.21: Outflow as Percent Inflow for Modeled Green Roof System of Varied Soil Moisture Thresholds	135
Figure 4.22: Wet Weather Outflow Hours for Varied Soil Moisture Thresholds	136
Figure 4.23: Wet Weather Outflow Volume for Varied Soil Moisture Thresholds	137
Figure 4.24: Total Inflow and Outflow of Modeled Green Roof System for Varied Contributing Drainage Areas.....	139
Figure 4.25: Green Roof Outflow as a Percent of Inflow for Varied Drainage Areas	140
Figure 4.26: Wet Weather Outflow Hours for Variations in Gray Roof Drainage Area.....	141
Figure 4.27: Wet Weather Outflow Volumes for Variations in Gray Roof Drainage Area	142
Figure 4.28: Normalized Wet Weather Outflow for Variations in Gray Roof Drainage Area...	143
Figure 4.29: Total Inflow and Outflow of Modeled Green Roof System for Variations in POP Thresholds	145
Figure 4.30: Total Outflow as a Percent of Inflow for Variations in POP Threshold	146
Figure 4.31: Wet Weather Outflow Hours for Variations in POP Threshold.....	147
Figure 4.32: Wet Weather Outflow Volumes for Variations in POP Threshold	148
Figure 5.1: CEER Green Roof and Controlled Cistern.....	156
Figure 5.2: View of Treatment Train from Lower Rain Garden	157
Figure 5.3: Rainfall Events from CEER Roof Rain Gage, 6/1/2016 to 7/12/2017.....	158
Figure 5.4: Sample Zones of Erosion and Deposition	160
Figure 5.5: Sediment Sampling Locations within Treatment Train	161
Figure 5.6: Storm Event Performance of Smart Green Roof.....	164
Figure 5.7: CEER Cistern Storage 4/1/16 to 7/10/2017	166
Figure 5.8: April 2017 to July 2017, CEER Cistern Water Level	167
Figure 5.9: Water Elevation in Treatment Train Infiltration Trench, 6/9/2016 to 3/15/2017	168
Figure 5.10: Performance of Pre-Retrofit Treatment Train	170
Figure 5.11: Sample Storm Response and Drawdown for Treatment Train Cisterns	172

Figure 5.12: Treatment Train Full Cistern Drawdown Events	173
Figure 5.13: Changes in Mean Particle Size of Sediments in the Treatment Train for February and May 2017	175
Figure 5.14: Vegetation Changes in Rain Garden 2 for Winter, Spring, and Summer	178
Figure 5.15: Overflow from Treatment Train, 3/31/2017 (Part 1)	179
Figure 5.16: Overflow from Treatment Train, 3/31/2017 (Part 2)	180
Figure 5.17: Treatment Train Infiltration Trench at Maximum Observed Level	181
Figure 5.18: Junction Box following 3/14/17 Snow Storm	182
Figure A1: Time-Series Results of RTC Green Roof Model – April 2016	195
Figure A2: Time-Series Results of RTC Green Roof Model – May 2016	195
Figure A3: Time-Series Results of RTC Green Roof Model – June 2016	196
Figure A4: Time-Series Results of RTC Green Roof Model – July 2016	196
Figure A5: Time-Series Results of RTC Green Roof Model – August 2016	197
Figure A6: Time-Series Results of RTC Green Roof Model – September 2016	197
Figure A7: Comparison of Green Roof Storage Volumes for RTC and Passive Systems – April, 2016.....	198
Figure A8: Comparison of Green Roof Storage Volumes for RTC and Passive Systems – May, 2016.....	198
Figure A9: Comparison of Green Roof Storage Volumes for RTC and Passive Systems – June, 2016.....	199
Figure A10: Comparison of Green Roof Storage Volumes for RTC and Passive Systems – July, 2016.....	199
Figure A11: Comparison of Green Roof Storage Volumes for RTC and Passive Systems – August, 2016	200
Figure A12: Comparison of Green Roof Storage Volumes for RTC and Passive Systems – September, 2016	200
Figure B1: Grain Size Distribution – Weir Box, February 2017	201

Figure B2: Grain Size Distribution – Weir Box, May 2017	201
Figure B3: Grain Size Distribution – Swale 1 Erosion, February 2017	202
Figure B4: Grain Size Distribution – Swale 1 Erosion, May 2017	202
Figure B5: Grain Size Distribution – Swale 1 Deposition, February 2017	203
Figure B6: Grain Size Distribution – Swale 1 Deposition, May 2017	203
Figure B7: Grain Size Distribution – Swale 1 Weir, February 2017	204
Figure B8: Grain Size Distribution – Swale 1 Weir, May 2017	204
Figure B9: Grain Size Distribution – Swale 2 Erosion, February 2017	205
Figure B10: Grain Size Distribution – Swale 2 Erosion, May 2017	205
Figure B11: Grain Size Distribution – Swale 2 Mid-Bank, February 2017	206
Figure B12: Grain Size Distribution – Swale 2 Mid-Bank, May 2017	206
Figure B13: Grain Size Distribution – Swale 2 Deposition, February 2017	207
Figure B14: Grain Size Distribution – Swale 2 Deposition, May 2017	207
Figure B15: Grain Size Distribution – Rain Garden 1, February 2017	208
Figure B16: Grain Size Distribution – Rain Garden 1, May 2017	208
Figure B17: Grain Size Distribution – Rain Garden 2, February 2017	209
Figure B18: Grain Size Distribution – Rain Garden 2, May 2017	209

NOMENCLATURE

AWA	Average Water Age
CMAC	Continuous Monitoring and Adaptive Control
ET	Evapotranspiration
O/Q_{out}	Outflow
P	Precipitation
PDSI	Palmer Drought Severity Index
PET	Potential Evapotranspiration
Q_{in}	Inflow
R_a	Solar Radiation
RTC	Real-Time Control
SCM	Stormwater Control Measure
SMAP	Soil Moisture Active Passive Satellite
SPEI	Standardized Precipitation Evapotranspiration Index
T	Temperature
T_R	Retention Time
V	Volume
λ	Latent Heat of Vaporization

ABSTRACT

Recent advances in stormwater management have shifted focus to using green stormwater infrastructure to capture runoff and more accurately simulate the natural hydrologic cycle in the built environment. Additional technologic advances have led to the availability of low cost sensors and controllers, making the creation of more intelligent stormwater networks feasible by allowing for continuous monitoring and adaptive control of sites. Several green infrastructure sites at Villanova University, including one green roof and a group of bioinfiltration stormwater control measures in series, were retrofitted with real-time sensors and controllers to provide continuous monitoring and adaptive control. Through a combination of modeling and monitoring of these two pieces of smart stormwater infrastructure, the ability of the systems to manage urban runoff was assessed and compared to pre-retrofit performance. Additionally, factors affecting the ability of real-time controlled systems to function, including forecast accuracy and regional climate trends, were analyzed to provide a comprehensive look at how smart green infrastructure can perform.

The results of the study indicate that smart stormwater systems have the ability to better manage runoff and further utilize natural hydrologic mechanisms (i.e. infiltration and evapotranspiration) than their passive green infrastructure counterparts. The increased ability for volume capture also indicates the ability to manage larger drainage areas with the same footprint green infrastructure by adding in real-time control capabilities. Additionally, potential exists to utilize publically available climate data such as drought indices, weather forecasts, and remote sensing to make more informed decisions in the control of stormwater management.

CHAPTER 1: INTRODUCTION

Water resources are one of the most important aspects of any society, the uses ranging widely from drinking to agriculture to energy production. As urbanization across the United States has increased, stormwater runoff has become one of the major sources of pollution for water bodies with 44% of rivers, 64% of lakes, and 30% of estuaries now considered impaired by the EPA (National Water Quality Assessment 2004). In many streams, watershed urbanization resulting in as little as 10% impervious cover has resulted in biologic impairment of the system (May et al. 1997). In order to combat the effect of urbanization on natural water bodies, recent efforts have focused on the use of source control via green infrastructure to more naturally simulate the hydrologic cycle in urban environments and increase the amount of urban runoff that either infiltrates or evapotranspirates (Walsh et al. 2005). The use of green stormwater infrastructure, also known as stormwater control measures (SCMs), not only prevents runoff from reaching traditional gray infrastructure but also provides water quality benefit to the runoff. This helps to address both the water quality and water quantity concerns associated with urban stormwater runoff. Additionally, recent focus within stormwater management has turned to creating smart systems that use continuous monitoring and adaptive control to create better performing stormwater systems (Kerkez 2016). By combining these two ideas, the use of green stormwater infrastructure and the implementation of smarter stormwater systems, this study sought to demonstrate how stormwater infrastructure could be optimized and retrofitted to increase the performance.

1.1 Literature Review

In recent years real-time control (RTC) has rapidly developed as a way to address stormwater management goals from a more adaptive and active perspective. Real-time control has been identified as a feasible solution for mitigating water quality problems associated with stormwater management especially in combined sewer communities where large water quality benefits can be achieved by simply shifting the timing of outflows and stopping runoff from entering combined sewers during peak flow periods when combined sewer overflows (CSOs) are occurring (Vitasovic et al. 1990; Cembrano et al. 2002; Vallabhaneni and Speer 2010). Many systems have already been optimized using real-time control by taking advantage of capacity in different parts of the sewer system and dynamically controlling sewers from a system-wide basis in order to avoid CSOs (Tetra Tech 2013). One example of such a system is the Municipality of Metropolitan Seattle that has employed a control system over the CSO region since 1973 (Vitasovic et al. 1990). The system relies on control of pumping and regulator stations to optimize the system and avoid CSOs. The control process relies on a complex hydraulic and hydrologic model that utilizes forecasted rain events six hours in the future, applying a control algorithm to discern the optimal control strategy to be employed by the pumps and regulators in the network to minimize flows to the wastewater treatment plant. This represents just one example of how real-time control has been used in water networks to achieve enhanced performance from an unchanged piece of infrastructure.

Many of the water based systems that used real-time control, until recently, represent end of pipe solutions where urban runoff is still allowed to enter into the sewer system and routed to wastewater treatment plants. While these solutions are clearly appropriate for avoiding CSOs, source capture via green infrastructure still stands as a preferable solution for preventing urban

runoff from ever entering a sewer (Walsh et al. 2005). Furthermore, because source capture prevents runoff from entering conveyance structures, it is a solution appropriate for both combined and sanitary sewers. Source capture solutions typically aim at employing green stormwater infrastructure, or infrastructure that tries to mimic natural hydrology by promoting infiltration and evapotranspiration, to capture stormwater runoff and remove it entirely from the standard stormwater conveyance networks. Overall, minimal study has gone into how these two stormwater solutions, real-time control and green stormwater infrastructure, can work together to create optimized solutions that address complex stormwater management goals.

One of the major ways identified for stormwater management to move forward and become truly smarter is utilizing rainwater harvesting in a more active and intelligent way (Reidy 2010). By combining the principles of detention storage to mitigate storm flows with RTC, more efficient systems are able to be created that not only capture stormwater runoff but also actively use the stored runoff during inter-event periods. While typically stormwater control measures and rainwater harvesting storage have acted as separate systems (Forasté and Hirschman 2010), RTC gives promise to combining the two through smarter controls so that runoff detained in stormwater control measures (SCMs) can be actively used for other purposes. Available uses for harvested rainwater include non-potable residential water supply, irrigation, and energy supply (Forasté and Hirschman 2010). By pairing a reuse of captured stormwater to the ability to actively control and manage systems, great potential arises for creating actively controlled stormwater networks that more efficiently deal with stormwater runoff (Quigley et al. 2008). Quigley et al. (2008) also point out the significant potential that exists with stormwater reuse and RTC just by retrofitting existing pieces of infrastructure with active management. Using controlled infrastructure to prevent

outflows from existing SCMs, storage can be prolonged giving more time for reuse during inter-event periods.

In order to utilize real-time controlled systems, sensors and valves on sites need to have the ability to continuously report data and make actionable decisions to control flows. Currently wireless sensor networks have developed far enough that they are generally low-cost and easily scalable, useful for applications in water management where continuous monitoring and adaptive control are desired (Quigley et al. 2008; Jin et al. 2010; Wong and Kerkez 2016; Mullapudi et al. 2016). In Mullapudi et al. (2016), a vision for system-wide adoption of real-time control is given where distributed networks operate together to maximize pollutant removal and optimize the resulting downstream water quality in watersheds. Because real-time controlled systems are inherently more adaptable through their control, systems like these could theoretically be tailored to meet site specific and complex stormwater management goals through watershed scale networks. While most of the current studies of RTC with stormwater management have focused on single site implementation (Kerkez et al. 2016), the availability of these low-cost sensors provides substantial potential for scaling the technology and seeing even more improvements to stormwater management on a watershed scale.

When looking for appropriate applications of real-time control with green infrastructure, analysis of existing green infrastructure was completed to determine performance areas that could see improvement through the use of active control. One common type of green infrastructure used in heavily urbanized areas is the green roof, a SCM that utilizes a vegetated media on top of buildings to capture rainfall and promote evapotranspiration. Traditional green roofs have been shown to provide both volume and peak flow reduction (Mentens et al. 2006) as well as provide non-water related benefits such as combatting the urban heat island effect (Dominique et al. 2014).

Especially in urban areas where rooftops can comprise a substantial portion of the impervious area (Frazer 2005), green roofs stand as a promising way to aid in stormwater management by increasing capture and promoting evapotranspiration.

While green roofs have been shown to manage peak flows and volumes effectively, the reliance of the systems on evapotranspiration as a removal mechanism provides an opportunity to create a more optimized system. In a green roof studied at Villanova University, it was determined that despite the promising performance of the roof, climatologically a substantial portion of the ET capacity of the roof remained unused due to lack of available soil moisture (Wadzuk et al. 2013). In a subsequent study of the same green roof, it was determined that evapotranspiration comprised over 50% of the water budget for the roof in the period of study resulting in an observed annual ET that was substantially higher than what is natural for the surrounding region (Zaremba et al. 2016). These studies would indicate that the potential for ET is substantial for green roofs and that if soil moisture is available, ET will occur at an effective (if long-term) rate. Linking these findings to the creation of smart stormwater systems, capacity already exists for more ET within green roofs, it just occurs during dry periods between events when water is not available. Therefore, an application for RTC exists where actively managed stormwater can be reused and managed by the green roof during periods where excess capacity is available.

Another common stormwater control measure that proves promising for smart systems is the rain garden. Rain gardens, vegetated SCMs that utilize a soil media to promote either bioretention or bioinfiltration, are effective for both volume reduction and water quality treatment (Hunt et al. 2006; Lord et al. 2013). Additionally, bioinfiltration SCMs in series, where the surface area for infiltration to occur is increased by placing bioswales or rain gardens in a chain, have been shown as a promising way to increase volume capture through promoting infiltration during storm

events (Lewellyn et al. 2016). Lewellyn et al. (2016) showed that despite the design of a bioinfiltration SCM in series for one inch (2.5 cm) of rainfall, the system generally outperformed this benchmark and was able to capture larger volumes due to infiltration that occurred during storm events. These results indicate that bioinfiltration SCMs can possess substantial potential for infiltration, again pointing to a place where optimization could occur through RTC. Similar to the idea of a smart green roof system, the application of rainwater harvesting to utilize a bioinfiltration SCM during dry periods stands as a viable option for creating smarter stormwater systems through the combination of RTC, rainwater harvesting, and green infrastructure.

1.2 Site Overviews

To study the performance of smart stormwater systems, three separate stormwater control measures (SCMs) on Villanova University's campus were retrofitted to include continuous monitoring and adaptive control. The sites include one green roof located on the Center for Engineering Education and Research (CEER), one set of bioinfiltration SCMs in series referred to as a Treatment Train, and one constructed stormwater wetlands that captures runoff from a substantial portion of campus. The three different SCMs provide a wide range of spatial scales with drainage areas ranging from just over 1000 square feet (the green roof) to over 42 acres (the constructed stormwater wetlands). With a similarly wide range of processes associated with the different SCM types, the three smart systems offer a view into how smart systems can function across a scales. For the purposes of this study, the CEER green roof and the Treatment Train specifically were examined. These two SCMs, described further in Sections 1.2.1 and 1.2.2, are similar in that both utilize storage as part of their RTC retrofit to actively manage harvested runoff

and create a smarter system. In studying how these systems perform and how they could be optimized, analysis was completed from both a modeling and an active monitoring perspective.

1.2.1 CEER Green and Gray Roof

The CEER green roof was initially constructed in the summer of 2006 as a retrofit to an existing impervious gray roof located over the CEER Holy Grounds coffee shop (Figure 1.1). The roof is in total 576 ft² in area, 450 ft² of which is covered in a growth media with a thickness of 4 inches. The green roof media is Rooflite MC Media, an engineered soil media from Skyland USA, LLC intended to maximize pore space and free up storage in the media for increased capture in the green roof. While the CEER green roof was originally designed to capture 0.5 inches (1.25 cm) of rainfall over the 576 ft² area, it has been shown to have the capacity to capture 0.8 inches (2 cm) of rainfall before significant outflow from the roof is experienced (Zaremba 2015).



Figure 1.1: CEER Green Roof Construction

Adding capacity to the roof below the grown media is a storage and drainage layer consisting of 1 inch of Optigreen waffled plastic sheets (Figure 1.2). The waffled layer, shaped similarly to an egg

carton, allows for drainage to occur from the green roof at high points in the waffled layer while still providing additional storage for the green roof. Drainage from this layer provides the primary mechanism for excess rainfall to be removed from the CEER green roof with outflows from the roof measured in a tipping bucket rain gage located below the green roof in the CEER Holy Grounds coffee shop.



Figure 1.2: Geotextile and Drainage Layer of CEER Green Roof

While the site existed as a typical green roof for over nine years, the green roof was retrofitted in 2015 to add in a smart component aiming at increasing the drainage area captured by the SCM and further utilizing the evapotranspiration potential of the green roof during dry periods. The motivation for this retrofit came from an analysis previously completed of the water balance of the green roof where it was shown that the total evapotranspiration potential of the roof far outweighed the amount of evapotranspiration that was occurring, this discrepancy was clearly due to the green roof not having water available during dry periods to reach the full evapotranspiration potential.

Figure 1.3 demonstrates the discrepancy between the potential and actual evapotranspiration. While the ET that measurably occurred on the green roof is less than the total rainfall volume, the total estimated ET capacity of the green roof far surpasses the total rainfall experienced. This discrepancy is clearly due to the hydrologic timing of the system, excess water falling during rain events and insufficient water available during dry periods to fully utilize the potential evapotranspiration.

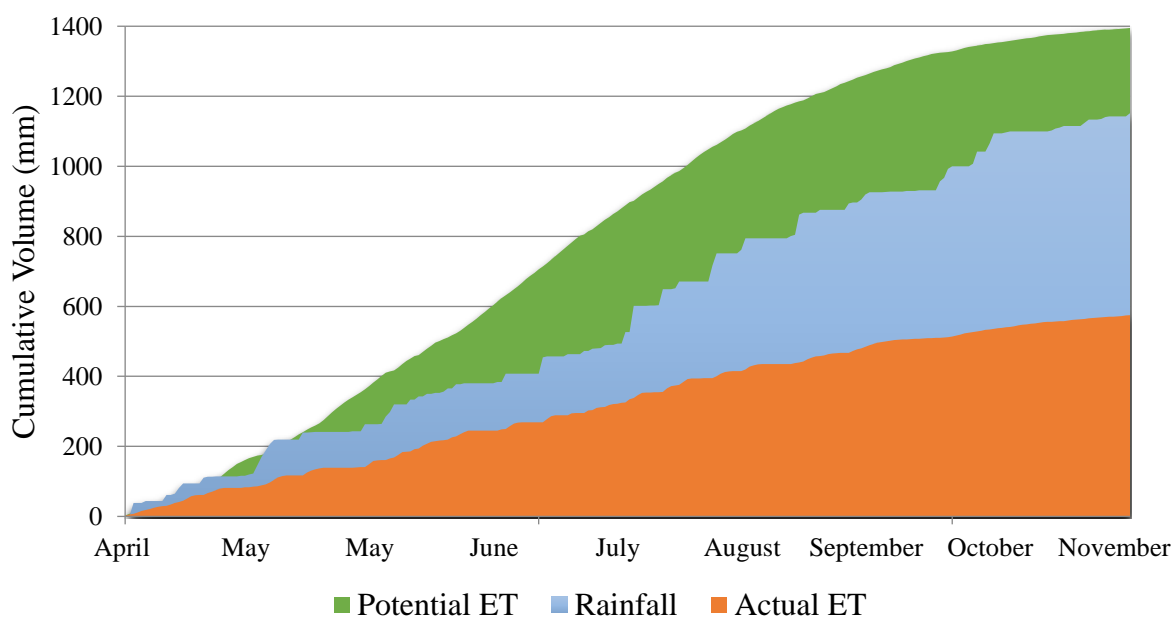


Figure 1.3: Sample Cumulative Potential ET, Actual ET, and Rainfall for CEER Green Roof

With this excess ET potential in mind, a rainwater harvesting cistern was added to the third floor of the CEER building which captures runoff from roof directly above it from an additional 800 square feet of impervious area. Figure 1.4 outlines the added drainage area and the location of the cistern added to CEER. The additional stored water is captured to irrigate the green roof during dry periods and utilize the evapotranspiration potential of the SCM. The cistern connects via a

pump to four sprinklers set up over the green roof media allowing for irrigation to occur directly from the stored rainwater.



Figure 1.4: Drainage Area and Cistern Added to CEER Green Roof System with RTC Retrofit

In trying to create a smart system, control of the green roof irrigation and management of harvested rainwater was automated using a cloud platform developed by OptiRTC (Section 1.2.3). The cistern itself operates with the goal of avoiding wet weather outflows by drawing down in advance of storms to create storage. Forecasts provided from the National Weather Service are used to make these decisions, with forecasts predicted with a probability of precipitation greater than 70% acted on. Additionally, the irrigation from the cistern to the green roof occurs automatically with the pump switching on when soil moisture values less than $0.16 \text{ ft}^3/\text{ft}^3$ are measured in the green roof soil media. Forecasts are also integrated into the irrigation logic with no irrigation occurring if a rainfall event is predicted. Figure 1.5 shows an overview of how the green roof currently appears as of May, 2017.



Figure 1.5: Overview of CEER Green Roof in May, 2017

As can be seen in Figure 1.5, the green roof also contains significant instrumentation that allows for performance to be monitored and be used in control decisions. Instrumentation includes eight soil moisture meters, four soil temperature meters, a full weather station, and a tipping bucket used as an outflow gage for the system. The cistern adjacent to the green roof also includes a pressure transducer level sensor and pump to operate the smart irrigation, the pump leading to the sprinklers located throughout the green roof.

1.2.2 Treatment Train

The second site retrofitted with RTC at Villanova University was a treatment train located near the Saint Augustine Center parking garage. The Treatment Train is a system of several SCMs in series that captures runoff from 14,000 ft² of impervious area draining from the top deck of the

Saint Augustine Center parking garage. Flows are routed from the parking deck down through a weir box and enters into a bioswale. The bioswale, a vegetated bioinfiltration SCM that also offers conveyance, is separated from a second bioswale by a weir with an orifice to pass flows. Following the bioswales are two additional bioinfiltration rain gardens, again separated by a series of weirs. An overview of the Treatment Train system is shown in Figure 1.6.



Figure 1.6: Overview of Treatment Train

When the Treatment Train was retrofitted to include real-time control in May 2016, the overflow from the second rain garden in the train was routed to flow into an underground cistern (Figure 1.7) with an additional storage capacity of 5,100 gallons. If the additional storage in the underground tanks is surpassed, flows are routed to an adjacent infiltration trench (Figure 1.8) which provides additional volume capture before overflowing to the storm sewer. The infiltration trench overflow mechanism is through permeable pavers placed on the surface of the infiltration trench. The infiltration trench itself is comprised of milk crates creating high void space, allowing for increased volume capture at the site.



Figure 1.7: Graf Carat-S Rainwater Tanks (Rain Harvest Systems)



Figure 1.8: Treatment Train Infiltration Trench

When the site was retrofitted to include the underground storage tanks, RTC was also added with the storage tanks reflecting the point of control for the system. The goal of the new Treatment Train was to increase capture and more fully utilize the hydrologic processes of the bioinfiltration SCMs in the system by running stored rainwater back through the bioswales and rain gardens. A pump was added to the underground storage tanks automated with RTC and logic was set up (again

using the OptiRTC cloud platform) to turn on the pump 24 hours after a rain event has occurred. Weather forecasts are also used at the Treatment Train to ensure that pumping does not occur prior to a predicted storm event.

Originally the Treatment Train was designed to capture one inch (2.5 cm) of rainfall volume over the contributing drainage area, about 75% of this coming from the bioinfiltration SCMs and the additional volume coming from the infiltration trench. Past study of the system indicated that the site often outperformed its design during large storm events due to infiltration that occurred over the course of rainfall events (Lewellyn 2015). When the system was retrofitted in 2016, the capacity was increased by adding the underground cisterns and the drainage area was also increased from an original 10,000 ft² to 14,000 ft². With the increased capture volume and ability to recycle water through the system to more fully utilize the infiltration capacity of the system, the retrofitted smart Treatment Train is analyzed for its ability to increase capture and reduce overflow from the site despite an increase in contributing drainage area.

1.2.3 Continuous Monitoring and Adaptive Control

For both the CEER green roof and the Treatment Train, real-time control was achieved using a cloud based platform from OptiRTC. Opti is a technology firm based in Boston that originally formed as a subset of Geosyntec Consultants and focusses on adding continuous monitoring and adaptive control to stormwater infrastructure (OptiRTC 2016). Control of stormwater infrastructure is achieved using control boards with embedded web servers that communicate with Opti's cloud platform to enact control decisions on actuated valves or pumps. Opti utilizes Microsoft Azure as a cloud platform and currently operates using several proprietary algorithms to achieve control.

1.3 Research Plan

The study completed took a comprehensive look at real-time controlled green stormwater infrastructure in order to better understand these systems and work towards optimizing their performance. Utilizing a combination of computer modeling and active site monitoring, different aspects of RTC systems were isolated and studied to gain insight and offer recommendations for future smart stormwater control measures. The main components of the research plan were as follows: an analysis of weather forecasts and uncertainty in the context of forecast-based controls for SCMs, investigation of publically available climate data sets and their application for use in smart stormwater systems, modeling of a smart green roof for performance optimization, and monitoring and evaluation of current RTC systems at Villanova University.

CHAPTER 2: FORECAST RELIABILITY

2.1 Introduction

When creating real-time controlled (RTC) stormwater systems, being able to have a system prepare for impending storm events is critical for optimal performance. This requirement naturally lends RTC systems to use rainfall forecasts to make operational decisions. Making decisions based on forecasted rainfall inherently introduces error and uncertainty into the control process, forecasts being imperfect at predicting exact rainfall volumes and timing. For this reason understanding the uncertainty that can be expected when relying on forecasted information for decision making is critical for designing RTC systems to perform optimally.

OptiRTC, the technology company managing the control of the RTC systems at Villanova University as well as one of the current leaders in real-time control stormwater technology, relies on forecast information for a number of different purposes in their systems. Forecasts are taken from the National Weather Service (NWS) and can be provided at a resolution of 2.5 km^2 (NOAA 2014). Quantitative precipitation forecasts (QPFs) are given for each six hour window up to 72 hours in advance, and probabilities of precipitation (POPs) are reported on a 12 hour basis, giving a probability of rainfall occurring in that 12 window from 0 to 100 percent. OptiRTC systems respond to the two forecasts when certain pre-designated thresholds are passed in terms of both a rainfall volume that the system is willing to accept and a probability of occurrence. These two parameters can be tailored to make the decision making process more or less conservative depending on the context and goals of the stormwater infrastructure. The majority of OptiRTC controlled systems have a storage component (e.g., a cistern) with a level sensor to yield a known depth-volume relationship. These OptiRTC controlled systems use rainfall forecasts to predict an expected volume of runoff that enters a stormwater control measure. By comparing this expected

volume to current volume in the storage device, there is a decision made whether or not to drain the system and create sufficient storage for the impending storm. Additionally, many sites utilize the immediate rainfall forecast for 0 to 6 hours in advance as an approximate check for whether or not it is currently raining. This method is used especially for cases where an on-site rain gage is not used.

Two of the current real-time controlled research sites on the Villanova University campus rely on forecasted rainfall information to make decisions. The CEER green roof and the Treatment Train both operate with RTC and utilize this forecast information. For the CEER green roof, stormwater runoff from the gray roof is collected in a cistern and stored to irrigate the green roof with forecast based RTC applied to ensure sufficient available storage to capture runoff from future storms. For the Treatment Train and CEER green roof system, forecasts are used to ensure irrigation does not occur directly prior to a storm event so that capacity in the system to manage a storm event is not lost. In the Treatment Train forecasts are used as well for an approximation of the time since rainfall occurred, information used to determine when irrigation should start to occur. The forecast reliability study sought to determine the effects of forecast uncertainties on these two distinct usages of forecast information in RTC.

The goals of the forecast accuracy study were to assess the two distinct uses of rainfall forecasts that are used for RTC stormwater systems: estimating an impending rainfall volume that a piece of infrastructure will receive and estimating the time passed since rainfall has occurred. Historic weather forecasts, both probabilistic and quantitative, were used from the National Weather Service for Villanova University campus to provide an accurate method of analyzing how accurate the forecasts were. A modeling approach was taken to also discern the effect of forecast accuracy in the context of RTC system performance.

2.2 Literature Review

In trying to address the complex and varied stormwater demands in urban watersheds, real-time control has been identified as a key method that can be used to more efficiently manage stormwater and lead to benefits from both a water quality and a water quantity standpoint (Wong and Kerkez 2016; Kerkez et al. 2016). Kerkez et al. also notes that while there is a clear benefit to integrating forecast information into RTC systems in order to prepare for impending storm events, there clearly exists inherent uncertainty when weather forecasts are introduced into the control structure. The majority of forecast-controlled systems currently used by OptiRTC compare the expected storm volume to the current volume of available storage remaining and uses this comparison to determine the appropriate storage state (OptiRTC 2017). Again, because of the uncertainty present in the rainfall forecasts, as well as smaller uncertainties related to sensor accuracy and hydrologic models for estimating runoff volume, decisions are predicated on information that carries with it substantial uncertainty.

Despite the clear issue of uncertainty carrying over to affect the performance of RTC stormwater systems, little research has investigated how these uncertainties translate to changes in operation. Of the limited modeling studies completed of RTC stormwater systems that utilize forecast information, many do not actually use historic forecast information, rather relying on the assumption of a perfect forecast and creating “forecast” information by using historic rainfall records (Joksimovic and Sander 2016, Lefkowitz and Bryant 2016). These studies simply manipulate the timing of the rainfall records, shifting the information to appear before storms occurred and allowing this to act as a forecast. While this method avoids the difficulties of acquiring historic weather forecast information, opting instead for the more widely available rainfall records, it removes all uncertainty from the decision making process for the simulations.

From Joksimovic and Sander's study it was determined that while retrofitting existing green infrastructure with RTC would not dramatically change sites' performance during large storm events in terms of peak flow reduction, over the course of a long term simulation up to a 90 - 100% increase in capture could occur from a RTC retrofit. This high level of capture is due to the effect of more common small storms and storms in series. Again, these values are likely high estimates due to the assumption of a perfect forecast built into the simulation. For this reason, Kerkez et al. (2016) suggests further research take place on how forecast uncertainties propagate into the performance of stormwater systems.

Outside of the context of stormwater management, extensive work has gone into improving weather forecasts and developing uses for their predictions. For example, study has gone into how QPFs could be used to preemptively determine areas at risk for flooding during typhoons in Taiwan, allowing for warnings to be disseminated in time to allow for evacuations and preparations (Lee et al. 2012). Pairing the QPFs with a conservative statistical model, the researchers were able to develop a methodology to quickly determine at risk locations for inundation during typhoons, albeit with substantial false alarms due to the conservative approach taken when considering life safety issues. This demonstrates a case where quantitative precipitation forecasts were effective in making decisions prior to storm event. Additionally, QPFs have been used with smaller scale models for predictive measures in reservoir management (Kardhana and Mano 2008). While there is substantial error from the uncertainties in forecasts when using QPFs for predictive modeling, it was shown that the error was less substantial for flow forecasting than when comparing predicted to actualized rainfalls

Clearly these forecast usages differ heavily from the approach taken with stormwater management (including not just on extreme events but all common rainfall events). Rather, in recent years the

aim with stormwater management is not just to consider these smaller, more frequent events, and focus on their management instead to have a larger day-to-day impact from the storms that in total represent the majority of events a site will experience (Lewellyn et al. 2016). This points to a need to investigate further how effective forecasts can be in making predictive decisions for all storm events, not just large-scale extreme events.

2.3 Methodology

To assess the two distinct usages for rainfall forecasts that are currently used for RTC stormwater infrastructure, several SWMM5 models were created to simulate typical configurations of RTC stormwater systems. The two base models created, one simple retention model that sought to maximize retention time and one simple detention time that sought to shift outflows to dry periods, were based on models used by OptiRTC to represent typical logic configurations of their system (Lefkowitz and Bryant 2016). For all models, forecast information was input as both the forecasts from the National Weather Service as well as synthetic perfect forecasts based on recorded rainfall history. This allowed for comparisons of the stormwater systems' performance to indicate how the uncertainty in forecasts affected the outcome of a RTC stormwater system.

2.3.1: Retention Model Setup

The first model created was a simple retention system that utilizes RTC in order to extend retention times in the basin for an assumed water quality benefit. The system is comprised of a 1 acre subarea of 100% impervious area that drains into a storage node sized for 1 inch of rainfall over the subarea (a volume of 3630 cubic feet). The outlet from the storage node is an orifice with a diameter of

0.0459 feet and a loss coefficient of 1.0, a combination sized to have the tank drawdown from full in 48 hours. The valve state is determined by a series of control rules described in Section 2.3.3 and operates to drain the storage in advance of a storm. The retention model is aimed at maximizing retention time and therefore the valve is only opened in the event of a forecasted storm or when an overflow from the system is inevitable. A conceptualization of the retention model can be seen in Figure 2.1.

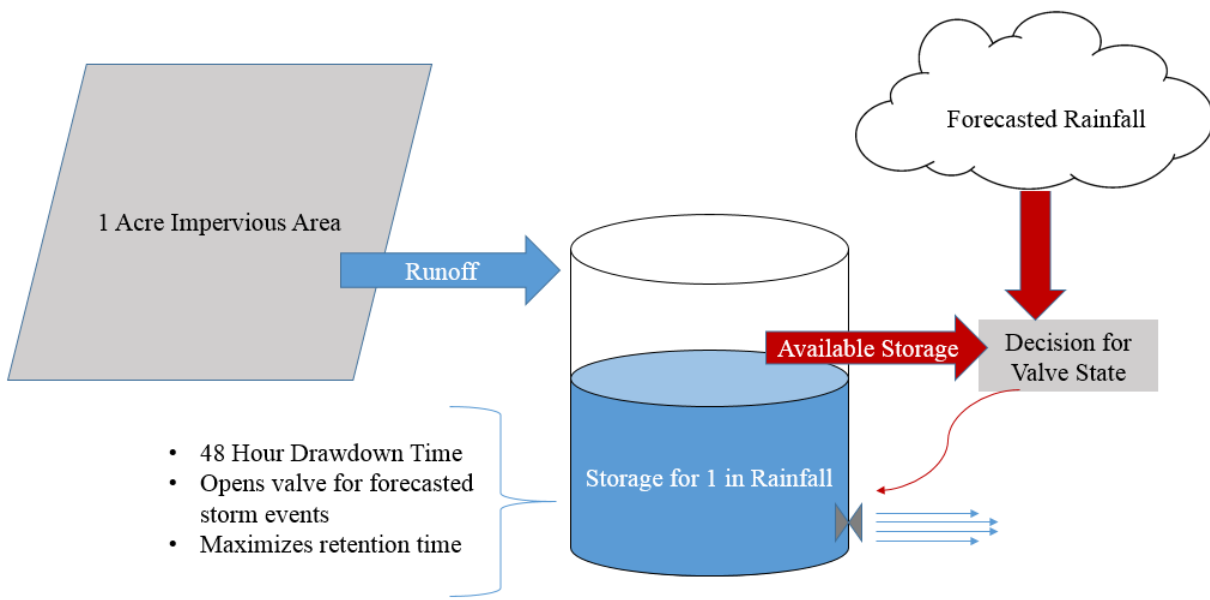


Figure 2.1: Retention Model Conceptualization

For simplification in the SWMM setup of the model, the subarea draining into the RTC cistern was set as a perfect square with no depression storage, meaning all rainfall that falls on the impervious surface would convert directly into runoff. The performance of the retention system was assessed based on its ability to avoid outflows during storm events when possible despite retaining storage after storm events. Because the only instance that causes the storage node to drain

is an actionable event, the performance of the forecast controlled system directly shows how the uncertainties in forecast affect the performance.

2.3.2: Detention Model Setup

In addition to the retention model, a simple detention model was created with the goal of shifting outflows from the wet weather window but without placing an emphasis on maximizing retention time. Once again the system was comprised of 1 acre of impervious area draining into a storage node with a volume of 3630 cubic feet, the equivalent of 1 inch over the drainage area. For the detention case the valve was set to drain the system not only when storms were forecasted in the future but also in the event that more than 6 hours had passed since the end of the previous storm. Rather than having a goal of maximizing retention time for an assumed water quality benefit, this system merely has the goal of avoiding outflows during storm periods. A conceptualization of the detention model can be seen in Figure 2.2.

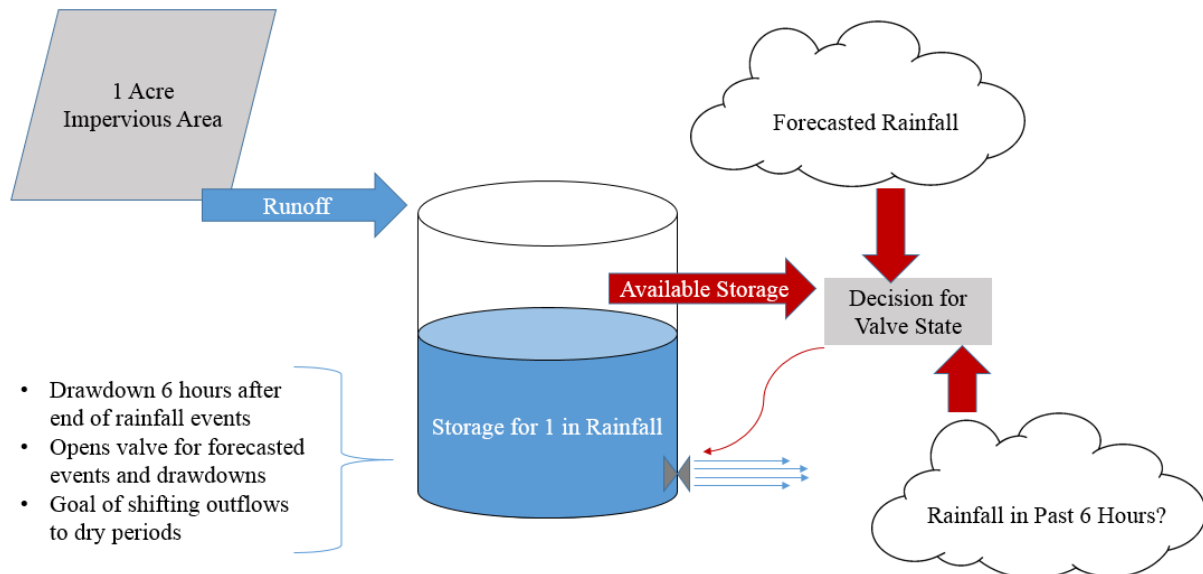


Figure 2.2: Detention Model Conceptualization

Again, the performance of the system was assessed based on its ability to avoid outflows during periods of rainfall. Because this system has as its main goal to shift outflows from the wet weather window, it was expected that performance would be greater when assessed from this metric than the retention system. The detention system allows the uncertainty associated with forecasts to be assessed in multiple ways however, both from the perspective of predicting storm events and ensuring sufficient volume as well as an approximate method to estimate the time since the last rainfall.

2.3.3: Forecast Based Controls

One of the most important aspects of the models was the integration of forecast information into the simulation. For these simulations, a forecast window of 6 to 48 hours in advance was used to check for predicted volume of runoff and a forecast window of 0 to 6 hours in advance was used as a check for impending extreme events where overflows are expected to be unavoidable. Forecast information was integrated into the SWMM model as a rainfall input file in time series form. These inputs were taken from National Weather Service forecasts for the Villanova Campus that were recorded by the OptiRTC platform. Because the RTC systems used by OptiRTC commonly only accept predicted forecasts with Probabilities of Precipitation (POP) greater than 70%, forecasts were only used in cases with a POP greater than or equal to 70% with all other rainfall forecasts set to zero. Rain files for each of the 6 hour windows (seven separate Quantitative Precipitation Forecast, or QPFs) were assigned to subcatchments with identical input parameters to the model's base subcatchment of 1 acre impervious area (Section 2.3.1 and 2.3.2) and all having a common outfall location. Setup of the forecast inputs in the SWMM GUI can be seen in Figure 2.3.

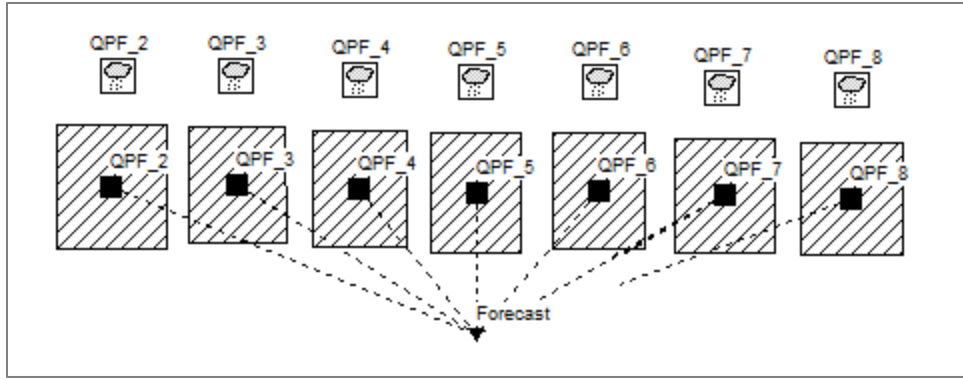


Figure 2.3: Forecast Inputs in the SWMM5 GUI

With forecasted runoffs from the next 48 hours all draining to the same node, a storm volume could be estimated by multiplying the flow (in cubic-feet per second) by the reporting time step of 1 hour to get volume in terms of cfs-hours. Through a series of control curves and hydraulic control rules, the simulation uses this volume to compare to remaining storage in the retention or detention storage node in order to decide whether or not to drain prior to an event. Based on the runoff volume projected from the forecasts, the volume is sorted into one of 20 categories that represent 5% increments of the storage volume. For each category, a control curve is used that makes a decision on the valve state based on the current storage volume. If the current storage volume available is less than the projected inflow volume, the outlet valve is set to 1 (or fully open). Otherwise, the outlet valve remains closed and is set to 0. The following represents a sample control rule and associated control curve:

```

Rule Forecast_50%
If Node Forecast Inflow > 0.4536
And Node Forecast Inflow <= 0.5040
And Node 1in_cistern Depth > 0
Then Orifice 1in_orifice Setting = Curve 50%

```

The rule, one of 20 that breaks the forecasted runoff volumes into ranges, first checks if the volume is between 0.4536 and 0.5040 cfs-hrs (0.45 to 0.50 inches of volume over the 1 acre drainage area). If this range condition is met and there is an additional check to make sure the tank is not empty, and if this is also found to be true the control setting for the outlet valve is directed to the control curve for this specific range of predicted inflows (Figure 2.4).

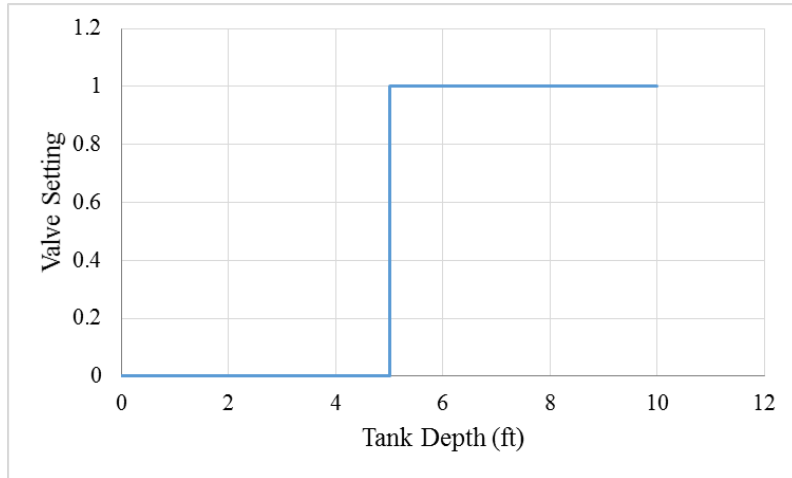


Figure 2.4: Sample Control Curve for Forecasted Inflow Volume at 50% of Tank Capacity

The control curves were created to be specific to each range of predicted inflows and are based on the available storage left in the cistern. If it is predicted that the current storage will be available to capture the storm volume, the valve will remain closed and stay set to 0. Otherwise the valve will be set to 1 and allowed to drain down until a time step is reached where it is determined that sufficient storage is available.

In addition to the forecast controls for the long-term forecast (48 hours in advance), logic was added to include a short term forecast (the immediate 6 hours) to make decisions in cases of large

and extreme events. The QPF for the 0-6 hour window is used again running over an identical subcatchment to the study area and draining to an outlet node (Figure 2.5).

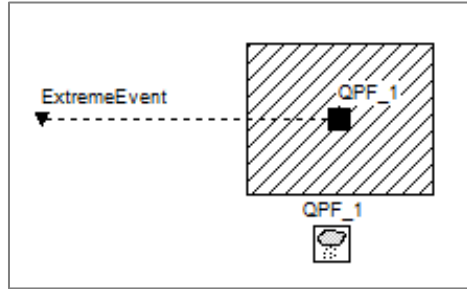


Figure 2.5: Extreme Event Check in SWMM GUI

The goal of the extreme event check was to ensure that in cases where an impending rainfall volume was large enough to overflow the storage node that the outlet valve would just remain open and act as a passive detention system for the duration of the storm. This overrides the standard logic which closes the valve during rainfall events in order to capture the storm and only takes action in cases of large events.

2.3.4: Rain Check Controls

A crucial component for the real-time control aspect of the models was the ability to check if rainfall had occurred during the preceding six hours. This check allows for the system to make sure that outflows occur during dry periods, therefore avoiding wet weather outflow. A challenge of achieving this goal using the SWMM5 model is that control rules that activate valve states in SWMM5 do not have the option of being based on information from a previous or future time step. In other words, control decisions must be predicated on information available in the current time step such as a model component's depth or flow or the simulation's date and time. Because the rain check controls require valve states to be decided based on whether it has rained in the past six

hours and not on conditions in the current time step, storage was used to determine the effect of past rain events.

In the SWMM model an additional subcatchment was created that drains into a storage node to be used for the rain check (Figure 2.6). The storage node was sized to equal the volume of 0.0001 inches of rainfall distributed over the 1 acre impervious area of the subcatchment, or 0.363 ft^3 of storage set full at 10 feet of depth. Because the rainfall inputs to the model are based on rain gages precise to 0.01 inches of rainfall, this ensures that any rainfall that occurs in the model will result with the storage being at capacity with all excess rainfall overflowing the node. To drain volume from the storage node in the rain check an orifice was placed at the base of the storage facility with an orifice coefficient of 1.0 and an area of 0.0015 ft^3 . This orifice was sized so that the storage node would drain from full in 6 hours, and because any amount of rainfall on the system results in a full storage node, this means the storage will always empty after 6 hours of no rainfall.

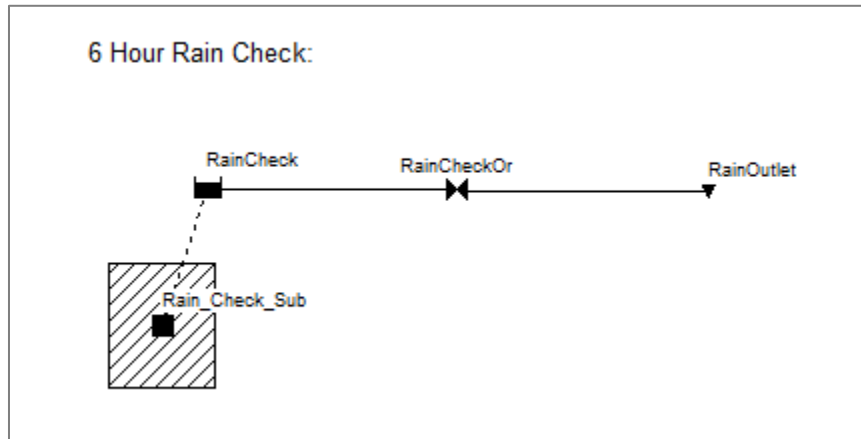


Figure 2.6: Rain Check Setup in SWMM5 GUI

Once the rain check storage node was created, determining whether or not rainfall had occurred in the past 6 hours could be determined in the time step based on whether or not the storage node had any volume in it. This simple binary check for any volume allows for an easy way at any point in

the simulation to determine if rainfall had occurred recently. An example of how the storage in the rain check changes over time with storms in series can be seen in Figure 2.7. This series of storms from May 1st to May 4th, 2016 demonstrates a range of storm volumes, with the minimum recorded value of 0.01 inch occurring at multiple points in the sequence. While fluctuations in storage can be seen throughout the course of the storm as intermittent dry periods less than 6 hours occur, it is clear that the storage node only empties when preceded by a 6 hour period of complete dry weather.

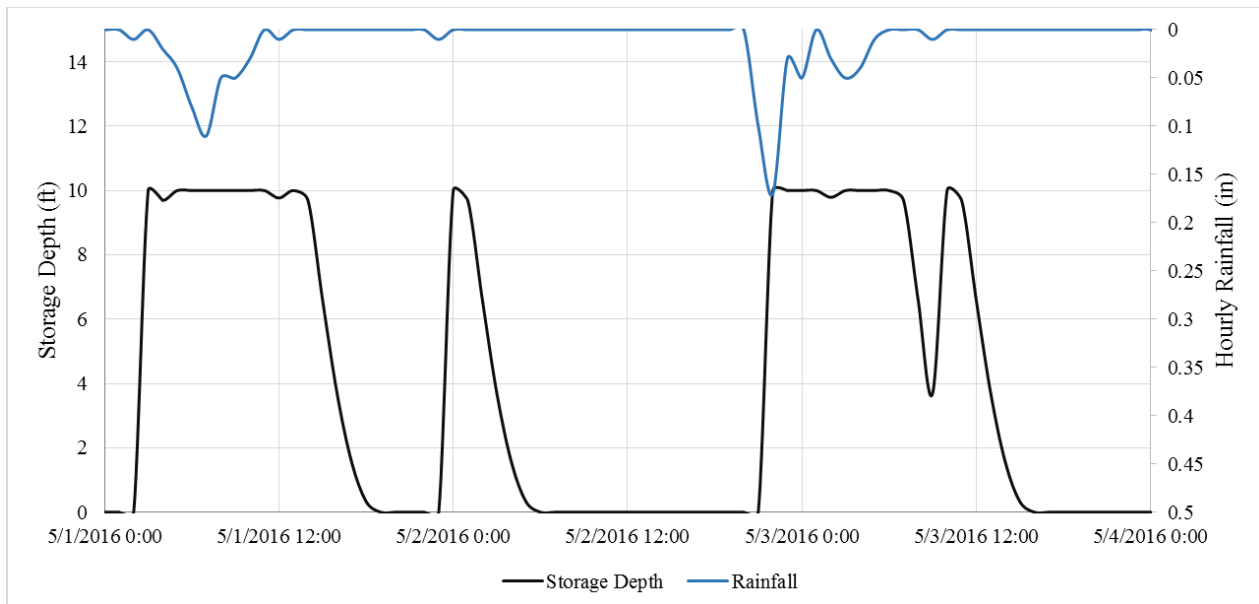


Figure 2.7: Example Rain Check Storage Response to Storms in Series

The rain check storage node was used to write a simple control rule for the system, telling the RTC storage facility to drain when it has been over 6 hours of dry weather. The standard SWMM control rules format was used, applying If/Then logic in the sequence of model attribute type, attribute name, control parameter, and finally a value. The rain check rule was written as follows:

```

Rule Drain
If Node RainCheck Depth < 0.01
Then Pump 1in_orifice Setting = 1.0

```

This control rule was applied in tandem with the forecast control rules to create a set of logic for the RTC on the stormwater systems. In the analysis of forecast accuracy the uncertainty associated with this rain check was also analyzed, as described in Section 2.3.5.

2.3.5: Model Runs for Forecast Analysis

In order to isolate the effect of forecast uncertainty on different aspects of the model’s performance, six different simulation runs were completed with varying inputs for the forecast information. In each case where a forecast could be used (forecasts for control decisions prior to storms and forecasts as a rain check after events), there existed the option to use either the forecasts recorded for Villanova University’s campus or a perfect synthetic forecast created from the historic rain data. Running simulations using the perfect forecast would represent the ideal case with deviations from these results reflecting the effects of forecast uncertainty. A summary of the six simulations completed with their usages of either real forecasts (denoted “forecast”) or perfect forecasts (denoted “rainfall”) can be seen in Table 2.1.

Table 2.1: Forecast Input Data Sources for Forecast Analysis Model Runs

Model	Forecast Rules	Rainfall Check
Retention Model (Retention time maximized for Water Quality)	Forecast	N/A
	Rainfall	N/A
Detention Model (Avoiding wet weather outflows)	Forecast	Rainfall
	Rainfall	Rainfall
Detention Model (Post-storm drawdown)	Forecast	Forecast
	Forecast	Rainfall

For all simulations a historic forecast and rainfall data was used spanning from April 1, 2016 to October 25, 2016. Rainfall records were taken from an on campus rain gage located at the stormwater wetlands, and forecasts were recorded by OptiRTC for the Villanova campus. While it is a relatively short simulation period, a variety of storms is still seen with six separate events (separated by 6 hours or more) seen with rainfall volumes above one inch and two events over two inches. Event totals for the simulation period can be seen in Figure 2.8.

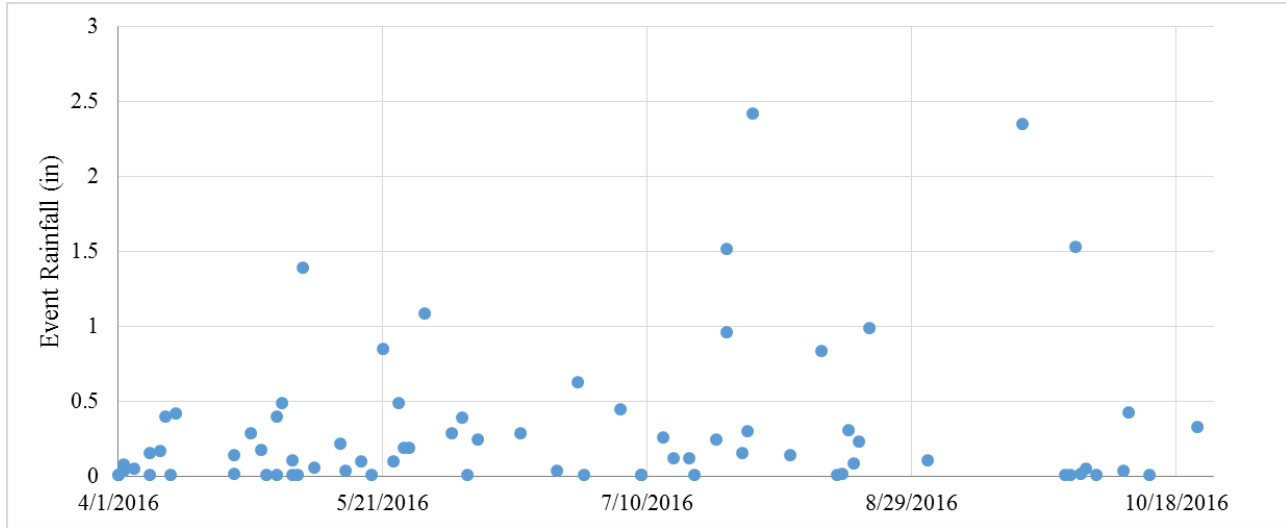


Figure 2.8: Rain Events in Long-Term Simulations

The variety of rainfall events present in the simulation allowed for the performance of the systems to be assessed in both typical cases that fall within the design goals of the systems (1 inch of storage) as well as larger events where overflows are expected. By running the systems with both perfect and real forecasts through a wide variety of hydrologic conditions, the overall deficit in performance from inaccuracies was expected to be seen.

2.4 Results

2.4.1 Forecast Accuracy for Simple Retention Model

The SWMM model of the simple RTC retention facility was run using both the perfect forecast and the real forecasts recorded for Villanova University's campus. To compare performance, the number of storm hours where overflow was experienced was recorded and compared for the two simulations along with the average outflow from the RTC retention storage node during wet weather periods. These values for both simulations can be seen in Table 2.2.

Table 2.2: Simple RTC Retention Performance with Real and Perfect Forecasts

	Forecast Used for Decisions	
	QPFs with POP > 70%	Perfect Forecast
Average Wet Weather Outflow (cfs)	0.0276	0.0169
Wet Weather Hours With No Outflow	195	206
Wet Weather Hours with Outflow	110	99
Percent Wet Weather Hours with No Outflow (%)	63.9	67.5

While it is clear that the performance of the system is worse when simulated with real forecasts rather than a perfect forecast, the decrease in performance is fairly minimal. Over the course of the 208 day simulation, there were 11 more hours where outflow occurred during a storm period when using the real rather than perfect forecast. This increase of 11.1% also resulted in the average wet weather outflow increase by a fairly substantial 63.3%, however this value is still a relatively low outflow value for an acre of impervious area. Philadelphia Water Department's current regulations set a maximum outflow for slow-release designs to 0.05 cfs per impervious acre of drainage area, a standard met on average even with the imperfections of rainfall forecasts (PWD GSI Planning and Design Manual 2016). Additionally, the change in wet weather hours where runoff was completely retained was from 67.5% to 63.9% when comparing the ideal and real forecast cases, respectively. While a decrease in performance, it shows that even with imperfect forecasts the system still has the ability to avoid wet weather outflows to near the ability of the perfect case.

For the decrease in performance between the simulations with real and perfect forecasts the discrepancies can be attributed to three unique cases: a storm was not predicted with high enough probability, a storm volume was underestimated, and a storm volume was overestimated. Sample time series results from these three cases can be seen in Figures 2.9, 2.10, and 2.11 respectively.

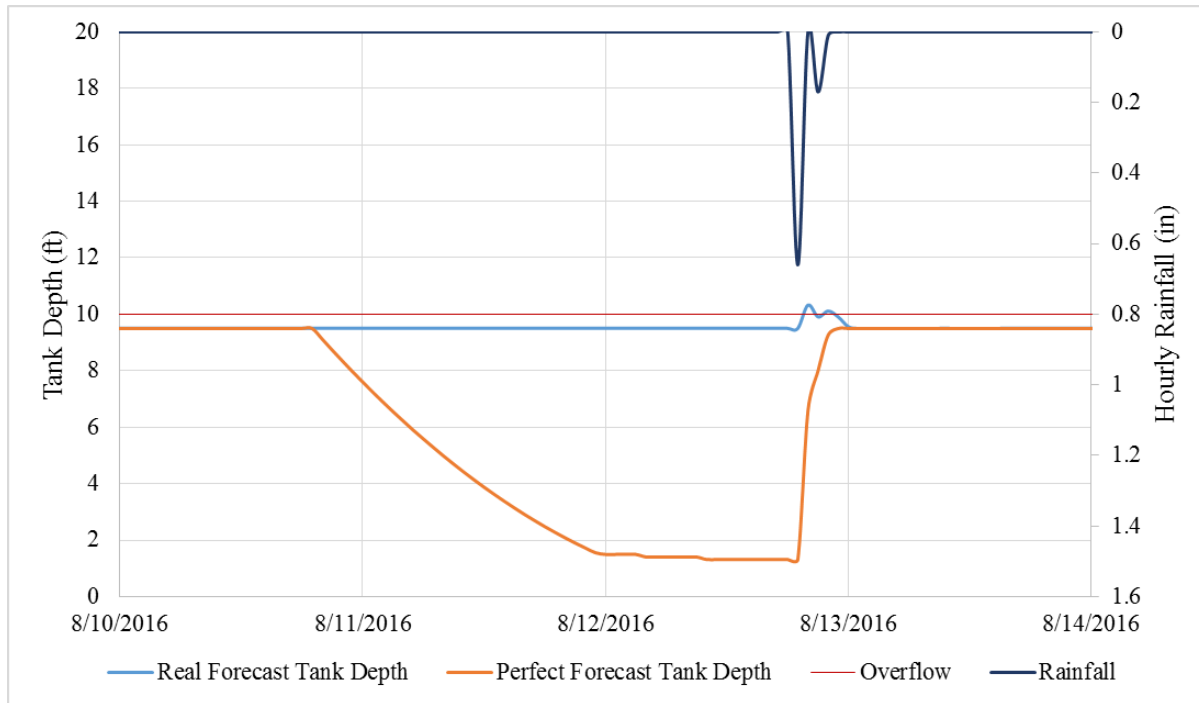


Figure 2.9: Forecast Inaccuracy – Storm Event not Predicted

Figure 2.9 demonstrates the case where a storm event was not predicted with a POP greater than or equal to 70%, resulting in the forecast not being considered for a RTC decision. In the perfect forecast case, the retention storage draws down to ensure sufficient room for the runoff volume however without a high enough probability of occurrence, the simulation with real forecasts takes no action. This results in the majority of storm volume overflowing from the system and is one of the causes of decreased performance from the perfect forecast case when comparing the overall performance in the two simulations. This represents the worst case scenario with forecast

uncertainty with no preparation made for a storm event and significant wet weather outflow occurring.

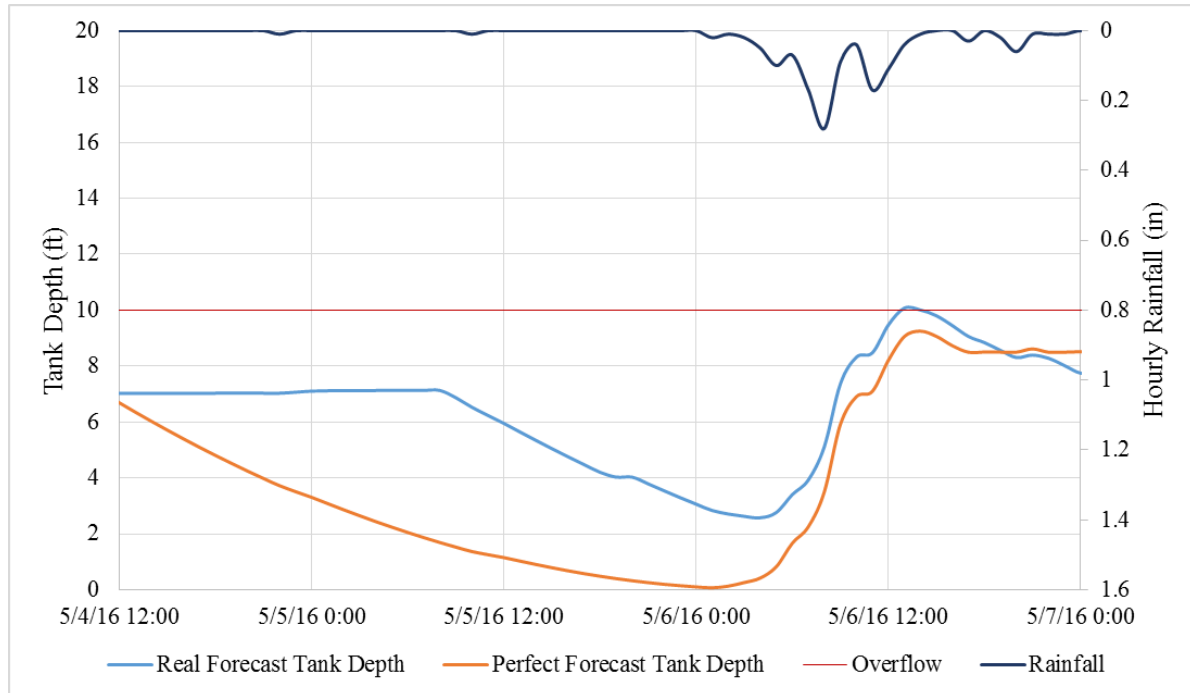


Figure 2.10: Forecast Inaccuracy – Storm Volume Underestimated

A more common occurrence related to forecast uncertainty seen in the simulation was a forecast that correctly predicted the occurrence of a storm, however had some error in the runoff volume that should be expected. Figure 2.10 shows the case where the predicted storm volume was less than the actual storm volume resulting in insufficient storage space being freed up prior to the storm event. While this still resulted in a slight overflow from the system, the performance was still better than that shown in Figure 2.9 where no action was taken. This demonstrates how decisions predicated on imperfect forecasts can still improve performance and lead to significant capture even if the exact predicted value is not perfect.

The last case shown in Figure 2.11 represents again when a storm event was predicted but the runoff volume forecasted did not exactly match what occurred. In this case the volume predicted was an overestimate, resulting in the retention storage node draining more than necessary to capture the storm volume. While the storm did not fill the cistern back to capacity, subsequent storms returned the system back to match the performance shown by the simulation with a perfect forecast.

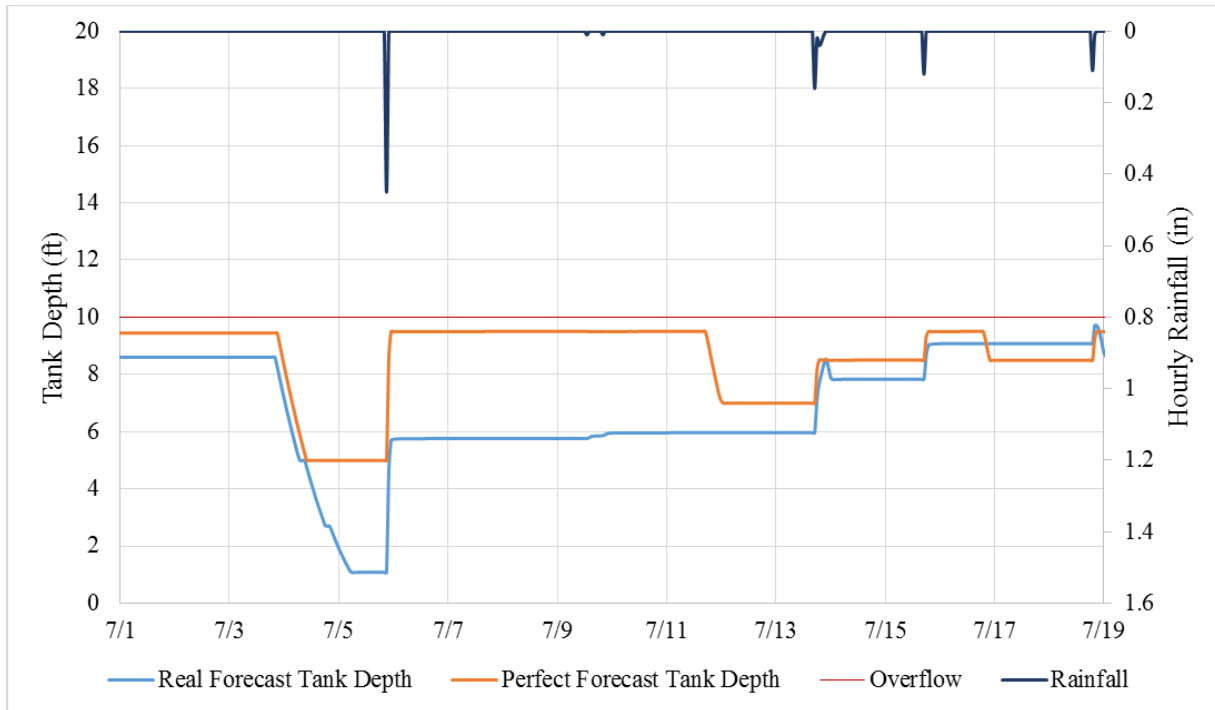


Figure 2.11: Forecast Inaccuracy – Storm Volume Overestimated

Figure 2.11 represents the ideal case for when a forecasted runoff volume is less than the experienced runoff volume. Though less stormwater remained captured after the event (which may be detrimental in the case of rainwater harvesting), an overflow was still avoided because sufficient storage was created to capture the entire storm. Furthermore, the system was self-correcting over time, eventually returning to a state similar to that of the perfect forecast simulation.

When looking at a typical deviation in performance between the systems with a real forecast and with a perfect forecast, the systems had average wet weather outflows of 0.0276 cfs and 0.0169 cfs, respectively. Analysis of rainfall record used with an assumed inter-event time of at least 6 hours showed that on average storms lasted for a duration of 5.04 hours. With these two values in mind, a typical storm overflow volume was calculated and compared for both simulation runs and is shown in Table 2.3 assuming the average wet weather outflow occurring constant throughout the average storm duration.

Table 2.3: Typical Overflow Volumes for Retention Model Simulation Runs

	Real Forecast	Perfect Forecast	Difference
Typical Storm Overflow Volume (ft ³)	501	307	194
Percent of Total Tank Volume (%)	13.8	8.46	5.34

The difference between typical outflow volumes for the two simulations was found to be 194 cubic feet, or 5.34% of the storage volume present in the RTC tank being simulated. This difference could be used to improve the performance of forecast based RTC systems and help take the uncertainty out of integrating forecast information into the RTC logic. For example if the target volume of the retention storage unit was set to be approximately 5.34% lower than the maximum volume of the tank, a buffer could be provided against uncertainties in the forecast causing unnecessary overflows during storm events.

2.4.2 Forecast Accuracy for Simple Detention Model

In addition to the simple retention RTC model created, another SWMM model was used to analyze the effect of forecast uncertainty which simulated a simple detention system with forecast based RTC. The detention model setup, as described in Section 2.3, operate with the objective of shifting outflows from the detention facility outside of the wet weather window. Performance is therefore evaluated based on the ability to avoid wet weather discharge, a goal that would be consistent with CSO communities' needs. Table 2.4 describes the performance of the system with the recorded forecasts of POP greater than or equal to 70% and for the hypothetical case of a perfect forecast.

Table 2.4: Simple RTC Detention Performance with Real and Perfect Forecasts

	Forecast Used for Decisions	
	QPFs with POP > 70%	Perfect Forecast
Average Wet Weather Outflow (cfs)	0.0223	0.0212
Wet Weather Hours With / Without Outflow	22 / 253	20 / 255
Percent Wet Weather Hours with No Outflow (%)	92.0	92.7

When comparing the two simulation runs, it is clear that forecast inaccuracies only slightly reduce the ability of the system to shift outflows from wet periods. The percent of storm hours where runoff was completely retained was reduced from 92.7% to 92.0% with just two more instances of overflow during the entire simulation. This shows that despite the reduction in performance, a forecast based method of shifting outflows from the wet weather window is still an effective way to manage stormwater runoff. The change in average wet weather outflow was also fairly minimal

with a 5.19% decrease in outflow from the perfect case. Both simulations remained well below the PWD requirement of 0.05 cfs per acre of impervious area for slow release systems.

With inaccuracies in the weather forecast, there exist two potential errors that the chosen prediction based on the POP and QPF can encounter: overprediction of incoming storm volume and underprediction of storm volumes. Both error cases have the potential to cause overflows during storm events. If a storm volume is overestimated to the point where an overflow is predicted, a system could discharge during a storm event to create sufficient room when that action may not have been needed. If a storm is underestimated, insufficient storage could be created and an overflow may ensue. Figure 2.12 shows an example of the overestimated case where an overflow during a storm event is caused by an inaccurate forecast.

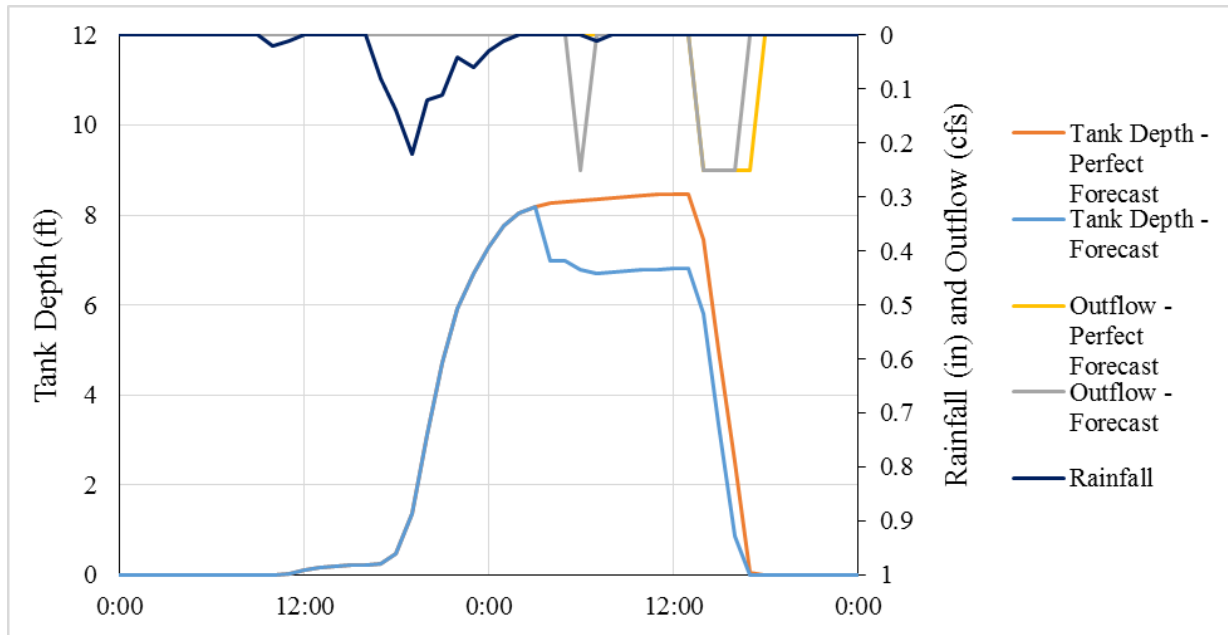


Figure 2.12: Storm on 5/21/2016, Comparison of RTC Detention with Real and Perfect Forecasts

In Figure 2.12 the overflow is caused by the RTC actively draining the system during the midst of a storm due to a high estimate of inflow volume. Because the detention system is drained relatively

shortly after storm events, this overestimation case was the only scenario seen where an overflow occurred in the system with a real forecast and not in the system with a perfect forecast.

2.4.2 Forecast Reliability as a Rain Check:

The other primary function that forecasts are used for in OptiRTC controlled systems is checking for the time period from when rainfall last occurred. While it would clearly be optimal to use real rainfall data for this check, currently the 0 to 6 hour forecast (QPF 1) is used to approximate the weather conditions and is necessary in cases where a site does not have an on-site rain gage. This approximation method is also used to determine when to pump water stored in the underground cisterns at Villanova's Treatment Train site, so understanding how the forecast uncertainty affects this function is clearly important for optimal performance of the site.

For the case where forecasted rainfall in the first QPF (0 to 6 hours in advance) is used as a check for whether rainfall occurred or not, the simplified model was run using a drawdown delay of 2 and 6 hours past the last period of rainfall with the simple detention model. Because the first QPF is for a 6 hour window, this delay in theory could have a range of six hours past the point of possible rainfall. In both cases to examine the variability associated with using the forecast as a rain check, the performance of the system was compared to a case where the real rainfall was used as a check, the ideal case for the system. Variations between the model performances could therefore be attributed to inaccuracies in the 0 to 6 hour forecast window. Results from the simulation with the 2 hour drawdown delay can be seen in Table 2.5.

Table 2.5: Wet Weather Outflow of RTC Modeled System with a 2 Hour Rain Delay Drawdown

	Real Rainfall for Rain Check	Forecasted Rainfall for Rain Check	Difference
Wet Weather Hours with Outflow (of total wet weather hours)	15 / 275	43 / 275	28
Percent Hours without Wet Weather Outflow	94.5%	84.4%	10.2%

Results from the comparison show decreased performance from the system that utilizes the first QPF for a rain check rather than the real rainfall. Overall a 10.2% decrease was seen in storm hours where no outflow was recorded from the systems. Because the only factor changed between the two models was the rain check input file, these discrepancies can be attributed to inaccuracies in the first QPF forecast. Because the time delay after rainfalls for when releases occur could have substantial effects on the way forecast inaccuracies propagate into the systems' performance, the same simulation was also run with a 6 rather than 2 hour delay for release past rain events. Results from this simulation can be seen in Table 2.6.

Table 2.6: Wet Weather Outflow of RTC Modeled System with a 6 Hour Rain Delay Drawdown

	Real Rainfall for Rain Check	Forecasted Rainfall for Rain Check	Difference
Wet Weather Hours with Outflow (of total wet weather hours)	22 / 275	51 / 275	29
Percent Hours without Wet Weather Outflow	92.0%	81.5%	10.5%

When using the 6 hour rain check a similar decrease in performance is seen when comparing the forecast based system to the real rainfall check, this time a 10.5% decrease in percent hours without wet weather outflow. These discrepancies where outlet valves are opened during periods where rainfall is still occurring can be linked to cases where a storm was not predicted with enough probability to be deemed real (in this case greater than or equal to 70% POP), causing the effects of that storm to be ignored in the logic. Two examples of this case in series that were found in the long-term simulation completed can be seen in Figure 2.13, comparing the expected performance if real rainfall is used as a rain check to the performance with the forecast based rain check.

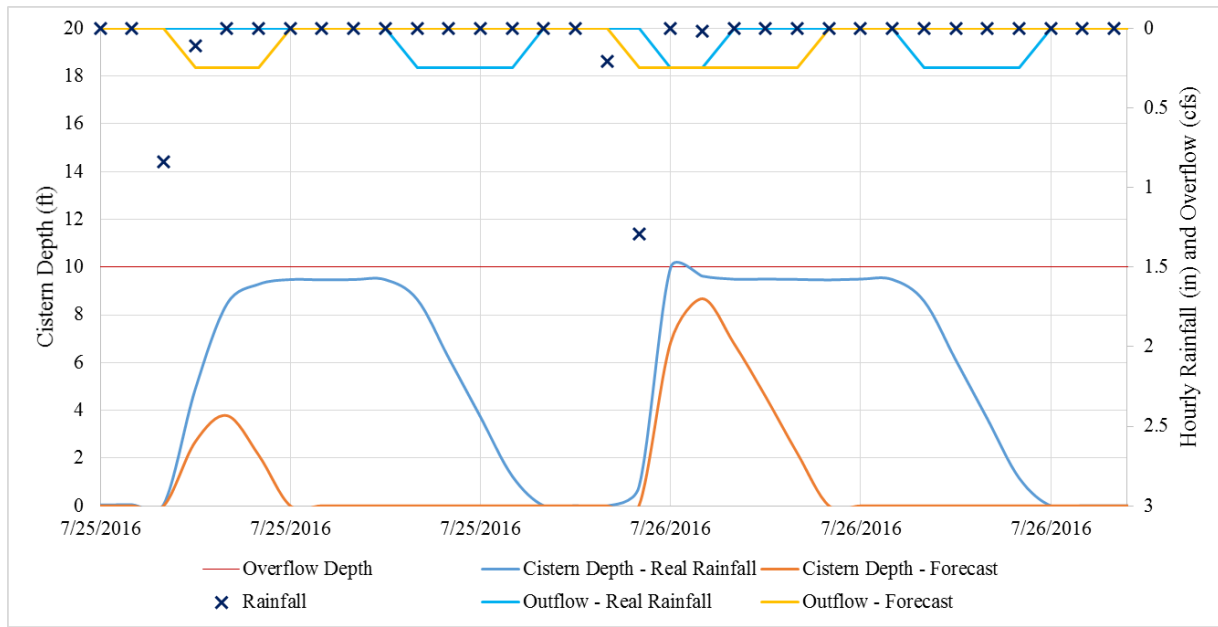


Figure 2.13: Overflow Cases Caused by Forecast Inaccuracy

For both storms the system using rainfall as a rain check performs ideally. The cistern fills with a closed valve during the storm (with the exception of one time step where the storage capacity was exceeded) and the cistern is drawn down 6 hours after the end of the storm. However, in these cases with the forecast as a rain check, neither storm was predicted with a probability above 70% resulting in drawdowns occurring while it was still raining.

While cases where outflows occurred during storm events due to errors in the forecasted rain check were relatively rare, they still resulted in an overall decrease in performance compared to the case where the actual rainfall record was used as a rain check. This indicates a place where there is room for improvement with RTC systems currently using this method because, unlike with forecast decisions that occur prior to storm events, there exists a viable alternative where an increase in performance would be seen. If on site rain gages are already in place or could be installed, using the actual rainfall record as the check for dry periods is ideal for optimizing RTC performance.

2.4.3 Probability of Precipitation Sensitivity

An important aspect of forecast usage in RTC stormwater systems is the probability of precipitation that is used to define an actionable event. For the previous analysis completed (Sections 2.4.1 and 2.4.3), a POP threshold of 70% was used based on standard practice with sites controlled by OptiRTC. This value was assessed by altering the POP threshold used to define an actionable event and comparing the performance of the simple retention system analyzed in Section 2.4.1. A retention system was chosen for analysis because the forecast uncertainties were shown to have a larger effect on the performance, meaning the effect in forecast uncertainty and POP threshold would be more visible in the results of the analysis. POP threshold values were altered from 10% to 100% and run through the same simulation described in Section 3. Storage depths modeled in each of the retention systems for varying POP thresholds are shown in Figure 2.14.

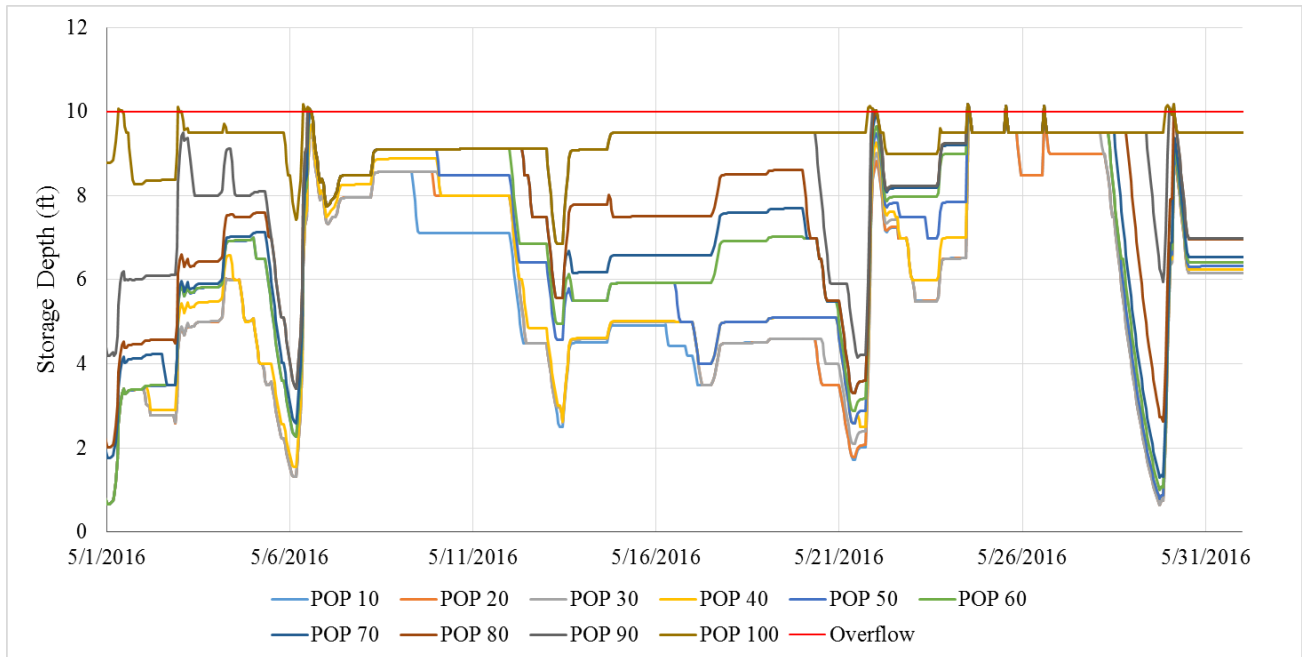


Figure 2.14: Tank Storage Depths for POP Sensitivity Analysis, May 2016

It is clear from looking at the time series storage results (Figure 2.14) that the POP threshold value chosen has a substantial impact on the performance of the retention system. Systems that only consider high POP values as actionable events (such as the POP 100 line) result in many overflows, this indicating that storm events occurred that were not deemed actionable. On the other end of the spectrum systems with very low POP thresholds (such as the POP 10 line) tend to draw down more frequently and to a greater extent. While this definitely avoids overflow events from happening, it is counterproductive to the water quality goals of increasing retention time. In order to better understand how these different factors work together, wet weather outflow hours, overflow events, and average retention times were calculated for each simulation run and are compared in Figures 2.15, 2.16, and 2.17, respectively.

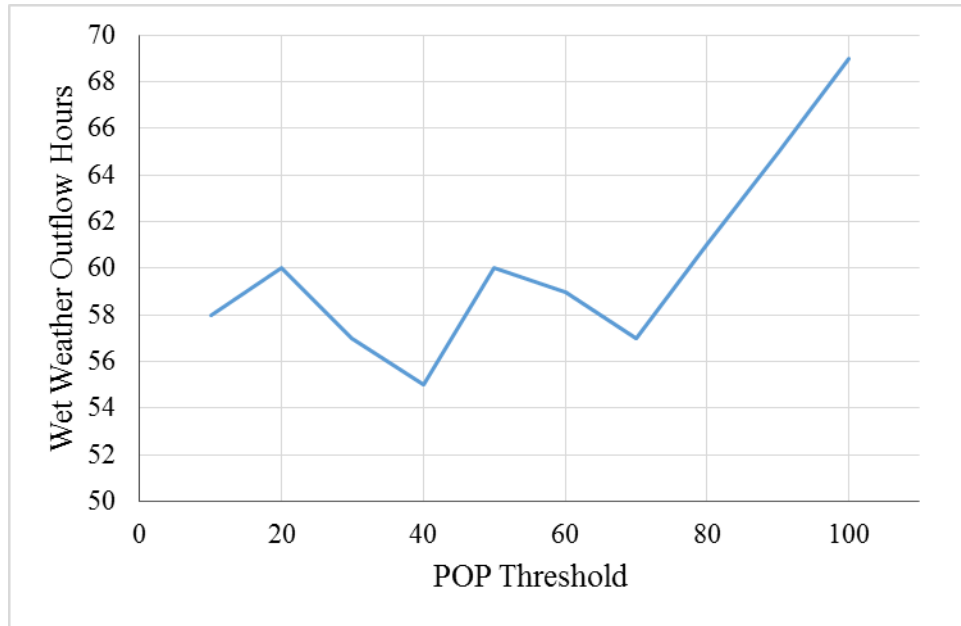


Figure 2.15: Wet Weather Outflow Hours for Changes in POP Threshold of RTC Retention System

As is expected, as the POP threshold increases, a corresponding increase in wet weather outflow is seen. The performance does show some variability at lower POP thresholds however, likely due to the balance between over-draining a system to prepare for a storm event (causing outflows during the beginning of storms) and not preparing enough for a storm. One of the local minimum values shown in the results is at a POP threshold of 70%, providing confirmation that this is a reasonable value to choose to define an actionable event. In addition to the wet weather outflow hours, the time when overflow was occurring from the systems was also examined. Overflow differs in that it is not controlled through the outlet orifice, rather just overflow from the top of the storage node. This is clearly less preferable and controlled outflow and again should be minimized for a design.

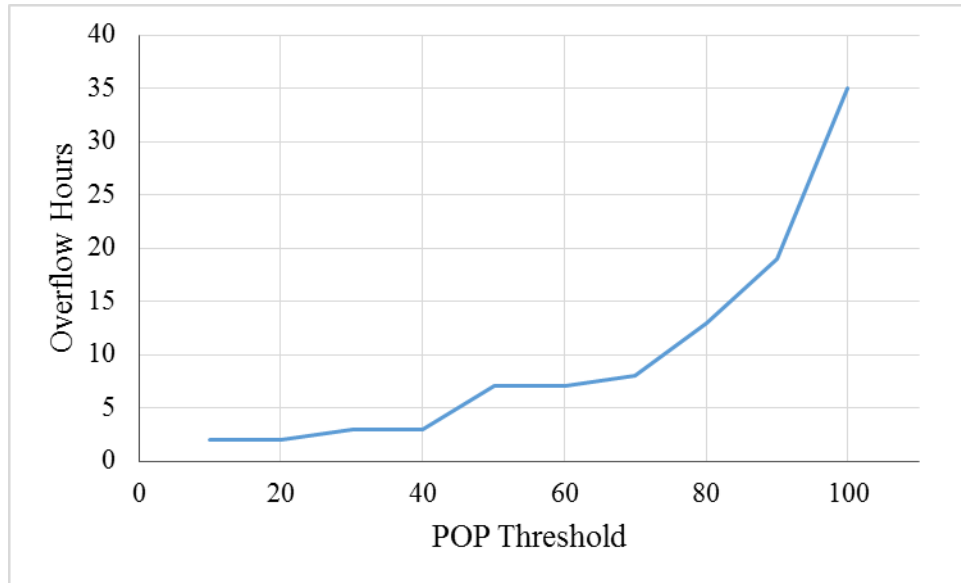


Figure 2.16: Total Overflow Hours for Changes in POP Threshold of RTC Retention System

Overflows occurring from the controlled storage facilities saw an increase as the POP threshold was increased. Increases were slow however until 70%, after which a sharp increase was seen until 35 hours of uncontrolled overflow occurred at the 100% POP threshold (compared to a minimum value of two hours at 10% POP). Again this shows 70% to be a reasonable selection for a POP threshold. While there is still more overflow than at the minimum point (eight hours rather than 2), this relatively small increase balances easily with the gains in performance seen when looking retention time (Figure 2.17).

To compare retention time for the different simulation runs, a methodology needed to be created to compute average retention time for the non-steady state system. The retention storage facility was assumed to act as a continuously stirred flow tank reactor (CSTR) where the parameter analyzed was time. With each time step, the average age of water in the tank was increased and combined in a volume weighted average with new runoff entering the system. Outflow then had an average retention time associated with it, allowing for a final flow-weighted retention time of

all outflow to be calculated. An overview of the retention time calculation can be seen in Equations 2.1, 2.2, and 2.3. AWA represents the average water age currently in the storage facility, V is the volume, Q represents flow, T_R is the calculated retention time, and Δt is the time step for the simulation.

$$\text{Equation 2.1} \dots \text{AWA}_{t+1} = \frac{(V_{av} * \text{AWA}_t) + Q_{in} * 0.5\Delta t}{V_{av} + Q_{in}\Delta t}$$

$$\text{Equation 2.2} \dots V_{av} = \frac{V_t + V_{t+1}}{2}$$

$$\text{Equation 2.3} \dots t_R = \frac{\sum(\text{AWA}_i * Q_{out_i})}{\sum Q_{out_i}}$$

Retention times were calculated for each simulation run and are shown in comparison to the POP threshold in Figure 2.17. As expected, as the POP threshold becomes larger and the actionable event becomes less frequent, the system is less likely to drain down to prepare for events and therefore results in larger retention times as a whole. Because the goal of the system in these simulations is to maximize retention time, the only time a drawdown is initiated is for a storm event. This results in a calculated retention time that represents an upper bound on what is possible to achieve in a smart retention facility.

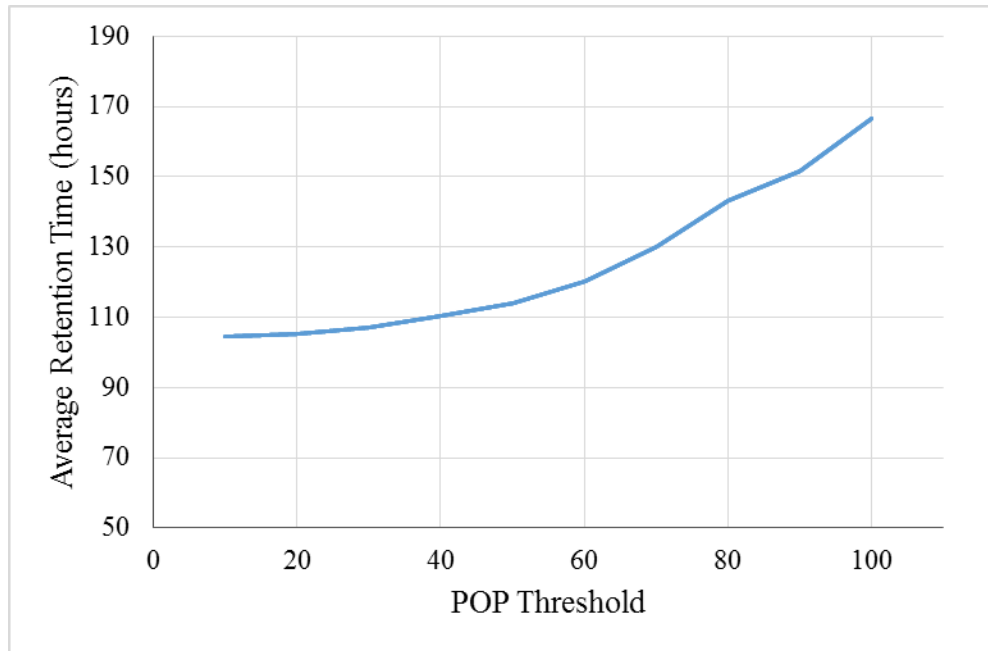


Figure 2.17: Retention Times for Changes in POP Threshold of RTC Retention System

When selecting a POP threshold to use for a facility, it is important to understand the context of the project and the water quality needs. Figure 2.17 clearly indicates that retention time can be substantially improved by choosing a more conservative POP threshold as less actionable events will occur, but this happens at the expense of in-storm performance (Figures 2.15 and 2.16). To better understand how these different factors work together, wet weather outflow (a metric trying to be minimized) and retention time (a metric trying to be maximized) were plotted against each other for changes in the POP threshold and are shown in Figure 2.18.



Figure 2.18: Comparison of Wet Weather Outflow and Retention Time for POP Sensitivity

Analysis

If the goals are minimizing wet weather outflow and maximizing retention time, Figure 2.18 indicates that a 70% threshold for actionable events stands as a good balance of the two. This point occurs as benefits in retention time are starting to increase more rapidly while the wet weather outflow hours stand at a local minimum. Again it is important to understand the specific needs of a project when choosing this value, some site contexts may place greater emphasis on one performance metric than another, but as a whole 70% is a reasonable value to select when designing for a control structure that utilizes forecast information.

2.5 Conclusion

2.5.1 Summary of Findings

To investigate the affect that forecast inaccuracy has on real-time controlled stormwater infrastructure a modeling approach was taken that compared systems with real and perfect forecasts for a variety of configurations. The results of the study indicated that inaccuracies in the forecast clearly lessen the efficacy of forecast based RTC systems. This determination was based on performance indicators such as number of outflows experienced from the systems during storm periods, as well as average outflows seen during wet weather. In both systems designed as basic detention and retention systems, a performance drop was noted when comparing the ideal case (synthetic perfect forecast) to the real case.

When looking at RTC systems that seek to maximize retention time while still avoiding wet weather outflows, the major way that forecast uncertainty affected the performance of the system was cases where storms were underestimated or not predicted at all with significant enough probability and an overflow occurred that could have been avoided. In total an 11.1% increase in overflow events was seen when switching from the perfect forecast case to the real forecast case, generally because of underestimated storm events where insufficient storage was created.

With the simple detention systems which did not try to retain captured stormwater after storm events, the overall ability of the system to avoid wet weather outflows was significantly better due to the system draining down after events. A slight performance drop was still seen though with a 5.2% increase in wet weather outflow and a 10% increase in wet weather outflow hours.

Overall, the results from both the retention and detention systems indicate that while a slight performance drop is expected from the ideal case, forecast based RTC still stands as an effective way to increase the capture of a stormwater system. In many cases the effects of forecast

uncertainty were dampened over time by extra space freed up in the systems during overpredicted events, resulting in a sufficient storage available for capture.

In addition to analyzing forecast uncertainty, the threshold for defining an actionable event was analyzed by performing a sensitivity analysis on the POP threshold. Results of the study indicate that a POP threshold of 70% stands as a good value when trying to balance competing needs of maximizing retention time and minimizing wet weather outflow. Wet weather outflow and retention time both saw increases as the POP threshold was increased, meaning that depending on the context of a site this value could be tailored to better suit the specific needs.

2.5.2 Design Recommendations

To combat the effect of forecast uncertainty in forecast based RTC, logic can be created with added conservatism to address these concerns. In cases where stormwater runoff is stored for long periods of time (such as a retention pond, rainwater harvesting, or Villanova's green roof system), the target permanent pool volume can be adjusted to leave extra storage for unexpected volume. The results of the modeling simulation for the retention system showed that on average for a typical storm, an extra 5.34% of the storage volume would be needed to prevent overflow during storm events that wouldn't be seen with a perfect forecast. When tackling the level of conservatism to be used when creating the control logic for a site, the context of the site and major goals also need to be considered. Because sometimes stormwater management goals can be competing (i.e. maximizing retention time while avoiding outflow during storm events), prioritizing objectives is crucial for developing logic appropriate for the context of the project.

For systems that currently utilize weather forecasts to approximate the time from the last rainfall, it is recommended that on-site rain gage information be used instead if possible. While like systems that utilize forecast information prior to storm events the performance is reduced only slightly when compared to (about 10% increase in wet weather outflows), this case represents a relatively easy and realistic place where RTC systems could be improved by integrating on site rainfall information from rain gages.

2.5.3 Future Work

Moving forward it is important to further monitor and evaluate the performance of SCMs that utilize forecast based control in order to assess the efficacy of forecasts usage in control decisions. While for this study two hypothetical and simple systems were used to evaluate the use of forecasts, it is necessary to also validate that these systems are working by implementing and monitoring green infrastructure that utilizes rainfall forecasts for decisions. Additionally, further sensitivity analyses could be completed on the forecast information to see if there are better ways to tailor a decision to the goals of a site. For example, the relationship between a predicted storm volume and probability of occurrence could be analyzed to see if the two pieces of forecast information could be used together to make more intelligent decisions.

CHAPTER 3: INTEGRATION OF PUBLICALLY AVAILABLE CLIMATE DATA

3.1 Introduction

While the stormwater control measure (SCM) research sites studied at the Villanova University campus are equipped with many real-time sensors and monitoring tools, the majority of SCMs lack the same level of data collection. Many decisions that RTC stormwater systems need to make are highly influenced by local climate trends and seasonal conditions. For example, systems that harvest and utilize rainwater for irrigation (such as the CEER Green Roof or Treatment Train at Villanova University's campus) want to be more conservative with their water usage during periods of drought and less conservative when storms are expected more regularly. While on-site weather stations and monitoring can be used to make these decisions, there also exist vast amounts of publicly available climate data that represent regional conditions and can be used to make decisions. This includes drought indices and remote sensors that have data sets publicly available for use by the general public.

For the purposes of this investigation, four separate sources of publicly available climate data were analyzed to determine their aptness for making control decisions. The data sources' aptitude was based on their correlation to on-site weather and hydrologic data collected as part of the Villanova Urban Stormwater Partnership's ongoing research on the Villanova University campus. Because the ongoing research involves a high amount of instrumentation and data collection, substantial data exists for comparison to the climate indices. The data sets analyzed were the Monthly Palmer Drought Severity Index, the Modified Weekly Palmer Drought Severity Index, the Standardized Precipitation Evapotranspiration Index, and the Soil Moisture Active Passive satellite.

3.2 Literature Review

3.2.1 PDSI

The Palmer Drought Severity Index (PDSI) was first developed in 1965 and has since become one of the most widely used drought indices in the United States (Heim 2002). The PDSI was created as a method to calculate a representative value for the intensity of droughts or wet periods based on the prevailing meteorological conditions from a specific site. The index is based on a simple hydrologic budget using historic meteorological data as well as the current month's data (Palmer 1965). The methodology for calculating the PDSI, as outlined in Palmer 1965, includes approximations of the major components of a hydrologic budget (rainfall, potential evapotranspiration, runoff, recharge, and loss) to estimate site hydrologic conditions. Rainfall, clearly one of the most critical components for determining drought, is used along with potential evapotranspiration, losses to the soil layer, and runoff to determine the moisture deficit. The PDSI relates the moisture deficit to historical, normal conditions to determine the severity of the drought with values ranging from -10 to 10. Negative calculated PDSI values indicate that conditions are drier than typical, showing drought conditions, while positive values indicate wetter than typical conditions. The PDSI is typically calculated monthly, however the same methodology has been applied to a weekly time step to get a shorter scale look at drought conditions.

While using the PDSI to quantify drought onset and duration, one shortcoming of the index is its subjectivity to the calibration period with historic meteorological data that did not enable comparison at different locations (Karl 1983; Wells et al. 2004; Vincente-Serrano et al. 2010). To address this deficiency, Wells et al. (2004) modified the PDSI to replace several empirical

constants within the water budget calculation with site specific calculated values. This method, called the self-calibrating Palmer Drought Severity Index, allows for better comparison of the calculated values spatially when looking at droughts with reference to historic climate conditions.

3.2.2 SPEI

The Standardized Precipitation Evapotranspiration Index (SPEI) was created to quantify drought using a multiscalar approach based on precipitation and temperature data. Similar to the PDSI, the SPEI is based on a water balance and uses historic data to quantify the level of drought severity. The SPEI bases its calculation on the difference between precipitation and potential evapotranspiration with calculations occurring on a range from a 1 month to 48 month basis (Vincente-Serrano *et al.* 2010). This variable temporal scale is one of the major aspects that differentiates the SPEI from the PDSI, a crucial component for addressing different hydrologic conditions when thinking about drought. Vincente-Serrano *et al.* (2010) notes that having this ability to change the time scale is key depending on what system or component is being analyzed; for analysis of soil water content or the headwaters of a river, a short term drought would be more prevalent, while more developed river systems, reservoirs, and groundwater storage would be more affected by medium to long-term droughts.

Precipitation and temperature (representing potential evapotranspiration) are the main water balance variables used for determining the SPEI (Vincente-Serrano *et al.* 2010). This methodology is a logical approach to quantifying drought periods with many previous studies indicating that precipitation is the most crucial variable for determining drought periods (Chang and Cleopa 1991; Heim 2002), however temperature still must be included because in some cases evapotranspiration (dependent on temperature) can represent a substantial portion of the water budget (Abramopoulos

et al. 1998). Therefore including both elements of the hydrologic budget when computing a singular index value to represent drought makes inherent sense.

3.2.3 SMAP Satellite

The Soil Moisture Active Passive satellite (SMAP) is a mission from NASA with the goal of measuring moisture content in the first two inches (5 cm) of the soil layer across the Earth's surface (SMAP Mission 2017). The satellite itself can measure moisture across the entire Earth's surface in 2-3 days, reporting out high resolution maps of moisture content for the entire globe several times per week. The satellite itself relies on a combination of radar (active) and radiometer (passive) measurements that measure radiant flux from the Earth's surface to calculate changes in soil moisture in the top level of the planet's surface (Entekhabi *et al.* 2014). The resulting data collected is processed and turned into several data products ranging from soil moisture readings on a variety of different spatial scales to indicators of freeze/ thaw state across the Earth's surface. For the purposes of this study, the Level 3 data products were used from the SMAP processed data which includes soil moisture conditions on available scales of 3, 9, and 36 kilometer grids based on the radar, radiometer and radar, and just radiometer readings respectively (SMAP Data Products 2017).

The SMAP mission operates with the objective of providing unprecedented access to global soil moisture and freeze/ thaw data on a high level of scale, resolution, and accuracy (SMAP Objectives 2017). The goals for the project include a better understanding of the processes that link water movements and the carbon cycle, a higher level understanding of global water flux, and the ability to better forecast climate and weather conditions such as droughts and flooding. With stormwater itself being an inherent function of climate conditions and changes in weather patterns, the SMAP

mission's goals provide promise for an application to the development of smarter stormwater systems that utilize climatologic data to operate more effectively.

3.3 Methodology

To assess the viability of using the monthly and weekly Palmer Drought Severity Indices, the Standardized Precipitation Evapotranspiration Index, and the Soil Moisture Active Passive satellite for control decisions at Villanova University, historic records of each of the climate indices were compared to local weather conditions at Villanova University and the greater Philadelphia region to discern any correlations between the two data sets. The goal of using the publically available climate data was to have a source of data that gives an approximate representation of local climate conditions, so for a data source to be viable it should reflect the weather conditions of the region. Depending on the time scale and the spatial range of the index being used, two historic weather records were used for the comparison: weather records recorded at Villanova University's Bioinfiltration Traffic Island (BTI) and the long-term weather records from Philadelphia International Airport.

At Villanova University's BTI, an actively researched bioinfiltration rain garden for the past 16 years, a wide range of hydrologic conditions are measured including precipitation, air and soil temperature, and soil moisture. Measurements are recorded every 5 minutes providing a high resolution record of weather conditions at the site. Clearly, one of the most important weather parameters when looking at the control of stormwater infrastructure is rainfall so availability of precipitation data was required to assess each of the climate indices. The rainfall record for the BTI for three recent years (May 2012 to December 2015) is displayed in Figure 3.1 demonstrating a record aggregated on a daily basis. Rainfall was summed on a daily basis to reflect the way the

SPEI and PDSI are calculated, summations completed based on time rather than a per event basis. While this can result in events split over a multiday period being shown as smaller, it better reflects the data set being compared.

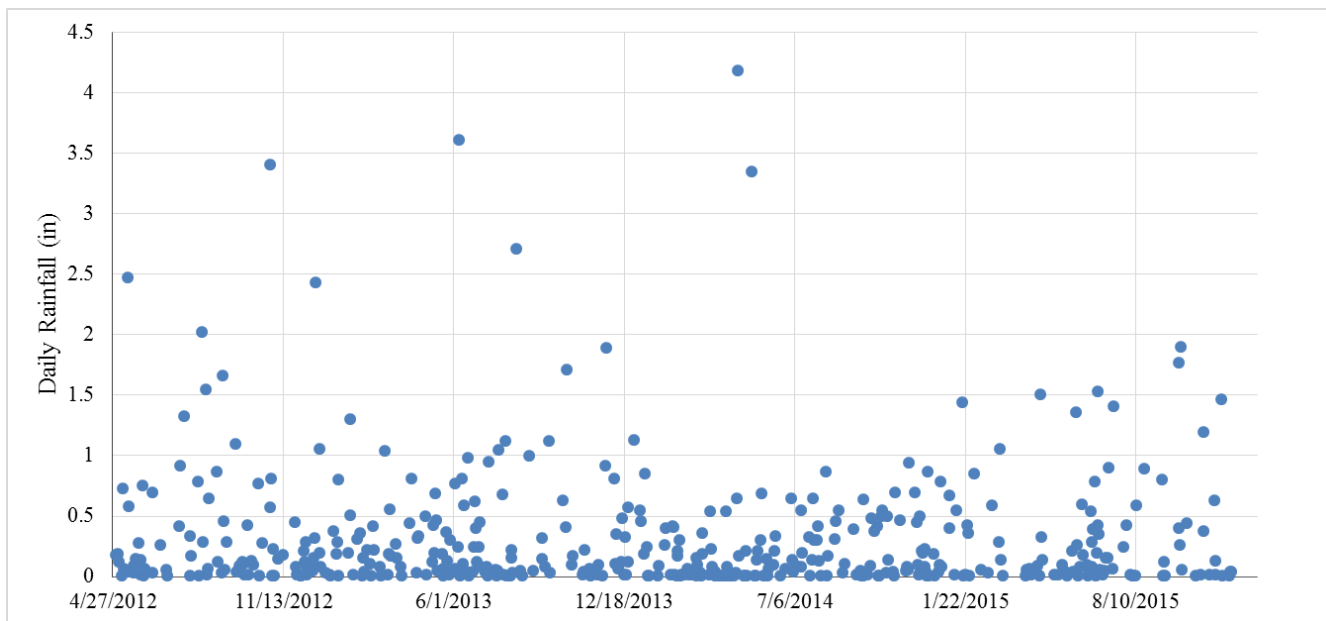


Figure 3.1: Historic Record of Rainfall at Villanova BTI (May 2012 to December 2015)

The historic record for the BTI (Figure 3.1) includes a variety of storm sizes, ranging from days that had over 4 inches (10 cm) of rainfall to many much smaller storms well below 1 inch (2.5 cm; a more typical storm for this region). The goal with utilizing publically available climate data is to capture these fluctuations between wet and dry periods without having extensive on-site instrumentation such as at Villanova's BTI.

While the BTI provides a high resolution and complete weather record for recent years at Villanova, some of the data sources analyzed (specifically the SPEI) have extensive records that far exceed the time period recorded by the BTI. To utilize this longer time span, the index was also compared to the weather records at the Philadelphia International Airport, one of the oldest and

most commonly used weather records for the greater Philadelphia area. The precipitation record for Philadelphia on a monthly basis from 1950 to 2016 is shown in Figure 3.2.

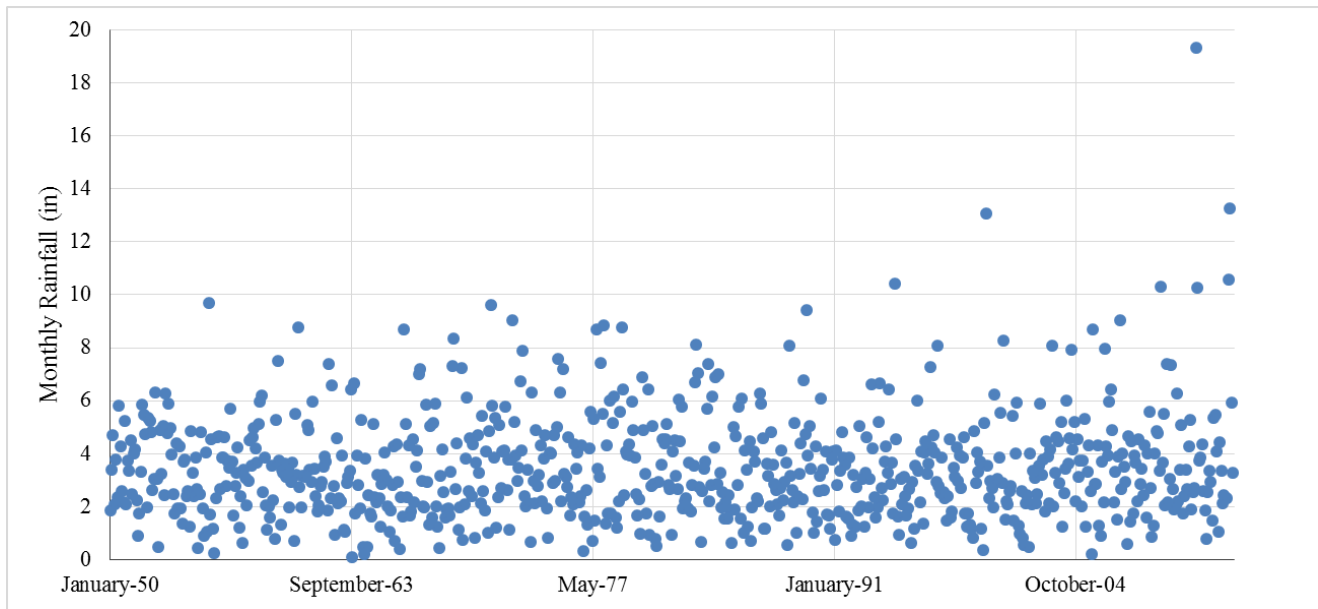


Figure 3.2: Historic Rainfall at Philadelphia International Airport (1950 to 2016)

Using the longer rainfall record at Philadelphia International Airport, a larger diversity in rainfall conditions can be seen. Monthly rainfalls at the site range from highs of almost 20 inches (51 cm) to lows below an inch (2.5 cm). Because more extensive history is available at the Philadelphia International Airport, more long-term climate changes and trends can be seen in the data analysis.

In addition to the rainfall records for both locations, air temperatures were also available for comparison to determine evapotranspiration potential. Daily average temperatures from Villanova's BTI were calculated and daily high and low temperatures were provided for the Philadelphia International Airport weather station.

3.4 Results

3.4.1 Monthly PDSI

The Palmer Drought Severity Index (PDSI) is published on a monthly basis and provides drought conditions on a local basis determined by comparing current conditions to historically average conditions for the site. The drought index was downloaded for Villanova, Pennsylvania and compared to local weather data collected (Villanova's BTI aggregated into months) to discern any correlations between the index and local conditions (Figure 3.3).

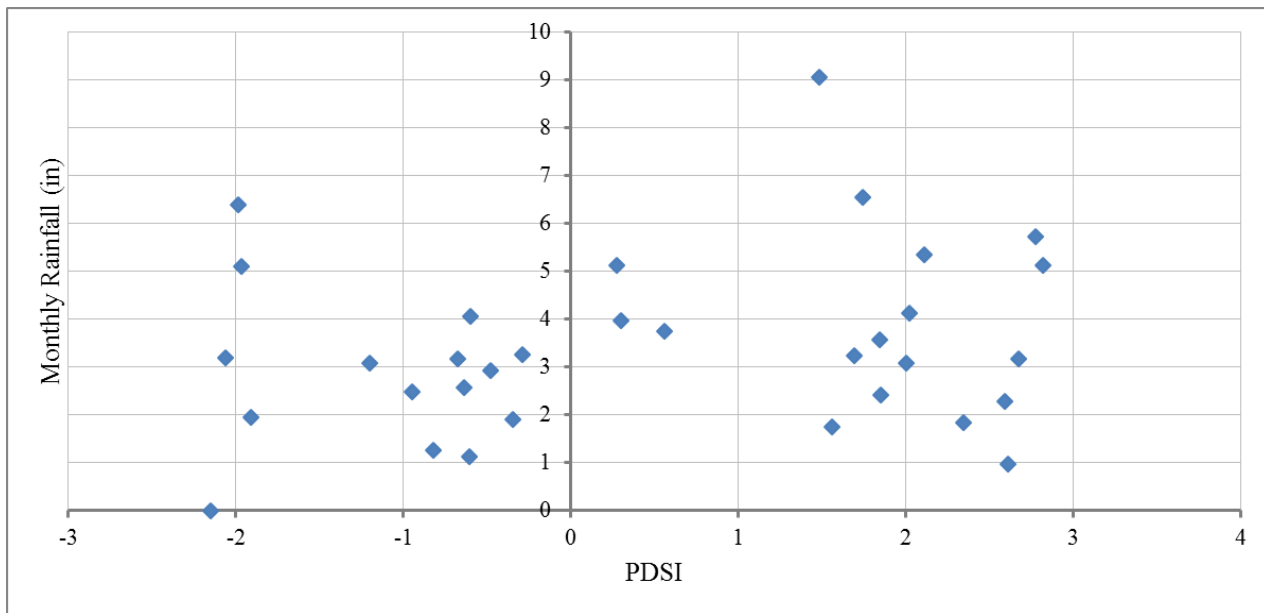


Figure 3.3: Monthly Comparison of Rainfall and PDSI at Villanova University

When comparing the monthly rainfall to the PDSI calculated for Villanova, Pennsylvania, there is no clear trend between the two data sets. While rainfall values for PDSI indices above zero are on average higher (3.95 inches) than those below zero (2.83 inches), there is too much scatter to make a statistical relationship between the two data sets. This would indicate that using the PDSI on a monthly basis is not an appropriate measure for the expected rainfall amount to occur during the

month. In addition to comparing the rainfall for Villanova, the average monthly temperatures were compared to their corresponding monthly PDSI values and the results displayed in Figure 3.4.

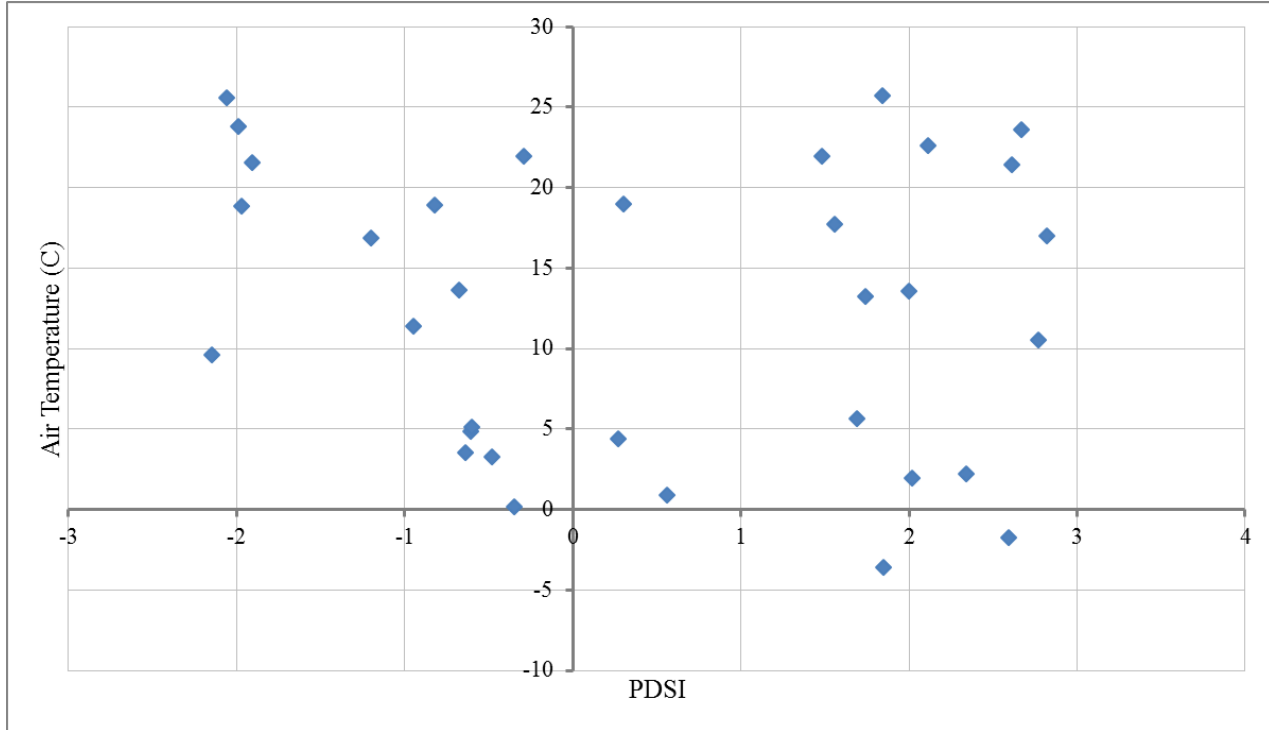


Figure 3.4: Monthly Comparison of Average Temperature and PDSI at Villanova University

Similar to the rainfall comparison, no clear trend can be seen when looking at the monthly temperature vs. PDSI data. The scatter seen in the comparison indicates that the monthly PDSI does not provide sufficient resolution to accurately capture the fluctuations in weather conditions at Villanova, making it an insufficient candidate for use in control decisions for RTC stormwater infrastructure. It was hypothesized that the PDSI was insufficient for use as a data source due to its high temporal resolution, the PDSI being calculated on just a monthly basis. To reduce the effects of the high time step, the modified weekly PDSI was next analyzed to determine if the PDSI could still be a viable option.

3.4.2 Modified Weekly PDSI

The Modified Weekly PDSI was investigated to see if the smaller time scale could provide enough resolution to provide an apt drought index for representing regional climate conditions at Villanova. Once again the drought index was compared to rainfall and temperature data measured at the Bioinfiltration Traffic Island on Villanova's West Campus to discern any trends between the two values. The rainfall comparison can be seen in Figure 3.5 while Figure 3.6 represents the comparison to weekly average temperatures.

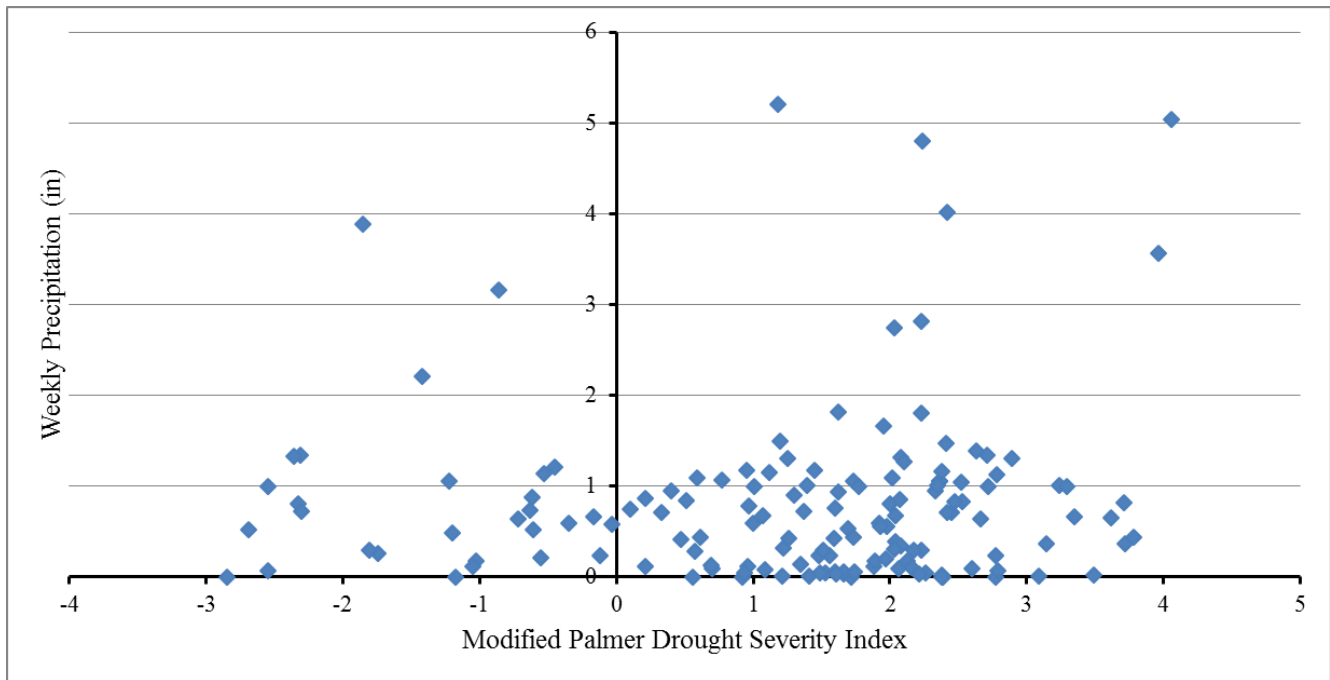


Figure 3.5: Weekly PDSI and Rainfall Comparison

While there is still substantial scatter in the comparison to weekly rainfall, there is a general upward trend of a PDSI rise corresponds with an increase in the weekly rainfall volume. While there are definitely outliers in periods that should be droughts (a PDSI value less than zero), the majority of large weekly rainfall volume occur when a PDSI greater than zero is seen. The amount of large weekly rainfalls that occur in periods of drought cause concern for the weekly PDSI to be

used as a drought index, the metric not representing overall precipitation trends as much as expected for the local weather conditions. Like with the monthly PDSI, the comparison indicates that the PDSI may not be an adequate representation of precipitation trends at Villanova, making it less valuable as a candidate for the basis of control decisions. While the precipitation relationship was not overly strong, there was a clearer trend seen in the comparison between the weekly PDSI and the average temperature at Villanova (Figure 3.6) - a decrease in temperature results in an increase in PDSI.

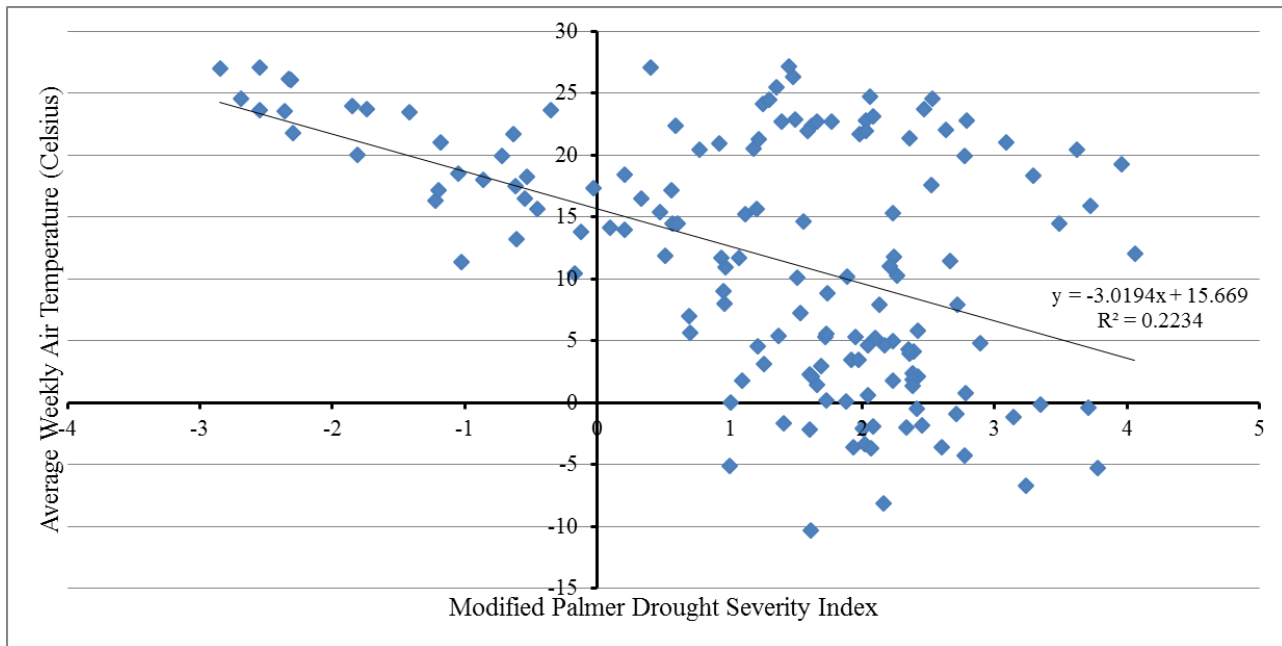


Figure 3.6: Weekly PDSI and Average Temperature Comparison

This relationship is very strong during drought periods when the PDSI is less than zero, however more substantial scatter occurs when the PDSI is greater than zero (indicating the conditions are no longer representative of a drought). When fitting a linear regression to the comparison, the slope shows a -3.02 degree Celsius change in average weekly temperature for every increase in PDSI with an R^2 value of 0.2234. This low correlation again is a function of the scatter associated with

non-drought periods, meaning that PDSI values above zero do not indicate much about the expected temperature for a region. If using the PDSI as an indicator of local climate conditions, values below zero do give meaningful information, indicating that relatively high temperatures can be expected. To examine this relationship further, the portions of data where PDSI values were less than zero were isolated and another regression was calculated. Figure 3.7 displays the average weekly temperature and PDSI comparison for PDSI values less than zero where dryer than typical conditions would be expected.

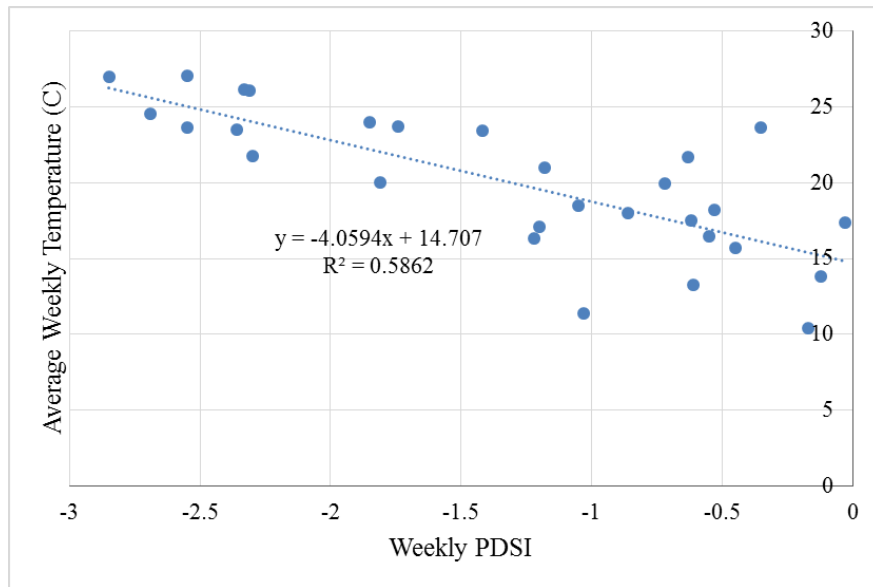


Figure 3.7: Average Weekly Temperature for PDSI Values Indicating Dryer than Typical Conditions

When the dry periods (as determined by weekly PDSI values) were isolated, the regression between average weekly temperature and the drought index becomes stronger with a linear fit and an R^2 value of 0.5862, substantially higher than when looking at all the data for wet and dry periods. Though with a slightly steeper slope than the regression with the entire data set, the comparison still indicates hotter temperatures on average when the PDSI reaches lower values and

extends towards drought conditions. This observation demonstrates that the weekly Modified PDSI stands as an appropriate way to determine if hotter, dryer conditions are expected at a site, especially when looking for indications of higher temperatures during periods denoted as dry. Additionally, 95% confidence limits were applied to the regression for drought condition PDSI values and is displayed in Figure 3.8.

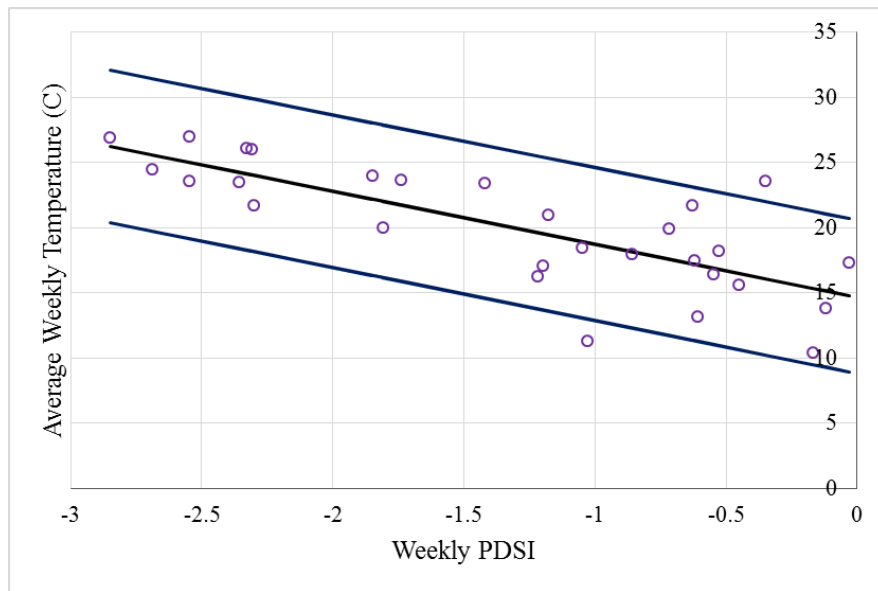


Figure 3.8: PDSI and Weekly Temperature Comparison for Dry Conditions with 95% Confidence Limits

The linear 95% confidence limits on the regression represent a +/- 5.87 degree Celsius range for expected average temperature based on the weekly calculated PDSI. The correlation appears stronger when a more severe drought is predicted (lower PDSI value), indicating that substantive meaning can be gained when very low PDSI values are calculated for a site. When applying this index to stormwater management, the PDSI could be used on a weekly basis to determine if a more conservative approach should be taken to storing water in cases of rainwater harvesting. That said,

the inverse case of this does not hold as strong with high PDSI values, indicating that this application is only appropriate in drought conditions.

3.4.3 SPEI

The Standardized Precipitation-Evapotranspiration Index, or SPEI, was analyzed and compared to local weather conditions in the Philadelphia region to discern trends and see if the index is representative of local climate trends. Because a vast amount of index history was available (ranging on a monthly basis from 1950 to present day), the index was compared to Philadelphia weather data collected at the Philadelphia International Airport where a long historical record exists. Initially the index was compared to the precipitation recorded at the Philadelphia International Airport using one month as the time step for calculating the SPEI (Figure 3.9). For the purposes of this study, SPEI values were used that were calculated on the first of every month starting in 1950 representing the hydrologic conditions of the previous month. While this method was used for a baseline comparison, the calculation theoretically can be updated on any timescale to provide an index of the previous month's climate conditions.

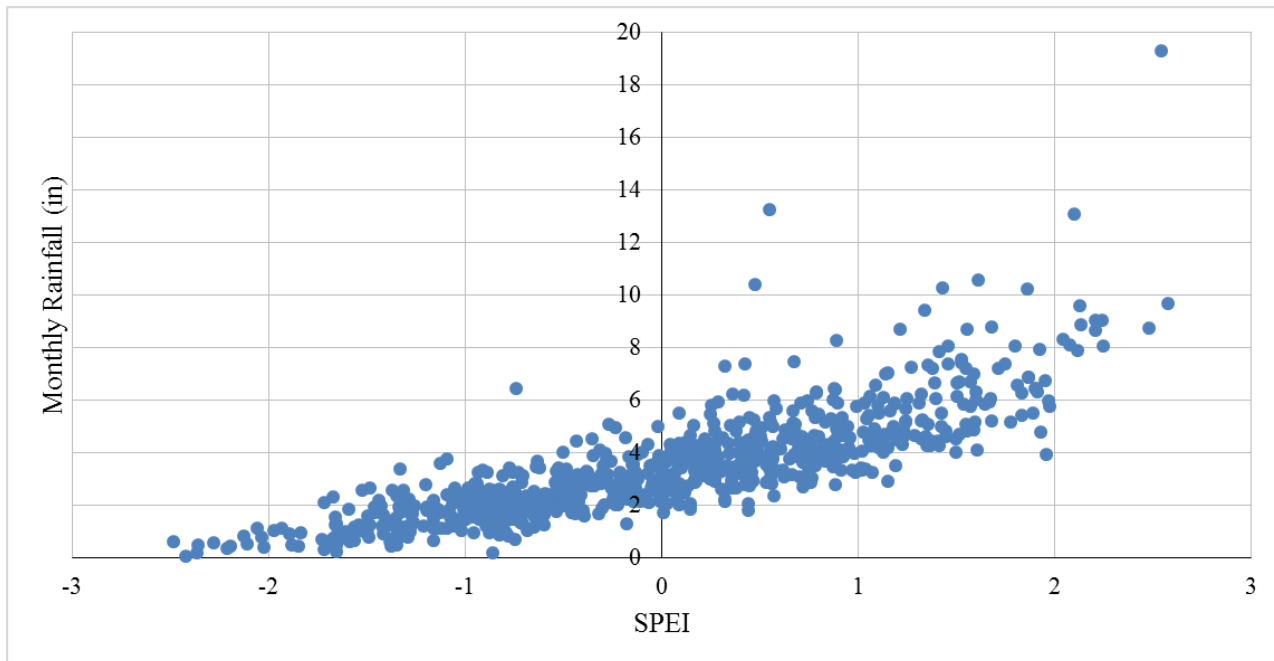


Figure 3.9: SPEI and Monthly Rainfall Comparison for Philadelphia, PA

While scatter still exists with the results, a clear upward trend can be seen with an increase in SPEI resulting in a corresponding increase in monthly rainfall. This trend, while clearly expected when looking at a drought precipitation-evapotranspiration index, is useful in that the correlation between index and precipitation is especially strong in the two extremes of the plot. This indicates that if the SPEI denotes a strong drought (for example, the region below -2), a very limited amount of monthly rainfall can be expected whereas periods of wet weather (for example, above 2 in Figure 3.9) are consistently high in monthly volume of rainfall. These general trends can help smart systems be more informed about the general climate trends in a region when deciding how conservative to be for purposes such as storing rainwater and preparing for storm events.

Using the comparison of monthly rainfall and the SPEI index for Philadelphia, a regression equation was developed for the dataset to predict monthly rainfall based on the current SPEI. The

best fit for the relationship was found to be an exponential growth function (Equation 3.1) that yielded an R^2 value of 0.71.

Equation 3.1: Philadelphia Regression for Monthly Rainfall and SPEI

$$P = 2.8959 * e^{(0.5445 * SPEI)}$$

The regression determined is fairly strong (as shown by the R^2 value of 0.71) and was used to determine error bounds for the relationship between monthly rainfall and the monthly SPEI. Residuals from the regression curve (Equation 3.1) were determined and the standard deviation of the regressions were used with a normal distribution to determine 95% confidence limits on the relationship between the monthly rainfall and the SPEI. Figure 3.10 shows the same comparison of data sets for Philadelphia as in Figure 3.9 with the regression curve and 95% confidence limits plotted.

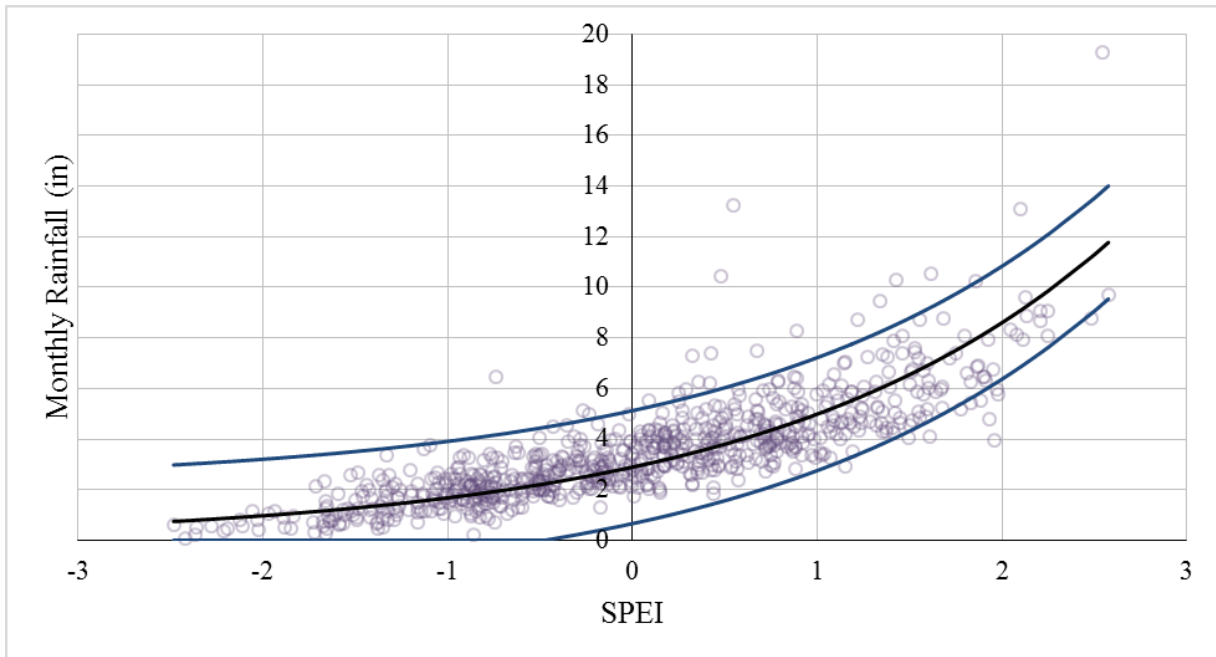


Figure 3.10: Confidence Limits on Monthly Rainfall Predicated on SPEI

Even with confidence limits the relationship shows a strong upward trend, again indicating that the SPEI represents a good method for determining the overall precipitation trends that can be expected in a region. For all the previous analysis completed, the SPEI was predicated on just a month of climate data. The SPEI allows a variable time step from which the index is calculated, ranging from a minimum value of 1 month to a maximum of 48 months. While the 1 month calculation was originally used because it reflects the most current climate conditions that have occurred, the longer duration calculations were also examined to see how they compared. Figure 3.11 shows the results when comparing the 1 month calculation (the minimum time step), the 48 month calculation (the maximum time step), and the 24 hour calculation (an intermediate time step).

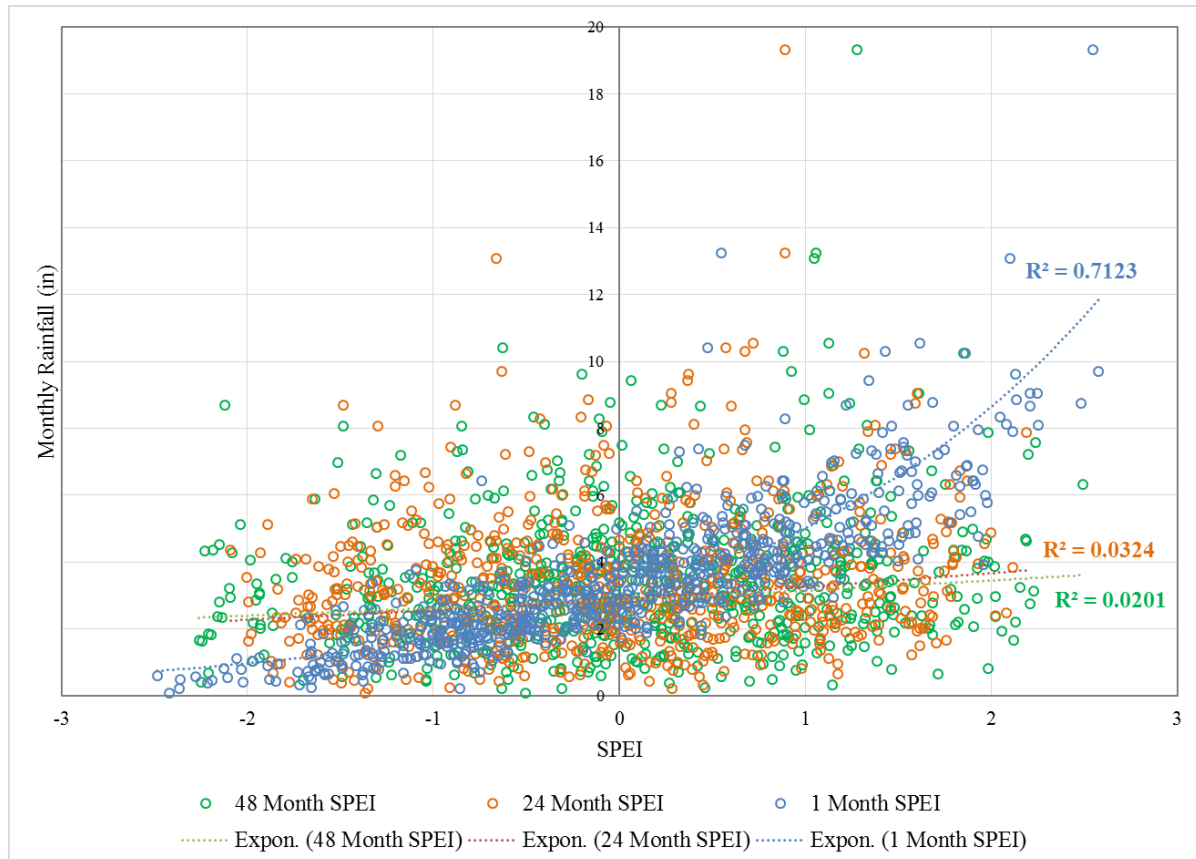


Figure 3.11: Comparison of Monthly Rainfall to SPEIs of Varying Computation Time Steps

The 1 month SPEI to monthly rainfall had the best relationship ($R^2 = 0.7123$). The SPEI data predicated on the previous 24 and 48 months of climate data did not have a good comparison against rainfall and the SPEI is mostly scatter. For the SPEI calculated with 24 and 48 months of data, the R^2 values for the best fit lines result in 0.0324 and 0.0201, respectively. These low values indicate no significance in the data and no discernable relationship between these higher time step SPEIs and the monthly rainfall for Philadelphia. Looking at the SPEI comparisons to rainfall for different temporal bases it is clear that the shortest time step (the one month calculation) is best for relating the drought index to the precipitation, which can be used in stormwater GI control decisions.

In addition to the rainfall comparison, the SPEI was compared to the daily temperatures measured in Philadelphia to quantify any correlation. While rainfall is clearly the most important factor that affects the performance of a stormwater control measure, temperature is critically important too due to its effect on evapotranspiration, as well as effects on infiltration rates in SCMs (Emerson and Traver 2008). Daily high temperatures and daily low temperatures were averaged monthly from Philadelphia and compared to the SPEI calculated on a one month time step. The resulting comparisons can be seen in Figures 3.12 and 3.13.

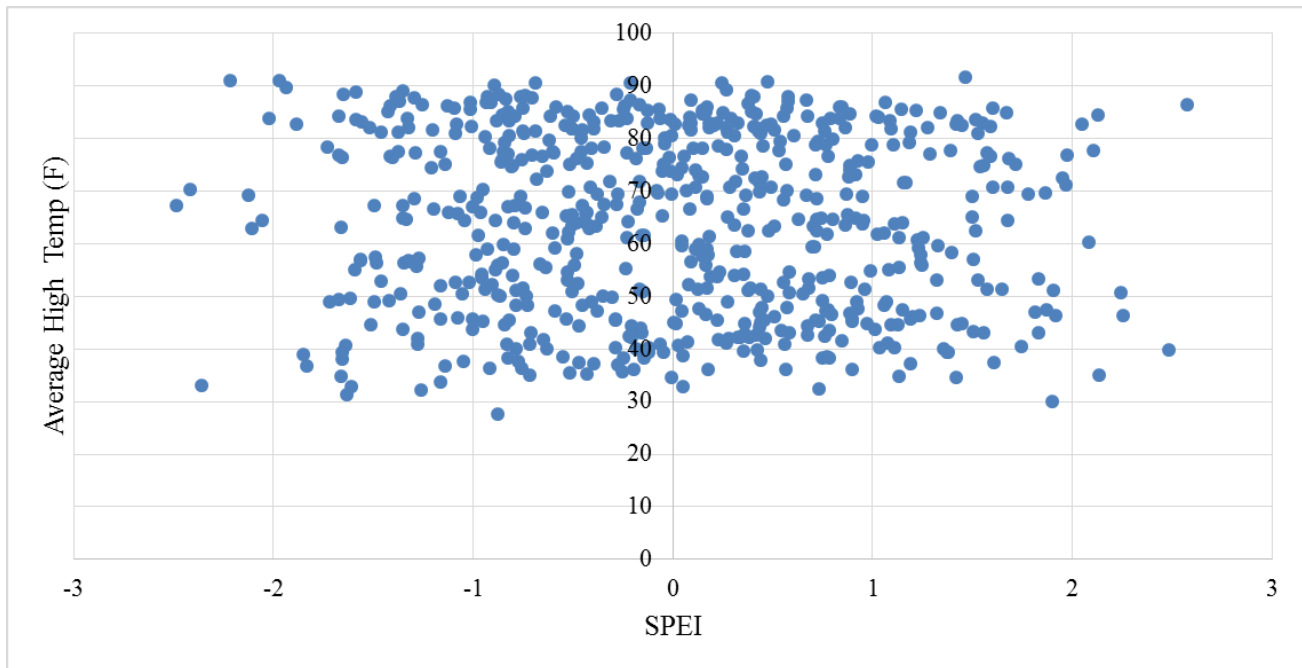


Figure 3.12: Monthly Average of Daily High Temperatures and SPEI Comparison

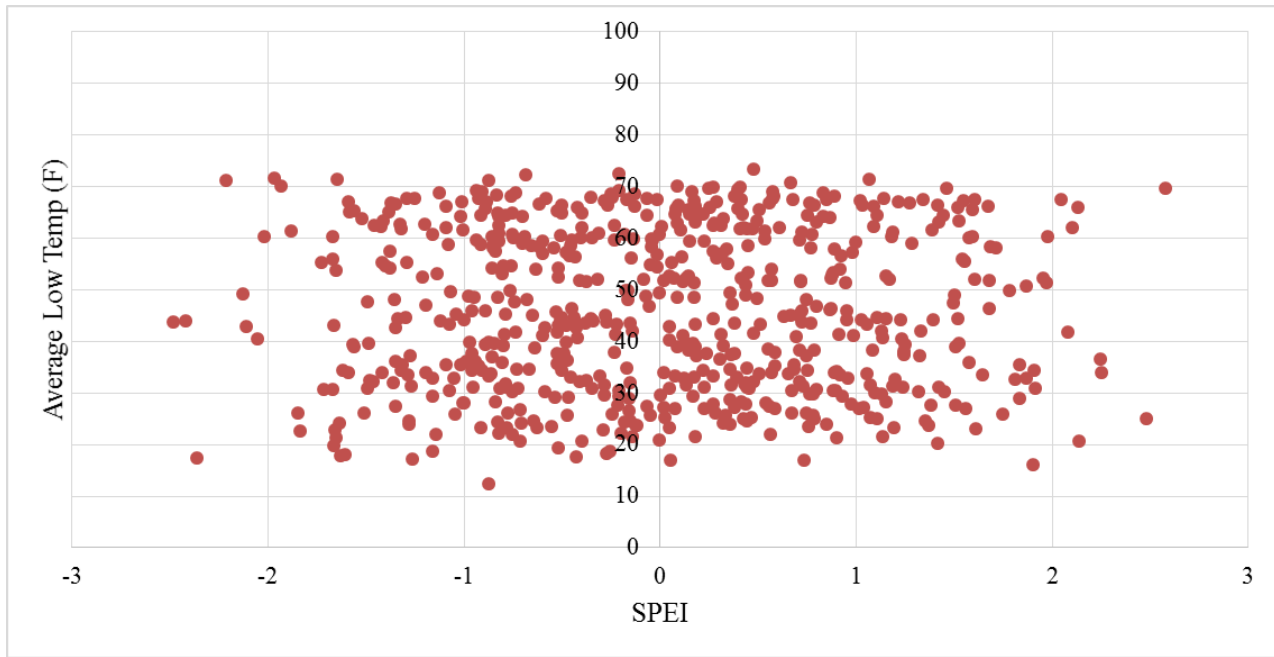


Figure 3.13: Monthly Average of Daily Low Temperature and SPEI Comparison

It is clear from both comparisons in Figures 3.12 and 3.13 that the monthly average temperatures do not correlate well to the SPEI when calculated monthly. This would indicate that the SPEI, though a drought index that takes into account both precipitation and evapotranspiration potential, is much more dependent and related to the rainfall experienced by a region. While ideally the index would provide a good measure of both climatological conditions, having a measure of rainfall potential for a month is still beneficial for making general decisions about the management of smart stormwater infrastructure.

Though the SPEI provides a promising option for making control decisions based on general weather trends, it does have the downside of being calculated and updated on a monthly basis. While this temporal resolution is fine enough to capture seasonal changes throughout the year, it lacks the resolution of some other drought indices analyzed (such as the Modified Palmer Drought Severity Index). However, the relationship demonstrated between precipitation and the index is stronger than the finer scale of the Modified PDSI, showing the balance that must be established between time scale and precision when looking at using these drought indices for making control decisions in stormwater management.

3.4.4 SMAP Satellite

In addition to the drought indices analyzed for use in determining climate trends, the SMAP satellite remote sensor was also looked at as a possible source of climate information. Unlike the other sources examined, the SMAP satellite serves to report just one hydrologic component (soil moisture) as a value rather than trying to create an index value to represent the overall climate conditions. The temporal basis of the SMAP satellite is dependent on the time it takes for the satellite to complete an orbit and pass over a certain location, with one orbit of the Earth taking

98.5 minutes. The satellite is able to get complete coverage of the Earth for soil moisture readings every 2 to 3 days, taking 2 days near the Earth's poles and 3 days for latitudes closer to the equator (NASA JPL 2017).

When downloading the data from the SMAP satellite, processed data is available aggregated on a daily basis which provides all the soil moisture readings taken in that day on a volumetric basis (cm^3/cm^3). Data is provided based on latitude and longitude for every location across the Earth, including a substantial amount of missing values due to the satellites ability to cover the Earth only every 2 to 3 days. Using a Matlab script, the data was processed to pull soil moisture values from the coordinates associated with Villanova University's campus to provide a comparison to the soil moisture measurements taken at stormwater control measures located on campus. Results from SMAP were compared directly to soil moisture data gathered from sensors located in the Bioinfiltration Traffic Infiltration Island on Villanova's West Campus. The comparison for soil moisture measured at 10 and 35 cm can be seen in Figure 3.14.

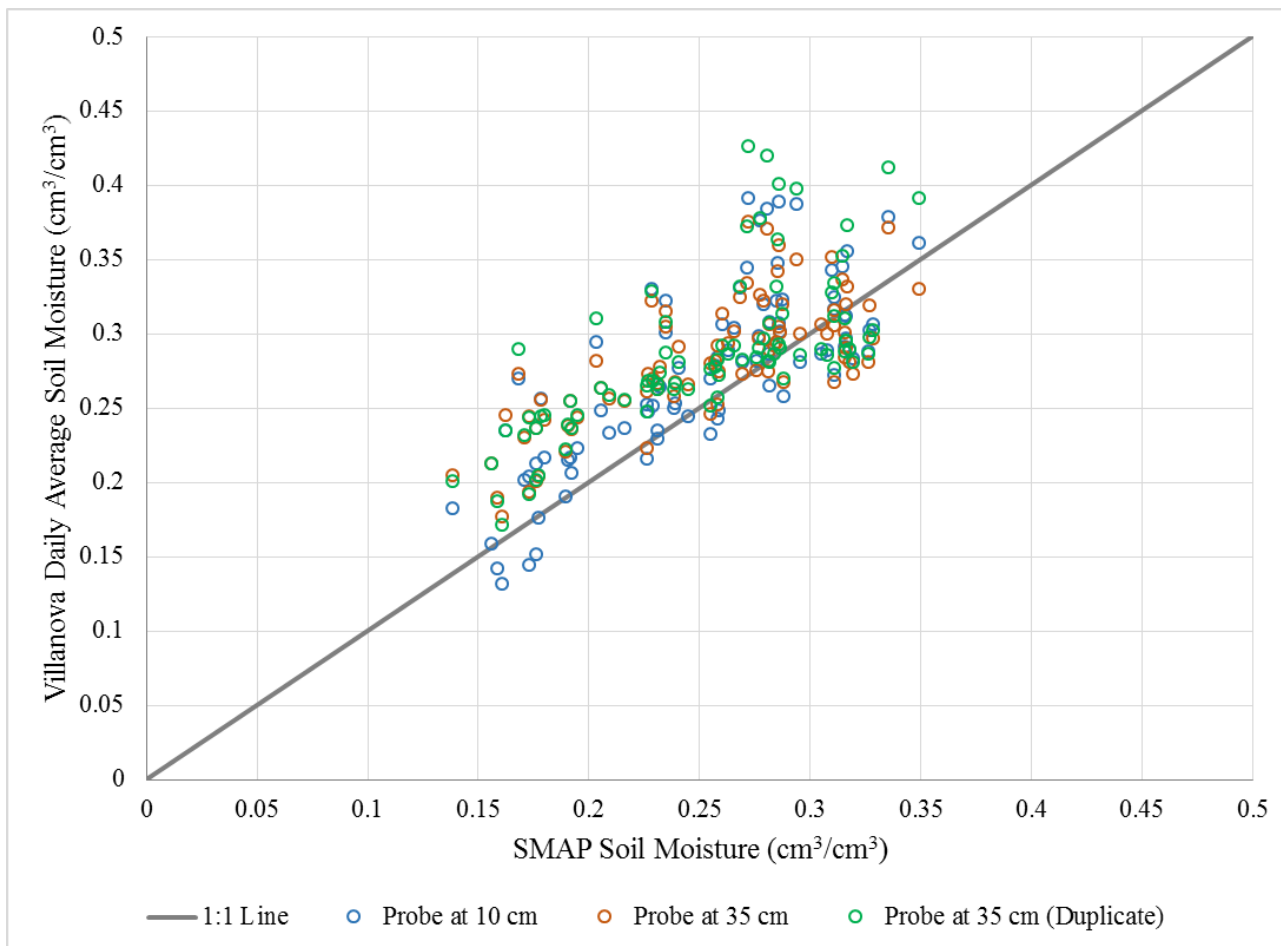


Figure 3.14: Comparison of SMAP Predicted Soil Moisture and On-Site Measured Soil Moisture

When looking at a direct comparison of the soil moisture measured on site at Villanova and from the SMAP satellite, there is a clear correlation between the two with data falling roughly on or above the 1:1 line. While there is some scatter, the trend still stays upward and fairly linear. To further characterize the correlation between the measured values on campus and those remotely sensed by the SMAP satellite, a paired t-test was completed on all three data sets (the 10 cm deep soil moisture probes and the two sets of 35 cm deep soil moisture probes) to see the statistical significance of the SMAP satellite for representing soil moisture conditions on Villanova University's campus.

In completing the t-test for all three samples, a statistically significant relationship between the SMAP and BTI soil moisture measurements was found for all three soil moisture meters. The t-statistics for the null hypothesis that the data sets were different was rejected for the 10 cm, 35 cm, and 35 cm duplicate samples with t-statistics of 5.61, 8.11, and 7.47, respectively. For all three places, the p value was well below 0.025, providing sufficient statistical significance for the SMAP measurements to be verified by the BTI soil moisture readings. While all had strong correlations, the highest was found to be for the soil moisture sensor at 35 cm in the BTI.

In addition to the paired t-test, 95% confidence limits were created to place a bound around the expected difference between the SMAP soil moisture readings and those at the BTI. All three soil moisture sensors had an average difference from SMAP less than zero, indicating the SMAP satellite typically reads lower than the on-site measured conditions within a SCM. The average differences along with the confidence limits are shown in Figure 3.15.

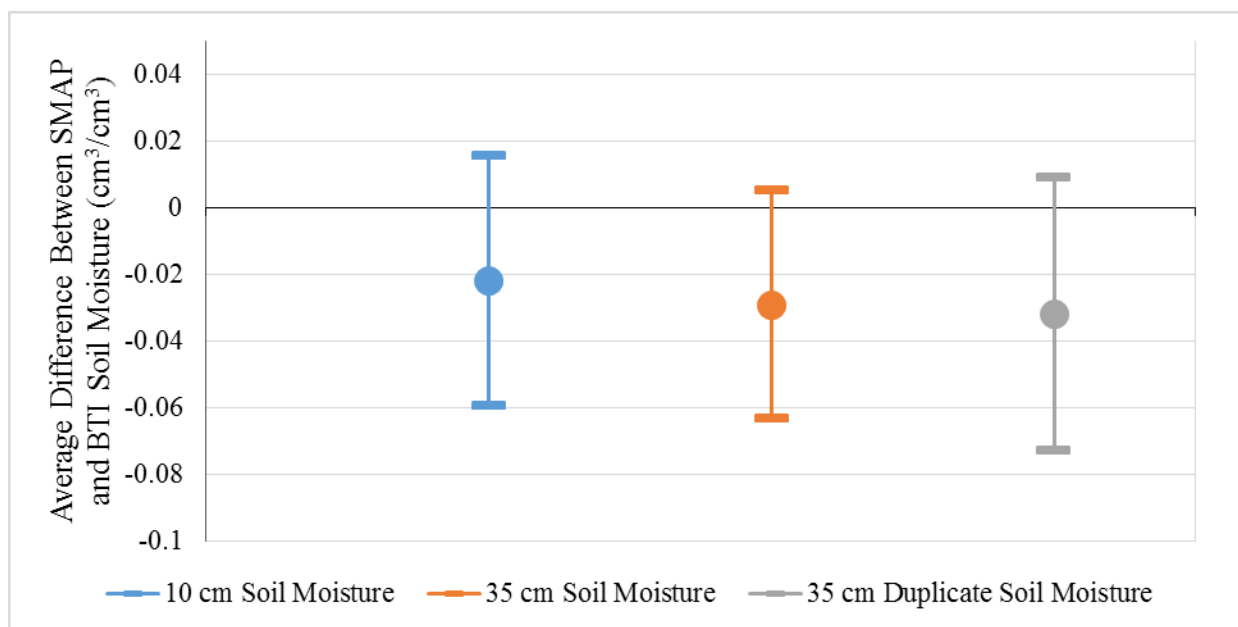


Figure 3.15: Average Difference in Soil Moisture Readings between SMAP and BTI

Measurements with 95% Confidence Limits

While the soil moisture probe at 10 cm had on average a difference from the SMAP satellite closest to zero, the error bound for the 35 cm probe was the smallest at just $0.069 \text{ cm}^3/\text{cm}^3$.

In addition to the comparison to site-specific soil moisture data, the soil moisture measured by the SMAP satellite was looked at with reference to rainfall measured at Villanova University to discern how reactions to storm events are seen in the SMAP output data. For the analysis, rainfall data was collected again from the Bioinfiltration Traffic Island and compared to the SMAP soil moisture readings. The time series results for a sample storm from the comparison can be seen in Figure 3.16.

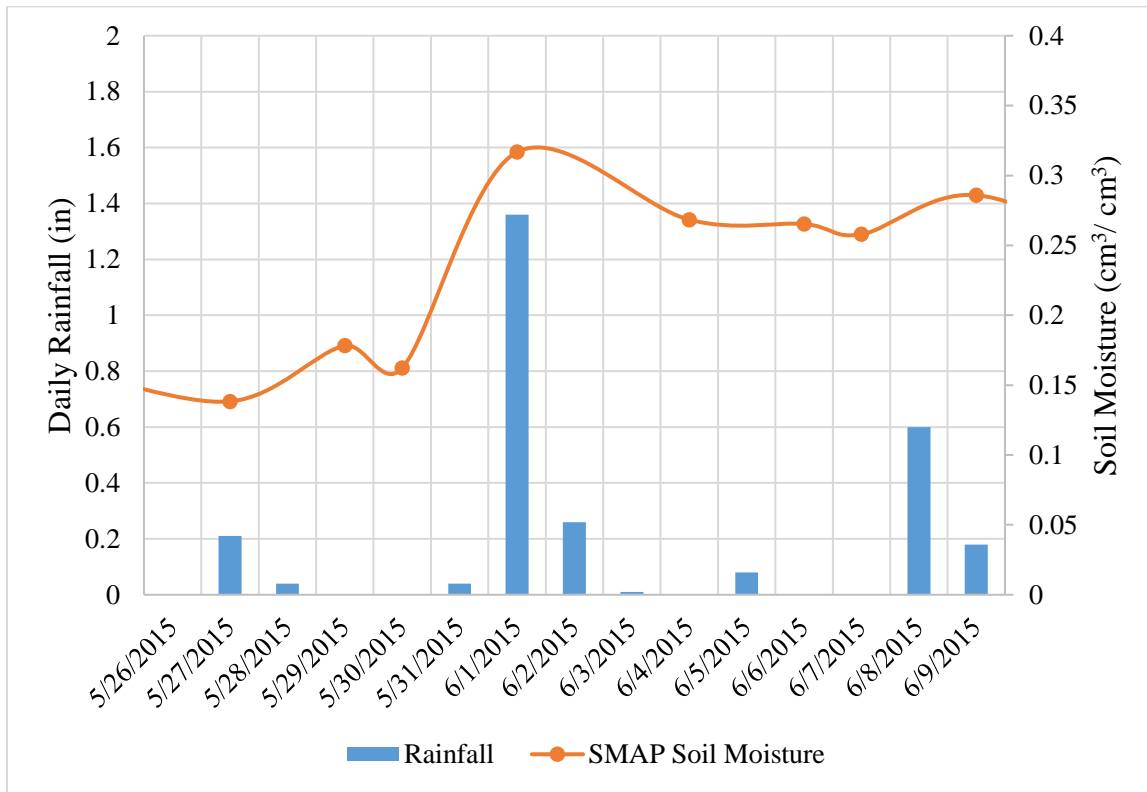


Figure 3.16: Sample Storm Response by SMAP Satellite

The time series results in Figure 3.16 indicate that the soil moisture readings from the SMAP satellite are adequately responding to storm events, with spikes in soil moisture seen after every

rain event. However, the response to events can be delayed based on the time period over which the storm occurs. Because the satellite takes 2-3 days to complete readings for the entire Earth, the increase in soil moisture from a storm sometimes is not read until several days after the event occurred (for example, the small storm that occurred on 5/27/2015). This could also result in a dampened response to a storm being read, the high soil moistures that one would expect directly following a storm having some time to be reduced via either infiltration or evapotranspiration. This phenomena could also explain the lack of response seen from the 6/5/2015 storm, a fairly small storm (about 0.1 inches) that resulted in negligible change in soil moisture when the SMAP satellite took a reading over Villanova the next day. As a whole, the general trend of the soil moisture readings makes sense when placed in the context of storm events at Villanova.

In addition to the comparison to storm events, results from the BTI 35 cm soil moisture meter, the probe determined via the paired t-test analysis to have the most significant correlation to the SMAP soil moisture, was plotted as a time series with direct comparison to the SMAP soil moisture values. The comparison, which yields similar overall trends in soil moisture as well as generally consistent values, can be seen in Figure 3.17.

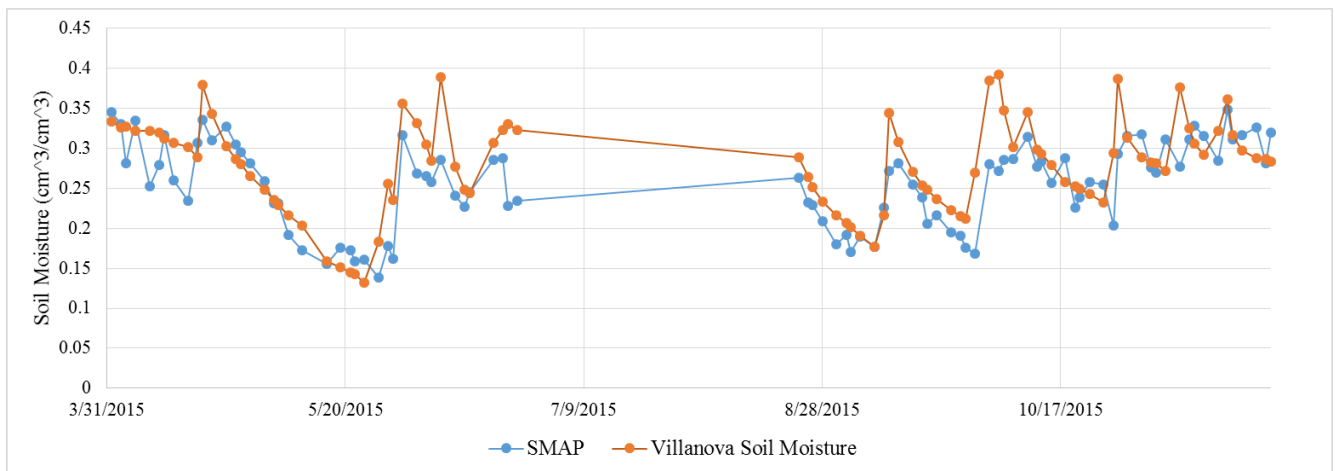


Figure 3.17: Time Series Results of SMAP and On-Site Soil Moisture Readings

The comparison of the BTI soil moisture readings and the sensed SMAP soil moisture values indicate that the SMAP satellite is an appropriate approximation for soil moisture conditions on site. While the readings lack the fine temporal resolution that on-site sensors can maintain, the free access to data provides a powerful mechanism to understand general trends in soil moisture at a site without utilizing any instrumentation.

While the SMAP readings proved to be a useful measure of the soil moisture expected within a region, the potential to use the soil moisture readings as approximations of overall weather trends was also analyzed. When looking at the time series results of the SMAP soil moisture readings and rainfall experienced, soil moisture reaches the highest peaks around periods with high volume storms (as would intuitively make sense). Therefore, the soil moisture readings were compared to cumulative rainfall in the preceding two weeks to understand if the sensors could be used as an approximation of generally wet or generally dry weather on a larger time scale (Figure 3.18). This analysis allows for the satellite to be compared more directly to the other drought indices analyzed, the PDSI and SPEI both representing general weather trends and dryness rather than a specific hydrologic value.

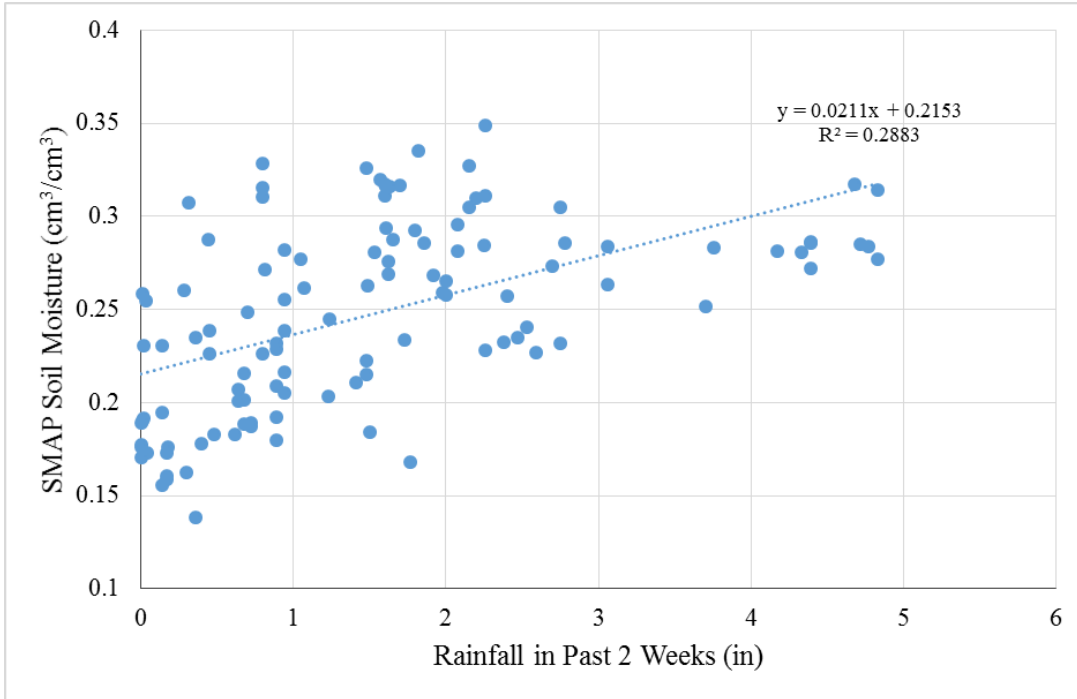


Figure 3.18: Recent Rainfall Comparison to SMAP Soil Moisture Readings

In comparing the recent rainfall (on a two week scale) to the SMAP soil moisture, a general upward trend can be seen with a substantial amount of scatter. When fitting a linear trend line over the data set, the slope shows a 0.021 increase in soil moisture for a corresponding increase in inch of bi

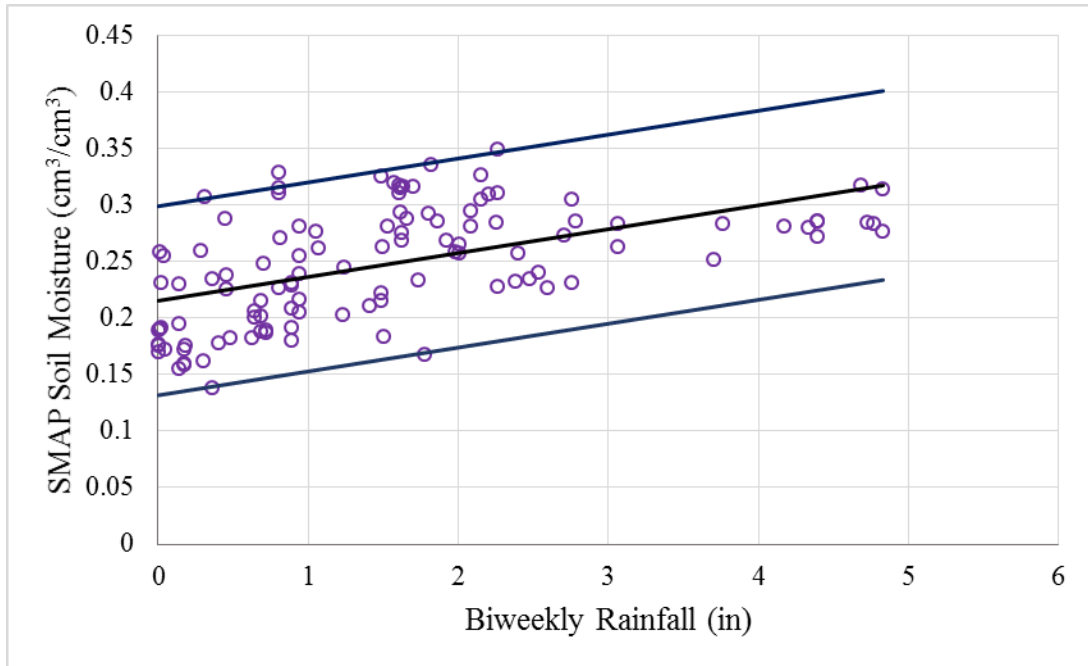


Figure 3.19: Rainfall in Past 2 Weeks and SMAP Comparison, 95% Confidence Limits

The results of the comparison with the confidence limits show that the soil moisture readings from SMAP do not provide an accurate representation of weather conditions on a longer temporal scale, even when just looking at a relatively small temporal scale of two weeks. The range associated with the 95% confidence limits of the relationship is almost as large as the total range for the data set (the range from wilting point to field capacity), indicating no clear statistical relationship between the soil moisture readings and rainfall. These results indicate that the SMAP satellite is an apt tool for measuring immediate meteorological events but lacks the ability to discern long-term trends as with the PDSI and SPEI. This short-term time scale though could be useful in stormwater management for making decisions about irrigation and use of captured rainwater.

3.5 Conclusion

To make real-time controlled stormwater systems smarter and make more informed decisions, having an idea of current climate trends and conditions is crucial. While having extensive on-site instrumentation to measure weather and hydrologic conditions is one way that this problem can be solved, there also exists substantial amounts of publically available climate information and indices that could be used to make more informed decisions in smart stormwater management. In analyzing multiple sources of climate data that are available publically, different trends and relationships were determined with respect to local climate conditions. These trends indicate that there is substantial potential for using publically available climate data to make informed decisions about stormwater systems.

One of the major sources of data that was analyzed were drought indices published to represent overall conditions, generally based on precipitation and temperature and their deviation from normal conditions. When looking at the weekly self-calibrating Palmer Drought Severity Index, it was determined that the index was apt at indicating dryer and warmer than usual conditions on a weekly basis with the highest correlation coming from the comparison between PDSI and weekly average temperature. Especially in cases where the PDSI was found to be low (less than zero, or dryer than normal conditions), a strong relationship existed that showed temperature steadily increasing as PDSI decreased. When looking at the relationship with precipitation, the PDSI did not perform as well as another drought index analyzed, the Standardized Precipitation Evapotranspiration Index. When basing the calculation of the SPEI on just one month of data (the shortest temporal scale available), a strong relationship between monthly rainfall and the SPEI was found that shows an increase in precipitation with an increase in SPEI.

Using both the PDSI and the SPEI in tandem could provide a better method of approximating the local weather conditions, the two indices both showing some promise at representing the overall weather conditions measured at Villanova while both also having some limitations. Because both scales operate in a similar way with negative values indicating dry conditions and positive values indicating wetter than usual conditions, looking at both indices could provide reinforcement that the condition determined by one index is really applicable to the situation. Additionally, the SPEI showed to be a better approximation of regional precipitation conditions while the weekly PDSI performed better at approximating temperature, together providing an overall picture of hydrologic conditions.

In addition to the drought indices analyzed, the SMAP satellite provides a promising method to gather climate data in relatively short time frames that could offer quicker updates on general moisture trends at a site. While unlike the drought indices this does not allow for general trends in weather patterns to be discerned, it does have the value of being updated every two to three days giving higher temporal resolution data from which decisions can be predicated on faster. Due to its high correlation to soil moisture readings taken at Villanova University in the bioinfiltration traffic island, the satellite also shows promise for use in cases where on-site instrumentation for soil moisture is not used. These measurements, paired with rainfall data, could provide a quick determination for actions such as irrigation when controlling complex stormwater reuse systems. While clearly not providing the high resolution that can be obtained with in situ measurements, the SMAP stands as a viable alternative when soil moisture conditions are required.

Future Work

Moving forward with the study of publically available climate data, some of the results need to be applied to smart stormwater networks in order to see how they can help improve the performance. Currently one of the best candidates for retrofit using a climate index at Villanova University's campus would be the CEER green roof system (Section 1.2.1). Because this system operates using smart rainwater harvesting and automated irrigation, applying knowledge of general climate conditions is important when making decisions about the duration and volume of irrigation that should take place. For example in light drought periods, heavier irrigation may be desired because a higher evapotranspiration potential is likely available. However, in a severe drought, more conservation of water needs to take place so that irrigation can continue to occur to maintain plant health on the roof. A balance between roof maintenance and stormwater management needs to occur when making these decisions, all within the framework of surrounding climate trends.

To try to address this goal, a basic framework was developed using the SPEI as a climate index. The goal of the process is to alter the intended irrigation volume based on the general climate trends. In order to do this, the SPEI needs to be recalculated on a daily basis to reflect the past month's climate trends. The SPEI is calculated by finding a moisture deficit for the month (D_i) which is approximated by the difference between precipitation (P) and potential evapotranspiration (PET). From this deficit value, a probability of exceedance is calculated based on a statistical distribution of all historic calculated deficit values (P). Based on several empirical constants (C and d values) and equations (Vincente-Serrano et al. 2010), the SPEI can then be calculated for the previous month. In order to complete this calculation, the statistical distribution of all deficit values will need to be calculated. An overview of the calculation process is as follows:

$$D_i = P_i - PET_i$$

$$SPEI = W - \frac{C_0 + C_1 W + C_2 W^2}{1 + d_1 W + d_2 W^3 + d_3 W^3}$$

$$W = \sqrt{-2\ln(P)} \quad P \leq 0.5$$

$$W = \sqrt{-2\ln(1-P)} \quad P > 0.5$$

Based on the calculated SPEI value, a multiplier will be applied to the intended irrigation volume in order to correct for climate conditions. The multipliers reach a peak at a SPEI value of -1 indicating slightly dry conditions where the evapotranspiration potential would be very high. In harsher drought conditions (less than -2), the multiplier drops below 1 to be conservative with water usage. Likewise in very wet periods the multiplier reaches smaller values in order to maintain the capacity of the green roof to deal with storm events. Figure 3.20 shows a draft of the multiplier curve to be used with the calculated SPEI to control the green roof irrigation.

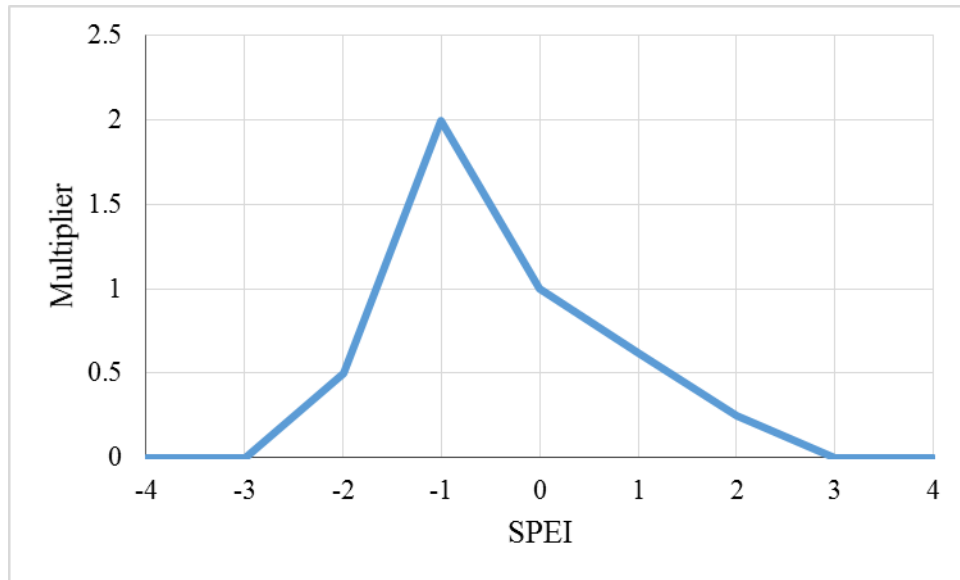


Figure 3.20: Green Roof SPEI Based Irrigation Multiplier

While clearly substantial work needs to go into place before this framework can be applied, this demonstrates just one example of how climate indices such as the SPEI or PDSI can be used to create smarter stormwater systems. As these smart systems continue to advance and become more

adaptable, performance monitoring needs to take place to quantify the benefit that is seen from these retrofits. Moving forward the green roof, with substantial monitoring equipment already in place, stands as an ideal candidate to demonstrate the use of climate data in the control of smart stormwater systems.

CHAPTER 4: MODELING OF REAL-TIME CONTROLLED SYSTEMS

4.1 Introduction

One of the main stormwater control measures (SCMs) that has undergone retrofits with real-time control (RTC) at Villanova University is the green roof on the CEER building. The stormwater system, described in Section 4.3.1, now captures stormwater runoff from both direct rainfall on the green roof and rainfall on an adjacent impervious roof area. Runoff from the adjacent impervious area is stored in a controlled cistern that uses weather forecasts to maintain sufficient storage to capture impending storm events. Water from the cistern is also pumped to irrigation sprinklers on the green roof during dry periods to utilize the evapotranspiration potential of the SCM. In total, the system represents a complex combination of storage, green infrastructure, and real-time control that functions together in order to optimize the capture of runoff from the CEER roof. Because the system has only been on-line for a short period of time (the site was declared online in April, 2016), a modeling approach was taken to study the site and determine the expected performance of the system. Furthermore, the model created was used to test different combinations of thresholds and factors used in the control decisions for the system.

4.2 Literature Review

Stormwater control measures (SCMs) are one way of managing stormwater that mimics natural hydrologic processes in order to reduce the effects of urbanization on the hydrologic cycle (PA BMP Manual 2006). Research into vegetated green roofs, one common type of SCM, has shown that a substantial portion of the hydrologic budget for green roofs come from evapotranspiration, providing a more natural mechanism to manage stormwater than direct release as runoff (Wadzuk et al. 2013, Zaremba et al. 2016). Despite the value in green roofs' ability to manage stormwater,

Wadzuk et al. (2013) point to the large evapotranspiration potential that is not realized by these systems when rainfall does not match the potential evapotranspiration. This study seeks to examine how the hydrologic timing of controlled SCMs, specifically a green and gray roof system, can be manipulated to more fully utilize the potential evapotranspiration while simultaneously managing a larger contributing drainage areas.

With the advent of many low-cost, real-time sensors and the capability to merge these technologies with developments such as the Internet of Things, there exists great potential within the field of stormwater management to integrate real-time information into control decisions (Wong and Kerkez, 2016). The potential configurations for real-time controlled (RTC) systems vary greatly, with benefits from both a water quality and water quantity standpoint being shown possible from various control configurations (Gaborit et al. 2013, Muschalla et al. 2014). Including controls on parts of stormwater systems such as valves or gates, retention times, timing of releases, and outflow rates can be manipulated to achieve water quality and quantity improvements. In cases of combined sewer systems where combined sewer overflows (CSOs) are the primary concern, real-time control has also been shown as a viable option for reducing CSO events (Cembrano et al. 2004).

An additional benefit of RTC systems shown in the studies by Muschalla et al. (2014) and Cembrano et al. (2004) is the ability to design systems to meet competing objectives. For example, trying to improve water quality by increasing retention time in storage facilities can impede the ability of a system to reduce peak flows in subsequent storms. However, RTC adds in dynamic capabilities that can better serve these sometimes conflicting goals. In this study, the full evapotranspiration potential of the green roof was attempted to be realized without impeding the ability of the roof to lower peak flows and capture runoff from storm events.

4.3 Methodology

4.3.1 Site Overview

The study site being modeled to demonstrate the use of RTC in stormwater systems is comprised of an extensive green roof and adjacent gray roof on the Center for Engineering Education and Research (CEER) at Villanova University (Figure 4.1). Runoff from the gray roof, an area of 800 square feet (74 m^2), is collected in a 500 gallon (1890 L) cistern while the 576 square foot (54 m^2) green roof collects only direct rainfall during storm events. The green roof itself has 4 inches (10 cm) of growth media overlaying a 1 inch (2.5 cm) storage and drainage layer created by a waffled plastic layer that creates large void space. A pump with four sprinklers (connected to 12 separate sprinkler heads) feeds water from the cistern to the green roof for irrigation during dry periods with the goal of fully utilizing the evapotranspiration potential of the green roof during inter-event dry periods.



Figure 4.1: Study Site Overview

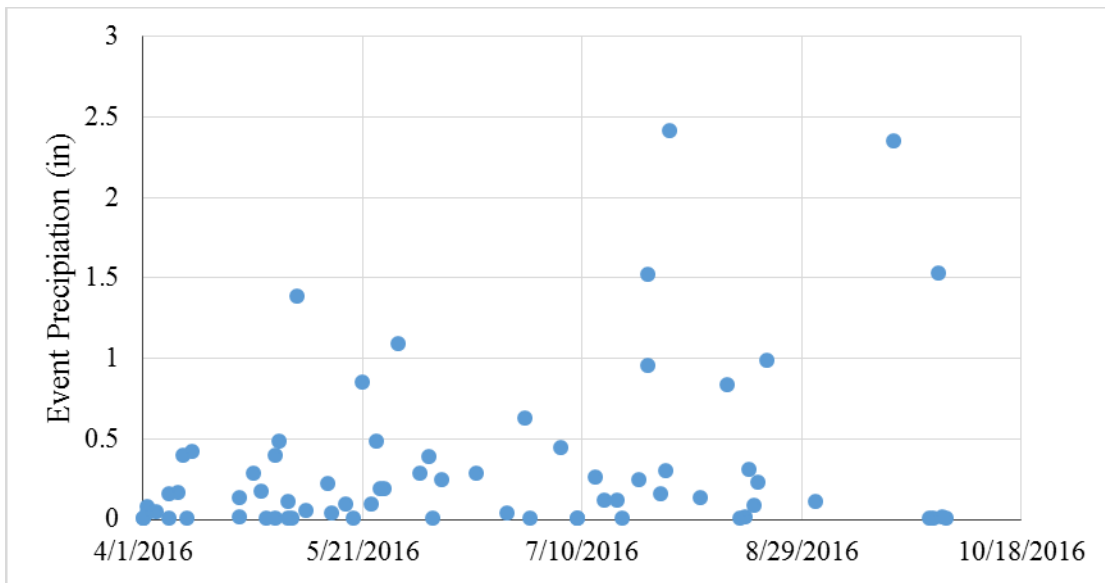
The green roof is heavily instrumented, providing a substantial amount of data to be used for calibration and validation of the model. Rainfall and weather data from the roof have been

measured since the site was first instrumented in 2008, meteorological data and outflow being recorded on a 5 minute basis. Outflow data from the site has been measured consistently since 2013, and evapotranspiration has been estimated using a weighing lysimeters since 2009. In 2015 the site underwent a retrofit to include the real-time controlled aspects described previously and simultaneously added additional monitoring equipment. This included eight soil moisture meters and four soil temperature meters, as well as the previously used meteorological station and outflow gage. Additionally, a pressure transducer was installed in the cistern to determine water volume in the tank. With the addition of OptiRTC technology which focuses on continuous monitoring and adaptive control (CMAC), the instrumentation reports collected data continuously in minute increments. The availability of data monitored from the site allows for a calibrated model to be created, matching historic performance of the system to create an accurate model representation of the physical system.

4.3.2 Data Acquisition

To model the long-term performance of the CEER green roof with real-time control retrofits, the EPA's Storm Water Management Model (SWMM) was selected for the modeling software. SWMM was chosen due to its ability to include control rules within long-term continuous simulations, as well as for its ability to model both the hydrologic and hydraulic components of urban stormwater systems (Storm Water Management Model Users' Version Manual 5.1 2015). A long-term simulation was desired for the project because of the focus on utilizing potential evapotranspiration from the green roof and to understand the influence of season. This process requires evaluation of not only storm events but also dry periods between storms, making the use of a long-term continuous simulation a natural choice to capture all these hydrologic processes.

For the long-term simulation, substantial hydrologic data was needed to model all of the processes associated with the green roof. This includes precipitation and temperature data measured on site to model rainfall and evapotranspiration, respectively. Rainfall events used in the simulation can be seen in Figure 4.2 with events summed for total rainfall volume based on a minimum six hour dry period between events to delineate storms. Rainfall data was collected from a tipping bucket rain gage located on the CEER roof, providing data from close proximity to the site being modeled.



bioinfiltration traffic island (BTI) on campus to calculate a potential evapotranspiration estimate using the Hargreaves equation (Equation 4.1). Daily maximum and minimum temperatures for the simulation are shown in Figure 4.3.

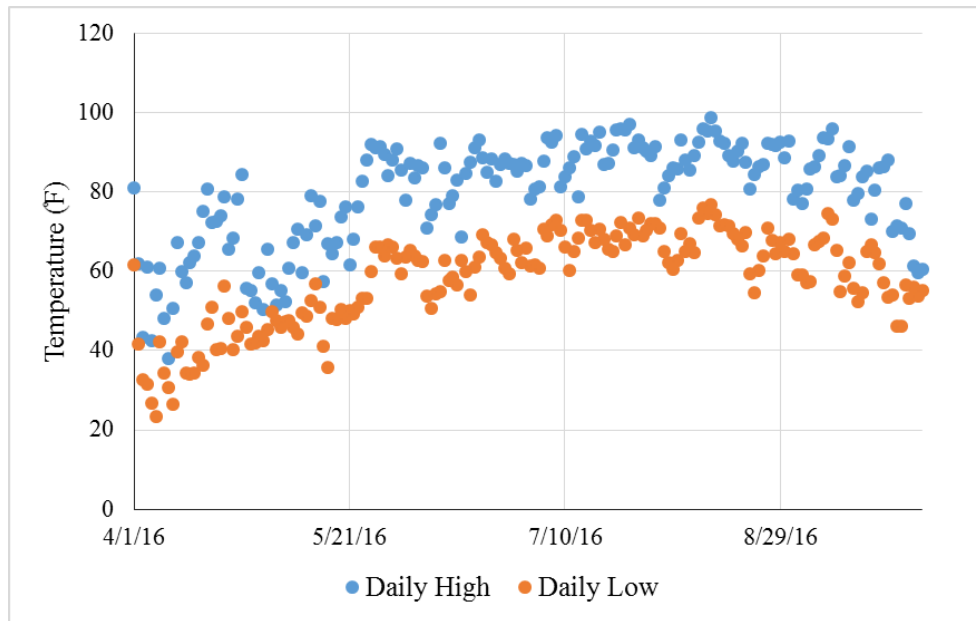


Figure 4.3: Daily Temperatures used for SWMM Climate File

In addition to the hydrologic data collected, historic weather forecasts were required to be integrated into the model to represent the forecast based controls used in the smart system. Forecasts were provided by the National Weather Service and are presented as both a probability of precipitation (POP) on a 0% to 100% scale and as a quantitative precipitation forecast (QPF) presented as a rainfall volume in inches. At each point in time, POP forecasts are presented representing 12 hour increments for up to 144 hours in advance and QPF forecasts are presented in 6 hour increments for up to 78 hours in advance. For this study, the QPF and POP data was used for a 48 hour future horizon.

4.3.3 Green Roof Model Development

Prior to the development of the RTC model of the retrofitted CEER green roof system, a model was created of the pre-retrofit green roof to have a calibrated base model for comparison to the RTC system. A storage node was used to represent the green roof, the volume of which represents the available pore space in the green roof media to capture stormwater. The green roof prior to the RTC retrofit only captured stormwater that falls directly on the roof as rainfall, so a subcatchment the size of the green roof (576 ft^2) was created with 100% impervious area and a large width (1000 ft) in order to transfer all runoff directly from the subcatchment into the green roof storage node. Depression storage was set to zero for the system to again allow for all runoff to be transferred to the green roof (as it would with direct rainfall) rather than be lost to initial abstractions in the model. An overview of the green roof model in the SWMM GUI can be seen in Figure 4.4.

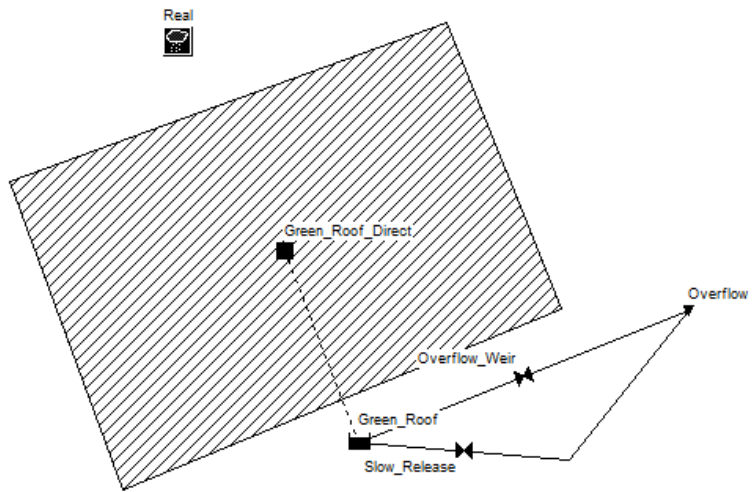


Figure 4.4: Green Roof Model in SWMM GUI

To model the outflow from the green roof, a combination of a weir and orifice were used to simulate the slow release outflows typically seen from the roof. During large rainfall events where the roof becomes saturated, outflow is immediately seen due to the drainage layer filling and draining from the system. However outflows are still seen for several days following large storm events due to water draining, representing soil moisture that falls between field capacity and saturation that is available to drain by gravity. A weir (“Overflow_Weir” in Figure 4.4) was selected to model the high outflows seen when the roof reaches saturation, and an orifice (“Slow_Release” in Figure 4.4) was chosen to represent the low flows seen following events. Together these were calibrated (Section 4.3.4) to represent the slow release phenomena typically seen with the CEER Green Roof.

One critical aspect of the green roof that needed to be captured in the model was the evapotranspiration from the roof, the primary mechanism for removing stormwater from the system. To model the potential evapotranspiration for the green roof (which serves as the maximum daily rate of ET given that water is available), the Hargreaves equation was used. The Hargreaves Equation (Equation 4.1) offers a good starting point to estimate the potential evapotranspiration of the green roof because of its relatively easy calculation which relies on just having daily maximum and minimum temperatures as inputs.

$$\text{Equation 4.1} \dots \dots \dots E = 0.0023\left(\frac{R_a}{\lambda}\right)T_r^{0.5}(T_a + 17.8)$$

In the Hargreaves Equation, R_a represents solar radiation ($\text{MJ/m}^2\text{d}$), λ is the latent heat of vaporization (MJ/kg), T_r represents the range of temperatures experienced in a day ($^{\circ}\text{C}$), and T_a represents the average daily temperature ($^{\circ}\text{C}$). The resulting E value (mm/day) represents the

calculated evapotranspiration rate for the day based on the daily maximum and minimum temperatures provided and applied to the surface area of the green roof storage node.

While Hargreaves Equation (Equation 4.1) provided a starting point for estimating potential evapotranspiration, the availability of measured ET data on site using weighing lysimeters allowed for a more accurate model of evapotranspiration to be developed. Previous green roof data suggested that as the soil moisture in the roof media decreased, less evapotranspiration was realized with highest ET rates measured directly after rainfalls when more water was available (Zaremba 2015). To represent this phenomena, the storage unit representing the green roof was given a curve where surface area increases with depth, allowing for more surface area available for evaporation as the storage unit is filled resulting in higher ET rates. The first estimate for an appropriate storage curve, where the total volume of the storage unit still matches the storage volume in the void spaces of the CEER green roof, can be seen in Figure 4.5.

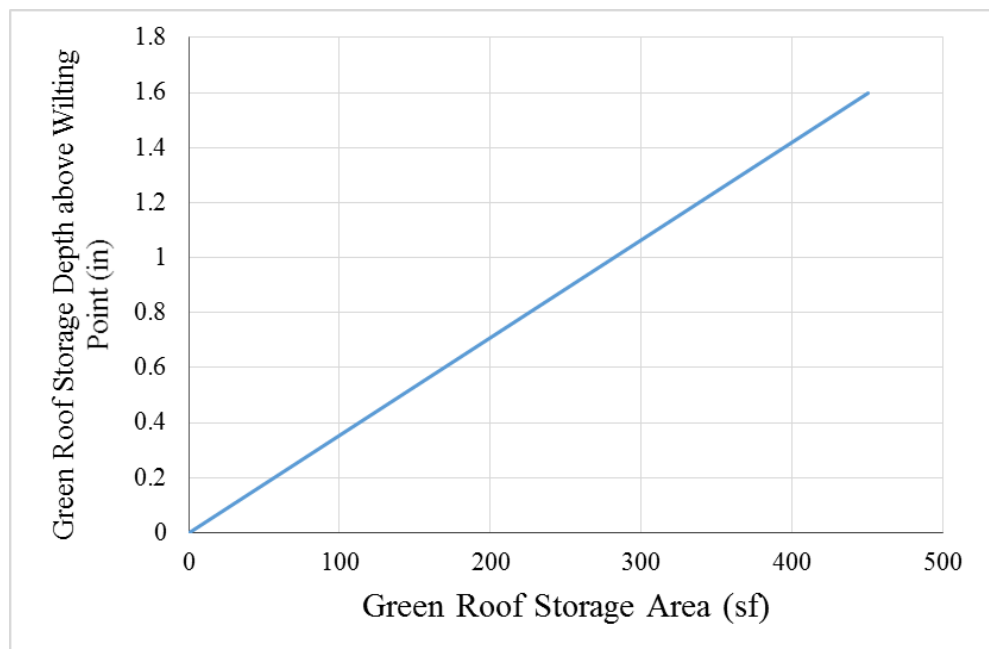


Figure 4.5: Original Estimate for Green Roof Storage Curve

After an initial storage curve was developed, the simulation was run using the data inputs described in Section 4.3.2 and the total evapotranspiration for the green roof was calculated based on a simple water balance of rainfall, outflow, and storage. Daily evapotranspiration values were then compared to ET values measured at Villanova University in the rain garden weighing lysimeters (Hess 2017) in order to provide comparison to typical SCM ET rates. Using these measured values, the storage curve was altered to match ET rates while maintaining the same total storage volume in the green roof storage node. The resulting altered storage curve can be seen in Figure 4.6.

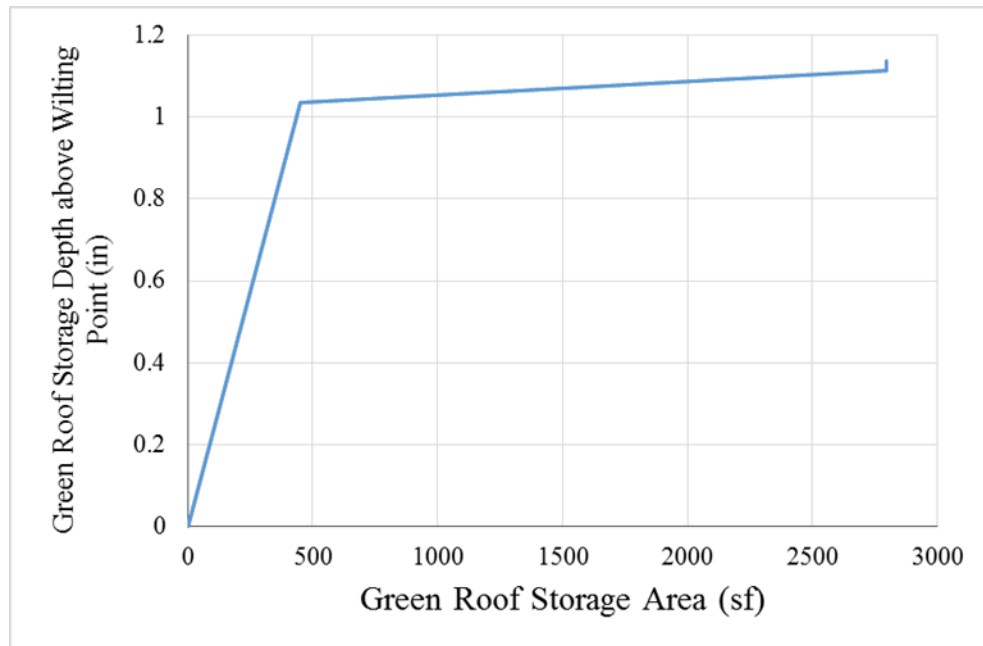


Figure 4.6: Final Storage Curve for CEER Green Roof Model

In order to match the measured and modeled ET rates, the surface area near the top of the storage curve was increased to match peak ET rates measured directly after large storm events. The final comparison between modeled ET from the green roof and measured ET from the rain garden weighing lysimeters for the calibration period can be seen in Figure 4.7.

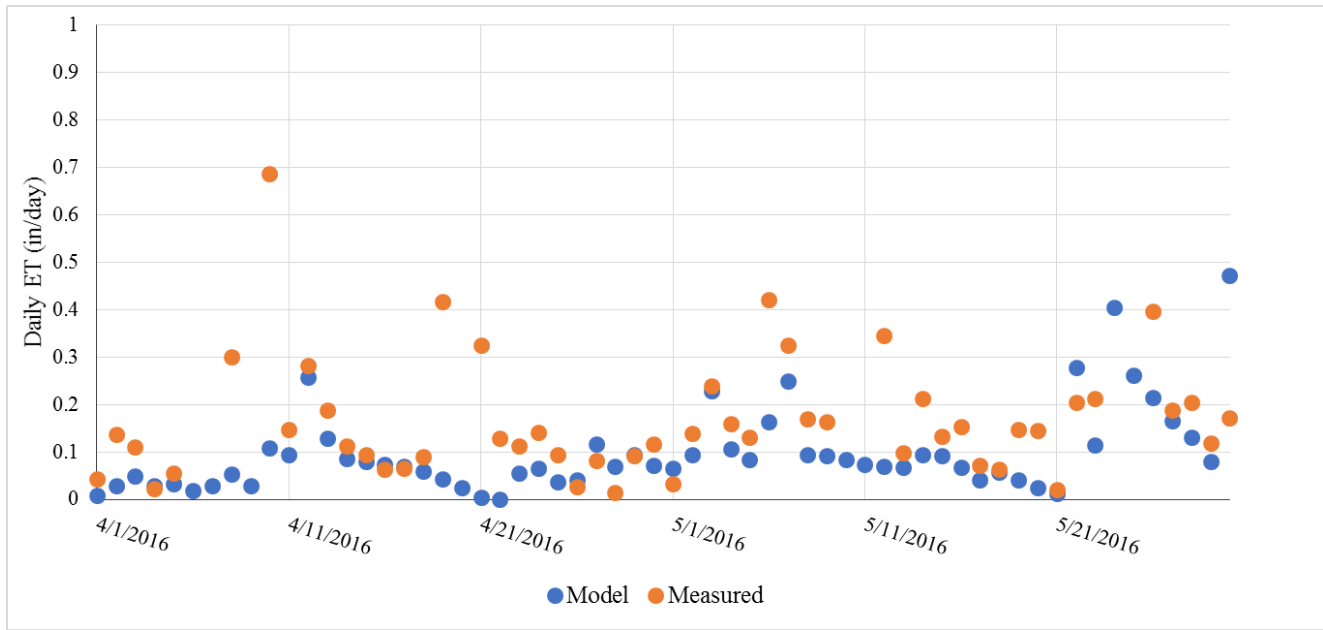


Figure 4.7: Daily Modeled and Measured Evapotranspiration

In order to discern the statistical correlation between the modeled and measured daily values of evapotranspiration, a paired t-test was performed on the two data sets with the goal of reaching 95% confidence that the two data sets have a residual of zero. For the final storage curve and temperature input values determined, a t-score of 2.07 was calculated which indicates a p value of 0.03, giving enough significance to accept the model for evapotranspiration. To visually check how the modeled and measured evapotranspiration values compared as well, the two data sets summed cumulatively over the time series being examined and plotted to see the correlation. The cumulative evapotranspiration measured and modeled can be seen in Figure 4.8.

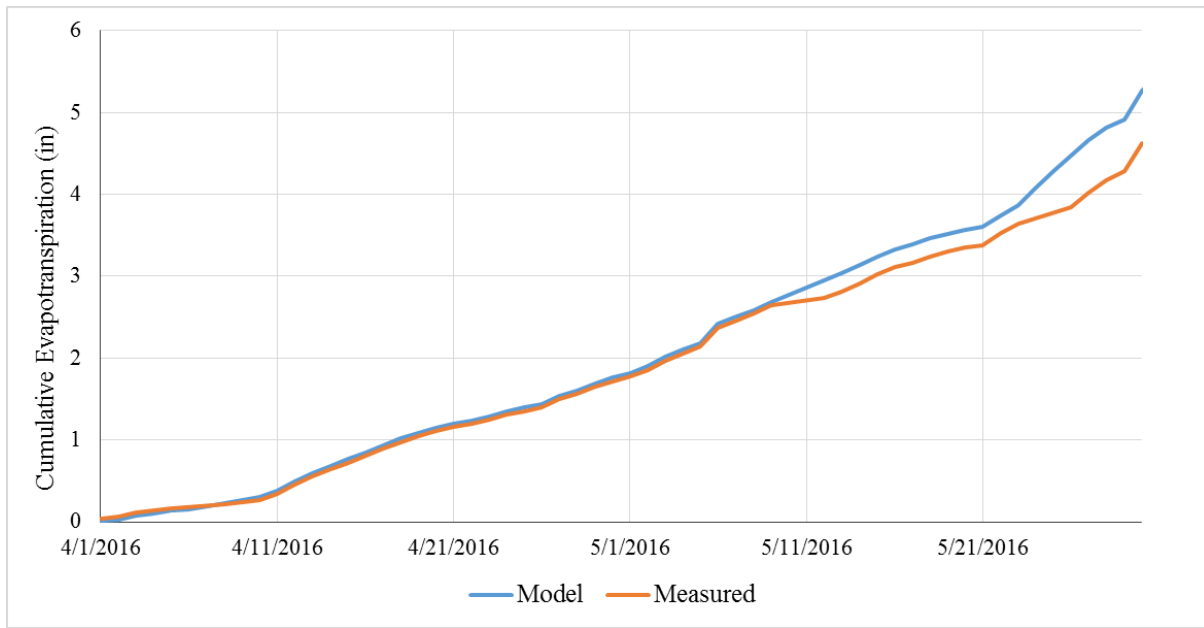


Figure 4.8: Measured and Modeled Cumulative Evapotranspiration for CEER Green Roof

The results clearly indicate similar trends between the two estimates of ET with just a slight deviation towards the end of the simulation. Once the storage curve was set for the green roof in the SWMM model the simulation was ready for calibration of outflow from the system.

For all model simulations completed, a 15 minute computational time step was used for creating runoff from the subcatchments (the hydrologic part of the model). A 60 second time step was designated for all hydraulic routing, of which there was very little in these simulations due to a lack of any conveyance systems. Reporting was done on a 15 minute basis to provide the same resolution as both the hydrologic calculations and the rainfall data, and results were eventually aggregated on a daily basis when considering performance in order to compare to the daily ET rates available from past study of the roof.

4.3.4 Green Roof Model Calibration

To create a model of the controlled green roof accurate to reality, the model was first calibrated to past performance data from the green roof prior to retrofit with real-time controls. Extensive study of the CEER green roof has previously been completed to measure the water balance of the SCM (Zaremba 2015) so storm responses were available for calibration and validation. To calibrate the overflow from the green roof, a storm event greater than 0.8 inches was required, this point being the roof's storage capacity and where overflow starts to occur. To first calibrate the model of the green roof, a storm from April 2014 was used with a total rainfall volume of 1.82 inches. The measured outflow from the system was compared to the model results and the orifice outlet to the modeled system adjusted until a high correlation between the data sets was found. The results of the final calibration simulation can be seen in Figure 4.9 aggregated on a daily basis.

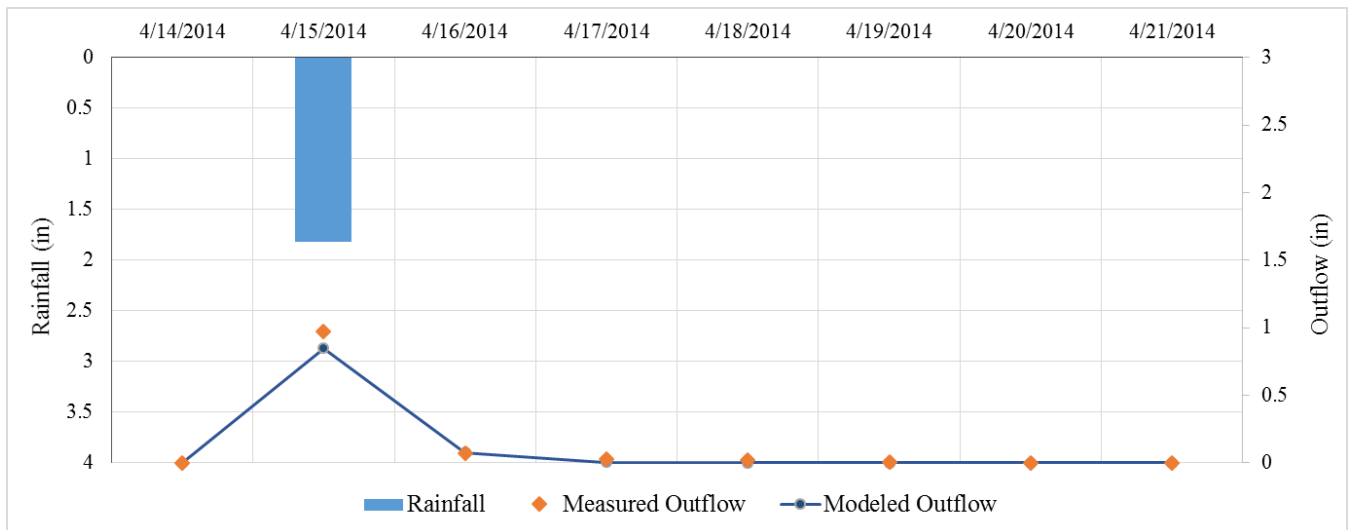


Figure 4.9: Model Calibration Run for Storm of $P = 1.82$ Inches

For the calibration run displayed in Figure 4.9, a Nash-Sutcliffe coefficient of 0.978 indicating a high correlation between the two outflow data sets. In order to achieve the calibration only the orifice (“Slow_Release” link in Figure 4.4) was adjusted, while the height to the weir outflow

remained constant because the green roof was well documented from previous study and relatively simple to model (this stayed constant at a stage and volume equivalent to the saturation point of the system). The results of the calibration yielded an orifice opening size of 0.00005 feet set at a height within the green roof storage node of 11.743 feet, a height representing the storage volume equivalent to the field capacity of the green roof media.

After the calibration simulation was completed, the calibrated green roof model was run again using rainfall data from a storm in May of 2014 with a total rainfall volume of 3.40 inches. This validation simulation can be seen in Figure 4.10.

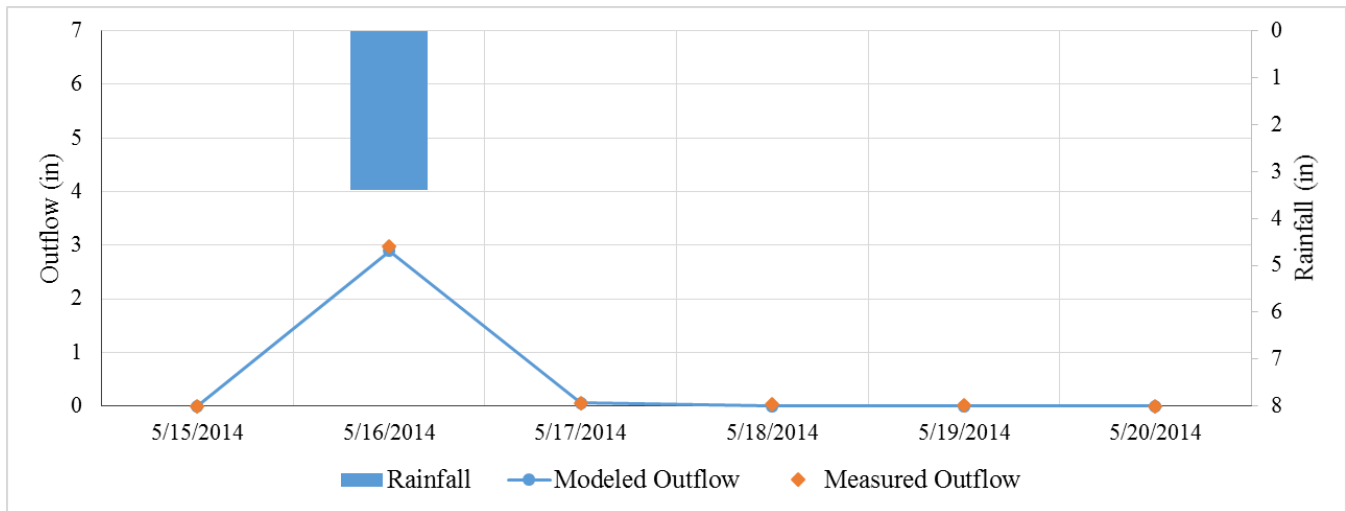


Figure 4.10: Model Validation Run for Storm of $P = 3.40$ Inches

The validation of the green roof model once again produced a high statistical correlation with a Nash-Sutcliffe coefficient of 0.989. The high correlation of both the calibration and the validation run indicate that the model of the original green roof system prior to retrofit accurately represents the hydrologic processes and responses of the green roof to storm events. Using this model as a baseline, real-time controls were added to the model in the green roof in order to simulate the retrofitted system with the additional gray roof contributing areas and controlled cistern.

In addition to the calibration of the outflow from the green roof, calibration was attempted using soil moisture data collected from the eight soil moisture meters located on the green roof. Because the volume of the green roof storage node in the SWMM model serves to represent a total volume of water held as soil moisture, the soil moisture data should provide a direct comparison to volume of water in the green roof model storage node. A sample of the soil moisture data collected for the green roof from the eight probes is shown in Figure 4.11.

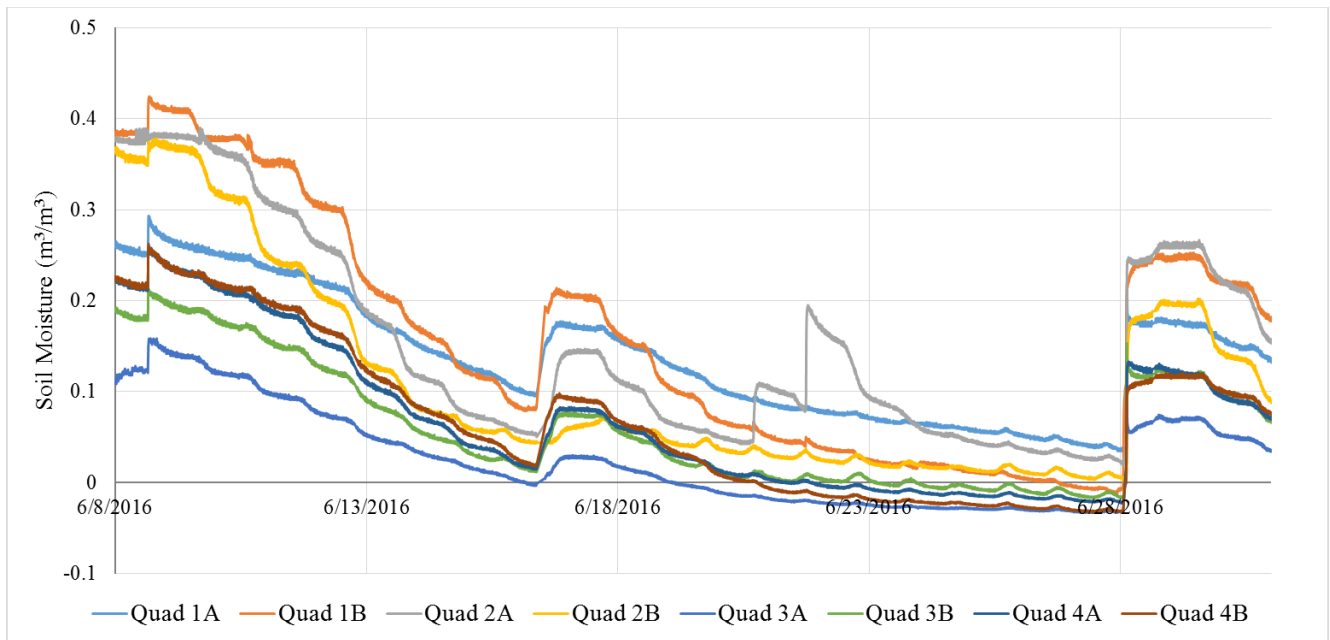


Figure 4.11: Sample Soil Moisture Data from CEER Green Roof

It is evident in Figure 4.11 that the soil moisture data collected from the green roof offers conflicting accounts of the soil moisture over time. Ranges of soil moisture values reported are shown to be as high as almost $0.3 \text{ m}^3/\text{m}^3$, or 30% of the total volume, clearly offering an unrealistic portrayal of the system's soil moisture. Additionally, negative values were recorded for some periods by five of the soil moisture meters, which are impossible and clearly do not represent the physical system. While all eight of the soil moisture probes give similar trends that recess during

dry periods and increase after rainfall events, the range of values is too large to draw any definitive conclusions. For this reason it was impossible to use the soil moisture data to calibrate the green roof model using any statistical correlations and the true soil moisture volume on the roof is still largely unknown. To provide a basic visual check to see if the general trends of the measured and modeled soil moisture volumes were the same, the modeled water volume in the green roof was compared to the average measured green roof soil moisture volume and is displayed in Figure 4.12. The period chosen for comparison represents a time where soil moisture data was available, negative values were not recorded, and the real-time control components (i.e. irrigation) was not being utilized.

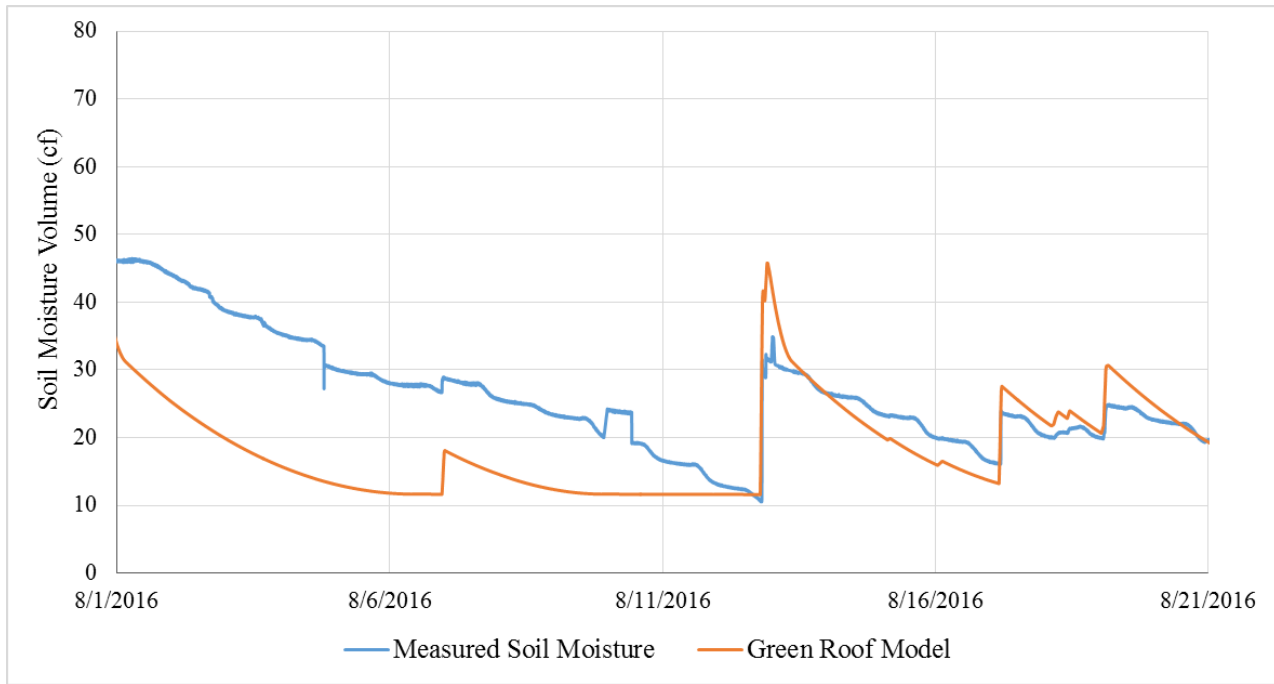


Figure 4.12: Average Measured and Modeled Soil Moisture Volume on CEER Green Roof

When looking at the overall trends displayed by the measured soil moisture in the CEER green roof, the modeled behavior provides a similar curve with soil moisture increasing and decaying over the same time periods. While there clearly does not exist substantial enough data for complete

calibration based on the soil moisture, the similarity in overall trends provides some confidence in the behavior described by the green roof model.

4.3.5 Real-Time Control Model Development

After the calibrated model of the passive green roof was created, the model was altered to include the real-time controls. The first aspect of the retrofitted RTC system to be modeled was the additional drainage area from the gray roof to be captured in the cistern in CEER. Because the drainage area is entirely impervious, the runoff from the roof can be simply modeled using the NCFS Curve Number method assuming a Curve Number of 98 for the 100 percent impervious area. The size of the drainage area (800 square feet) is small enough that the timing of the system is not critical, most of the runoff from storm events immediately transferring from the roof to the cistern within one reporting time step of 15 minutes.

From the subcatchment representing the gray roof portion of the system (Figure 4.13), runoff is routed to a storage node representing the cistern with a volume of 500 gallons. Outlets from the cistern are modeled as an orifice (“Drain_Valve” in Figure 4.13), a weir (“Overflow”), and a pump (“Irrigation”) to represent the three primary mechanisms for water exiting the tank. The orifice allows for the cistern to draw down water levels based on controls, the weir allows for excess water to exit the system during large storm events, and the pump provides the connection between the cistern and the green roof for irrigation purposes.



Figure 4.13: CEER Gray Roof and Cistern in SWMM GUI

When the model was adjusted to include RTC, the green roof drainage area and storage model remained the same, adjusted only by having the pump (“Irrigation” node) connect flows from the RTC cistern to the green roof when activated. Figure 4.14 provides an overview of the different components of the site added into the model of the smart system. The red outlined area represents the additional drainage area capture from the impervious gray roof, and the cistern shows the controlled storage unit used to capture the additional runoff and irrigate the green roof.

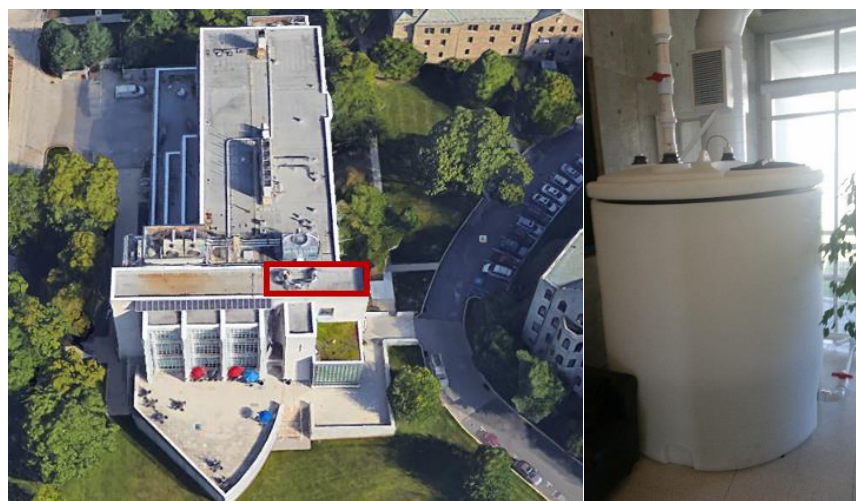


Figure 4.14: CEER Gray Roof and Cistern

In order to model the controls used on the green roof system, the SWMM hydraulic controls module was used to input control logic into the SWMM simulation to be evaluated every time step. The first aspect to set controls for was the cistern, which operates by checking the weather forecast and consequently draining down in advance of storms to ensure sufficient storage to capture storm events. These controls operate and are modeled in the same way that the smart retention systems in Chapter 2 were modeled and follow the same control structure as outlined in Section 2.3.3. Again the forecast based controls relied on the Quantitative Precipitation Forecasts (QPFs) for Probability of Precipitation (POP) values above 70% looking on a horizon of 48 hours into the future. An expected inflow volume from future storms is calculated at each time step, compared to the current storage volume in the cistern, a decision and potential action is made based on the available cistern storage.

In addition to the cistern storage which is managed by weather forecast based controls, control decisions were written to automate the green roof irrigation schedule by activating the pump connecting the cistern to the green roof. This decision was based on a soil moisture threshold where if the soil moisture (represented as total storage volume in the SWMM model) dropped below a certain value, the pump would turn on to move stored runoff to the green roof. The initial value for the soil moisture threshold was taken to be $0.16 \text{ ft}^3/\text{ft}^3$ and the control rule was written as follows:

Rule Soil_Moisture

If Node Green_Roof Depth < 11.727 ft

And Node Forecast Inflow = 0

Then Pump Irrigation Setting = 1.0

Else Pump Irrigation Setting = 0

The control logic here seeks to irrigate when the soil moisture drops below the threshold (the threshold here displayed as the depth equivalent to the desired storage volume) while avoiding wetting the soil when a storm is forecasted. A simple binary system is used with the pump either being fully on (pump setting equal to 1.0) or fully shut (pump setting equal to 0). Together with the forecast-based controls operating the cistern, the logic combines to create a smart system that seeks to more fully utilize captured runoff while still avoiding outflows during wet weather.

4.3.6: Sensitivity Analysis Setup

In addition to the simulation runs created for the baseline passive and RTC green roof models, additional simulation runs were completed to analyze the sensitivity of different parameters on the model results, as well as to see how the parameters could be adjusted to optimize the performance of the RTC green roof. The most crucial parameters identified were the soil moisture irrigation threshold, the controlled cistern storage capacity, and the probability of precipitation threshold used for the forecast decision.

The soil moisture threshold was identified as an important aspect of the system because this value is what determines when irrigation occurs. This value requires balancing competing objectives, with the goal to utilize harvested rainwater ideally having a high soil moisture threshold so more water is utilized in opposition to the goal of reserving green roof capacity for impending storms wanting a low soil moisture threshold. The sensitivity analysis used a range of soil moisture values from the estimated green roof media wilting point to the field capacity, which is the span of soil moisture values with water available for evapotranspiration. Input values used for the soil moisture threshold sensitivity analysis can be seen in Table 4.1.

Table 4.1: Input Values for Soil Moisture Threshold Sensitivity Analysis

Storage Volume (cf)	Threshold Depth (ft)	Equivalent Soil Moisture
11.65	11.65	0.072
13.14	11.657	0.081
14.64	11.663	0.090
16.13	11.670	0.099
17.63	11.676	0.108
19.12	11.683	0.118
20.61	11.690	0.127
22.11	11.696	0.136
23.60	11.703	0.145
25.09	11.709	0.154
26.59	11.716	0.164
28.08	11.722	0.173
29.57	11.729	0.182
31.07	11.736	0.191
32.56	11.737	0.200
34.06	11.738	0.210
35.55	11.739	0.219
37.04	11.740	0.228
38.54	11.741	0.237
40.03	11.742	0.246
41.52	11.743	0.256

The cistern capacity primarily affects the ability to capture runoff from the gray roof. In addition, cisterns without sufficient storage could also limit the ability to irrigate the green roof when there is soil moisture capacity available. Inversely, a very large cistern would likely be unnecessary if the volume of runoff captured far outweighs the evapotranspiration capacity of the green roof. Starting from the baseline (i.e., 1 inch capture over the drainage area in the cistern), the size of the gray roof drainage area was altered from -50% to +200% in order to vary the cistern capacity. A summary of the simulation runs completed for the drainage area sensitivity analysis can be seen in Table 4.2.

Table 4.2: Sensitivity Analysis Inputs for Variations in Gray Roof Drainage Area

Percent Change	Capacity* (in)	Drainage Area (ft ²)
-50%	0.50	400
-25%	0.75	600
-20%	0.80	640
-15%	0.85	680
-10%	0.90	720
-5%	0.95	760
0	1.00	800
5%	1.05	840
10%	1.10	880
15%	1.15	920
20%	1.20	960
25%	1.25	1000
50%	1.50	1200
100%	2.00	1600
200%	3.00	2400

*Capacity is the rainfall capture over the drainage area

The last parameter looked at in the sensitivity analysis was the Probability of Precipitation (POP) threshold used to determine when to act on a predicted rainfall event. For this analysis, the POP was adjusted to range from zero to 100% in increments of 10% as reported from the National Weather Service. The POP threshold is important because it determines what certainty is high enough to believe a storm is coming. If this value is set very low, the system would likely act on many storms that end up not occurring. If this value is set very high, the chances that no action is taken in preparation of a storm that does occur becomes larger. Again, choosing a threshold value

for control decisions requires balancing different objectives to find a middle ground. By looking at how adjustments in these three influential factors affect the performance of the smart green roof system, the system can be designed for a more optimal performance.

4.4 Results

4.4.1 Baseline Model Results

Once the green roof model was calibrated and altered to include real-time controls, the simulation run was completed for the period spanning April 1, 2016 to October 1, 2016. The full RTC model provides an example of how the different processes, from capture of the gray roof runoff kept in storage to the evapotranspiration prompting green roof irrigation, could be used together to create a smarter and more efficient stormwater network. Sample time series results for one month of the simulation (May 2016) are shown in Figure 4.15 with the modeled storage in the green roof (as soil moisture; “Green Roof” as orange line) and controlled cistern (“Cistern” as blue line) shown with respect to rainfall events. The volume where the green roof (“GR Overflow” as gold line) and cistern overflow (“Cistern Overflow” as green line) are provided to show the bounds of the system. For full results across other months in addition to May 2016, see Appendix A.

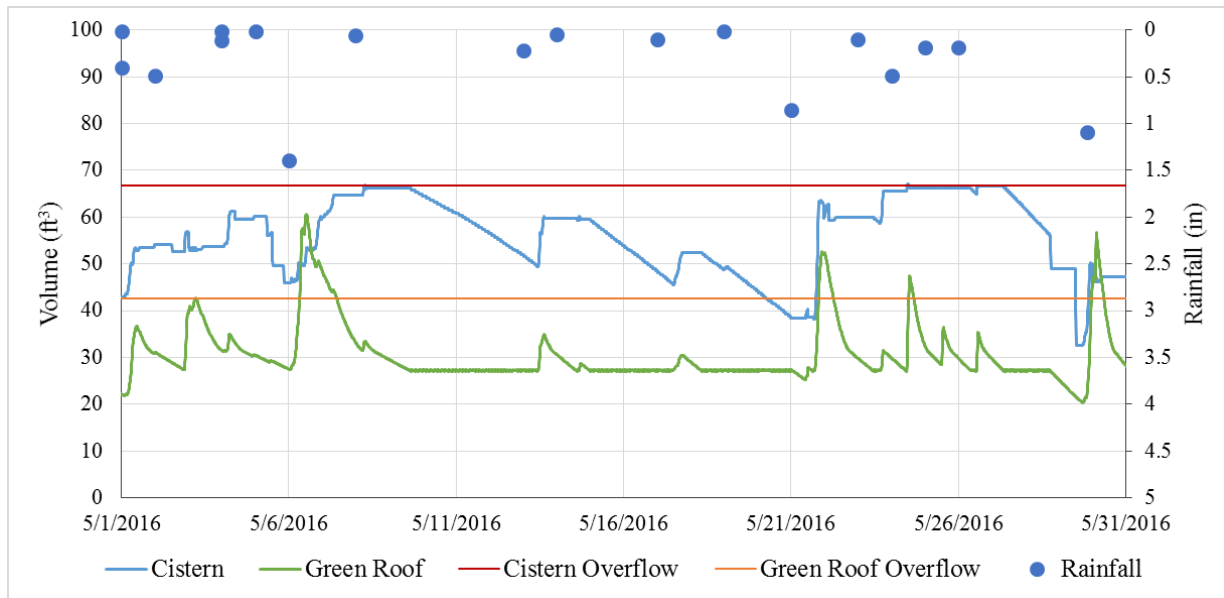


Figure 4.15: Sample Time-Series Results of RTC Green Roof Model for May, 2016

The results in Figure 4.15 demonstrate most of the expected components of the RTC green roof system, with the actively controlled cistern making decisions to both draw down and create storage for impending storms as well as irrigate the green roof during dry periods. For the dry period experienced around May 10th, the soil moisture (green roof volume hit it's threshold of 0.16 ft³/ft³) and the cistern can be seen drawing down as stored water is used to irrigate the green roof to maintain the target soil moisture volume. Later on May 30th when a larger storm occurs (greater than the 0.8 inch capacity of the green roof), the cistern can be seen drawing down in advance of the storm to free up storage while the irrigation to the green roof stops (and the soil moisture drops below the irrigation threshold) to prepare ensure sufficient capacity in the green roof as well.

One of the main changes between the passive system and the retrofitted RTC system was the increase in drainage area due to the addition of the 800 square foot gray roof drainage area and associated cistern. For direct comparison between the two model simulations, results were normalized over a watershed area and calculated in terms of a water depth in inches. Outflows

were recorded and aggregated on a per storm event basis and were plotted against the total rainfall volume experienced for the storm (Figure 4.16) in order to demonstrate the typical outflow response to storms of varying sizes. Storms events were determined by setting a minimum inter-event dry period of six hours. Prior to the expected overflow point (0.8 in), no overflow is expected. After the expected overflow point, outflow is assumed to be equal to the rainfall (inflow) and is a 1:1 line on Figure 4.16.

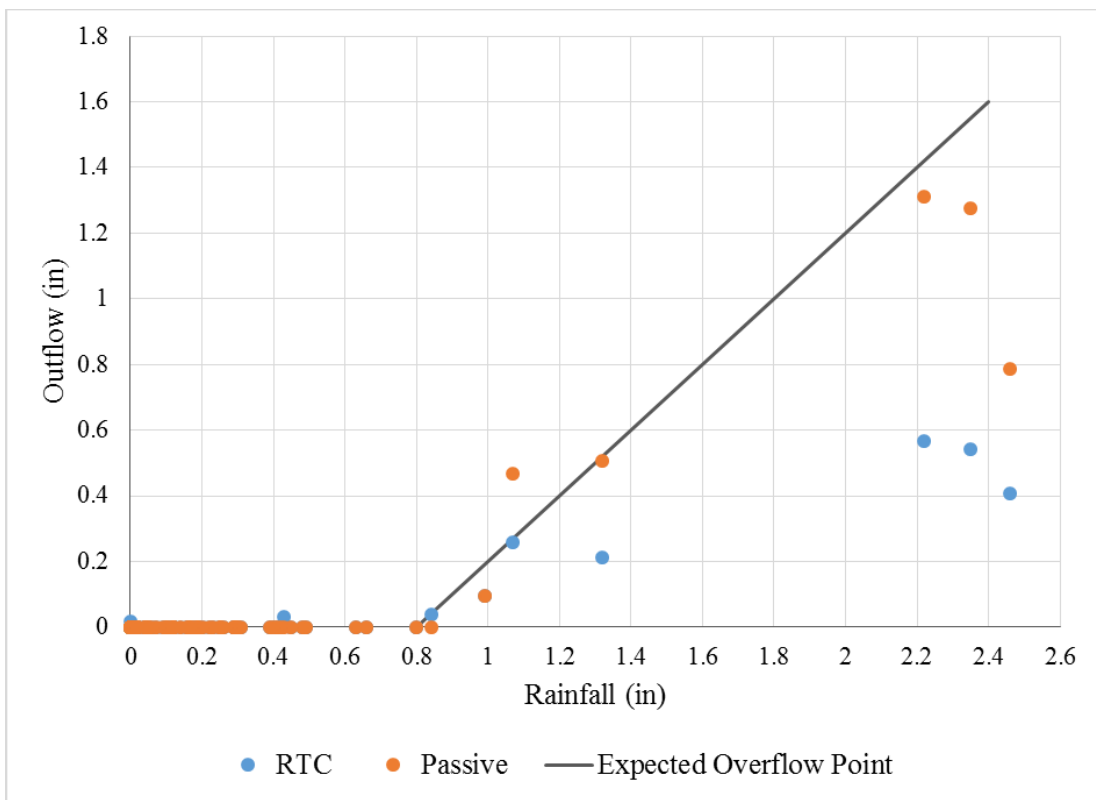


Figure 4.16: Rainfall and Outflow from Passive and RTC Green Roof Models

For the passive system, the system performs as expected with rainfall events less than 0.8 inches resulting in no outflow while events greater than 0.8 inches resulting in outflow. Generally the outflow from the passive green roof is close to the excess volume over the first 0.8 inches (the point demonstrated by the Expected Overflow Point line). When comparing this to the RTC green

roof results, the system still generally was able to capture events entirely when below 0.8 inches with a few exceptions (2 events of the 70 within the simulation). For the larger events where overflow is expected, the overflow volume was generally less than that of the passive green roof when normalized on a watershed basis. While some outflows were caused by the retrofit around 0.4 inches that would not occur with the original passive system, this overall indicates an increase in performance by the retrofitted system, especially for large rainfall events. This performance benefit holds implications for CSO communities especially, where larger events typically cause CSOs to occur. By minimizing the outflow, the system mitigates the impact on a combined sewer system whereas the passive system does not provide as much a buffer.

After the model simulations were run of the passive green roof and retrofitted real-time controlled green roof, the two simulation results were compared further to discern expected performance changes after the RTC retrofit of the system. For each system, the total cumulative rainfall and overflow were recorded and the evapotranspiration calculated. With no infiltration from the system, ET was approximated as simply the difference between rainfall and outflow from the system (Equation 4.2). Analysis of other extensive green roofs has shown this to be a good approximation for calculating ET, the mass balance retention being equal to the long term ET from green roofs (Gregoire and Clausen, 2011).

Cumulative performance plots for the passive green roof and RTC roof are shown in Figures 4.17 and 4.18, respectively. Additionally, individual rain events, determined by a minimum intermediate dry period of six hours, were plotted against the cumulative performance curves to show the effect that individual events have on the performance of the passive and RTC green roof systems.

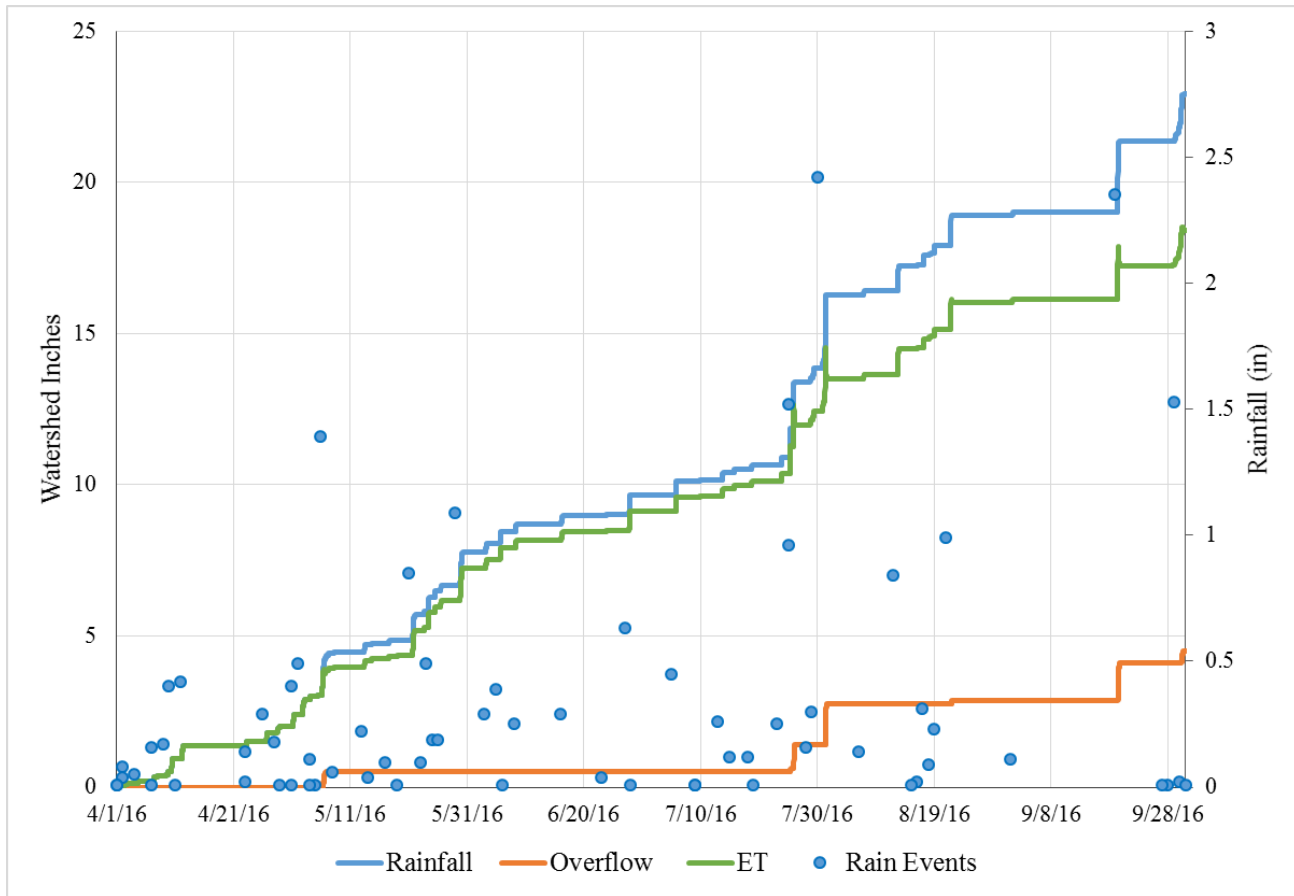


Figure 4.17: Cumulative Rainfall, Overflow, and ET from Passive Green Roof

The results of the passive system follow largely what was expected of the system based on past study of the CEER roof. In total, 22.93 inches of rainfall occurred during the simulation with 4.50 inches of the rainfall resulting in overflow, the remaining 18.43 inches being captured by the green roof and removed via evapotranspiration. When comparing these results to the individual storm events, gains in the overflow cumulative curve typically occur with rainfall events near or exceeding 0.8 inches of rainfall, the amount previously shown to reach the storage capacity of the green roof media (Zaremba 2015). These performance curves from the passive green roof set a baseline of performance for which to compare the retrofitted RTC system to (Figure 4.18).

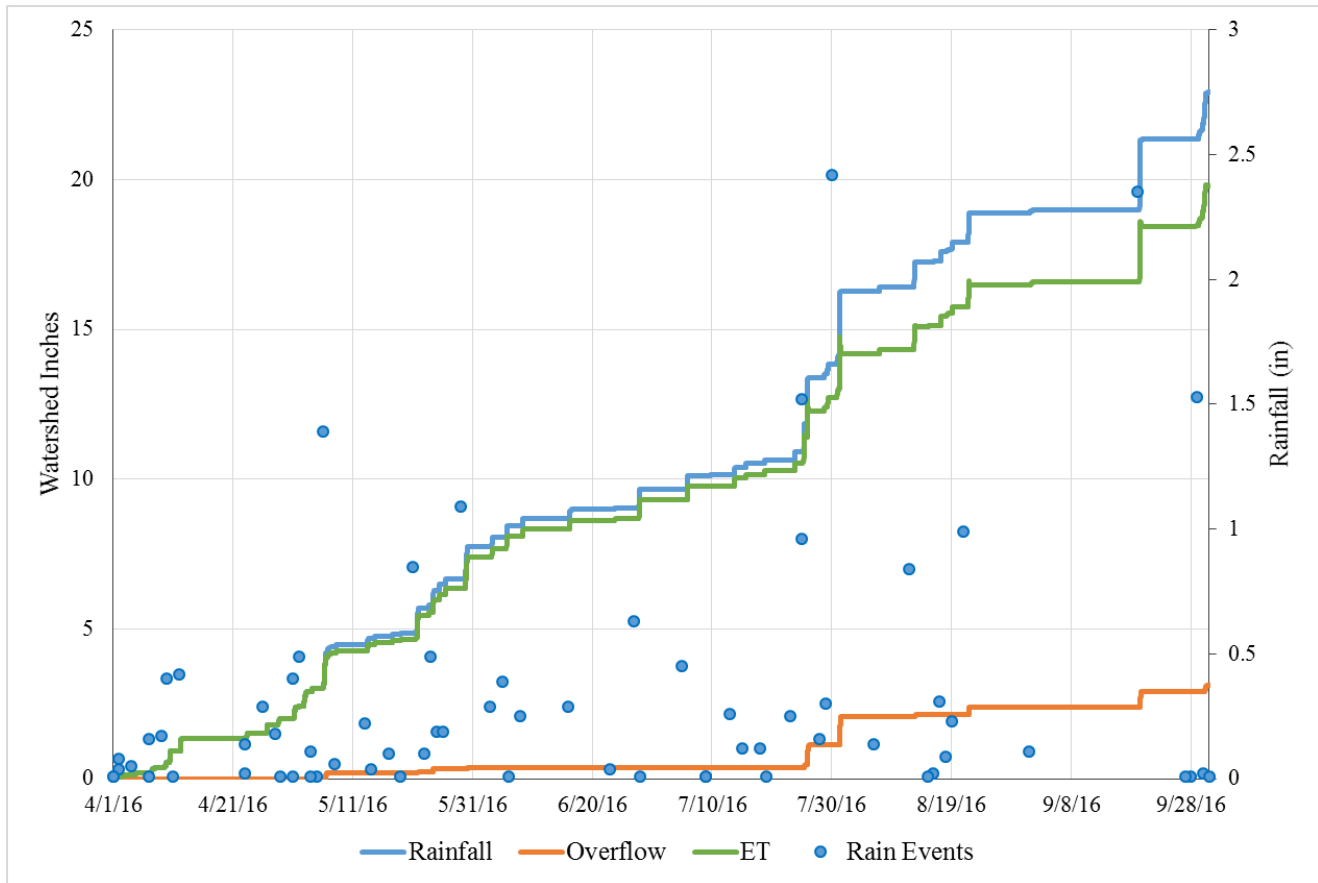


Figure 4.18: Cumulative Rainfall, Overflow, and ET from RTC Green Roof

The performance of the real-time controlled green roof system was largely similar to the performance of passive green roof when looking at the simulation results on a watershed basis. Again a total of 22.93 inches of rainfall occurred over the course of the simulation, this time with only 3.12 inches resulting in overflow and the remaining 19.81 inches being captured and removed via evapotranspiration. This shows that despite the increase in contributing area (an additional 800 square feet of entirely impervious area), the performance of the system on a watershed basis was actually improved when RTC components were utilized.

While overall the results of the modeling study show promise for the RTC system, one goal of the retrofit was to make sure that the performance of the green roof itself did not suffer during rain

events. This could occur when irrigation of the roof happens prior to a rain event, thus limiting the storage capacity in the roof and potentially causing overflows that would not otherwise have occurred. To analyze this aspect of the performance, the captured volume within the green roof was compared for the modeled passive and smart systems for the duration of the long term simulation. Figure 4.19 shows sample results from the two systems for the month of May, 2016 with results from other months available in Appendix A.

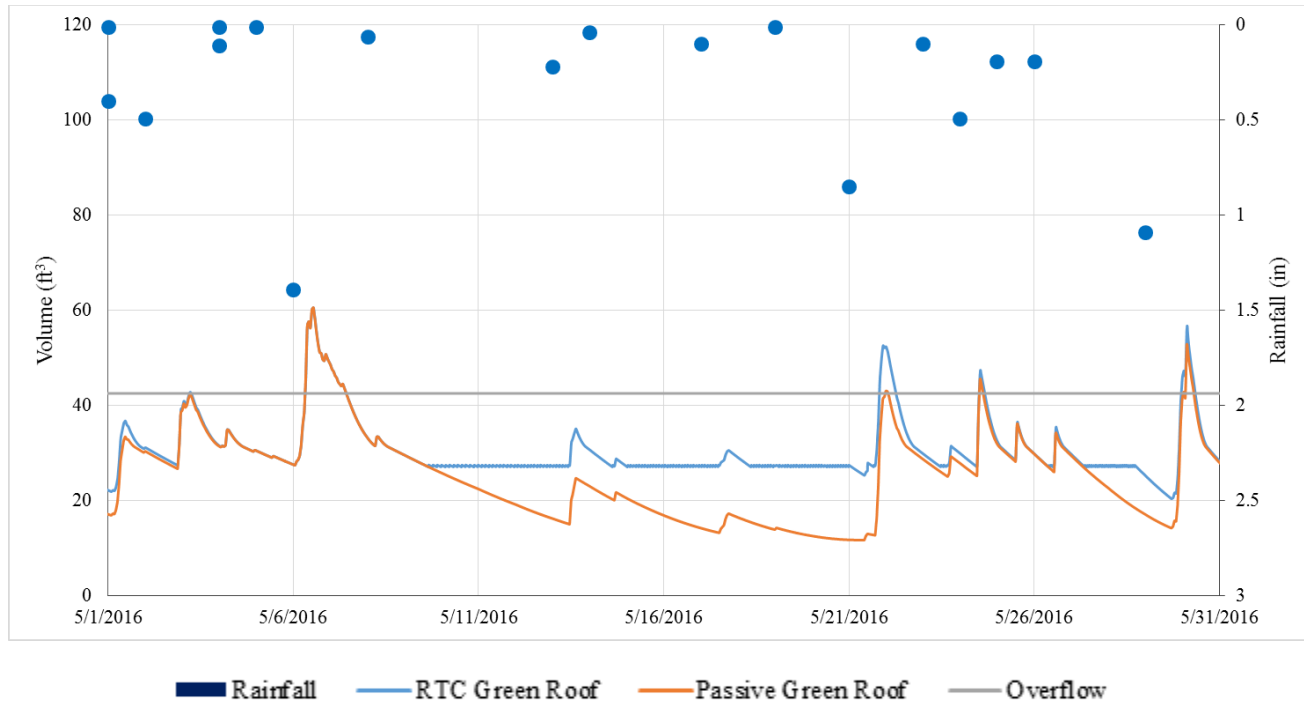


Figure 4.19: Sample Comparison of Green Roof Storage Volumes for RTC and Passive Systems

While overall the two systems showed similar performance, there were occasional events where an overflow was predicted in the RTC system but not in the original passive system (for example, the storm on May 21st). Looking overall at the two systems, metrics were calculated in order to analyze the performance of the green roof during storm events and are displayed in Table 4.3.

Table 4.3: Performance Metrics for Modeled RTC and Passive Green Roofs

	Passive Green Roof	RTC Green Roof	Percent Change
Overflow Volume (in)	4.50	3.12	-30.7%
Overflow Volume (gallons)	1600	2680	67.4%
Capture Volume (in)	18.43	19.81	7.50%
Capture Volume (gallons)	6620	16990	157%
Average Wet Weather Outflow (gpm)	0.059	0.108	83.2%
Wet Weather Outflow Volume (gallons)	980	1790	83.2%

When looking at the results from both the passive and RTC simulations of the CEER green roof, it is again apparent that when looking on a watershed basis the system saw a marked improvement. This was indicated by a substantial decrease (30.7%) in overflow from the system and an increase (7.50%) in the volume captured and removed via evapotranspiration. However, when looking at the timing of the system, the RTC green roof had an overall increase in average wet weather outflow rate as well as wet weather outflow volume (both at 83.2%) indicating that the addition of the controlled cistern in some cases caused a reduction in capacity of the actual green roof. Moving forward with the sensitivity analyses on different aspects of the simulation, the goal is to reduce this phenomenon and gain the increase in overall capacity while still maintaining performance of the green roof during storm events.

While the results of the baseline model indicate performance benefits on a watershed basis when looking at the pre and post-retrofit systems, it is also important to recognize that further benefits exist due to the inclusion of additional impervious area in the RTC green roof's drainage area that otherwise would drain directly to the storm sewer. When considering the passive system with the impervious roof as an entire watershed, wet weather outflows would be seen during every event regardless of rain volume due to the impervious nature of the roof. To better understand these benefits from a volume perspective, Table 4.4 shows the expected outflow from the pre and post retrofit systems when considering the impervious gray roof in both cases.

Table 4.4: Performance Metrics for Modeled RTC and Passive Green Roofs (Including Passive Gray Roof)

	Passive Green Roof with Impervious Gray Roof	RTC Green Roof	Percent Change
Overflow Volume (in)	15.2	3.12	-79.5%
Overflow Volume (gallons)	13000	2680	-79.5%
Capture Volume (in)	7.71	19.81	157%
Capture Volume (gallons)	6620	16990	157%
Wet Weather Outflow Volume (gallons)	12400	1790	-85.6%

When considering the entire watershed prior to retrofit, the performance benefits from creating the smart green roof system are even clearer with a 157% increase in capture and 79.5% decrease in overflow. Wet weather overflow shows even more substantial benefit with 85.6% of the pre-

retrofit wet weather overflow being removed. These benefits clearly stem from taking a substantial amount of impervious area that was previously unmanaged (800 square feet) and adding it to a system that allows for capture to occur. The benefits of a smart system are highlighted here with the ability to manage larger watersheds while still utilizing the same piece of green infrastructure that was already existing.

4.4.2 Soil Moisture Threshold Sensitivity Analysis

After the initial simulation runs were completed for the passive and controlled green roof systems, additional model runs were completed to analyze the sensitivity of the RTC system to different parameters used in the control decisions of the system. The first parameter to be analyzed was the soil moisture threshold which is used to determine an irrigation action. In the actual CEER roof system, the control process occurs by checking the soil moisture meters on the green roof and comparing the value to the irrigation threshold. When the soil moisture recedes below this value, the pump from the cistern to the green roof is activated and the sprinklers irrigate the roof. To see the effect of this irrigation threshold on the system's performance, simulation runs were completed ranging from the wilting point to the field capacity of the green roof media as described in Section 4.3.6. Soil moisture values were represented as total volumes of water in the green roof for purposes of the model.

Once the simulation runs were completed for the various soil moisture values tested as the threshold point for irrigation, several metrics of performance were compared across the range of soil moistures tested. First, an overall water balance was created for the system looking at what volume of runoff on the green and gray roofs ultimately ended up as outflow from the cistern and what was ultimately removed via evapotranspiration (the two mechanisms available for water to

leave the green roof system). The results of the water balance for each of the soil moisture sensitivity runs for a constant inflow of 22.93 inches is displayed in Figure 4.20. For the sensitivity analyses performed, the same simulation period spanning April to October of 2016 was used with total inflow and outflow volumes from the entire period considered.

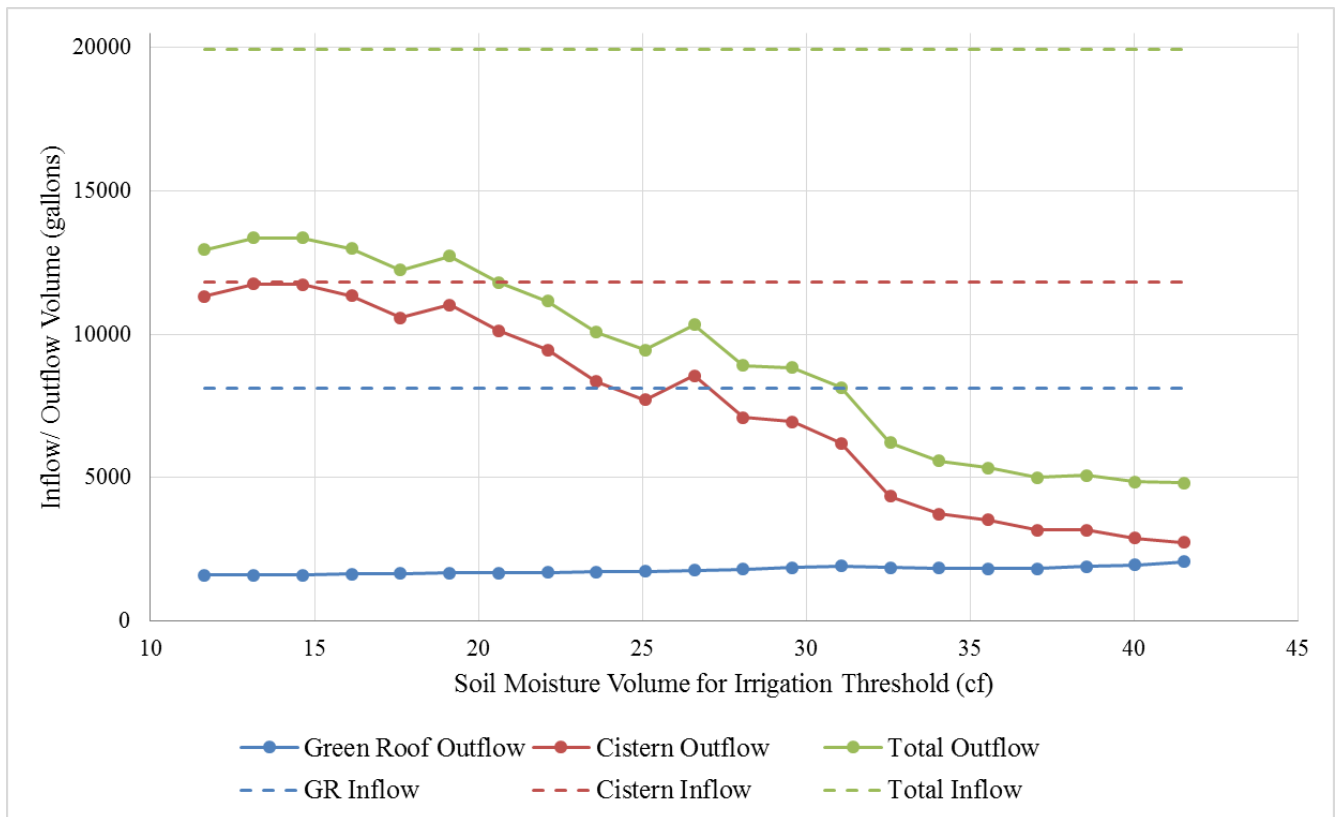


Figure 4.20: Total Inflow and Outflow to Modeled Green Roof System for Varied Soil Moisture Thresholds

Figure 4.20 displays the total inflow and outflow from the green roof, cistern, and total system for all time periods of the simulation runs. While clearly outflow is expected from the larger storm events, this aims to show the amount of capture that was able to be achieved and the amount of water that was removed via evapotranspiration, a process that in the natural hydrologic cycle is the largest mechanism (Hornberger et al. 2014). While the performance of the green roof (outflow)

does not change much depending on the threshold, the total outflow and cistern outflow vastly decrease as the threshold is increased. This makes sense because as the threshold increases, stored water is more frequently removed from the cistern because the irrigation threshold is more quickly achieved. Additionally, the results showed the cistern to be the largest contributor to outflow from the system, which again makes sense because it has the largest drainage area and relies on the green roof for any removal mechanism besides release and outflow. Figure 4.21 shows the same outflow results reported as a percent of the inflow.

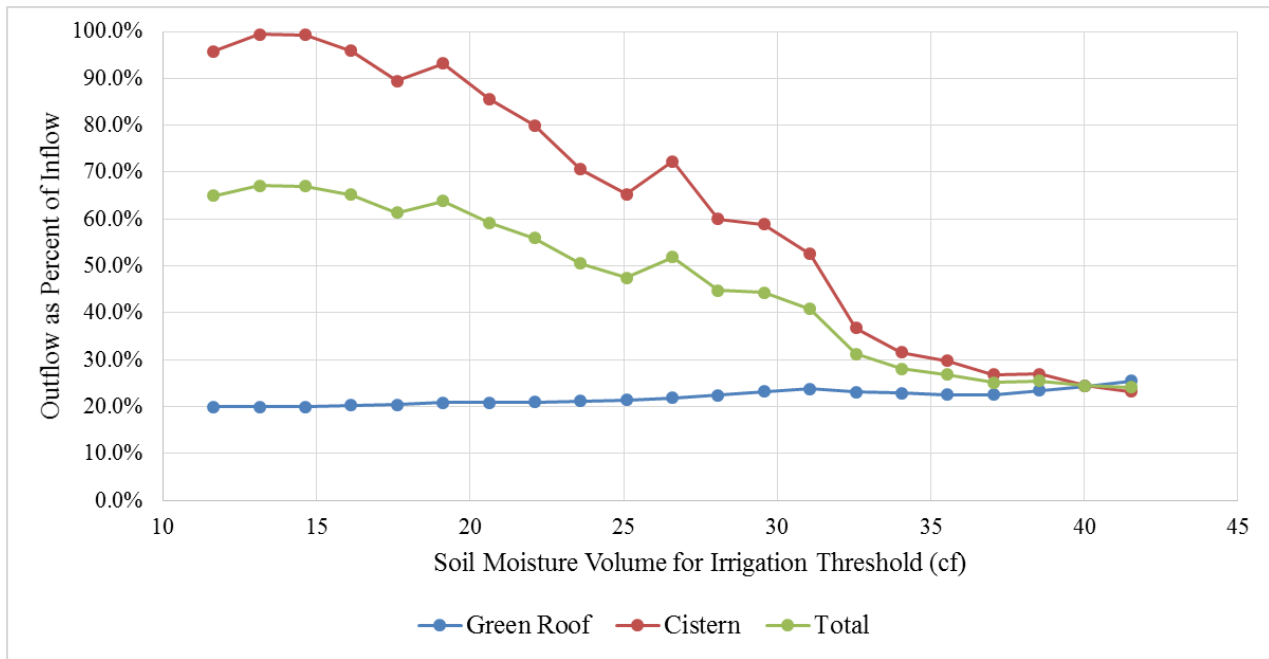


Figure 4.21: Outflow as Percent Inflow for Modeled Green Roof System of Varied Soil Moisture Thresholds

The results of the sensitivity analysis also indicate a point of diminishing returns, with a threshold above 32 cubic feet of soil moisture storage resulting in minimal additional capture benefits when looking at outflow as a percent of inflow. This point would indicate the most optimal point to set the irrigation threshold at, the benefit past this point not being substantive but still keeping the

threshold low enough to avoid causing additional outflows from the green roof from excess irrigation. The initial baseline simulation (and the current green roof system) operate with a threshold of 26.0 ft^3 ($0.16 \text{ ft}^3/\text{ft}^3$) indicating that the performance would likely be increased if the soil moisture threshold were raised to a value such as 32 ft^3 . In order to analyze these relationships and see how the irrigation threshold affects the timing of the system, outflows that occurred during storm events were also analyzed for both the controlled cistern and the green roof. Figure 4.22 displays the total hours recorded where outflow was occurring during storm periods while Figure 4.23 shows the total volume of overflow that occurred during rainfall events. For both these factors the goal is to minimize the outflow experienced during wet weather while still utilizing fully the stormwater captured, as shown in Figures 4.20 and 4.21.

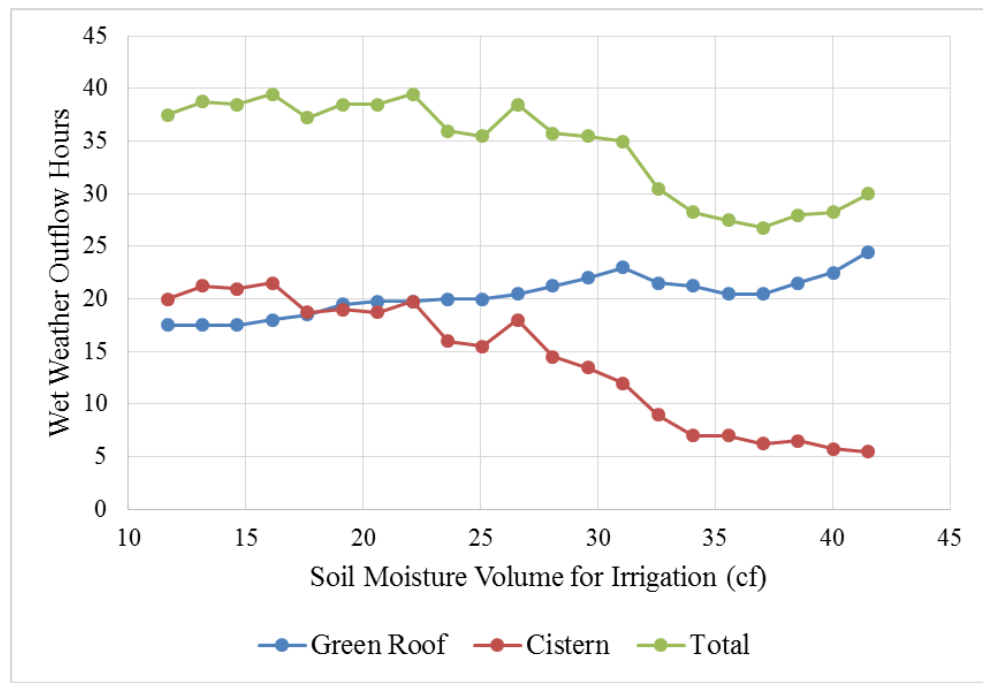


Figure 4.22: Wet Weather Outflow Hours for Varied Soil Moisture Thresholds

Looking at the wet weather periods experienced during the different simulations, the amount of time where outflows occurred decreased as a whole as the soil moisture irrigation threshold was

increased. This did not occur uniformly throughout the system though with an overall increase in wet weather outflow hours from the green roof and an overall decrease from the cistern. These results make sense though because as capacity is freed up in the cistern by irrigation (which occurs more frequently when the irrigation threshold is higher), the capacity in the green roof is correspondingly decreased. The results show thought that the cistern's capture area has a greater effect on the overall system, with optimal performance coming in the range of 30 to 40 cubic feet of storage in the green roof (a soil moisture equivalent of about 0.19 to 0.24 ft^3/ft^3 by volume). When looking at the wet weather in terms of volume rather than time increments (Figure 4.23), these results are generally corroborated with the increase in soil moisture threshold showing an overall increase in performance.

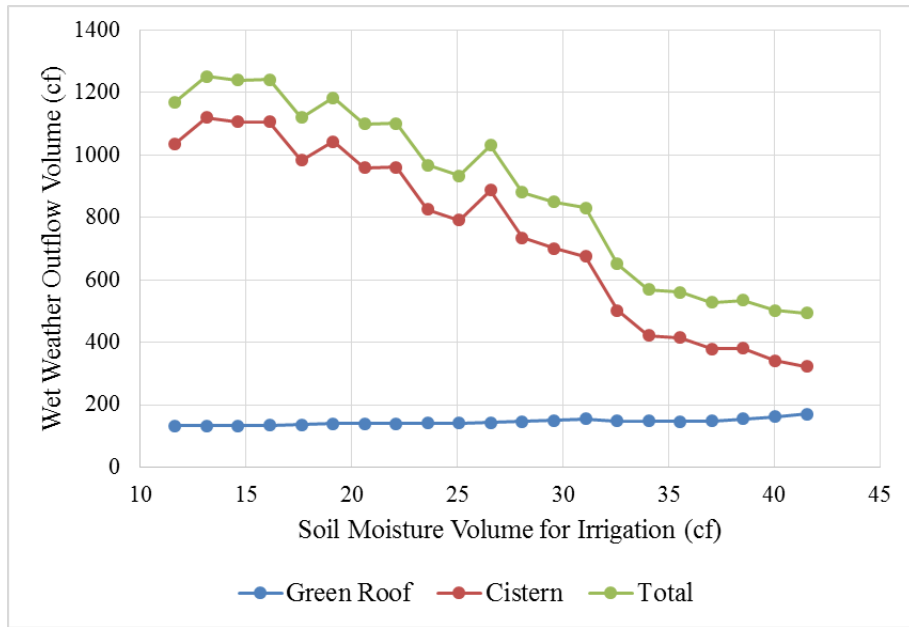


Figure 4.23: Wet Weather Outflow Volumes for Varied Soil Moisture Thresholds

In terms of both volume and hours of outflow, the controlled cistern saw a vast decrease as the threshold for irrigation was increased. This intuitively makes sense because as the irrigation threshold is increased, the soil moisture value at which the irrigation pump is triggered is reached

more easily and the captured runoff is therefore pumped to the green roof more liberally. Because the benefits of increasing the soil moisture threshold are generally diminished after passing around 32 cubic feet of storage, a threshold around this point would likely make a good candidate for the optimized soil moisture threshold, relating to a soil moisture equivalent of about 20% ($0.20 \text{ ft}^3/\text{ft}^3$). Again this value is slightly higher than the soil moisture threshold currently used ($0.16 \text{ ft}^3/\text{ft}^3$), indicating that performance benefits could be gained by altering this value.

4.4.3: Drainage Area Sensitivity Analysis

In addition to the sensitivity analysis performed on the soil moisture threshold for the green roof mode, a sensitivity analysis was also performed on the size of the drainage area contributing runoff to the cistern from the gray roof. The goal of this sensitivity analysis was to alter the capacity of the cistern for different capture amounts; altering the drainage area results in different rainfall depths the cistern has the capacity to capture. Drainage areas ranged from changes of -50% to +200%, as described in Section 4.3.6. The resulting total inflow and outflow of each component of the system can be seen in Figure 4.24.

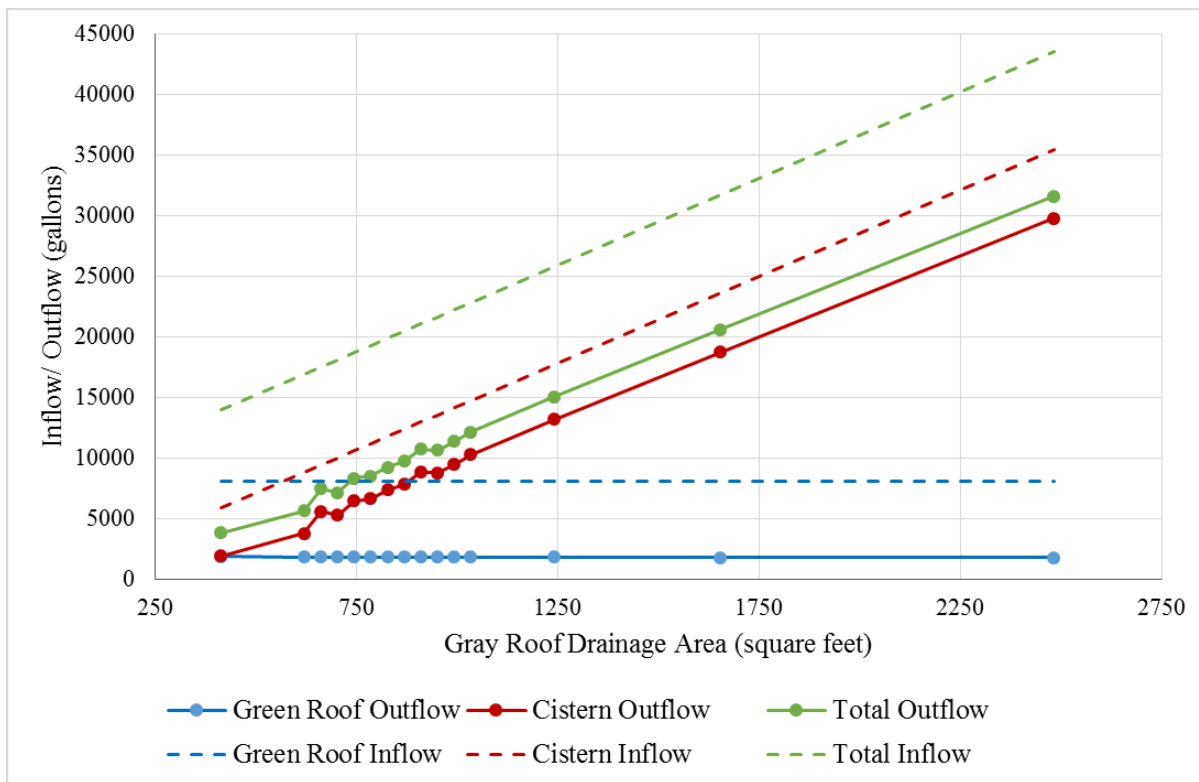


Figure 4.24: Total Inflow and Outflow of Modeled Green Roof System for Varied Contributing Drainage Areas

The results of the sensitivity analysis on drainage area indicate that the green roof outflow was not substantially affected by changes to the gray roof's drainage area. This indicates that the irrigation to the green roof was not limited by the tank volume and that the range of values simulated for gray roof drainage area still provided sufficient water to maintain the green roof performance. Outflow from the cistern, however, saw an expected increase as increases in drainage area were seen. This represents a cut in the capacity for capture in the cistern, the storage potential dropping to a minimum of 0.25 inches of storage capacity when the drainage area is the largest. To further examine the effect that changing the storage capacity of the cistern had on the performance of the green roof and the ability to capture and manage stormwater runoff, the outflow from the cistern,

green roof, and total system were reported as a percent of the inflow to each component and is displayed in Figure 4.25.

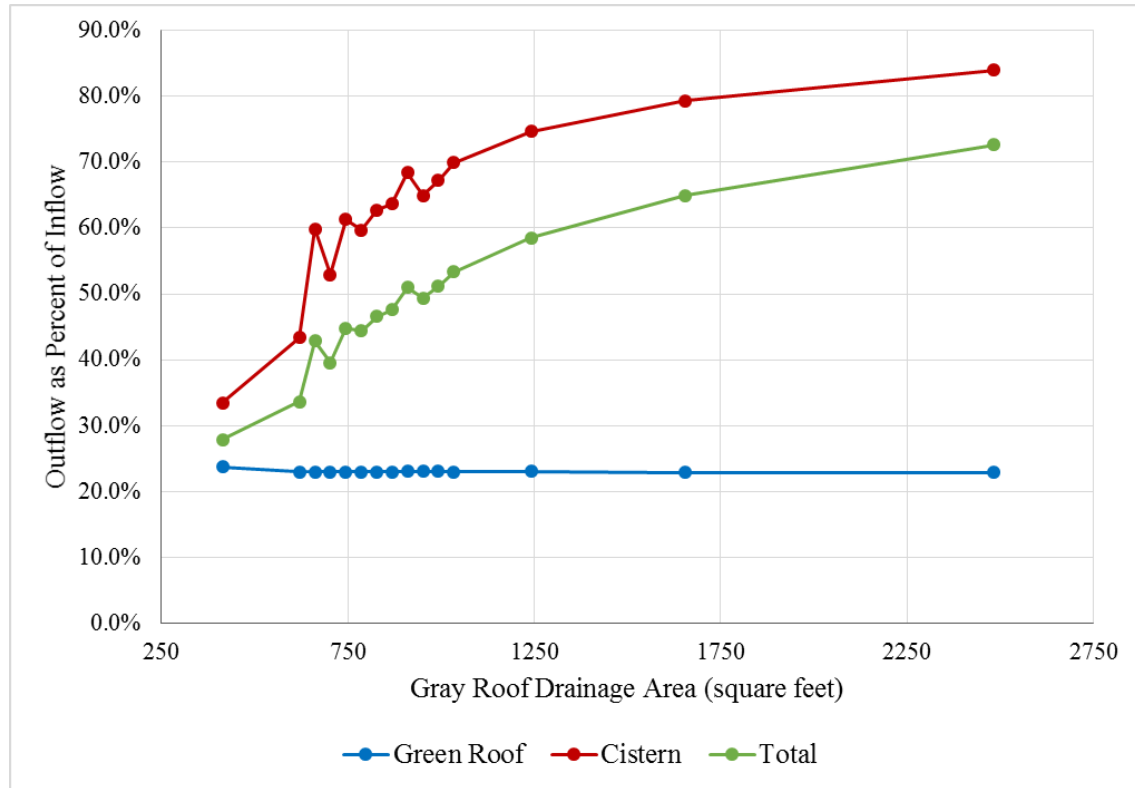


Figure 4.25: Green Roof Outflow as a Percent of Inflow for Varied Drainage Areas

Again the results of the simulation indicate that changes to the drainage area had minimal effects on the performance of the green roof itself, with the outflow to the system staying fairly constant at around 23% of the inflow. The cistern ranged from a minimum of 33.5% to a max of 84.0% representing a large change depending on the capacity of the cistern relative to the drainage area. This again makes sense with the performance benefits of a RTC system being lost as the capacity of the cistern is decreased because even with smart controls, the cistern is limited by the lack of sufficient volume to capture inflows.

In addition to the total inflow and outflow experienced during the simulation, the system was also analyzed specifically for wet weather periods to better understand the hydrologic timing and how the RTC system performed during storm events. To see how the in-storm performance changed with changes to the drainage area, the time during storm events that outflow occurred was summed for both the green roof and the controlled cistern and is reported in Figure 4.26.

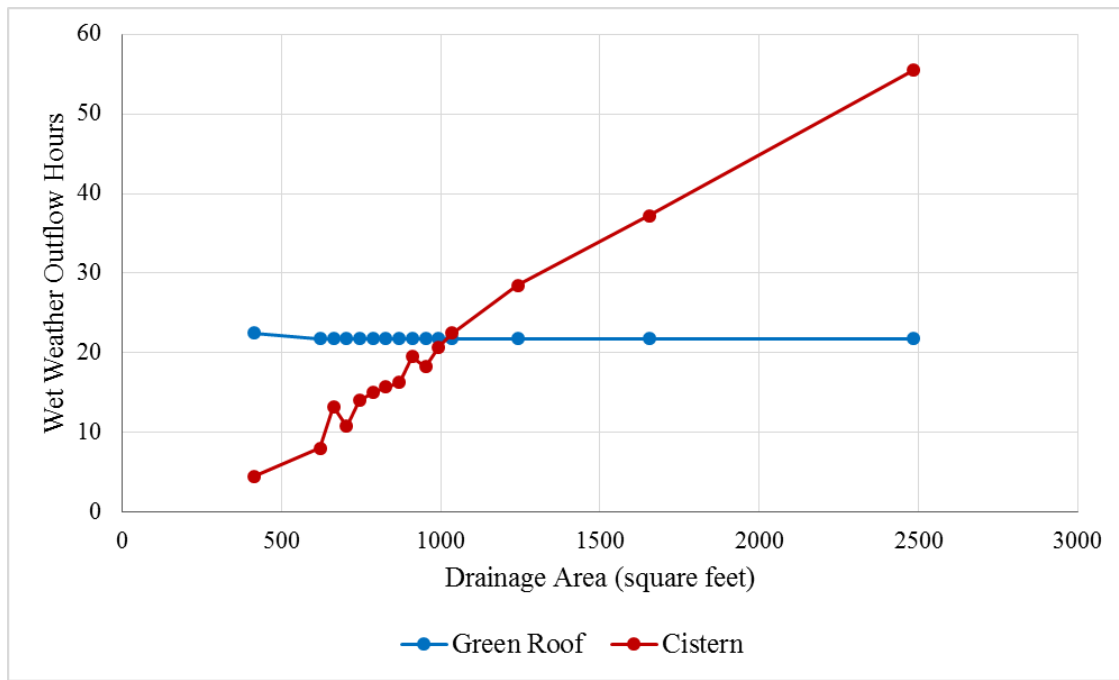


Figure 4.26: Wet Weather Outflow Hours for Variations in Gray Roof Drainage Area

The green roof again sees a constant value reported for wet weather outflow hours for all changes in gray roof drainage area. This indicates that the system was not limited for the different runs by the ability to irrigate the roof (where one might expect to see an increase in wet weather outflow hours), rather maintaining a fairly constant performance throughout the simulation runs. The cistern saw a decrease in performance that occurs fairly linearly as the drainage area increases. This indicates that not only is the total outflow increased when the cistern capacity is reduced, but also the outflow duration experienced during wet weather. These results are notable especially for

CSO communities where the ideal performance would have no outflow to the combined sewers during storm periods in order to avoid overflows. To further examine the performance during storm periods, the volume of overflow that occurred while a storm was happening was also calculated and is displayed in Figures 4.27 and 4.28 as both a total volume and a normalized volume over the watershed area.

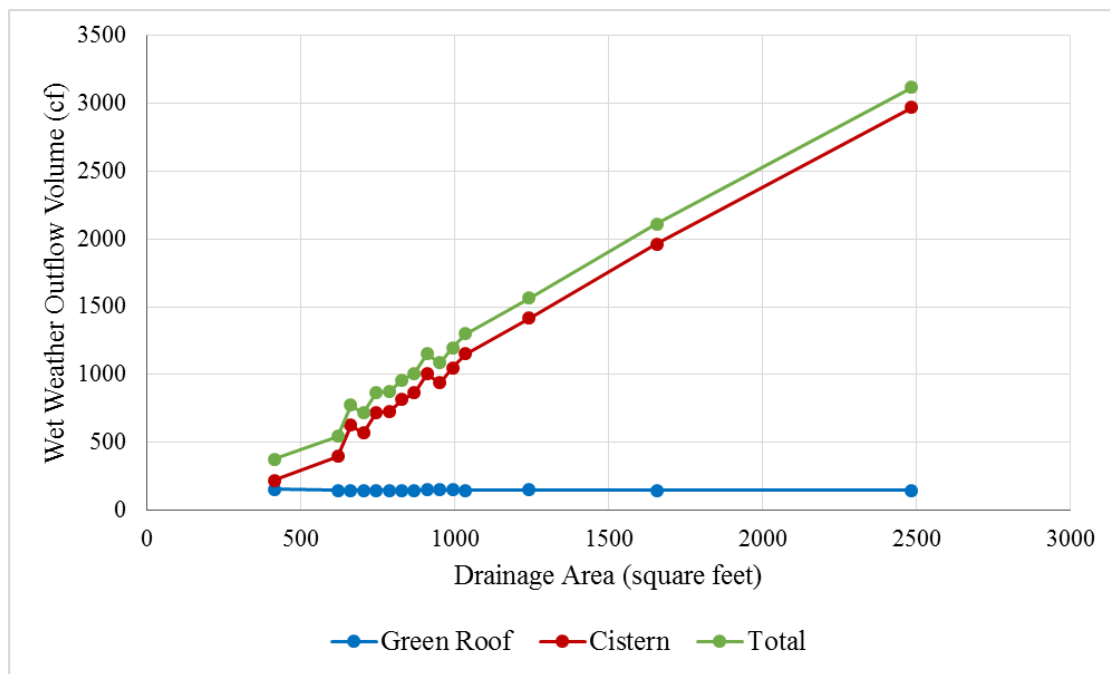


Figure 4.27: Wet Weather Outflow Volume for Variations in Gray Roof Drainage Area

When looking at the wet weather outflow volume as a total volume, an expected linear increase is seen in total outflow from the system as the drainage area increases. This makes sense because after a certain point, the system is limited by the capacity of the cistern and all additional inflow will result in immediate outflow. Looking at the wet weather outflow volume normalized over the watershed area however, the system reaches a limit in terms of outflow where increases in drainage area stop resulting in an equivalent increase in outflow (Figure 4.28).

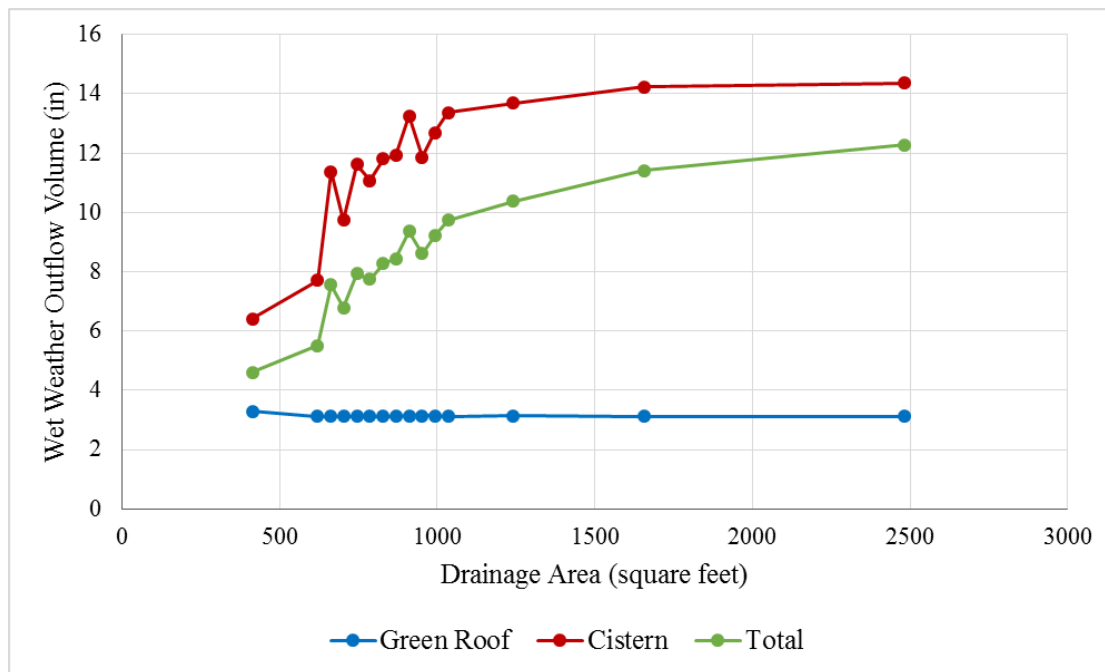


Figure 4.28: Normalized Wet Weather Outflow for Variations in Gray Roof Drainage Area

Figure 4.28 demonstrates how as the drainage area increases and the capacity of the system decreases, the outflow from the cistern begins to level off around 14 inches with the total outflow reaching a maximum of around 12 inches. Again the green roof performance does not substantially change across the changes in drainage area, indicating that the green roof aspect of the system is not limited by an availability of water for any of the scenarios tested.

Overall these results demonstrate the balance that needs to be achieved when selecting a cistern size and corresponding drainage area. While a small drainage area to cistern size ratio would clearly maximize performance (the smallest drainage areas saw the least amount of overflow by all metrics tested), this is clearly not economical when constructing a stormwater control measure. Covering the same amount of drainage area would then lead to many additional cisterns, a cost likely not worth the achieved benefit in performance. Likely the one inch sized cistern currently

being used at the CEER green roof (indicated on all figures by a drainage area of 800 ft²) stands as a good balance with fairly minimal outflow yet still a larger drainage area being captured.

4.4.4: Probability of Precipitation Threshold Sensitivity Analysis

When looking at RTC systems that utilize weather forecasts, one of the most obvious sources of uncertainty in the controls stems from the use of forecasts that clearly lack exact accuracy. In an attempt to improve the use of weather forecasts in RTC stormwater systems, the NWS Probability of Precipitation (POP) is used to determine when forecasts should be acted on. Once a certain pre-defined POP threshold is passed, the system recognizes the storm as an impending event and acts to ensure storage to capture the storm. If this threshold is not passed, no action will be taken related to the storm. To determine what probability threshold to act on and yield the best performance from the CEER green roof system, a sensitivity analysis was performed by altering the POP threshold for action from 10% to 100% chance of precipitation. Figure 4.29 demonstrates the resulting total inflows and outflows from both the green roof and the controlled cistern from the duration of the simulation.

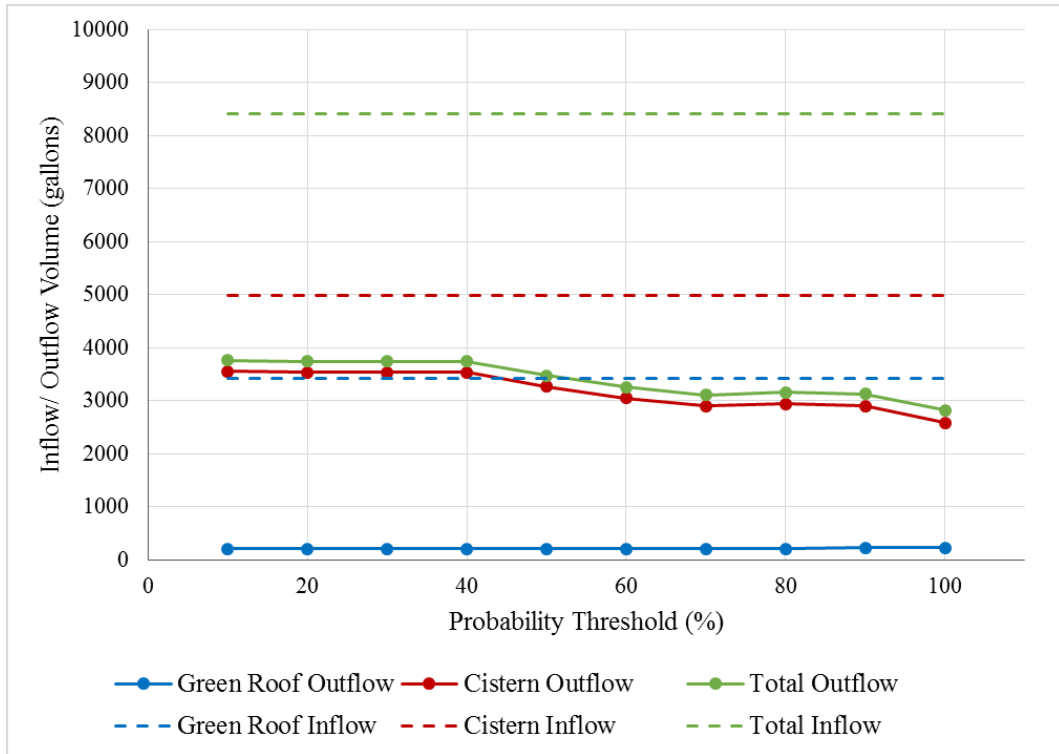


Figure 4.29: Total Inflow and Outflow of Modeled Green Roof System for Variations in POP Threshold

As can clearly be seen in Figure 4.29, the POP threshold at which decisions occur largely does not affect the performance of the green roof system in terms of total outflow. While a slight decrease is seen as the threshold is increased towards 100%, the overall change is minimal. These results can be explained by the use of weather forecasts in the system: forecast based decisions usually just shift outflows from the wet weather window by freeing up storage in the cistern. Therefore, in total the percent of runoff captured and evaporated is not expected to change, rather just the timing at which the outflow occurs. This phenomena is further demonstrated in Figure 4.30 which shows the outflow from each component of the system as a percent of the inflow. While the two components of the system (green roof and controlled cistern) differ in their ability to remove outflows, the values remain relatively constant across the extent of the sensitivity analysis.

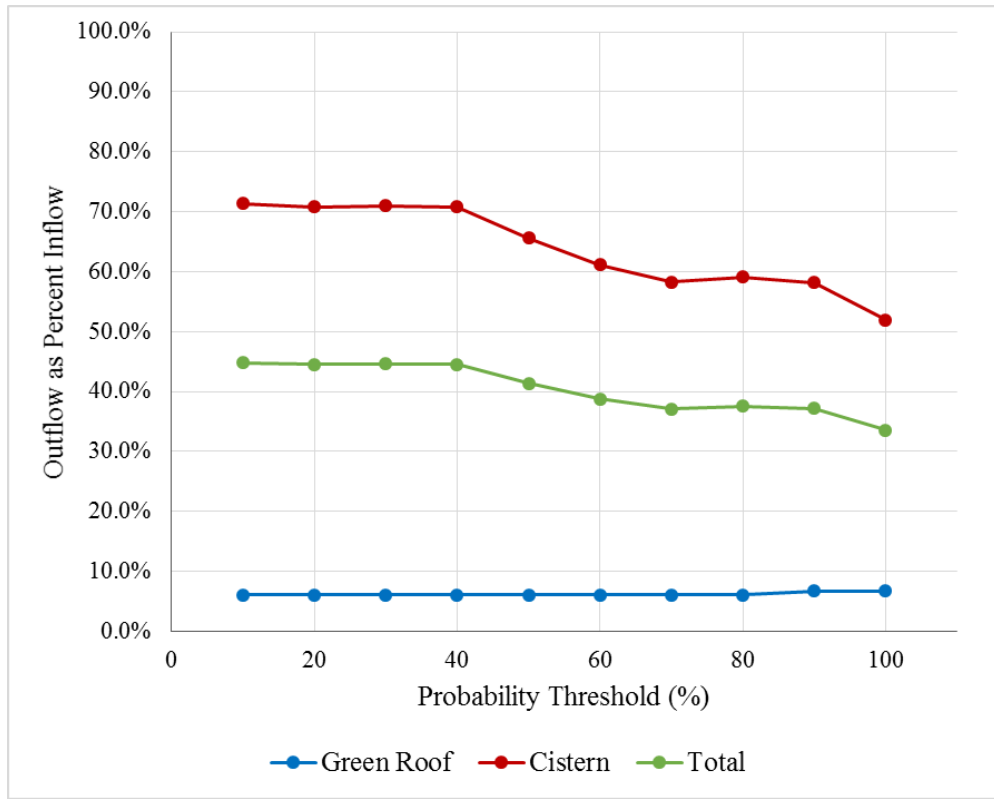


Figure 4.30: Total Outflow as a Percent of Inflow for Variations in POP Threshold

Again when looking at total outflow from the system, minimal changes are seen as the POP threshold is altered. The cistern outflow has the most substantial change, dropping from 71.4% to 52.0% of inflow that is converted to outflow. This drop can be explained by the system more readily acting, both in terms of irrigation to the green roof and drawdowns in preparation for storms, when the probability of precipitation that is deemed acceptable is lower. Despite the slight increase in total capture and evapotranspiration, the major difference between the simulation runs with different POP thresholds comes when analyzing the timing of outflows from the system (a factor more heavily related to the weather forecast based controls). The total hours of wet-weather outflow experienced from both the green roof and the cistern can be seen in Figure 4.31.

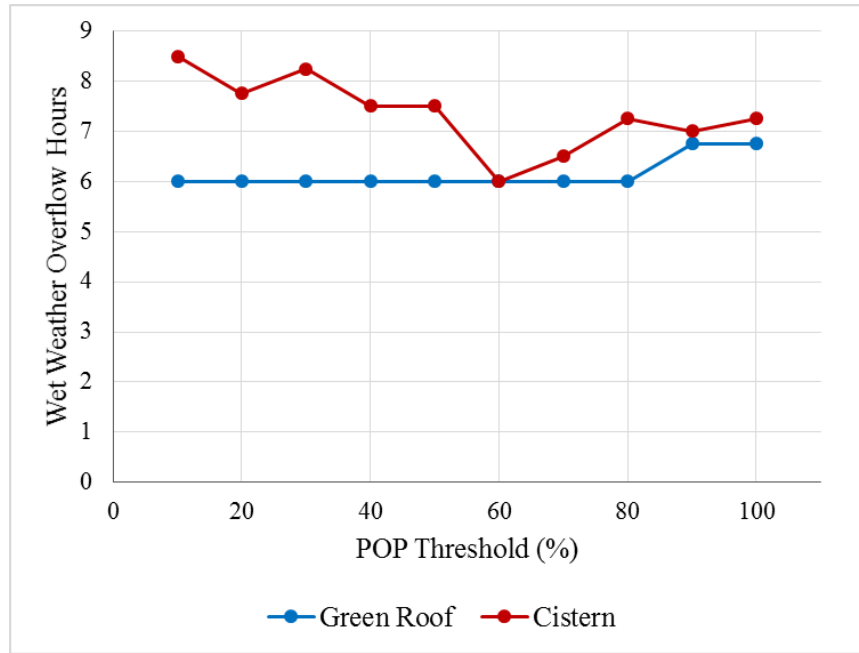


Figure 4.31: Wet Weather Outflow Hours for Variations in POP Threshold

When utilizing weather forecasts, a balance needs to be struck between overly conservative POP thresholds (i.e. 100%) where overflows could occur from a system not acting on enough impending storms and not conservative enough thresholds (i.e. 10%) where outflows are released too easily. In the results of the sensitivity analysis for the CEER green roof system, the POP threshold shown to have the smallest amount of time where wet weather outflow was occurring was 60%. While the outflow from the green roof did not change substantially, the cistern wet weather outflows saw a drop from a maximum of 8.5 hours to a minimum of 6.0, a change of 29.4%. In addition to the timing of outflows from the system, the volume of outflow that occurred during wet periods was also analyzed to better understand how the POP threshold affects the timing and volume of outflows from the system. The total wet weather outflow volume for each of the different simulation runs is shown in Figure 4.32. Green roof outflows were left off Figure 4.32 because they remained at a constant value for the duration of the POP sensitivity analysis.

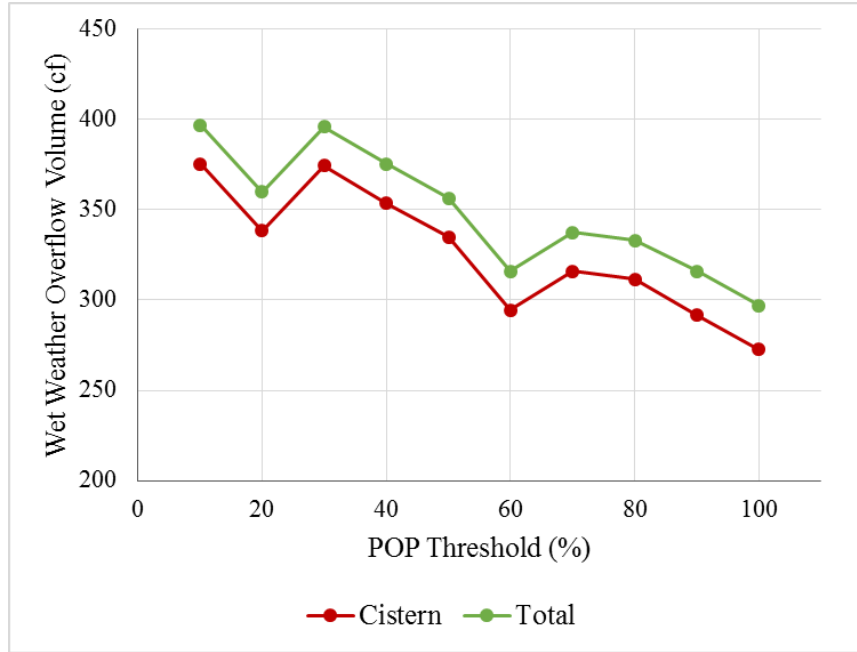


Figure 4.32: Wet Weather Outflow Volumes for Variations in POP Threshold

Overall the lowest wet weather outflow volume seen was experienced when the POP threshold was set to 100%. A local minimum is seen at a POP threshold of 60% again however, which when paired with the results looking at the timing of outflows (Figure 4.31) indicates that a threshold of 60% provides an overall good balance of conservatism when looking at forecast information. Moving forward these simulation results could be used to alter the actual operations of the CEER green roof system, adjusting the POP threshold value so less wet weather outflows are experienced and performance can be optimized.

The results of the POP sensitivity analysis did differ slightly from the POP sensitivity analysis performed in Chapter 2 looking at a simple retention system. For the retention system, ideal performance was achieved at a threshold of 70% rather than 60% POP. These results would indicate that for different system goals, different thresholds may be appropriate for the logic configuration. In the case of the retention system, a balance of conservatism needed to be struck

to maintain a high retention time (achieved by a higher POP threshold) and minimize wet weather outflow (achieved by a lower POP threshold). In the case of the green roof, retention time was not a factor considered in performance. This likely contributed to a lower POP threshold being appropriate when considering ideal performance. Overall the CEER green roof represents a complex case where factors such as irrigation, evapotranspiration, and controlled storage work together to create an effective stormwater management system making the different ideal POP threshold unsurprising. For most simple cases (such as the hypothetical systems described in Chapter 2), a threshold of 70% is still appropriate.

4.5 Conclusion

The results of the study overall point to real-time control being an effective way to retrofit existing green infrastructure to increase the capacity of the system. This was demonstrated initially by comparing the performance of the original CEER Green Roof to the retrofitted and controlled smart Green Roof which included a substantial increase in contributing drainage area. Despite the increase in drainage area, an overall increase in performance was noted. This again points to the ability of RTC systems to manage larger watershed areas because of the increased adaptability and control provided with real-time systems. When looking at the outflow normalized over a watershed basis, a 30.7% decrease in outflow volume was noted while a 7.50% increase in capture volume was seen. While this increase in benefit seems fairly minimal, when looking at the total volume (rather than normalized over the watershed area) the changes are even more dramatic with a 157% increase in capture volume. While the total overflow volume did see an increase in the simulation when RTC was implemented (67.4%), the benefits are still clear due to the substantially larger drainage area being treated by the system when the RTC was included.

In addition to the baseline comparison of a passive and RTC green roof system, a sensitivity analysis was performed to see how different key parameters included in the RTC design affect the performance of the green roof. For this study the parameters analyzed were the soil moisture irrigation threshold, the drainage area and capacity of the controlled cistern, and the probability of precipitation threshold. For the performance of the green roof (independent of the controlled cistern), the soil moisture threshold had the highest effect on the ability of the green roof to capture storm events. For the other two parameters analyzed, the effects were seen more magnified in the performance of the controlled cistern and its ability to shift flows out of the wet weather window. When choosing design parameters for systems like the CEER green roof, priorities need to be established in order to achieve the desired performance. For example, with the CEER green roof, outflow from the cistern could be minimized by increasing the soil moisture threshold, however this results in a corresponding decrease in green roof capacity. For the purposes of this study, priority was given to maintaining the capacity of the green roof during rain events, giving preference towards utilizing the green infrastructure component of the system rather than just the cistern.

4.5.1 Design Recommendations

In analyzing the results of the modeling simulations for the CEER green roof, one of the key focuses was maintaining the performance of the green roof during storm events. This expressed itself as a minimization of wet weather outflow, both in terms of total volume and in timing, from the green roof over the length of the simulation. In addition, the total capture of the system was analyzed to see the amount of runoff that was ultimately removed from the storm sewers by the evapotranspiration potential of the green roof. Because the RTC retrofit was completed to harness

this evapotranspiration potential not being utilized during dry periods, this was another significant factor in determining ideal design parameters.

When looking specifically at the CEER green roof being studied, several design recommendations can be made based on the results of the multiple sensitivity analyses in order to improve the overall performance of the system. The first parameter analyzed was the soil moisture threshold used to determine when it would be appropriate to irrigate. Determining this value requires a balance of both conservatism towards maintaining green roof capacity while still irrigating enough to utilize the runoff being stored in the controlled cistern. The results of the sensitivity analysis indicate that the current soil moisture threshold at 16% is likely lower than it needs to be, with a threshold at a higher value such as 20% being a better candidate to fully utilize the stored runoff in the cistern while still maintaining the capacity of the green roof.

In addition to the soil moisture threshold, the POP threshold was also examined for trying to optimize the control decision process of the system. The results of the sensitivity analysis indicate that a 60% POP threshold stands as the best value to balance the need to be conservative with acting on impeding storm events while still providing enough ability to prepare for impending storm events. An intermediate value like 60% makes sense with what is expected, the relatively high number stopping the system from acting on too many low probability events that likely will not happen while the 40% of actionable POP values still giving the system a large window for preparing for storms. Similar to the soil moisture threshold, this value is an easy design parameter to change and gain performance improvements from without needing to make alterations to the physical site setup. While this differs slightly from the ideal threshold discussed in Chapter 2 (70% POP), the different goals and configuration of the system cause the ideal threshold to change from the simple retention case.

The last aspect of the system to be analyzed in the sensitivity analysis was the drainage area, changes to the gray roof drainage area designed to reflect changes to capacity in the controlled cistern. Unlike the other parameters analyzed, less of a balance needs to be struck from a performance basis when looking at the cistern capacity with a larger cistern capacity (i.e. smaller drainage area) clearly resulting in better performance. Rather the balance with the cistern capacity is from a more economic standpoint, trying to get a maximized performance benefit from the cistern without investing in too large a piece of infrastructure. While the largest capacity cisterns clearly have the best performance, a one inch sized cistern (what is currently in place at the site) was shown to still be on the better end of performance with enough capacity that the irrigation of the green roof was not limited by a lack of stored runoff.

4.5.2 Future Work

Moving forward with the analysis of the CEER green roof smart system from a modeling perspective, additional work can be done to ensure that the system is working at its most optimized potential. While the model was calibrated with the recorded data available, mostly from the perspective of the passive system, once more data collection has been completed for the RTC system the model should be further validated in order to ensure that the SWMM model accurately represents what is physically happening in the system. Calibration done in this study showed a high correlation between the model and the passive green roof in terms of outflow and evapotranspiration, however the inflow and outflow to the controlled cistern lacks substantial analysis at this point. Additionally, if the soil moisture meters present in the green roof media become more reliable, this could provide another point of comparison to further validate that the RTC model is performing correctly.

In addition to further validating the model, additional runs can be done to see how the system can be further isolated. The current sensitivity analysis relied on looking individually at three different parameters: the soil moisture irrigation threshold, the drainage area, and the probability of precipitation threshold. This allowed for ideal thresholds and parameters to be chosen for the system as it currently works, however having a calibrated model of the system allows for even further experimentation with the setup of the system. Many of the ideas presented in Chapter 3 (an overview of publically available climate data that could be included in the logic of smart stormwater systems) could be applied to the SWMM model of the smart green roof in order to test ideas before implementing them. These include using the Standardized Precipitation Evapotranspiration index to change thresholds based on the level of dryness.

While the modeling study performed in this study was created to be highly specific to the CEER green roof currently being studied at Villanova University, the ideas presented could easily be applied to other smart systems and RTC retrofits. The forecast-based control aspects developed to model the OptiRTC logic could be applicable to any controlled storage unit and could easily be applied to models of other stormwater control measures. Additionally, a better understanding of how control logic thresholds affect the performance of a site should clearly be a focus as more smart systems are designed and implemented in stormwater management. Optimizing these parameters offers a way in which performance benefits from the system can be gained without any additional expenses or physical changes to a site.

CHAPTER 5: PERFORMANCE OF REAL-TIME CONTROLLED SYSTEMS

5.1 Introduction

Throughout the study, the idea of smart stormwater networks that utilize a combination of green infrastructure and real-time control has been discussed. While trying to achieve optimal performance of these systems, it is important to look at smart systems already deployed in order to better understand how they are functioning and performing. At Villanova University's campus, multiple stormwater control measures have already been retrofitted with RTC in order to create smarter control of stormwater management and stand as examples of how green infrastructure can utilize RTC to become smarter, more adaptive systems. Two such systems in particular are to be assessed for performance for the time since the retrofits of the SCMs occurred in early 2016: the CEER green roof and the Saint Augustine Center Treatment Train. With substantial study of both sites already completed prior to the retrofits as smart systems, a point of comparison already exists for the baseline performance of the sites. Both sites also have in common the addition of impervious drainage area when the retrofits occurred with the goal being to manage greater contributing drainage areas with the same green stormwater infrastructure ground footprint.

Looking at the performance of the CEER green roof and the Treatment Train, several different performances indicators were considered. For both systems, the ability to capture storm events and add volume removal stood as the main indicator of performance. While existing data provided the pre-retrofit system's abilities to capture different storm volumes, the new comparison was done in the context of the retrofitted system with increased drainage area. The CEER green roof saw an increase from 576 ft² to 1376 ft² while the Treatment Train saw an increase from 10,000 ft² to 14,000 ft². In addition to the storm capture, the control of the CEER rainwater harvesting cistern

was assessed and a sediment analysis was completed within the Treatment Train to better understand the morphology of the SCM. All these analyses work together to demonstrate how the two smart systems are performing and provide baseline results to help enact future improvements to the systems.

5.2 Literature Review

The two systems analyzed in this study are the CEER green roof, a green roof SCM, and the Treatment Train, a bioinfiltration SCM. As discussed in previous sections (Section 1.1), both green roofs and bioinfiltration systems stand as effective ways to manage stormwater from both a volume capture and water quality standpoint (Hunt et al. 2006; Mentens et al. 2006; Lord et al. 2013; Dominique et al. 2014). The two systems specifically studied here have also been shown to be effective stormwater control measures from a volume capture standpoint, both systems studied extensively as passive systems before being retrofitted with real-time control (Wadzuk et al. 2013; Zaremba 2015; Lewellyn 2015; Zaremba et al. 2016; Lewellyn et al. 2016). With the promise of real-time controlled systems improving and changing the way stormwater infrastructure operates (Kerkez et al. 2016), these specific systems have been altered to reflect smarter systems that rely on continuous monitoring and adaptive controls to more effectively manage urban runoff.

5.3 Methodology

5.3.1 Project Description

The two smart systems monitored in this study were the CEER green roof and the Saint Augustine Center Treatment Train. A full description of both sites can be found in Sections 1.2.1 and 1.2.2. Both systems rely on additional storage to increase the total capture of SCM as well as a real-time controlled pump to utilize the stored water during dry inter-event periods. Standing as examples of how intelligent storage can be used to more fully utilize the hydrologic functions of green infrastructure, analysis of the systems is important for understanding the benefit and moving forward with design of these smart systems. Figures 5.1 and 5.2 show an overview of the two systems discussed.

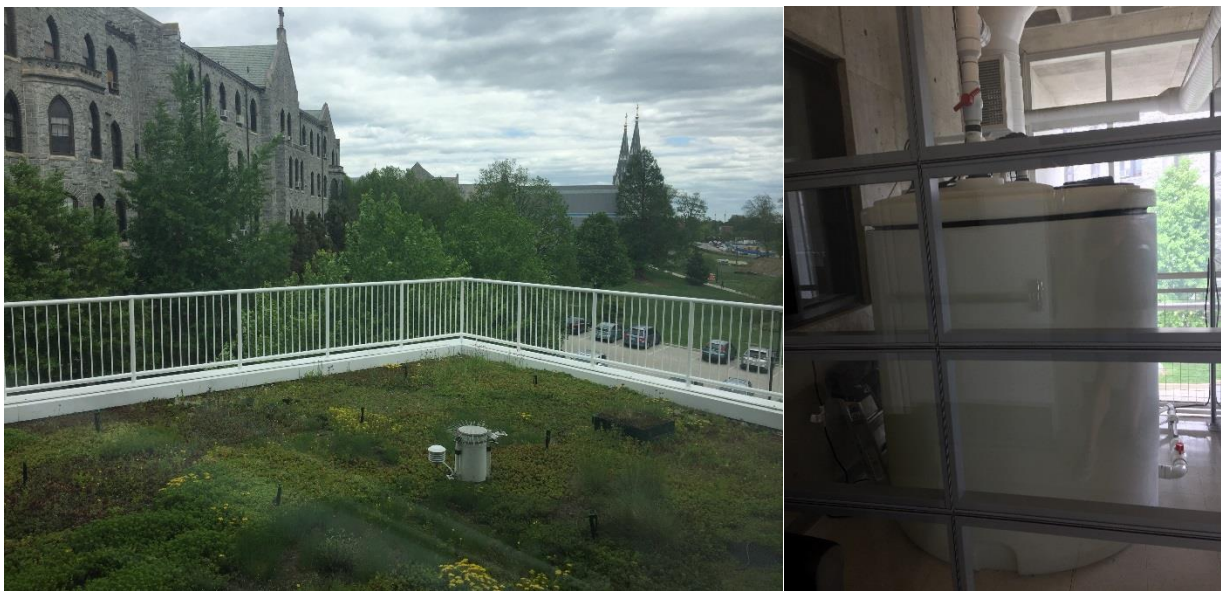


Figure 5.1: CEER Green Roof and Controlled Cistern

The CEER green roof system operates by capturing runoff from an impervious section of the CEER building, storing it in a cistern that is controlled using a pump and actuated valve, and utilizing the stored runoff to irrigate the green roof during dry periods. The cistern operates

independently to drain down and create storage for impending storms, pumping water as needed to the green roof when capacity is available. As described in Section 1.2.1, the goal of the system is to utilize the full evapotranspiration potential of the green roof without decreasing the overall capacity of the system.



Figure 5.2: View of Treatment Train from Lower Rain Garden

The Treatment Train is a stormwater system that combines several SCMs in series to increase capture and promote infiltration. The train is comprised of two bioswales, two rain gardens, underground storage cisterns, and an infiltration trench. Real-time controls are applied to the underground storage using a pump to route stored runoff back to the beginning of the system during dry periods when infiltration capacity is available in the bioinfiltration portions of the system.

Again weather forecasts are used along with real-time sensing and monitoring in order to create the smart infrastructure.

In the period since the smart systems were online, rain gage data has been recorded using a tipping bucket rain gage located on the roof of the CEER building. Because rainfall is clearly the driving variable in understanding the performance of stormwater sites, having a complete record of rainfall is important for analysis of the smart systems. Figure 5.3 shows the storm events experienced from June 2016 to July 2017, events defined as rainfall periods separated by six or more dry hours.

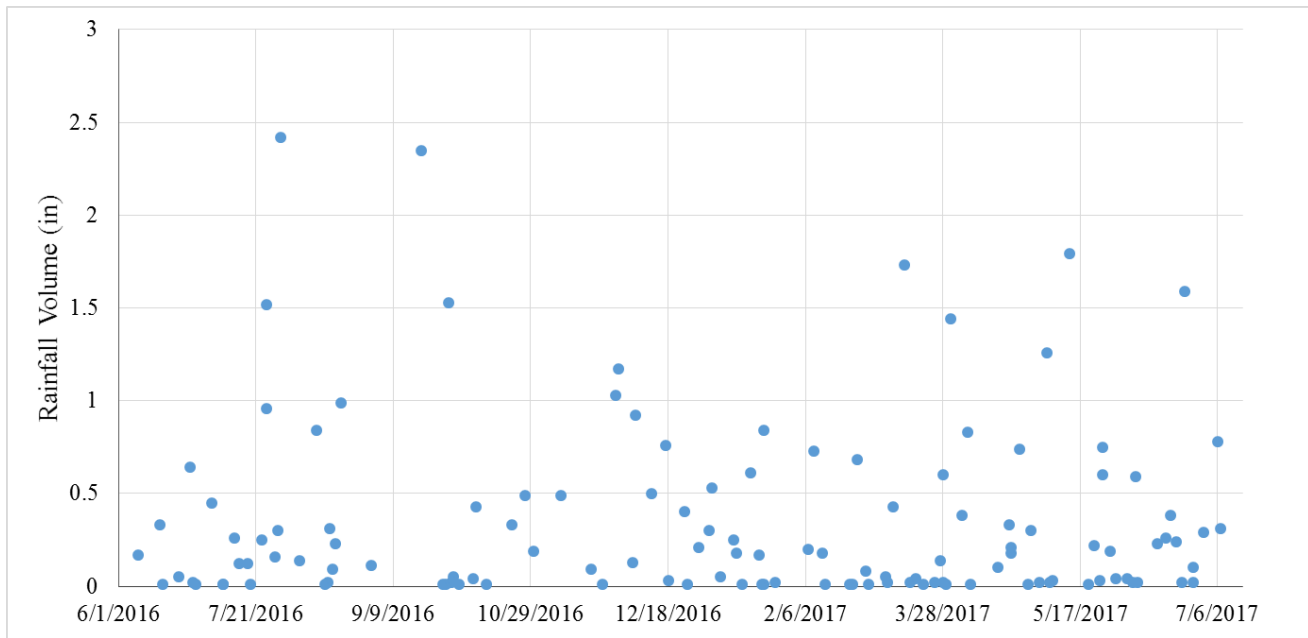


Figure 5.3: Rainfall Events from CEER Roof Rain Gage, 6/1/2016 to 7/12/2017

Clearly there exists a wide variety of storms to look at in the analysis of the green roof and Treatment Train performance, the record including two storms above 2.0 inches (5 cm), seven storms above 1.5 inches (3.8 cm), and 11 events exceeding 1.0 inches (2.5 cm). In total 44.14 inches of rainfall was recorded at the site. Understanding the smart infrastructure response to storm

events in the context of total storm volume is a crucial component moving forward with the performance monitoring of sites.

5.3.2 Site Monitoring

Both the CEER green roof and the Treatment Train are heavily equipped with monitoring equipment so the performance of the systems can be quantified. The monitoring relies on the OptiRTC cloud platform which constantly monitors and reports data collected on site. A full list of parameters monitored at both the green roof and Treatment Train are shown in Table 5.1.

Table 5.1: Green Roof and Treatment Train Site Instrumentation

Parameter	CEER Green Roof		Treatment Train	
Rainfall	x			
Air Temperature	x			
Relative Humidity	x			
Soil Moisture	x	Green Roof Media (8)	x	Rain Gardens (2 shallow, 2 deep), Bioswales (2 shallow, 2 deep)
Soil Temperature	x	Green Roof Media (4)		
Water Level	x	Cistern	x	Cisterns, Weir Box, Rain Gardens (2), Bioswales (2)
Water Temperature	x		x	
Inflow			x	V-Notched Weir
Outflow	x	Tipping Bucket and Thelmar Weir		

Using the data collected from the monitoring equipment displayed in Table 5.1, a comprehensive look was able to be taken at the performance of the systems throughout their lifespan as a real-time controlled system. The combination of weather station data giving the driving hydrologic

conditions as well as in-situ measurements provide a substantial data set to be used in the analysis of both the green roof and Treatment Train performance.

5.3.3 Sediment Grain Size Analysis

One aspect of the performance analysis for the Treatment Train centered on morphology of the system and the changes to sediment characterizations seen throughout the SCM. A visual inspection of the site completed in February 2017 revealed distinct areas of erosion and deposition within the Treatment Train (Figure 5.4), which were selected as sampling locations for measuring the mean grain size of sediments present. The goal of this portion of the study was to understand how the morphologic changes were occurring within the Treatment Train and relate these changes to the system performance. While observation of changes in sediment characteristics will take further time, baseline values were established (February 2017) and reassessed in May 2017.



Figure 5.4: Sample Zones of Erosion (Left/ Center) and Deposition (Right)

Mean grain sizes were determined by taking a surface sample of sediments from each sampling locations identified and performing a sieve analysis of the sample following ASTM C136. Samples were taken by lightly scraping the surface of the soil media, attempting to obtain representative samples of the sediments seen throughout the Treatment Train. Figure 5.5 shows the locations of sampling throughout the Treatment Train as well as the observed process in each location (i.e. erosion or deposition). Long-term changes, especially in areas noted for erosion or deposition visually occurring, will be examined to see the stability of the structure and how the system could be expected to change through a project lifecycle.

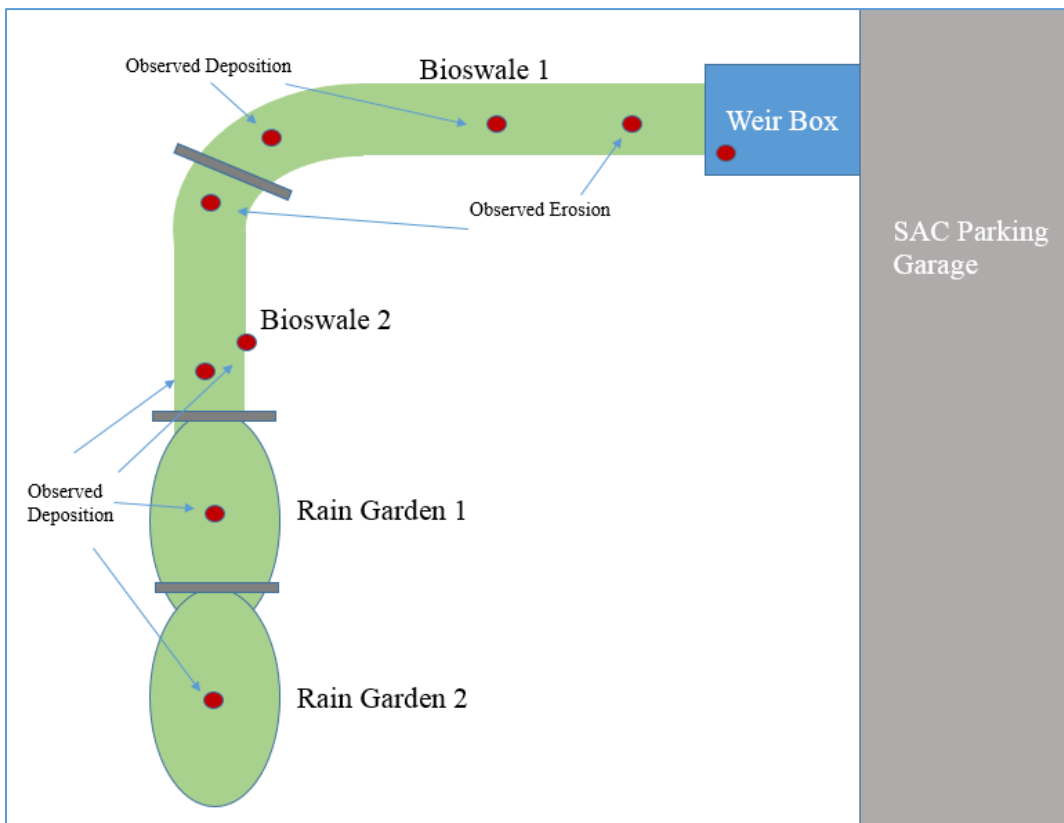


Figure 5.5: Sediment Sampling Locations within Treatment Train

Samples collected from the surface of the weir box (a concrete box that provides flow measurement and conveyance into the first bioswale) provide a baseline of particles that are entering the system

through runoff from the parking deck. Each subsequent sample allows for the changes that occur throughout the system, with larger particles expected on the surface of zones showing erosion and lower mean grain sizes in zones of deposition.

5.4 Green Roof Results

5.4.1 CEER Green Roof Performance

In analyzing the performance of the CEER green roof, one of the primary objectives was to ensure that outflows from the green roof did not occur for storm events of a manageable size. The original design of the green roof planned for the first 0.5 inches of rainfall to be captured. Previous analysis of the green roof, however, has indicated that storm events equal to 0.8 inches or less should result in negligible outflow from the roof, so this value was taken as the standard to compare against when looking at the newly retrofitted green roof with smart capabilities. Table 5.2 shows all events from June 2016 to July 2017 (the period where smart irrigation was occurring) that resulted in overflow. Green indicates overflow that would be expected to occur based on previous study of the roof, yellow shows events that were between the design capacity (0.5 inches) and the observed capacity (0.8 inches), and orange reflects overflow events from rain events less than the design capacity of 0.5 inches.

Table 5.2: Green Roof Rain Events with Outflow

Event Start Date	Total Rainfall Volume
7/31/2016	2.42
8/21/2016	0.99
9/19/2016	2.35
9/29/2016	1.53
10/9/2016	0.43
10/27/2016	0.49
11/9/2016	0.49
11/29/2016	1.03
11/30/2016	1.07
12/6/2016	0.92
12/12/2016	0.5
12/17/2016	0.76
12/24/2016	0.40
12/29/2016	0.21
1/2/2017	0.53
1/12/2017	0.43
1/18/2017	0.61
1/22/2017	0.84
2/9/2017	0.73
2/12/2017	0.18
3/14/2017	1.73
3/27/2017	0.76
3/31/2017	1.44
4/4/2017	0.38
4/6/2017	0.83
4/26/2017	0.74
5/5/2017	1.26
5/13/2017	1.79
5/25/2017	1.35
6/24/2017	1.59

For the 13 month period analyzed, 30 overflow events were recorded for a total of 126 events registered by the CEER rain gage. While overall this reflects good performance of the system, there were still eight rainfall events less than the design capacity of 0.5 inches that resulted in outflow, indicating that some capacity of the green roof has been lost. To better understand patterns

associated with the overflow events, a time series was created showing both captured and overflow events throughout the year (Figure 5.6).

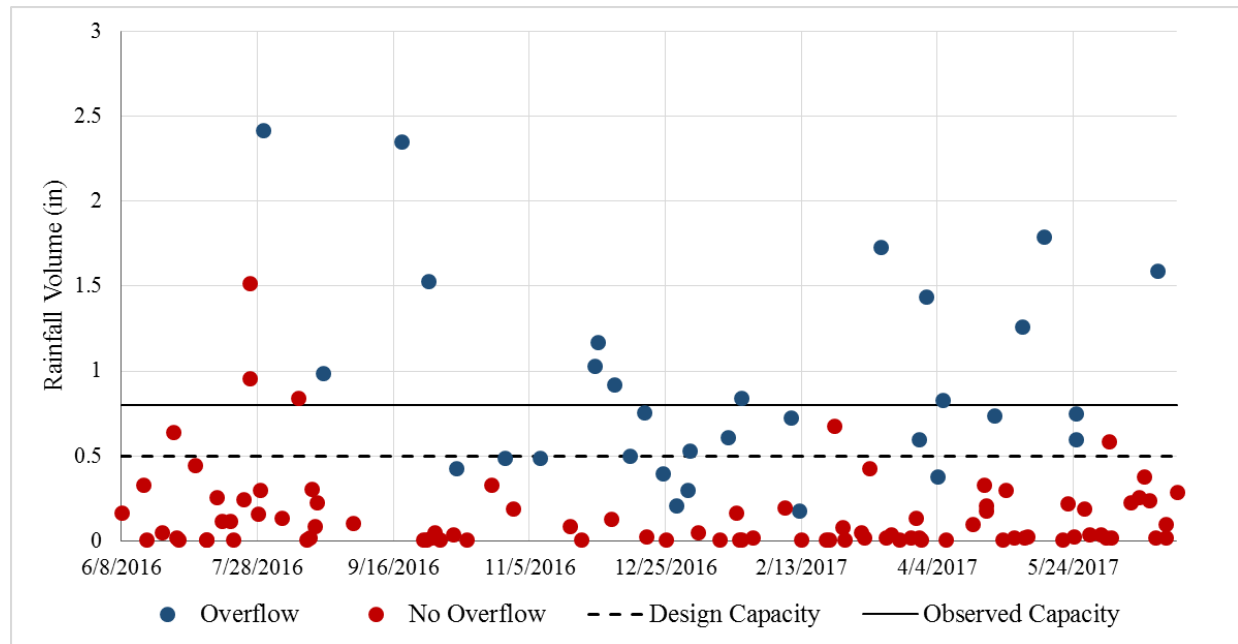


Figure 5.6: Storm Event Performance of Smart Green Roof

Figure 5.6 indicates that some of the overflow trends seen in the green roof are seasonal, with the majority of the outflow events below design capacity occurring during the winter season. During this period the smart irrigation portion of the green roof system was not operating (see winterized state in Figure 5.7), so this indicates that other factors were influencing the performance deficit seen in the system. A likely cause would be the lower ET potential experienced during winter (potential evapotranspiration is a function of temperature and plants, the driver for transpiration, are dormant during the winter), resulting in the green roof taking longer to remove ET available soil moisture between storm events. This paired with the high frequency of events seen in December 2016 (8 storms greater than 0.05 inches within the month compared to an average of 6 storms per month on record) likely caused the underperformance of the system.

The performance of the system when dewinterized (before December 2016 and after April 2017) shows promise for the smart system. Only one event (April 4, 2017) resulted in overflow that was below the design capacity and just five resulted in overflow that were below the observed capacity of 0.8 inches. When taking into consideration the 139% increase in drainage area that occurred with the retrofit, this performance indicates that the system is overall managing the watershed well. When it is considered that any rainfall event resulted in outflow from the pre-retrofit system from the impervious CEER roof now being captured, even having just five overflow events from rainfall volumes less than 0.8 inches indicates an improvement in the ability to capture runoff.

5.4.2 Controlled Cistern

Another aspect of the green roof system to be assessed is the controlled cistern, a piece of gray infrastructure that relies on weather forecasts and controls to route stored rainwater to the green roof and avoid outflows during wet weather. The ability for the cistern to create storage for impending events was analyzed by looking at the volume in the tank over time as rain events happened. Figure 5.7 shows the full set of water surface elevation data available for the period on record where the green roof operated as a smart system.

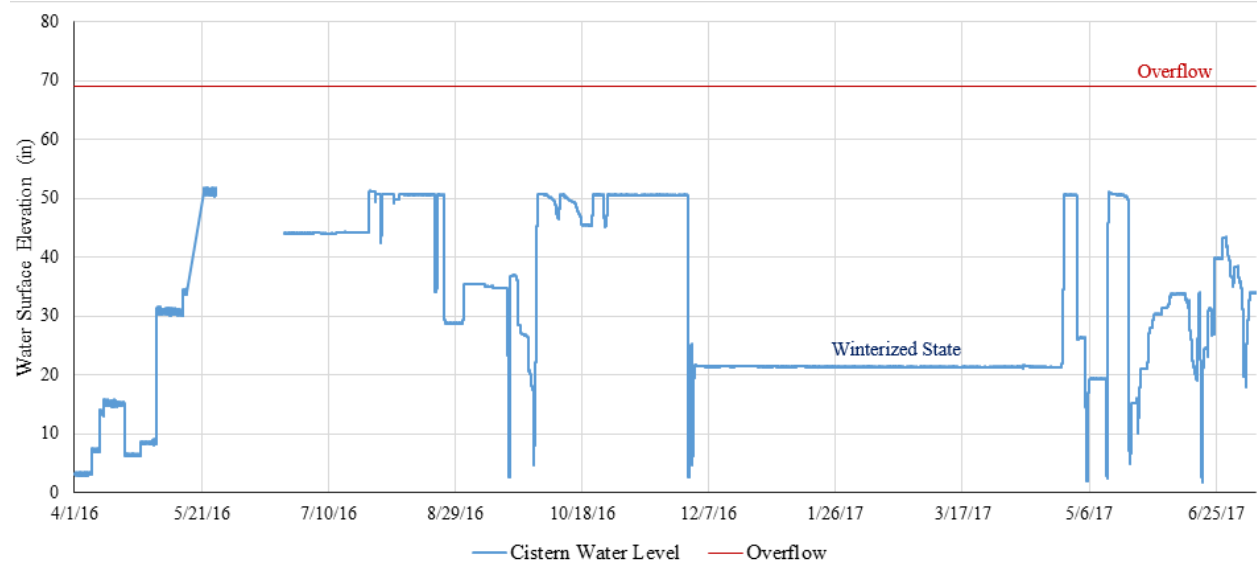


Figure 5.7: CEER Cistern Storage, 4/1/16 to 7/10/2017

Results of the system thus far have shown no overflows caused to the cistern. Currently target volumes for the storm in inter-event periods is set at 75% of the total volume, explaining why typical volumes rest below the full capacity of the system. The cistern is sized for a one inch storm over the added impervious area and a number of storms on record far exceed an inch of volume (Figure 5.4), so this indicates that not as much flow as expected is entering the cistern on a regular basis. Drawdowns prior to storm events, especially those that have occurred in 2017 since the system has been de-winterized, have shown to overestimate the inflow volume resulting in the cistern storing less than full capacity. Moving forward the drainage area needs to be investigated entering the cistern in order to have full capacity of the system. Figure 5.8 demonstrates the period after dewinterization in 2017 when the difference between expected and experienced inflow volume seems to differ substantially (i.e., when the cistern water level does not return to 51 in).

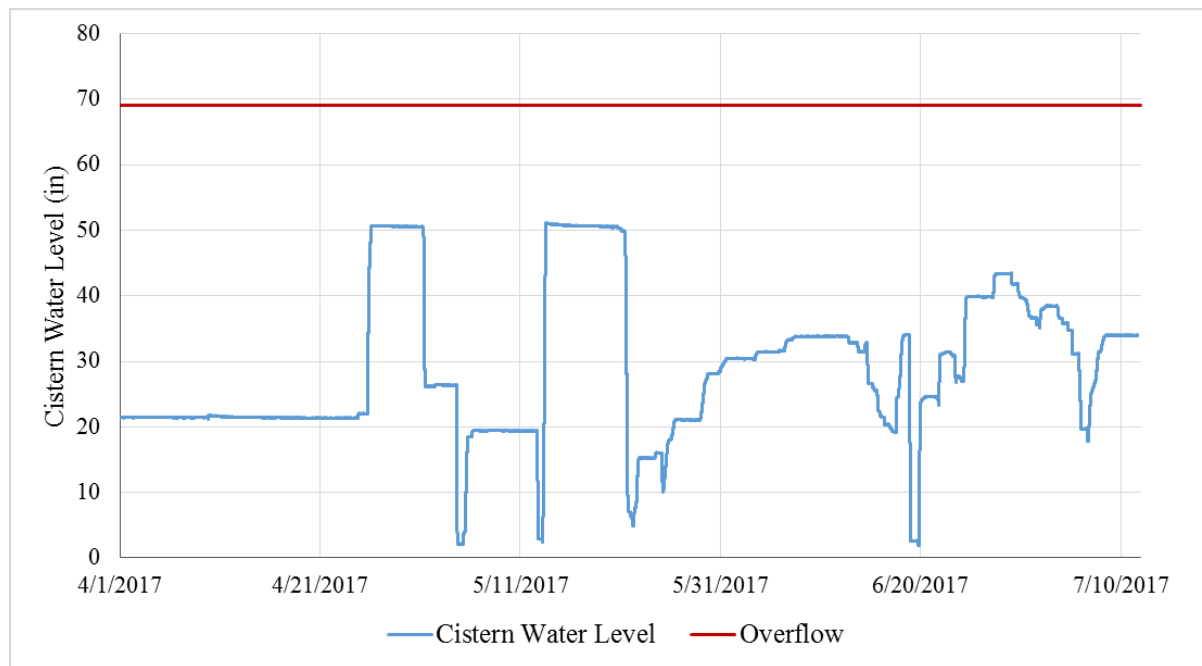


Figure 5.8: April 2017 to July 2017, CEER Cistern Water Level

While the discrepancy between expected and observed inflow has helped result in no overflows from the CEER cistern, it is still problematic in that the cistern is being underutilized and not providing the expected benefit, as modeled in Chapter 4. Again this discrepancy should be investigated more and steps taken to ensure that the full drainage area of the CEER impervious roof is being routed to the controlled cistern. Not only will this increase capture from the impervious areas of the roof, but it will also ensure sufficient stored water to provide irrigation benefits to the green roof.

5.5 Treatment Train Results

5.5.1 Treatment Train Storm Capture

When monitoring the performance of the Treatment Train, one of the most important aspects of the performance was the ability of the system to capture storm events and reduce the amount of

overflow that occurs to the downstream storm sewers. In measuring the SCMs ability to capture storm events, the number of overflow events were compared to the storm events experienced at the site since the retrofit to include real-time control. Figure 5.9 demonstrates the water surface elevation in the infiltration trench (the last point before overflow of the system) for the available record. Overflow from the infiltration trench is designed to occur when the water surface reaches an elevation of 4.2 feet, however overflows have been observed to occur from the system when the water level is slightly lower at 4.1 feet. Both possible overflow points were considered when analyzing the water surface elevations of the infiltration trench throughout its monitoring history.

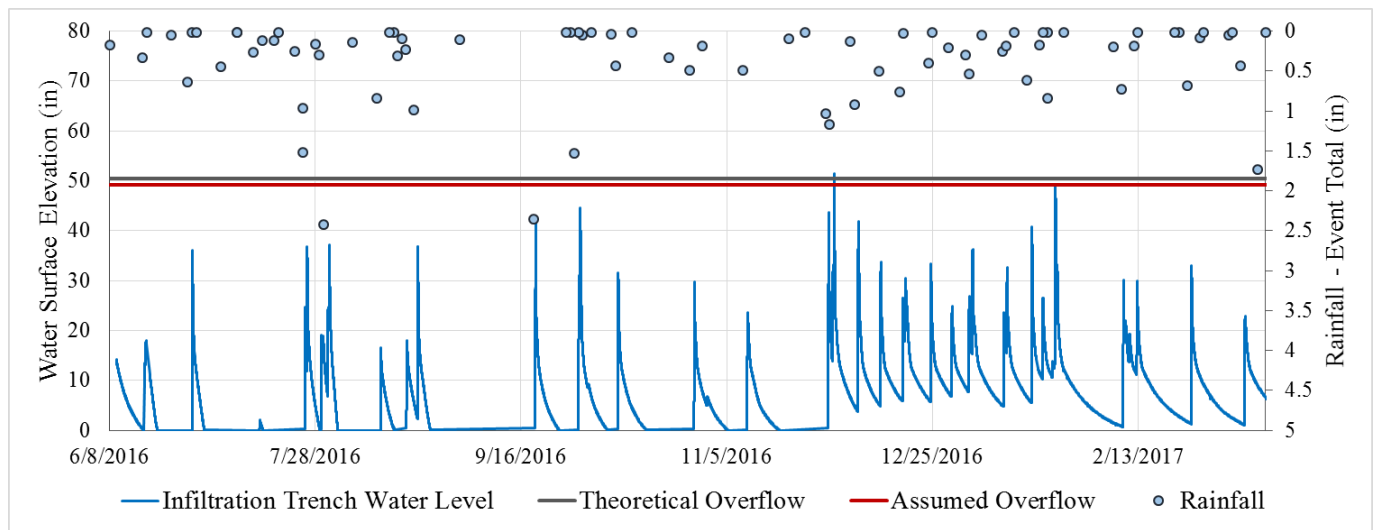


Figure 5.9: Water Elevation in Treatment Train Infiltration Trench, 6/9/2016 to 3/15/2017

As can be seen in Figure 5.9, the Treatment Train maintained its volume capture ability throughout its existence as a smart system. Previous examination of the Treatment Train (prior to retrofit – Figure 5.10) has indicated that the predicted capacity of the system is vastly underestimated, with most large events reporting more substantial capture than expected. The performance as a smart system continues to reflect this trend with only one overflow event observed despite 11 events exceeding the design capacity of one inch. The results also show seasonal trends experienced with

the Treatment Train, with performance in July far exceeding the design capacity. The one overflow that did occur was in December, a period where slower infiltration rates could be expected due to the change in temperature and corresponding increase in viscosity.

In total 80 events occurred (with the precision of the rain gage used measuring any event that exceeded 0.01 inches of rainfall) since the Treatment Train's history as a smart system, again with just one overflow from an event with a total rainfall volume of 1.17 inches, which directly followed a previous event of 1.03 inches for a total rainfall volume of 2.20 inches occurring over two days.

While the minimum event separation time of six hours still occurred (12 hours of dry time separated the two events), this still reflects a substantial amount of rainfall in a short period of time, making an overflow not unwarranted. To better understand the response of the Treatment Train to different rainfall events, several of the larger events were isolated and examined for storm statistics, as shown in Table 5.3. Events chosen represent when overflow occurred (the 11/30/2016 event) as well as other events that resulted in near-overflows spanning a large portion of the year.

Table 5.3: Storm Statistics for Major Rainfall Events at Treatment Train

Storm Start Date	Rainfall Volume (in)	Event Duration (hours)	Peak Hourly Intensity (in/hr)	Average Intensity (in/hr)	Peak Infiltration Trench Level (in) *
7/30/2016	2.42	17	1.44	0.14	37.2
9/29/2016	1.53	32	0.26	0.048	44.6
11/29/2016	1.03	15	0.22	0.069	43.7
11/30/2016	1.17	15	0.29	0.078	51.4
1/22/2017	0.84	41	0.15	0.012	49.0

* Overflow assumed to occur at 49.2 inches

It is clear in Table 5.3 that there are a variety of factors that affect the ability of the Treatment Train to capture storms ranging from storm duration to intensity and time of year. It is clear that seasonal trends have a substantial role, the two highest elevations the infiltration trench reaching in November and January (despite the January 22nd storm having a storm volume of 0.84 inches). This would indicate that infiltration capacity plays the largest role in the Treatment Train's ability to manage storms, which further ties into duration affecting the system. The second longest duration storm analyzed resulted in only 44.7 inches for peak infiltration trench level, despite having 1.53 inches of rainfall. This indicates that allowing time for infiltration to occur substantially improves the performance of the SCM.

As a whole, the performance since the smart retrofit has shown improvements based on the previous system. Looking at events greater than 0.05 inches, the RTC Treatment Train completely captured 80 of 81 events, or 98.8% of the storm events. The pre-retrofit system saw a capture rate of 90.8% of storms, or 198 of the 218 recorded over 0.05 inches. Results from previous study of the Treatment Train (prior to the RTC retrofit) are shown in Figure 5.10 (Lewellyn 2015).

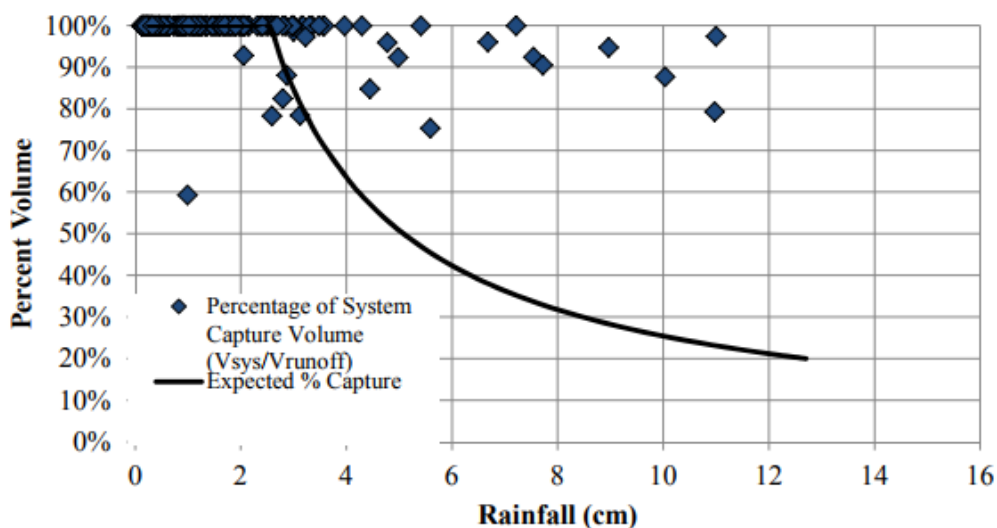


Figure 5.10: Performance of Pre-Retrofit Treatment Train (Lewellyn 2015)

When comparing the performance of the pre-retrofitted system to the current smart Treatment Train, performance has been enhanced from the added smart controls. While more data needs to be collected in order to draw further conclusions, the added storage from the underground cisterns paired with the controlled pump appear to increase the ability of the system to capture storm events despite the 40% increase in directly connected impervious area. The pre-retrofitted system (Figure 5.10) still had performance better than expected with many large storms receiving less overflow than predicted, however with the smart system the majority of events show no overflow (with the exception of one event). As study is continued and larger events are experienced, this comparison can be continued to see the further effect of smart controls on the system.

5.5.2 Infiltration Capacity of Treatment Train

When looking at the performance of the Treatment Train after being retrofitted as a smart system, one of the main goals was to ensure that the system still maintained its resiliency and ability to manage storm events even after managing a larger drainage area. While the underground cisterns provide substantial additional capture to deal with the enlarged drainage area, because the treatment train operates by pumping stored runoff back to the top of the SCM the ability for the SCM to infiltrate and evapotranspire stormwater at reasonable rates is still required. In order to see how infiltration rates varied since the retrofit with RTC, the pumping time to draw down the underground cisterns from full were compared for the year of monitoring available. Because level sensor data in the rain gardens was unavailable for much of the year, this was used as an approximation to represent infiltration rate. Figure 5.11 demonstrates sample results from a drawdown event, showing a typical period analyzed.

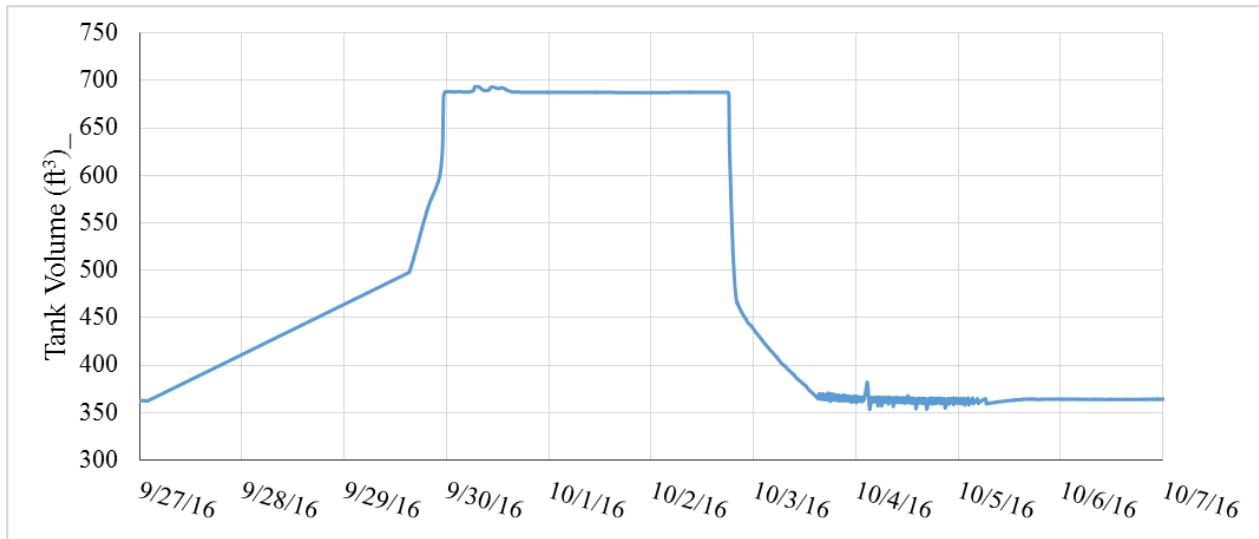


Figure 5.11: Sample Storm Response and Drawdown for Treatment Train Cisterns

Figure 5.11 clearly demonstrates how a cistern drawdown from full typically occurs at the Treatment Train with runoff stored in the cistern being pumped back to the beginning of the SCM at the first bioswale. When drawdowns from full occur, monitoring of the site has shown that the volume pumped exceeds the capacity of the bioswales and rain gardens, resulting in some water flowing back into the cistern. Pumping continues until the target volume (set at half the total capacity of the cisterns) is reached. This indicates that the time it takes for the system to stop cycling through pumping gives a sense of how long the SCM takes to infiltrate enough water to ensure sufficient capacity for the pumped water. Without level sensor data from the entire monitoring period available, this metric stands as the best way to understand how the infiltration rate in the Treatment Train has changed over the course of its current lifespan. A comparison of these pumping times for the Treatment Train through summer of 2016 to summer of 2017 is shown in Figure 5.12.

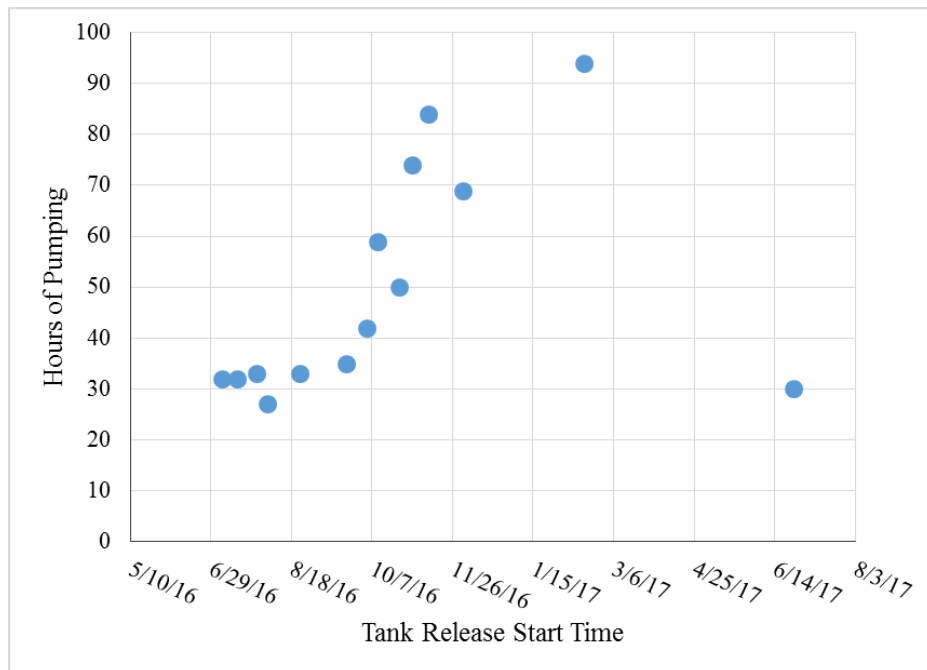


Figure 5.12: Treatment Train Full Cistern Drawdown Events

While data was not available from March 2017 until mid-June, the results still indicate that changes in the infiltration rate seen throughout the year were largely seasonal rather than indicative of a loss of performance from the Treatment Train. Pumping times vastly increased from late fall into winter of 2016, resulting in a maximum pumping time of 94 hours (a factor of 3.48 times larger than the minimum pumping time measured). Through September 2016 the average drawdown time was 32.0 hours but quickly rose to an average of 67.4 hours in late fall and winter, an increase by a factor of 2.11. Though minimal measurements are available for the spring and summer of 2017, a measurement taken on June 25, 2017 shows the pumping time to return to 30 hours, a value within range of the typical measured values in the summer months of 2016. While further data collection is clearly necessary, this overall indicates that the changes in infiltration rate seen were largely seasonal and the performance of the Treatment Train has not been reduced by the retrofit with a larger drainage area and addition of real-time control.

While the changes shown in infiltration rate (longer pumping times denoting slower infiltration rates) are of a substantial and fairly large scale, the range seen is not unusual for seasonal changes in stormwater control measures. In Emerson and Traver's 2008 article, "Multiyear and Seasonal Variation of Infiltration from Storm-Water Best Management Practices," the hydraulic conductivity of several rain gardens were shown to be directly correlated to temperature with high infiltration rates experienced with hotter temperatures. Additional seasonal variation was demonstrated in the ponding times of the rain gardens with longer ponding times experienced in late winter and shorter ponding times in summer. Despite the seasonal variations, the study also pointed to no long-term degradation in infiltration capacity. These results corroborate what was measured in the Treatment Train, with the change in infiltration rates seen likely due to seasonal variation rather than any reduced long-term capacity.

5.5.3 Particle Size Analysis

In addition to the monitoring of the drawdown times in the treatment train, sediment gradations were monitored throughout the Treatment Train in order to understand any changes to the morphology of the system. With a change to the drainage area a corresponding alteration to the flow regime during storm events can be expected in the treatment train with higher wet weather flows expected. Additionally, while flows recycled through the system from the pump are generally low, the retrofitted smart system does increase the residence time of water in the system, therefore providing additional time for settling of sediments to occur. Because of these changes sieve analyses were performed for multiple locations throughout the Treatment Train (Figure 5.5) on a quarterly basis in order to see how sediment characteristics changed over time. Results for the February 2017 and May 2017 sieve analyses are shown in Figure 5.13.

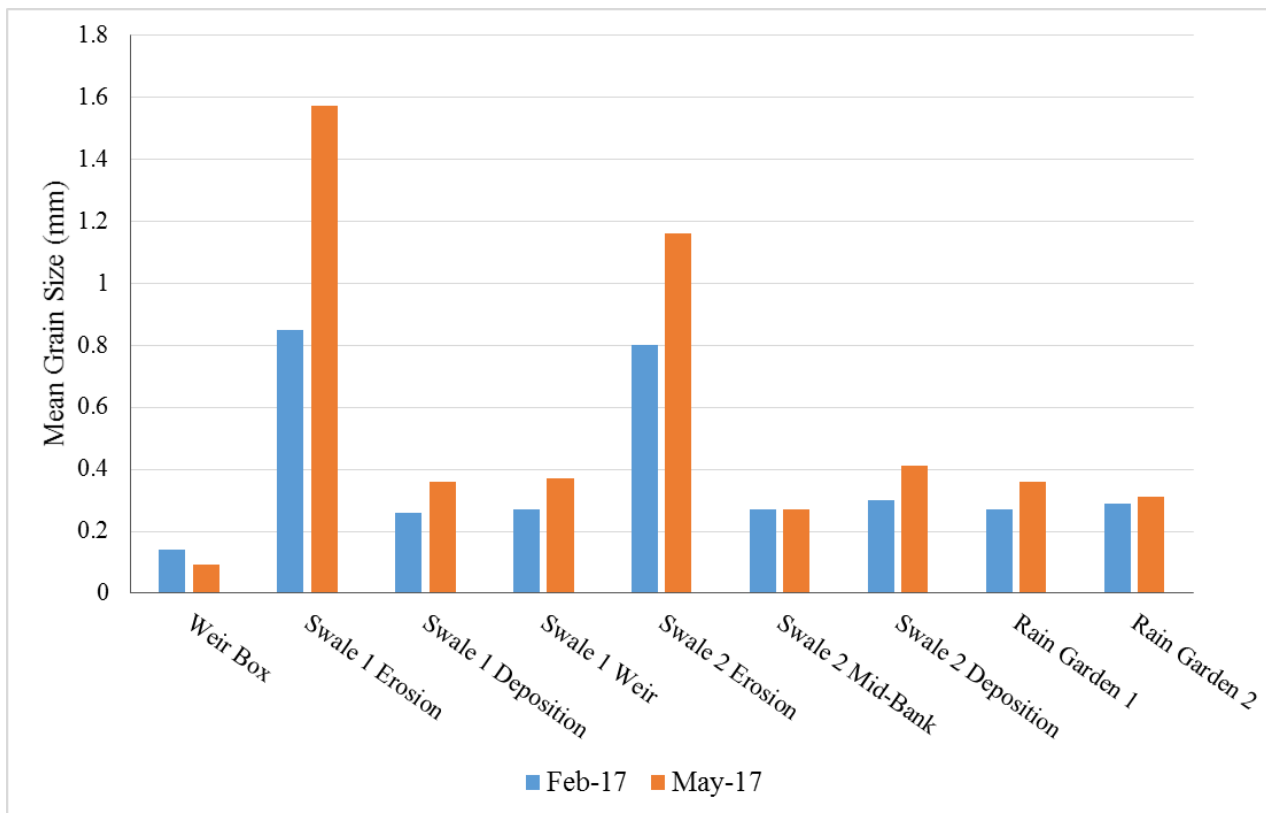


Figure 5.13: Changes in Mean Particle Size of Sediments in the Treatment Train for February and May 2017

Figure 5.13 shows that the sediment sampling completed throughout the Treatment Train in May saw an overall increase in mean particle size from February, the only exception being the sediment within the inflow weir box which noted a slight decrease in sediment size. Table 5.4 displays the same mean grain sizes determined for the Treatment Train along with the percent change noted from February to May. Complete sieve analysis results and the full particle distributions for each sample may be found listed in Appendix B.

Another clear trend seen in the results of the sieve analyses is the sharp increase in mean particle size seen in areas that erosion was being noted. While this is the expected result, smaller sediment sizes are expected to be washed away in areas where flow is forcing erosion, the trend is still clear

with sharp increases in particle size seen in both locations of erosion. These trends also held through the three month period between testing, with the two erosion sites marking the largest grain sizes in both February and May. Table 5.4 further shows the results of the sieve analyses with percent changes in grain size seen between February and May 2017.

Table 5.4: Changes in Mean Particle Size in Treatment Train, February to May 2017

Sampling Location	February Mean Grain Size (mm)	May Mean Grain Size (mm)	Change
Weir Box	0.14	0.094	-32.9%
Swale 1 Erosion	0.85	1.57	84.7%
Swale 1 Deposition	0.26	0.36	38.5%
Swale 1 Weir	0.27	0.37	37.0%
Swale 2 Erosion	0.80	1.16	45.0%
Swale 2 Mid-Bank	0.27	0.27	0.0%
Swale 2 Deposition	0.30	0.41	36.7%
Rain Garden 1	0.27	0.36	33.3%
Rain Garden 2	0.29	0.31	6.9%

This overall increase in mean grain size of sediments distributed throughout the system indicates that finer sediments are being washed away through the winter. In both zones where erosion and deposition were observed this trend held, with the only decrease in sediment size seen in the weir box and the only identical value seen in a sample taken at mid-bank in the bioswale. The average increase in particle size seen was 27.7%, with the erosional sites increasing by an average of 64.9% and the depositional sites by an average of 25.4%.

The results of the particle size analysis hold implications for green infrastructure designs that provide conveyance, the erosional and depositional processes needing to be considered to ensure a sustainable piece of infrastructure is built. Areas where ponded water was allowed to occur (the rain gardens and backwater zones prior to the bioswale weirs) displayed depositional characteristics while areas that conveyed higher flows (directly following the weirs in the bioswales) exhibited erosion. While so far the changes exhibited in the Treatment Train are mostly small, it will be important to continue monitoring to better understand how these considerations play into the design of green stormwater infrastructure.

5.5.4 Potential Factors for Sediment Results

The changes in sediment characterization seen so far through grain size analyses in the Treatment Train indicate that some morphology is occurring throughout the SCM. In trying to understand the causes of these changes it is also important to assess other changes to the system that have occurred along the same temporal scale. One notable example is the changes to vegetation experienced throughout the year, with the seasonal difference between winter and summer vegetation being substantial. Figure 5.14 demonstrates the changes in vegetation noted in 2017 for the second rain garden in the Treatment Train from pictures of the system taken in February, May, and July.



Figure 5.14: Vegetation Changes in Rain Garden 2 for Winter (Left), Spring (Center), and Summer (Right)

It is clear that vegetation in the summer is much more established than in the early spring, with the winter lacking vegetation altogether due to the use of deciduous shrubs and seasonal plantings. These changes could help explain the changes in sediment size, the vegetation allowing for additional capture and stabilization by adding resistance to flows through the system. As sampling continues in the future and a multi-year analysis is completed, this hypothesis can be further tested by looking at the seasonal changes in sediments throughout the SCM.

5.5.5 General Performance Notes

In the year of operation for the Treatment Train as a smart system, several additional performance characteristics have been noted from a qualitative standpoint that are important considerations when moving forward with the system. From several field visits during large storm events (events with enough rainfall volume to cause an overflow from the Treatment Train to the storm sewer), it was determined that the overflow mechanism that was designed for does not function correctly.

In no storm event was outflow observed through the permeable pavers, excess flows rather exiting the system uncontrolled over the Treatment Train berm in several locations. While this still resulted in outflows reaching the storm sewer inlet located in the adjacent street, this is clearly not the ideal functionality of the system. Figures 5.15 and 5.16 show overflows occurring for a storm event on 3/31/2017 with a rainfall volume of 1.44 inches. While many storms of this volume had been shown to be captured in the past (Lewellyn et al. 2016), this storm occurred directly after a storm of 0.79 inches, the back to back storms likely decreasing the capacity of the system.



Figure 5.15: Overflow from Treatment Train, 3/31/2017 (Part 1)



Figure 5.16: Overflow from Treatment Train, 3/31/2017 (Part 2)

Figures 5.15 and 5.16 demonstrate the overland flow occurring from the Treatment Train to the adjacent street, a problem that should be addressed moving forward with the study of the system. These occurrences indicate that the top elevation of the infiltration trench, where outflows are intended to occur through the permeable pavers, is at high enough elevations that overflow occurs prior to this within the bioinfiltration portion of the Treatment Train. Figure 5.17 shows the highest observed water elevation of the infiltration trench, still below the overflow point designed for the system.



Figure 5.17: Treatment Train Infiltration Trench at Maximum Observed Level

Overflows across the bioswale and rain garden berms could be problematic for the structural integrity of the system, additional overflows potentially causing erosion and therefore even further problems with overflow. Moving forward a complete survey of the site should be completed in order to correct the elevation difference between the infiltration trench overflow and the rain garden berms.

In addition to the problems experienced with overflows during large storm events, several new issues arose with the Treatment Train site that illustrate some of the operational considerations that come with implementing smart stormwater networks. Following a snow storm on 3/13 to 3/14/2017 that resulted in a combined total of 6.0 inches of snowfall, snow removal equipment scraped a plastic valve box that served as a junction for wires coming from sensors located throughout the Treatment Train (Figure 5.18). The incident severed all wires in the junction box

and resulted in a loss of monitoring capabilities for the remainder of the winter and spring for the Treatment Train.



Figure 5.18: Junction Box following 3/14/17 Snow Storm

Because smart systems rely on continuous monitoring to make control decisions, this resulted in a loss of control on the system while the monitoring equipment was not functioning. As a whole this occurrence illustrates the importance of communication with maintenance crews that operate around sites utilizing RTC and of planning to protect smart systems from accidents.

5.5 Conclusion

The preliminary results acquired from monitoring the performance of two of the smart stormwater systems at Villanova University (the CEER green roof and Treatment Train) indicate that smart systems are effective ways to improve the performance of green stormwater infrastructure. While further study needs to be completed to show the long-term implications of adding real-time control to SCMs, both systems displayed an ability to manage stormwater for rainfall volumes within their

design capabilities despite an increase in contributing drainage area. These results show RTC as a promising way to retrofit systems in order to increase the capture across a larger drainage area without altering the structure of an SCM.

The green roof analysis showed that while a substantial amount of outflow occurred from the system during small events (events less than the predicted overflow point of 0.8 inches), the majority of these performance deficits came during the winter when the smart irrigation portion of the system was not active. Furthermore, in many cases during the summer (when the ET potential of the system is expected to be at its highest), the system performed better than expected by capturing entire storm events larger than 0.8 inches. Considering that the capture for the green roof increased by 139%, the ability for the green roof to still manage storm events during effectively points to the promising ability of smart stormwater systems.

Unlike the green roof, the Treatment Train saw an overall increase in performance even without considering the additional drainage area that was added with the RTC retrofit. In the period of record for infiltration trench water level data (June 2016 to March 2017), only one overflow event was noted despite the 81 events experienced. This high capture rate exceeds the performance seen by the system prior to the RTC retrofit, indicating that the additional underground storage and ability to recycle runoff from the storage back through the bioinfiltration system is an effective way to manage stormwater. Furthermore, analysis of the system's infiltration capacity has shown minimal changes since the retrofit occurred other than seasonal fluctuations, indicating that the changes to the system have not adversely affected its ability for infiltration (the most crucial hydrologic mechanism for a bioinfiltration SCM). While slight changes to the sediment characteristics were noted from February to May of 2017 indicating that some erosion and

deposition are occurring within the SCM, a longer record of grain size data needs to be established before further conclusions are drawn.

Overall the results of the analysis point to substantial benefits being possible by creating smart stormwater systems that integrate both green infrastructure and real-time control components. While these systems make sense to help combat the negative effects of urban runoff, they come with several design considerations that are not typical of traditional stormwater control measures. Because these smart systems rely on substantial monitoring and data utilization, on-site sensing equipment will generally be required in some capacity. For this reason additional maintenance and security measures need to take place in order to ensure the longevity of the sites. The example set by the Treatment Train shows how this comes into play, with all smart aspects of the system being offline for 3 months due to a snow maintenance accident that resulted in all remote sensing capabilities being lost. As long as these additional considerations are taken into account, the smart Villanova stormwater sites stand as examples of how real-time control can be used to retrofit existing green infrastructure to create more efficient and effective stormwater management.

6 CONCLUSIONS

Throughout the study, smart stormwater management has been analyzed from both a theoretical and practical perspective utilizing both in-situ measurements and hydrologic modeling. A comprehensive approach was taken that included analysis of forecast uncertainty used in the RTC decision making process, modeling and monitoring of existing smart stormwater sites, and analysis of publically available climate data that could be integrated into smart stormwater management to make more informed decisions. While there are many factors that affect the performance of green infrastructure that has been retrofitted with real-time controls, the overall results indicate that these smart systems are highly adaptable and have the capability to manage larger drainage areas while still providing a substantive benefit.

6.1 Forecast Uncertainty

Currently one of the main practices used in smart stormwater management is the integration of forecast information to make predactive control decisions to prepare for storm events. While inherent uncertainty is introduced into the control structure when this is done, weather forecasts still stand as a useful tool in stormwater management. A modeling study was completed to compare smart stormwater systems that used weather forecasts to theoretical systems that used a perfect forecast. While there was a deficit in performance seen in the forecast based systems, an ability was still shown to actively manage stormwater and create an overall benefit. Comparing the ideal case (the perfect forecast) to the real case, the average increase in overflow between the two systems represented 5.34% of the storage volume when looking at a per-event basis. This deficit in performance could therefore be in part mitigated by applying further conservative measures to

the control decisions, for example leaving an extra 5% free tank volume when setting a target volume for drawdowns.

In addition to the analysis of forecast uncertainty, a sensitivity analysis was completed by running long-term simulations that utilized forecast-based controls and varying POP (probability of precipitation) thresholds. The POP threshold defines what an actionable event for a system is and ranged from 0% to 100%. When taking into consideration multiple and competing objectives, for example maximizing retention time for water quality benefit while minimizing the amount of wet weather outflow that occurs from a system, a value of 70% was deemed appropriate for the operation of most forecast-controlled systems. This value balanced the need for increasing retention time while still maintaining event performance. These results also further demonstrate how parameters could be tailored to fit specific site needs, for example if retention time took precedence over wet weather flows, the POP threshold could be increased so more runoff were retained. This point is further illustrated with the study of the specific CEER green roof site (Chapter 4) where a POP threshold of 60% was deemed best to meet the goals of increased capture and reduced in-storm runoff, the ideal value changed to meet the specific site goals.

6.2 Integration of Climate Indices

While the majority of the work done at the Villanova University smart sites relied heavily on in-situ sensing for making control decisions, there exists significant potential from using the vast amount of publically available climate data published from a variety of sources. To determine how these could be used effectively within the context of the Villanova sites, several sources of climate data [the Palmer Drought Severity Index (PDSI), the Standardized Precipitation Evapotranspiration Index (SPEI), and the Soil Moisture Active Passive (SMAP) satellite] were

analyzed over multiple time scales to see how they correlated to measured weather conditions at Villanova University. Results showed that the PDSI, when calculated on a weekly basis, was apt at indicating dryer periods (especially from a temperature standpoint) but had little correlation when rainfall was high than average. The SPEI had promising results with a significant correlation between measured monthly precipitation and the index value, showing promise for use as a drought index. Finally the SMAP demonstrated a useful way to give current regional soil moisture information, the measurements taken on a 2 to 3 day basis providing significant correlation to soil moisture readings taken on site at Villanova.

With a better understanding of how these indices and data sets relate to Villanova's weather conditions, methodologies can now be developed to incorporate these data sets into the control structures of smart stormwater systems. One application (as outlined in Section 3.5) would be to use the SPEI, calculated for a month's worth of weather conditions and updated on a daily basis, to indicate the volume of irrigation that should occur. This could help ensure that during extreme dry periods that water is being conserved and that when a greater ET potential exists, it can be fully utilized. Moving forward ideas like this need to be applied to stormwater management and further methodologies developed for including climate data in stormwater control structures.

6.3 Analysis of Villanova Smart Stormwater Systems

Two stormwater control measures at Villanova University were retrofitted to include real-time control with the goal of creating smarter stormwater networks that can more actively manage urban runoff. The two systems, the CEER green roof and the Treatment Train, both have active undergone active monitoring to allow for the performance to be quantified since they went online as smart systems in the summer of 2016. While data collection is still preliminary and should be

continued to further quantify the benefit of smart stormwater systems, both systems show a maintained ability to provide volume reduction to storm events while managing an increased drainage area. The green roof, which saw an impervious drainage area increase of 139%, demonstrated a relatively sustained ability to capture storm events when compared to the pre-retrofit performance. The benefits here clearly relate to the management of a larger drainage area. The Treatment Train, which saw a 40% increase in impervious drainage area, has demonstrated an increased ability to capture storm events with only one overflow from the system of the 81 storm events measured (with events defined as volumes greater than 0.05 inches).

In addition to the active monitoring of the two smart stormwater sites, a modeling study was completed for the CEER green roof to better understand the complex interactions between control processes that are occurring. After a calibrated model of the pre-retrofit passive green roof was created, the model was altered to include the controlled cistern and a control structure to provide the adaptive control to the system. The baseline results of the model, a simulation run using parameters that matched the current setup of the system, indicate that when comparing the entire watershed (including the added impervious area from the CEER roof) a substantial performance benefit is gained by including the smart control logic. Overall a 79.5% reduction in total outflow was predicted with a 157% gain in total capture volume by the green roof. When considering outflow that occurred just during storm periods, a value that should be minimized especially in the context of CSO communities, an 85.6% reduction in flows was predicted.

In addition to the baseline model, several sensitivity analyses were performed where key control parameters were altered to see the affect that they had on the model results. The aim of these simulation runs were to see on a long-term basis how these parameters could be optimized to increase the performance of the systems. The parameters analyzed were the soil moisture threshold

for irrigation, the capacity of the CEER cistern, and the POP threshold for defining an actionable event. The results indicated that performance benefits could be achieved by increasing the soil moisture threshold from $0.16 \text{ ft}^3/\text{ft}^3$ to $0.20 \text{ ft}^3/\text{ft}^3$, maintaining the current volume of the cistern, and by reducing the actionable event threshold to a 60% probability of rainfall (currently the system operates at 70%). While the results of the forecast analysis indicated that for a generic system 70% is the ideal threshold for forecast POP, with the specific goals of this green roof system 60% resulted in more deal performance.

In addition to the monitoring and modeling perspectives taken when looking at the smart stormwater systems at Villanova, some key observations were made throughout the process of implementing these systems. While much of the maintenance for smart SCMs will remain the same as passive systems, additional care needs to be taken during maintenance because of the larger amounts of sensors that need to be on site in order for a smart system to operate. Significant setbacks occurred to the Treatment Train site at Villanova because of sensors being damaged during routine maintenance around the site, indicating the need for a defined maintenance plan and communication about instrumentation on site.

6.4 Future Work

The results discussed in this thesis reflect a preliminary attempt to examine the factors related to smart stormwater management and better understand how to optimize their performance. Moving forward additional work needs to be done to ensure that using these types of systems remains feasible and can be easily implemented. Aside from the continuation of site monitoring and analysis, methodologies that utilize publically available climate data (such as the SPEI) should be implemented at the Villanova smart system sites to demonstrate how this would function. With a

smart system in place that relies less heavily on in-situ measurements, the ability to bring smart stormwater systems to scale would be vastly increased. Additionally, this would demonstrate a way that systems would be truly “smart”, not just reacting to in-situ conditions but making decisions based on overall climate trends and processes.

Another area that could be expanded upon in the future is analysis of forecast uncertainty across different climate regions. While this study utilized forecast information and rainfall data from Villanova because it was being applied to the Villanova smart systems, it will be important to understand regional variability in weather forecasts to design for systems at scale. A simple modeling approach (such as the methodologies presented in Chapter 2) could be taken with different regional rainfall and forecast inputs to see how uncertainty affects smart stormwater management under a variety of weather patterns.

Finally, as smart stormwater systems continue to grow in use, further analysis of their performance and effectiveness needs to be analyzed so that future sites can be improved in their design. Currently many RTC systems operate as retrofits of existing systems, but as new sites are brought online, RTC can be used as a design tool to plan for the way a system is going to operate. The results of this study have indicated that by adding real-time controls to SCMs, the drainage area the SCMs can manage is able to be increased. This holds implications for design of new sites because a smaller SCM could now be used to manage the same amount of impervious area. Overall, the application of real-time control in green infrastructure holds promise for making smarter, more efficient stormwater systems.

REFERENCES

Abramopoulos, F., Rosenzweig, C., and Choudhury, B. (1988). "Improved Ground Hydrology Calculations for Global Climate Models (GCMs): Soil Water Movement and Evapotranspiration." *Journal of Climate*, 1(9), 921–941.

Cembrano, G., Quevedo, J., Salamero, M., Puig, V., Figueras, J., and Marti, J. (2004). "Optimal control of urban drainage systems. A case study." *Control Engineering Practice*, 12(1), 1–9.

Chang, T. J., and Cleopa, X. A. (1991). "A Proposed Method For Drought Monitoring." *Journal of the American Water Resources Association*, 27(2), 275–281.

Dominique, M., Tiana, R. H., Fanomezana, R. T., and Ludovic, A. A. (2014). "Thermal Behavior of Green Roof in Reunion Island: Contribution Towards a Net Zero Building." *Energy Procedia*, 57, 1908–1921.

Emerson, C. H., and Traver, R. G. (2008). "Multiyear and Seasonal Variation of Infiltration from Storm-Water Best Management Practices." *Journal of Irrigation and Drainage Engineering*, 134(5), 598–605.

Entekhabi, D., Yueh, S., O'Neill, P. E., Kellogg, K. H., Allen, A., Bindlish, R., Brown, M., Chan, S., Colliander, A., Crow, W. T., Das, N., De Lannoy, G., Dunbar, R. S., Edelstein, W. N., Entin, J. K., Escobar, V., Goodman, S. D., Jackson, T. J., Jai, B., and Johnson, J. (2014). "SMAP Handbook: Soil Moisture Active Passive." *Jet Propulsion Laboratory*, NASA.

Forasté, J. A., and Hirschman, D. (2010). "A Methodology for Using Rainwater Harvesting as a Stormwater Management BMP." *Low Impact Development 2010*.

Frazer, L. (2005). "Paving Paradise: The Peril of Impervious Surfaces." *Environmental Health Perspectives*, July, 113(7), 456–462.

Gaborit, E., Muschalla, D., Vallet, B., Vanrolleghem, P. A., and Anctil, F. (2013). "Improving the performance of stormwater detention basins by real-time control using rainfall forecasts." *Urban Water Journal*, 10(4), 230–246.

Gregoire, B. G., and Clausen, J. C. (2011). "Effect of a modular extensive green roof on stormwater runoff and water quality." *Ecological Engineering*, 37(6), 963–969.

Hargreaves, G. H. (1974). "Estimation of Potential and Crop Evapotranspiration." *Transactions of the ASAE*, 17(4), 0701–0704.

Heim, R. R. (2002). "A Review of Twentieth-Century Drought Indices Used in the United States." *Bulletin of the American Meteorological Society*, 83(8), 1149–1165.

Hornberger, G. M., Wiberg, P. L., Raffensperger, J. R., and D'Odorico, P. (2014). *Elements of physical hydrology*. Johns Hopkins Univ Press, Baltimore.

Hunt, W. F., Jarrett, A. R., Smith, J. T., and Sharkey, L. J. (2006). "Evaluating Bioretention Hydrology and Nutrient Removal at Three Field Sites in North Carolina." *Journal of Irrigation and Drainage Engineering*, 132(6), 600–608.

Jin, N., Ma, R., Lv, Y., Lou, X., and Wei, Q. (2010). "A novel design of water environment monitoring system based on WSN." *2010 International Conference on Computer Design and Applications (ICCDA)*.

Joksimovic, D., and Sander, M. (2016). "Performance Modelling of Actively Controlled Green Infrastructure Options in a Mixed Use Neighborhood Retrofit." *World Environmental and Water Resources Congress 2016*.

Kardhana, H., and Mano, A. (2009). "Uncertainty on a Short-Term Flood Forecast with Rainfall-Runoff Model." *Advances in Water Resources and Hydraulic Engineering*, 88–92.

Karl, T. R. (1983). "Some Spatial Characteristics of Drought Duration in the United States." *Journal of Climate and Applied Meteorology*, 22(8), 1356–1366.

Kerkez, B., Gruden, C., Lewis, M., Montestruque, L., Quigley, M., Wong, B., Bedig, A., Kertesz, R., Braun, T., Cadwalader, O., Poresky, A., and Pak, C. (2016). "Smarter Stormwater Systems." *Environmental Science & Technology*, 50(14), 7267–7273.

Lee, C.-S., Ho, H.-Y., Lee, K. T., Wang, Y.-C., Guo, W.-D., Chen, D. Y.-C., Hsiao, L.-F., Chen, C.-H., Chiang, C.-C., Yang, M.-J., and Kuo, H.-C. (2013). "Assessment of sewer flooding model based on ensemble quantitative precipitation forecast." *Journal of Hydrology*, 506, 101–113.

Lefkowitz, J., and Bryant, S. (2016). "Meeting Competing Stormwater Management Objectives: A Nationwide Assessment of Forecast-Integrated Real-Time Control." *World Environmental and Water Resources Congress 2016*.

Lewellyn, C. (2015). "A Hydrologic Evaluation of Pretreatment and Variations in Seasonal and Large Storm Performance of Infiltrating Stormwater Control Measures." thesis, Villanova.

Lewellyn, C., Lyons, C. E., Traver, R. G., and Wadzuk, B. M. (2016). "Evaluation of Seasonal and Large Storm Runoff Volume Capture of an Infiltration Green Infrastructure System." *Journal of Hydrologic Engineering*, 21(1), 04015047.

Lord, L. E., Komlos, J., and Traver, R. G. (2013). "Evaluation of Nitrogen Removal and Fate within a Bioinfiltration SCM." *World Environmental and Water Resources Congress 2013*.

May, C. W., Horner, R. R., Karr, J. R., and Welch, E. B. (1997). "Effects of Urbanization on Small Streams in the Puget Sound Lowland Ecoregion."

Mentens, J., Raes, D., and Hermy, M. (2006). "Green roofs as a tool for solving the rainwater runoff problem in the urbanized 21st century?" *Landscape Urban Plann.*, 77(3), 217–226.

Mullapudi, A., Wong, B. P., and Kerkez, B. (2017). “Emerging investigators series: building a theory for smart stormwater systems.” *Environ. Sci.: Water Res. Technol.*, 3(1), 66–77.

Muschalla, D., Vallet, B., Anctil, F., Lessard, P., Pelletier, G., and Vanrolleghem, P. A. (2014). “Ecohydraulic-driven real-time control of stormwater basins.” *Journal of Hydrology*, 511, 82–91.

“National Water Quality Inventory: Report to Congress.” (2004). *National Water Quality Inventory: Report to Congress*, rep., United States Environmental Protection Agency.

NOAA. (2014). “NDFD Definitions.” *NDFD Definitions*, National Weather Service, <<http://www.nws.noaa.gov/ndfd/definitions.htm>> (Jul. 31, 2017).

“Opti Story.” (2016). *Opti*, OptiRTC, <<https://optirtc.com/about>> (Jul. 29, 2017).

“Ottawa River CSO Reduction.” (2013). *TetraTech.com*, Tetra Tech.

Palmer, W. C. (1965). “Meteorological Drought.” *US Department of Commerce, Weather Bureau*, 45.

Philadelphia Water Department (PWD) (2016). “Green Stormwater Infrastructure Planning & Design Manual.”

Quigley, M., Rangarajan, S., Pankani, D., and Henning, D. (2008). “New Directions in Real-Time and Dynamic Control for Stormwater Management and Low Impact Development.” *World Environmental and Water Resources Congress 2008*.

Reidy, P. C. (2010). “Integrating Rainwater Harvesting for Innovative Stormwater Control.” *World Environmental and Water Resources Congress 2010*.

Rossman, L. A. (2015). Storm Water Management Model User’s Manual Version 5.1. U.S. Environmental Protection Agency, Cincinnati.

“SMAP: Data Products.” (2017). NASA, NASA, <<https://smap.jpl.nasa.gov/data/>> (Jul. 31, 2017).

“SMAP: Mission Description.” (2017). NASA, NASA, <<https://smap.jpl.nasa.gov/mission/description>> (Jul. 31, 2017).

“SMAP: Objectives.” (2017). NASA, NASA, <<https://smap.jpl.nasa.gov/objectives>> (Jul. 31, 2017).

“Standard Test Method for Particle-size Analysis of Soils.” (2010). American Society for Testing and Materials (ASTM C136).

Vallabhaneni , S., and Speer, E. (2010). “Real-Time Control to Reduce Combined Sewer Overflows.” *WaterWorld*.

Vicente-Serrano, S. M., Beguería, S., and López-Moreno, J. I. (2010). “A Multiscalar Drought Index Sensitive to Global Warming: The Standardized Precipitation Evapotranspiration Index.” *Journal of Climate*, 23(7), 1696–1718.

Vitasovic, Z., E.D. Speer, and R. Swarner. "Real Time Control for CSO Reduction." (1990) Water Environment and Technology, Vol. 2, No. 3.

Wadzuk, B. M., Schneider, D., Feller, M., and Traver, R. G. (2013). “Evapotranspiration from a Green-Roof Storm-Water Control Measure.” *Journal of Irrigation and Drainage Engineering*, 139(12), 995–1003.

Walsh, C. J., Roy, A. H., Feminella, J. W., Cottingham, P. D., Groffman, P. M., and Morgan, R. P. (2005). “The urban stream syndrome: current knowledge and the search for a cure.” *Journal of the North American Benthological Society*, 24(3), 706.

Wells, N., Goddard, S., and Hayes, M. J. (2004). “A Self-Calibrating Palmer Drought Severity Index.” *Journal of Climate*, 17(12), 2335–2351.

Wong, B. P., and Kerkez, B. (2016). “Real-time environmental sensor data: An application to water quality using web services.” *Environmental Modelling & Software*, 84, 505–517.

Zaremba, G. (2015). “Evapotranspiration Measurement and Modeling for a Green Roof.” thesis, Villanova.

Zaremba, G. J., Traver, R. G., and Wadzuk, B. M. (2016). “Impact of Drainage on Green Roof Evapotranspiration.” *Journal of Irrigation and Drainage Engineering*, 142(7), 04016022.

APPENDIX

Appendix A: RTC Green Roof Model Results

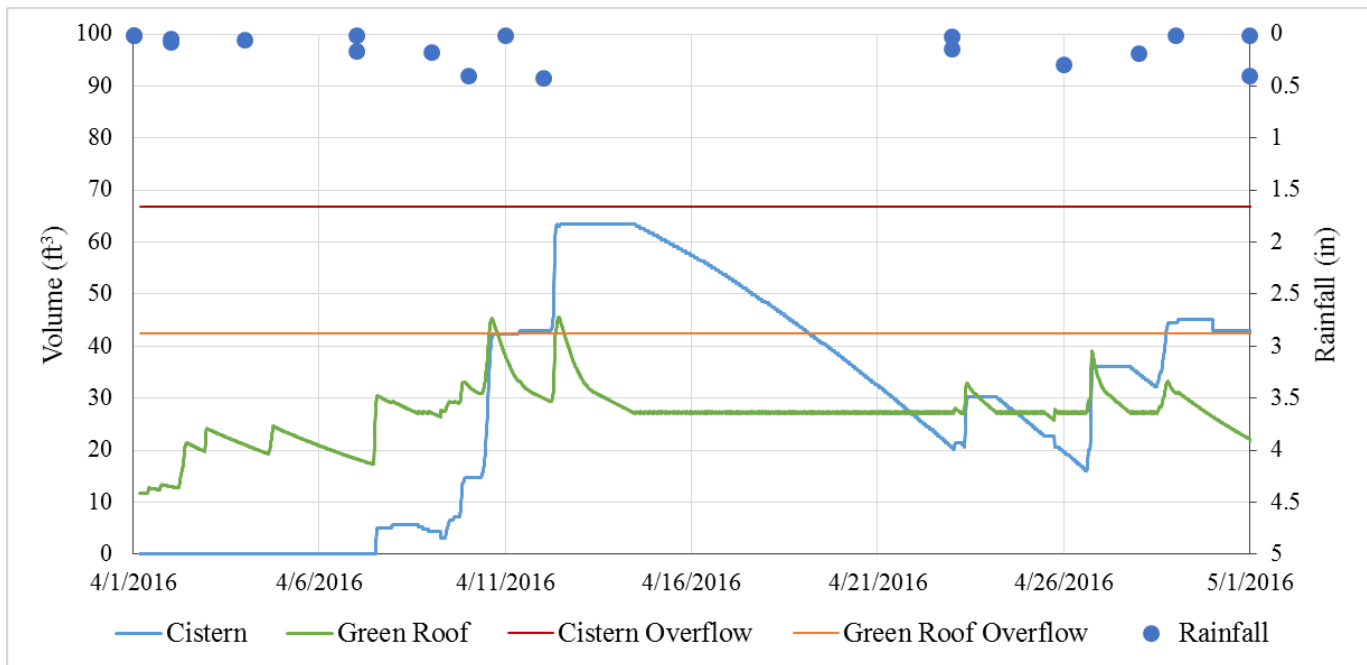


Figure A1: Time-Series Results of RTC Green Roof Model - April, 2016

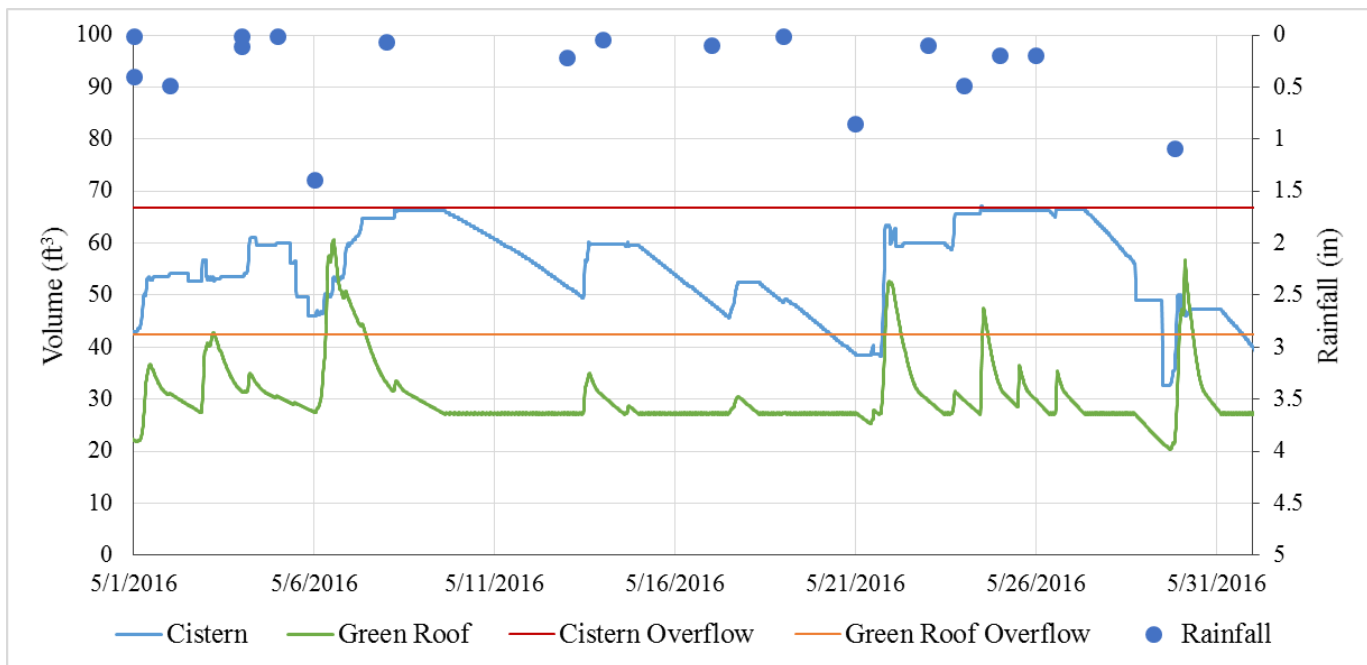


Figure A2: Time-Series Results of RTC Green Roof Model - May, 2016

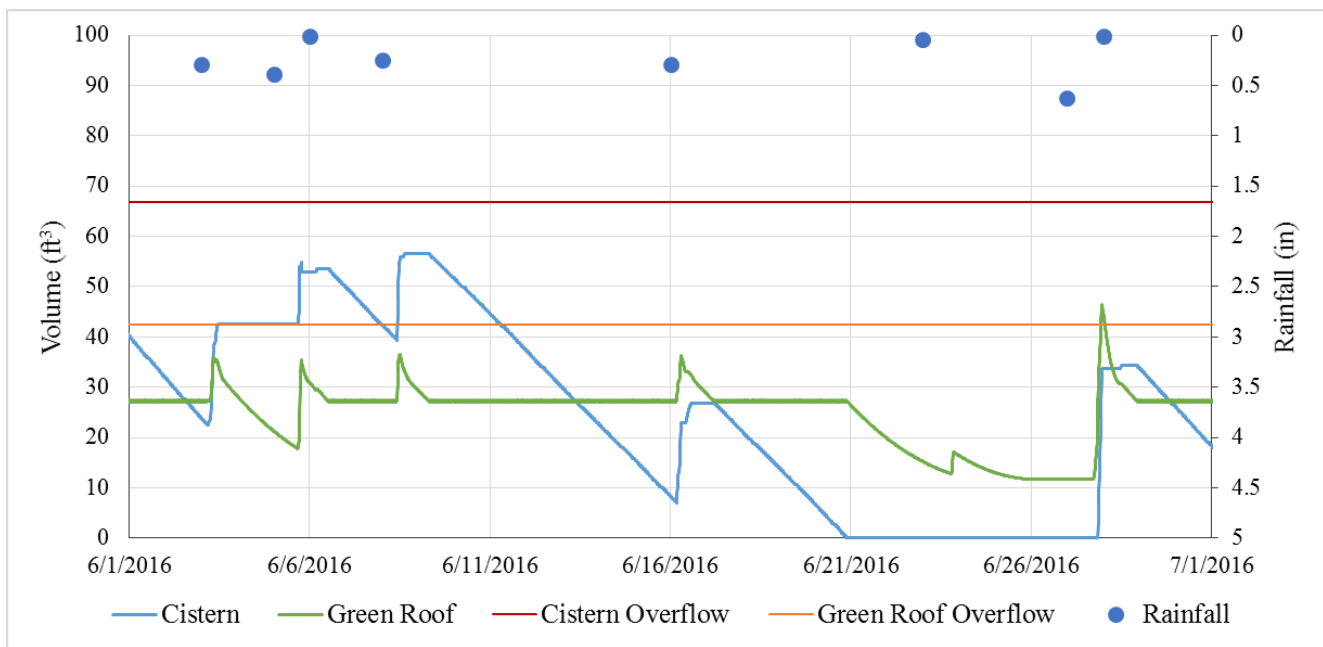


Figure A3: Time-Series Results of RTC Green Roof Model - June, 2016

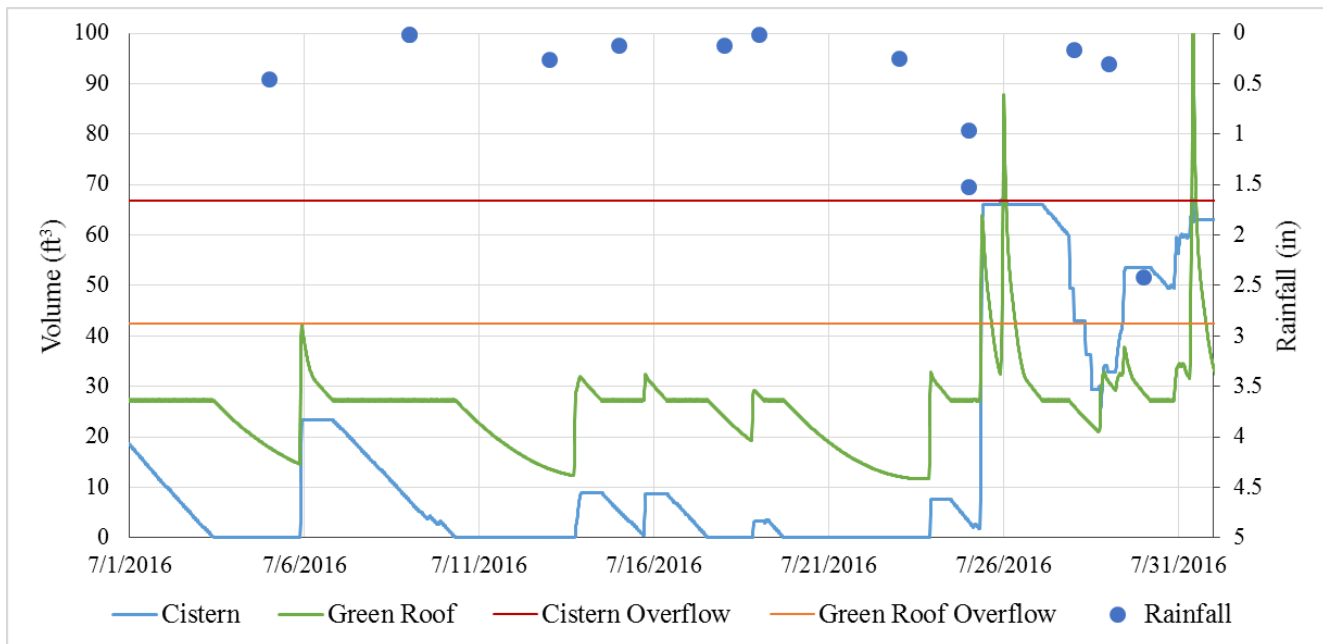


Figure A4: Time-Series Results of RTC Green Roof Model - July, 2016

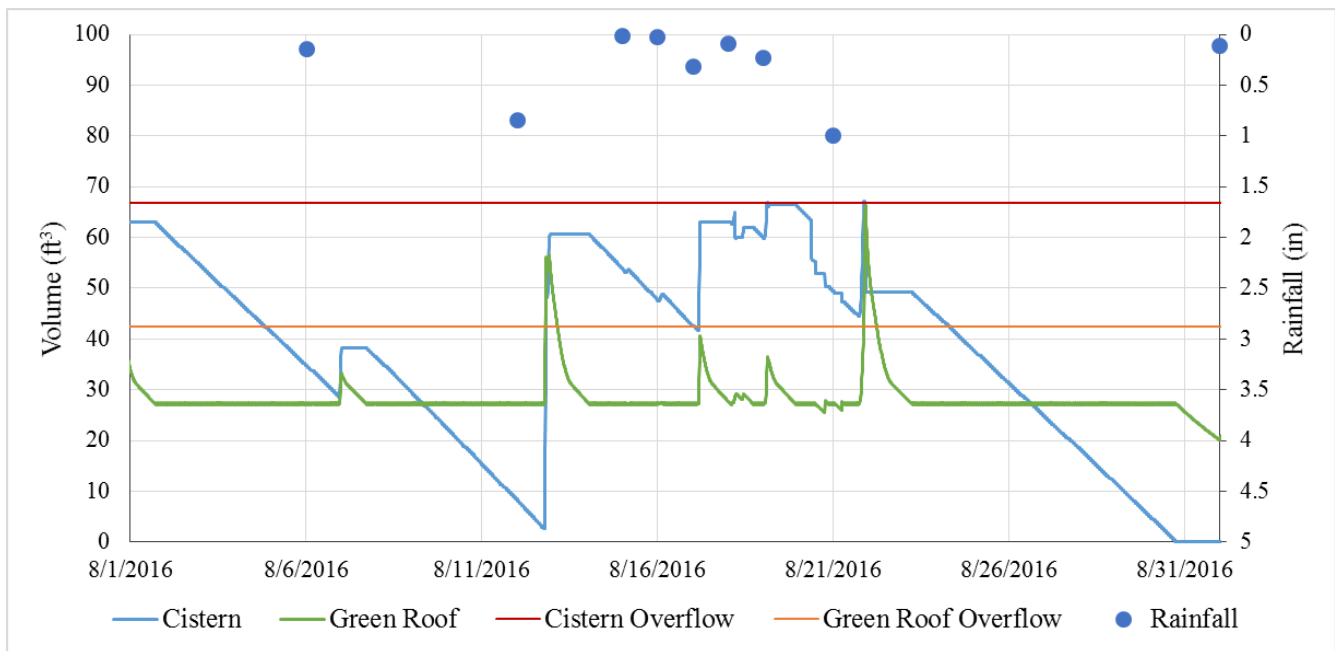


Figure A5: Time-Series Results of RTC Green Roof Model - August, 2016

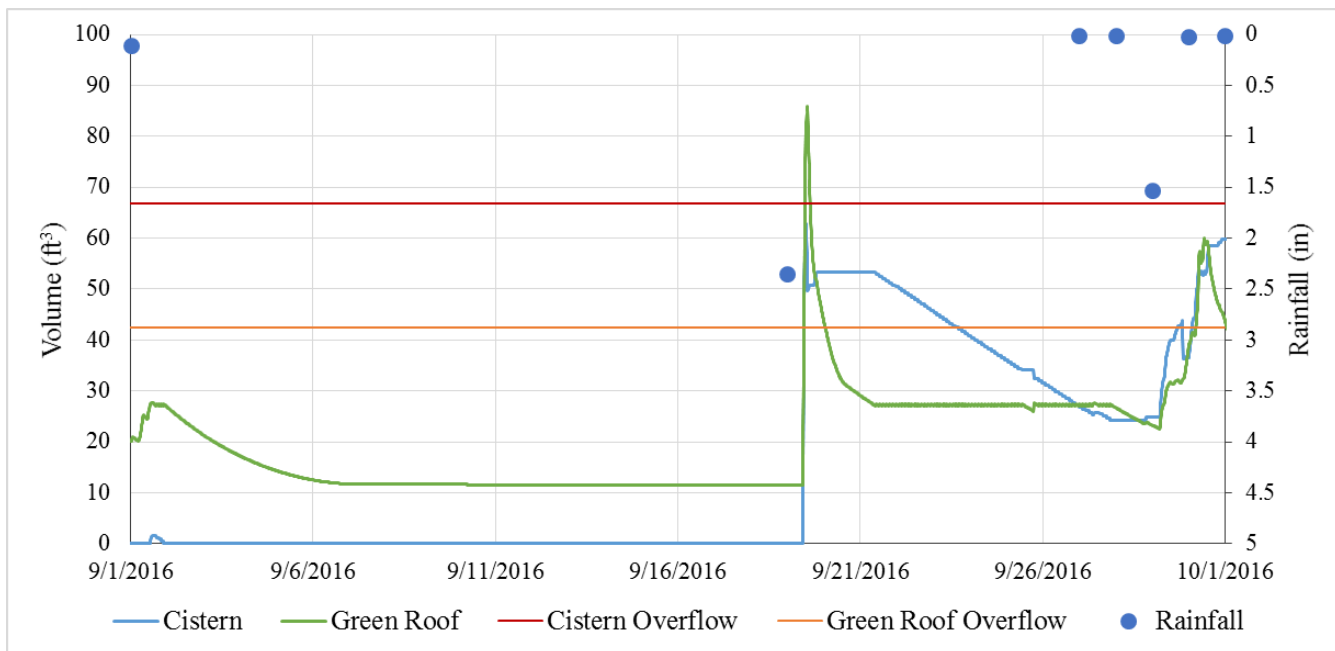


Figure A6: Time-Series Results of RTC Green Roof Model - September, 2016

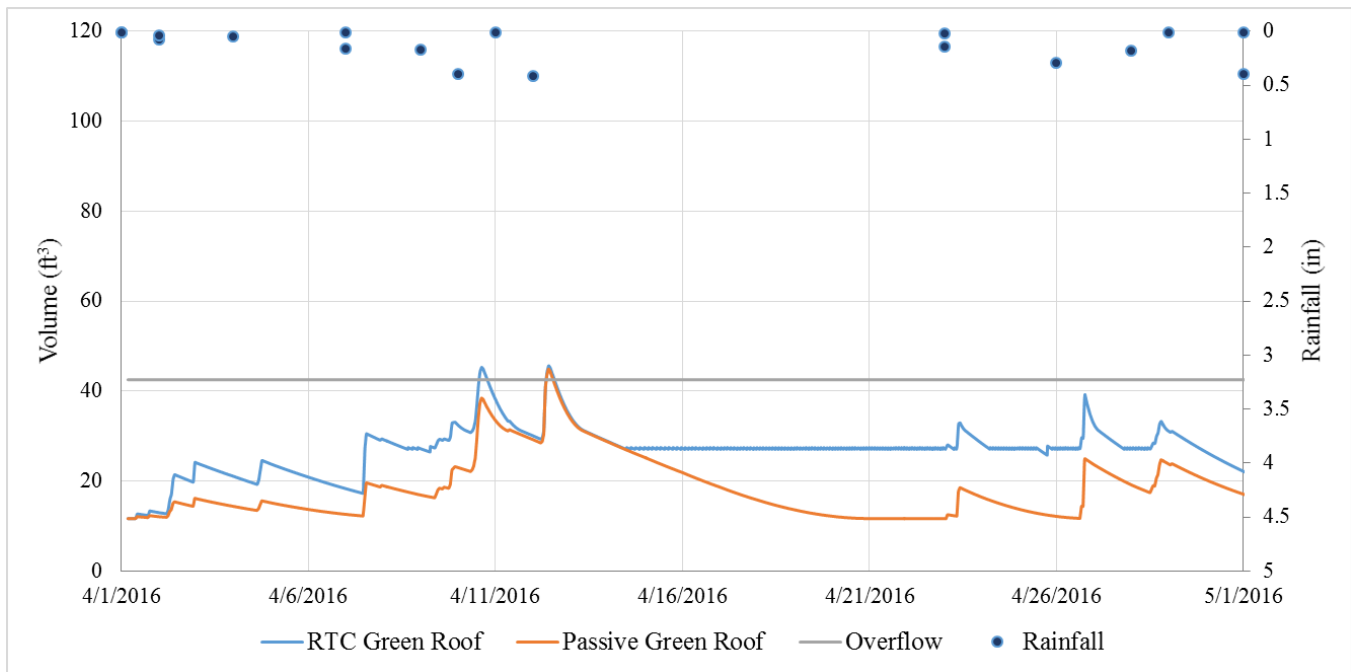


Figure A7: Comparison of Green Roof Storage Volumes for RTC and Passive Systems – April, 2016

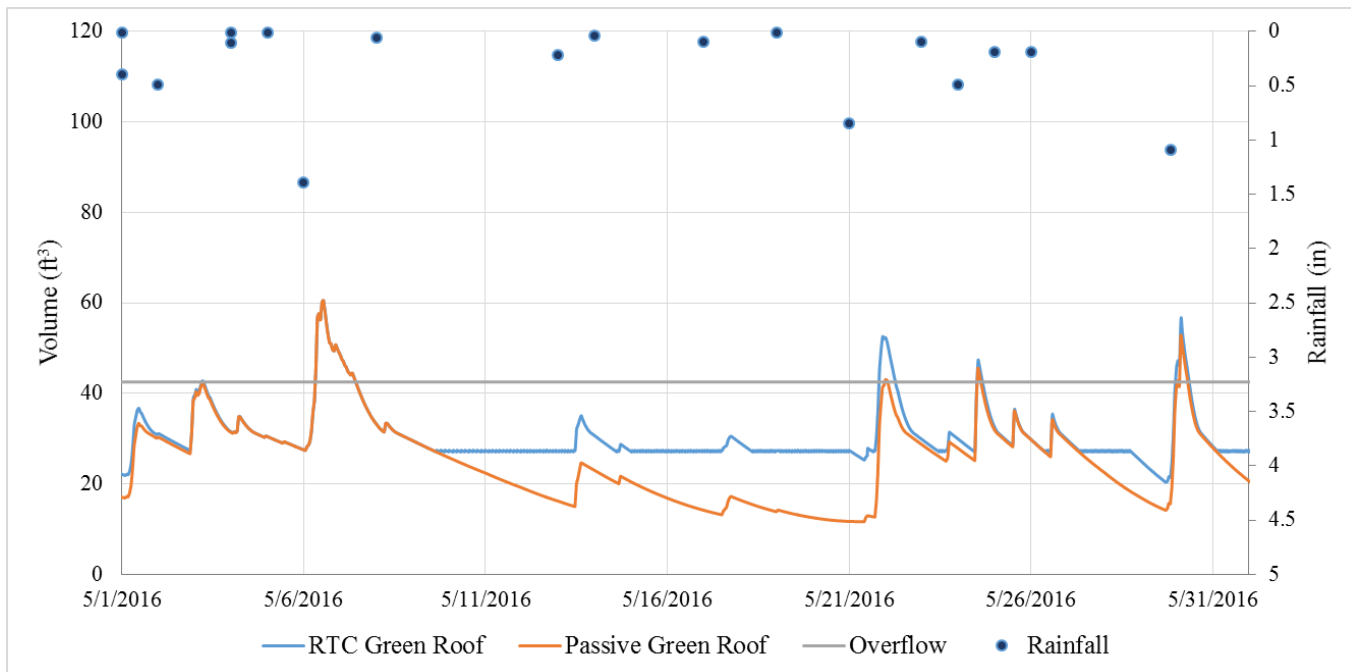


Figure A8: Comparison of Green Roof Storage Volumes for RTC and Passive Systems – May, 2016

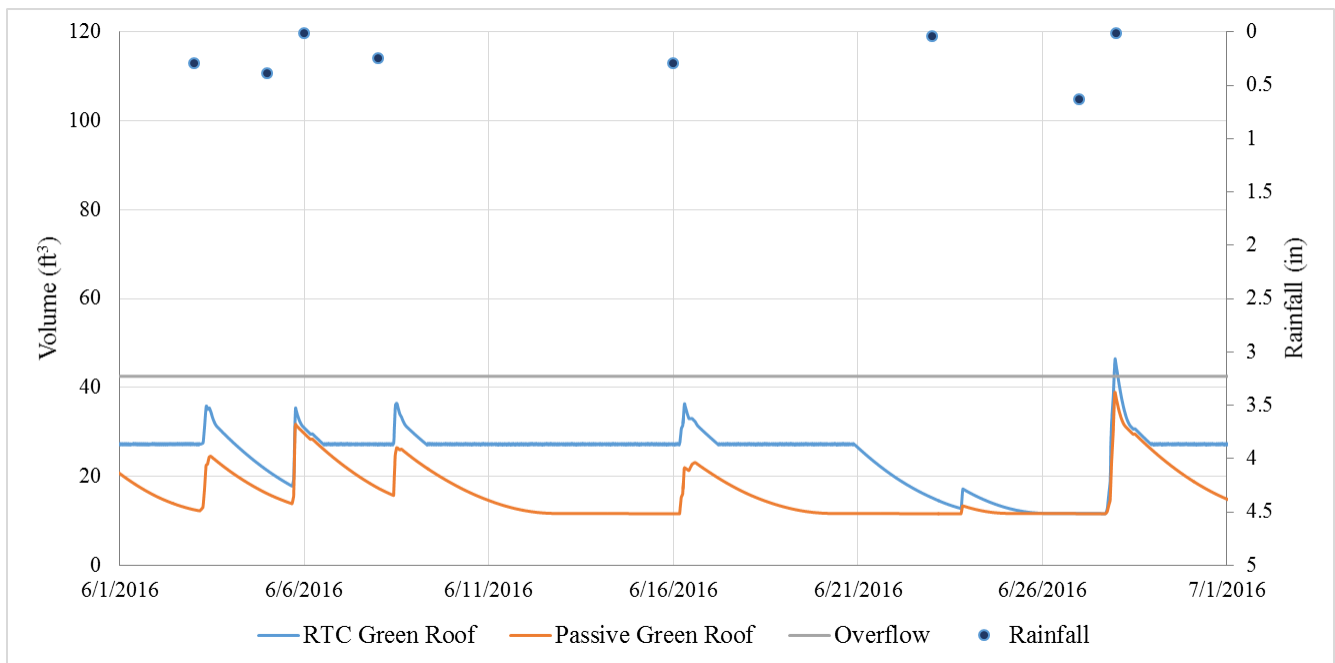


Figure A9: Comparison of Green Roof Storage Volumes for RTC and Passive Systems – June, 2016

2016

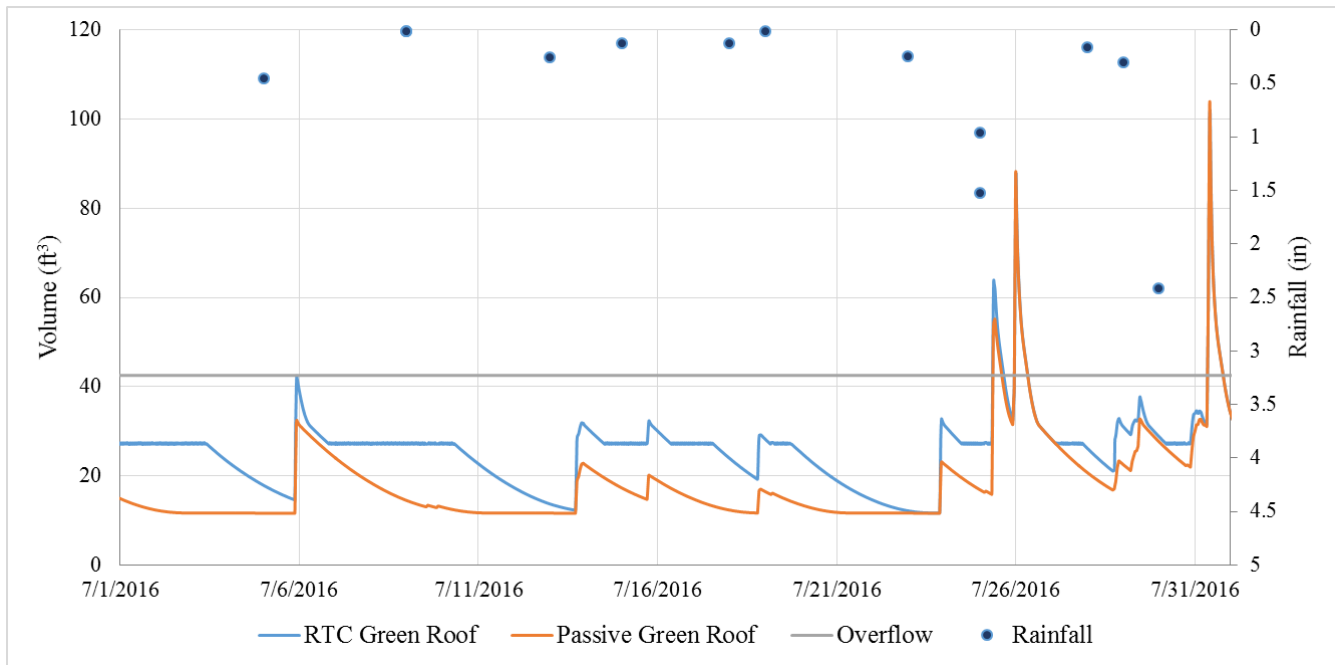


Figure A10: Comparison of Green Roof Storage Volumes for RTC and Passive Systems – July, 2016

2016

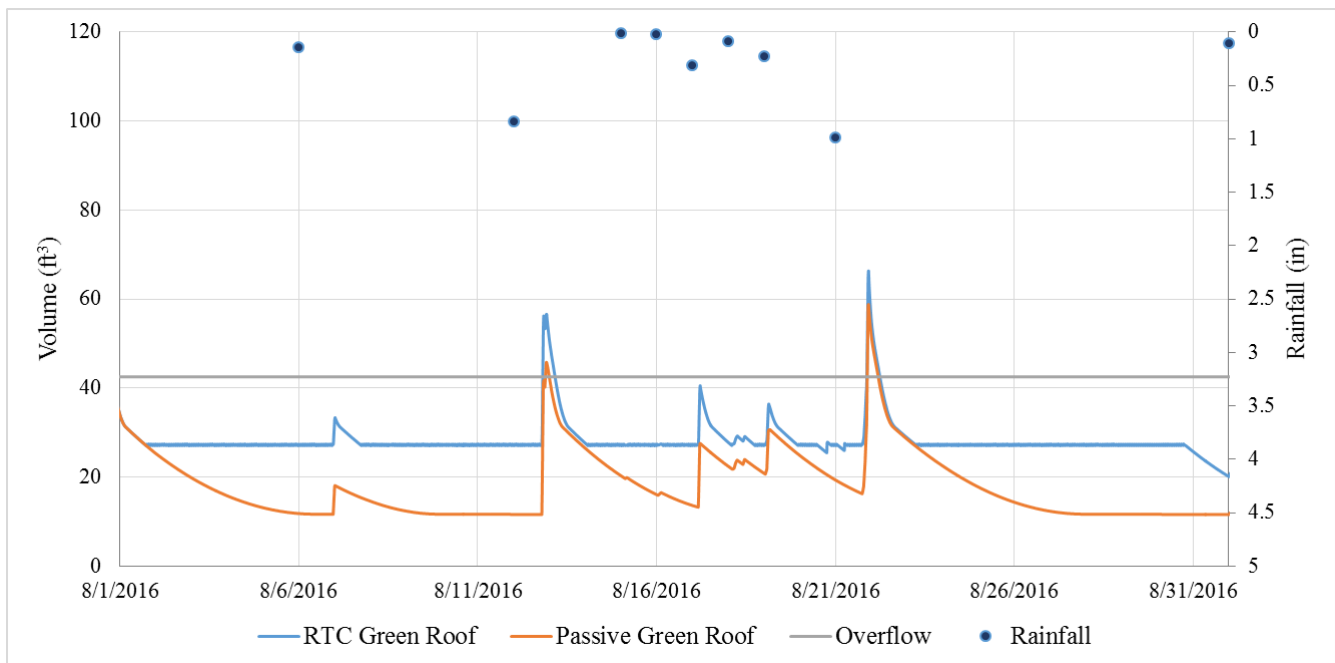


Figure A11: Comparison of Green Roof Storage Volumes for RTC and Passive Systems –

August, 2016

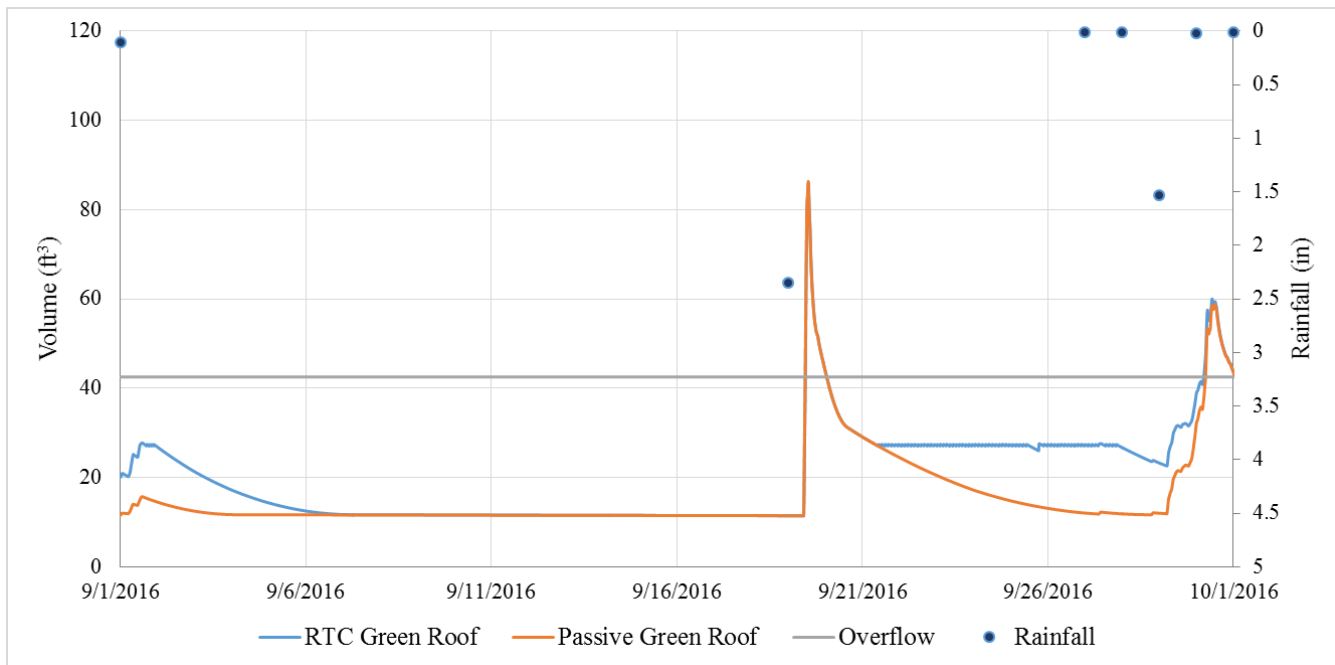


Figure A12: Comparison of Green Roof Storage Volumes for RTC and Passive Systems –

September, 2016

Appendix B: Treatment Train Sediment Analysis

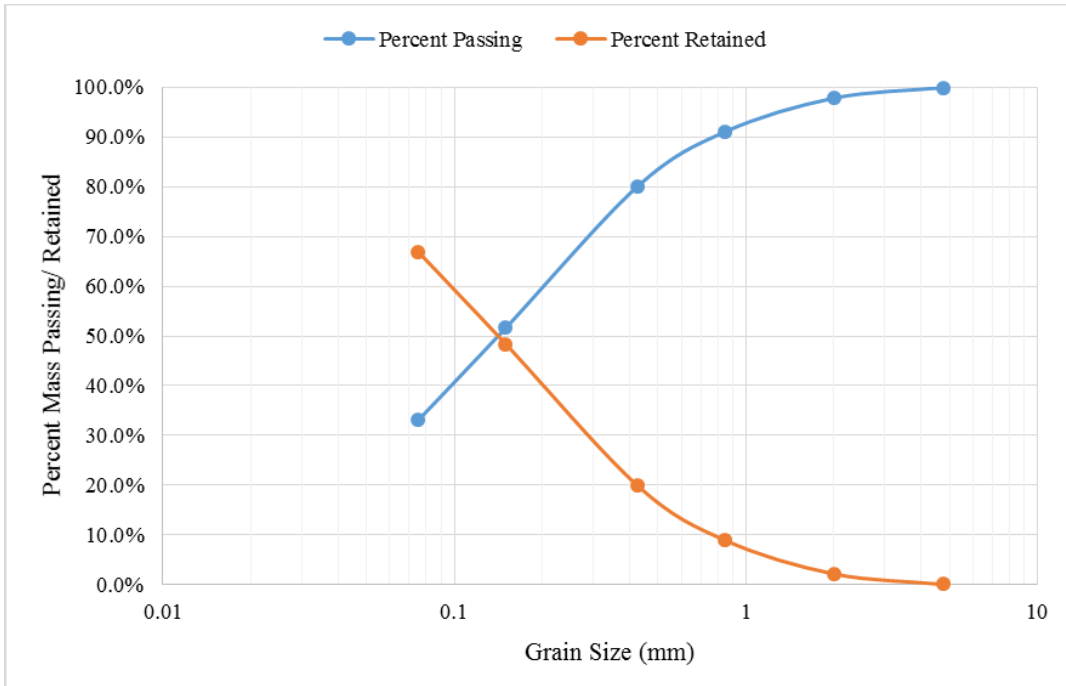


Figure B1: Grain Size Distribution – Weir Box, February 2017

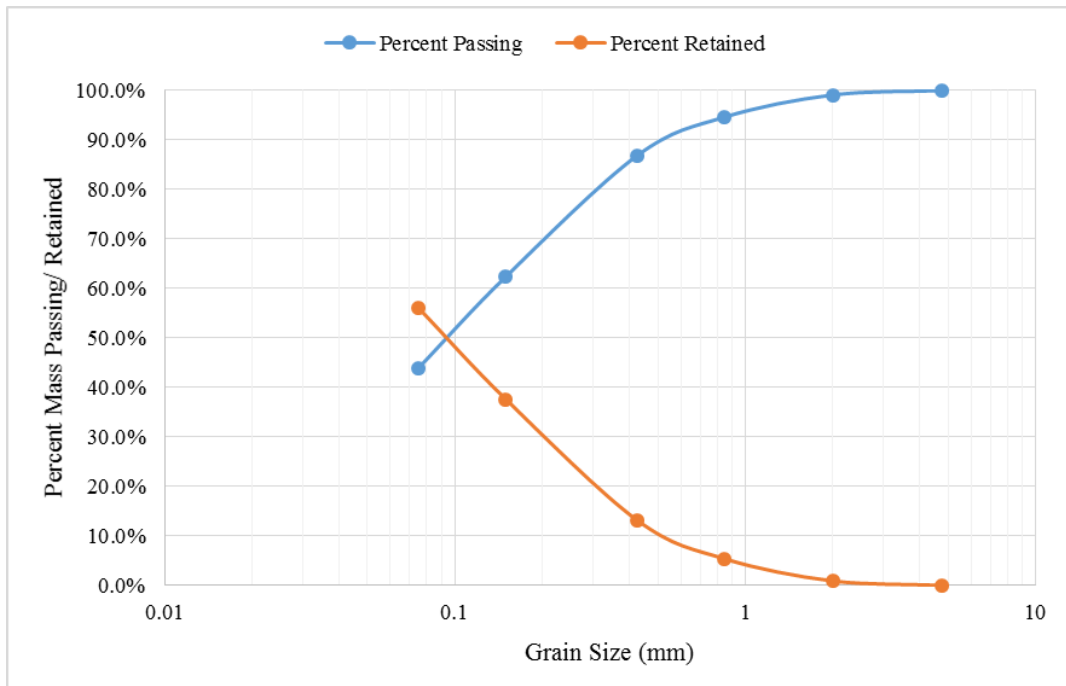


Figure B2: Grain Size Distribution – Weir Box, May 2017

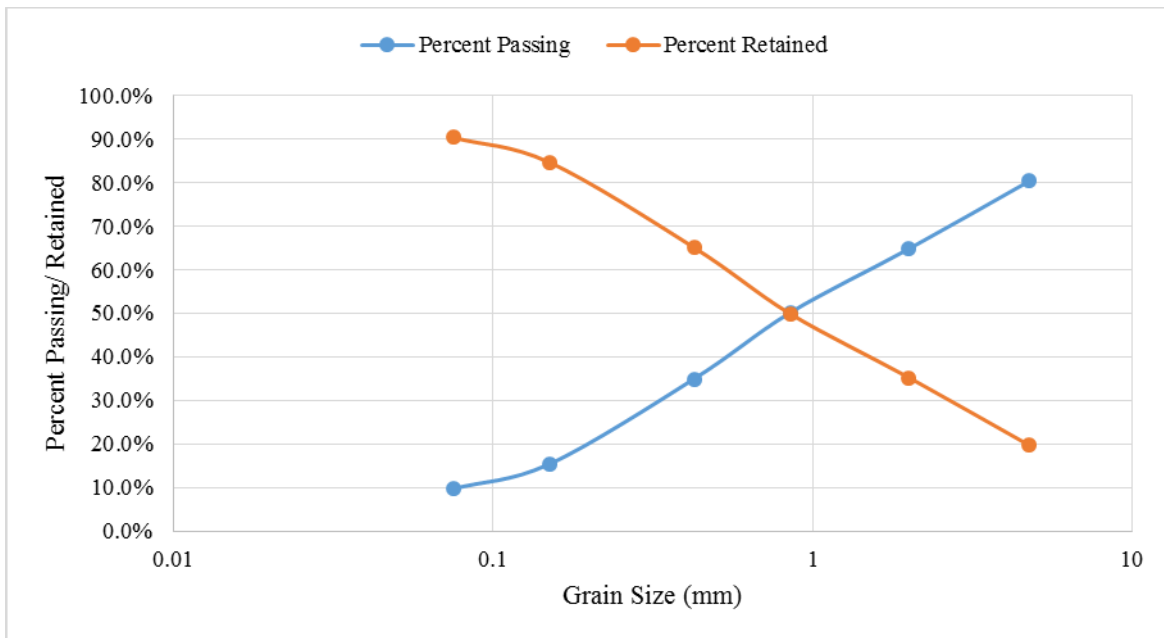


Figure B3: Grain Size Distribution – Swale 1 Erosion, February 2017

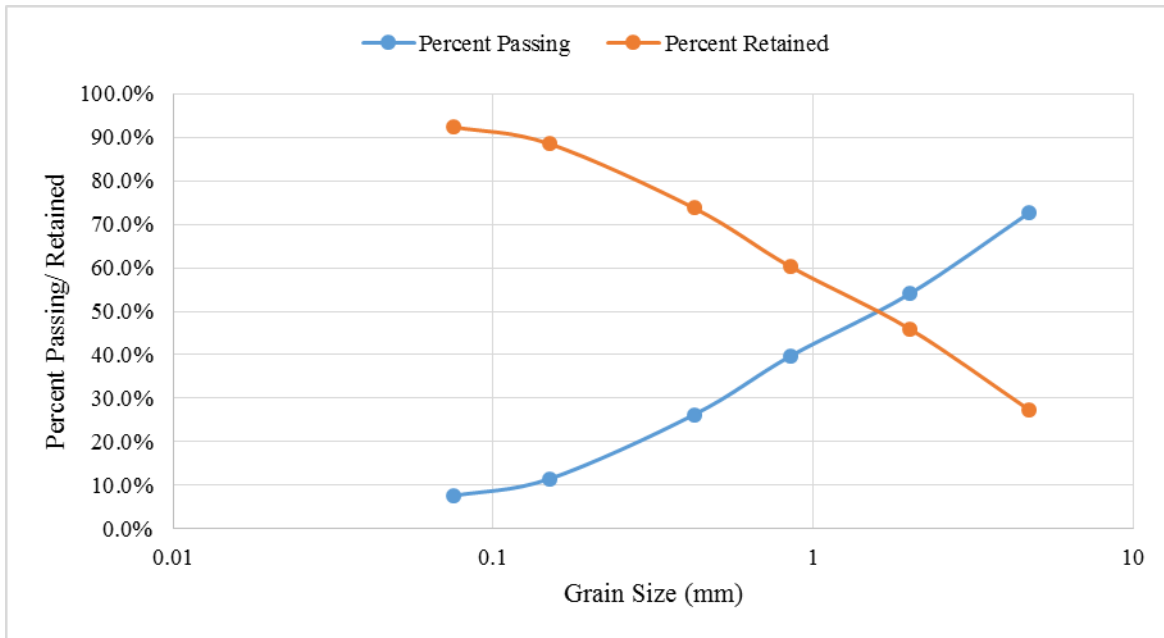


Figure B4: Grain Size Distribution – Swale 1 Erosion, May 2017

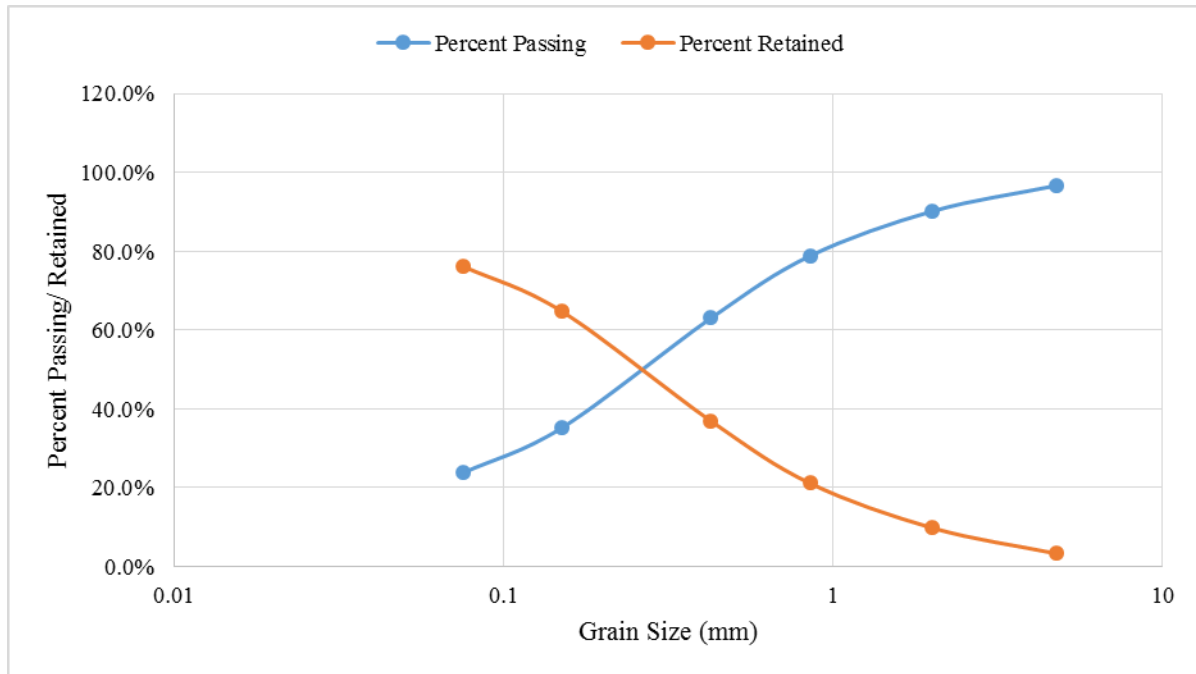


Figure B5: Grain Size Distribution – Swale 1 Deposition, February 2017

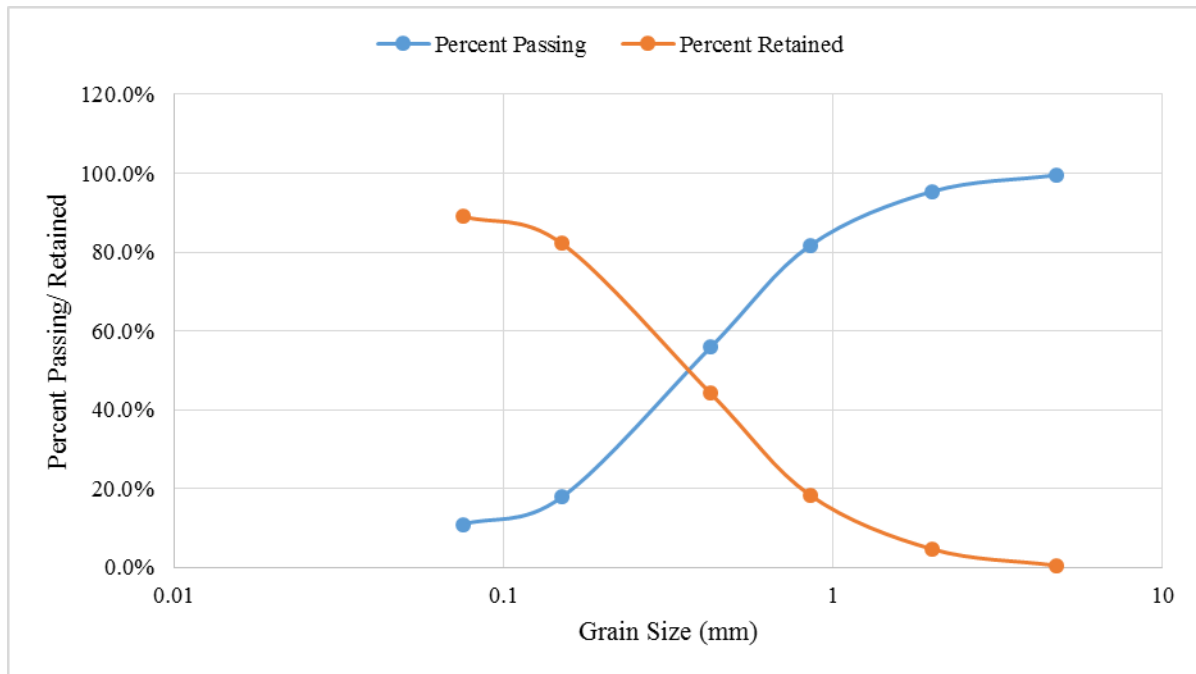


Figure B6: Grain Size Distribution – Swale 1 Deposition, May 2017

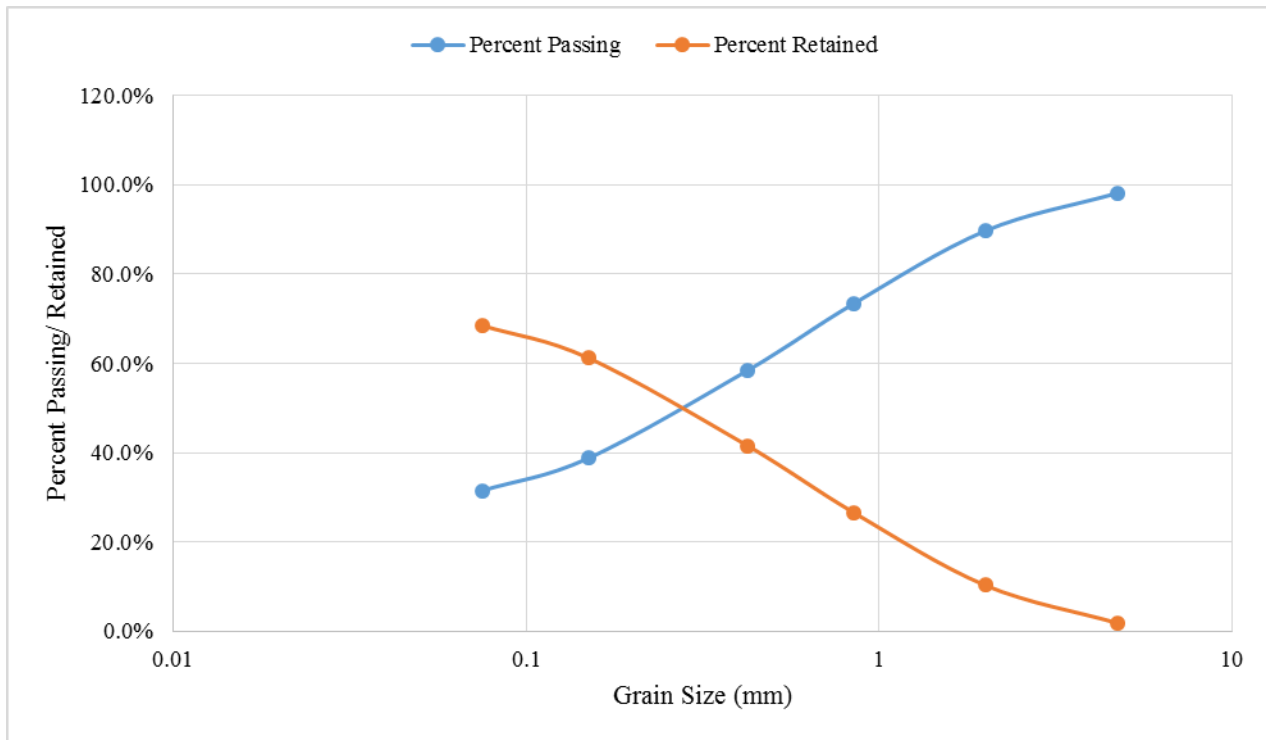


Figure B7: Grain Size Distribution – Swale 1 Weir, February 2017

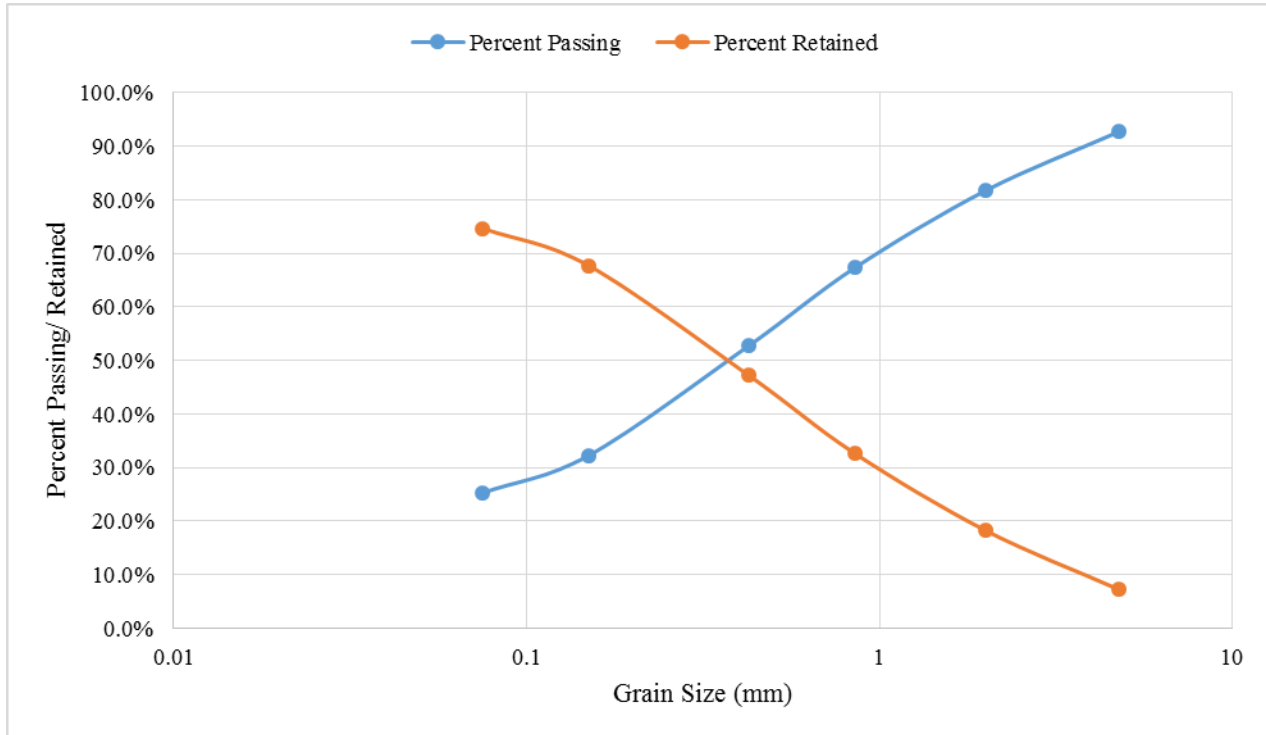


Figure B8: Grain Size Distribution – Swale 1 Weir, May 2017

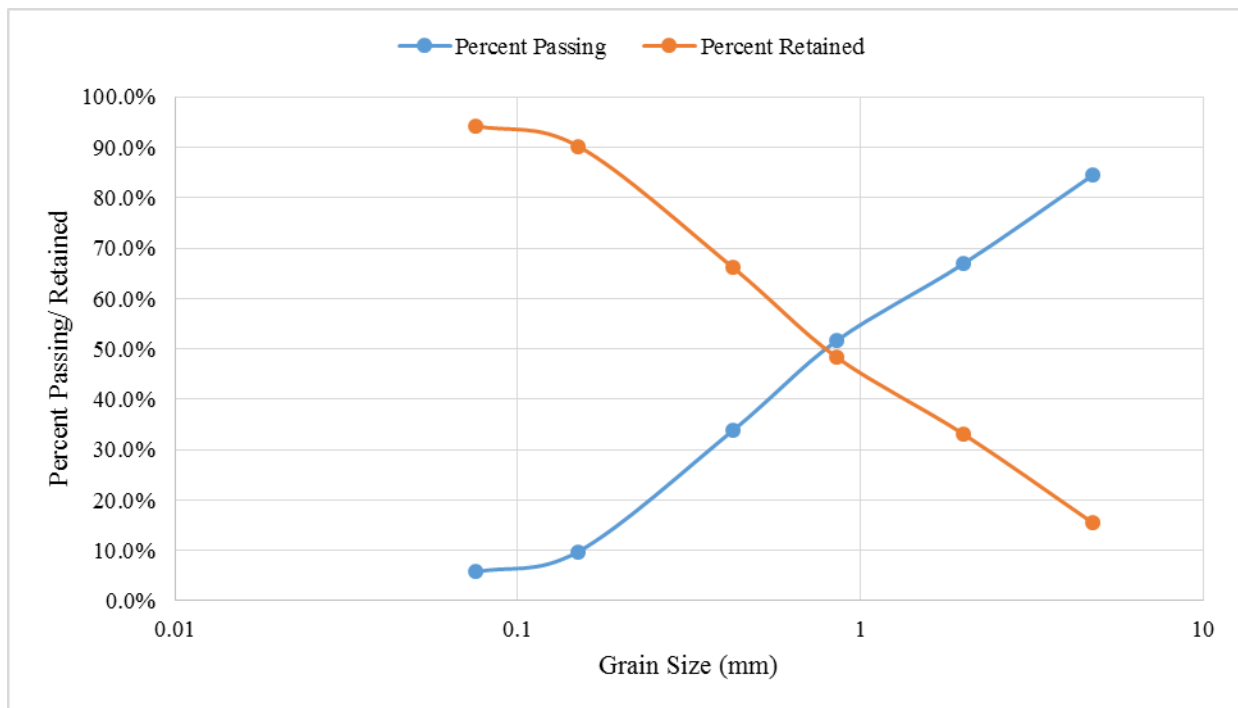


Figure B9: Grain Size Distribution – Swale 2 Erosion, February 2017

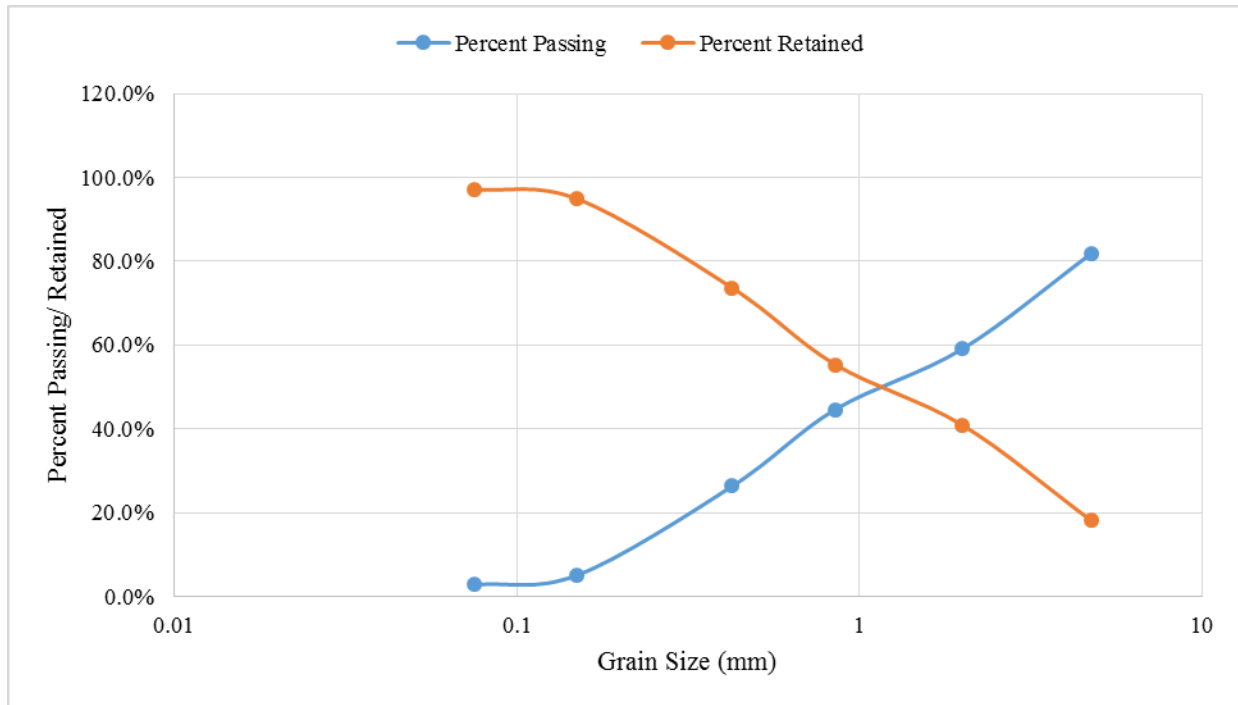


Figure B10: Grain Size Distribution – Swale 2 Erosion, May 2017

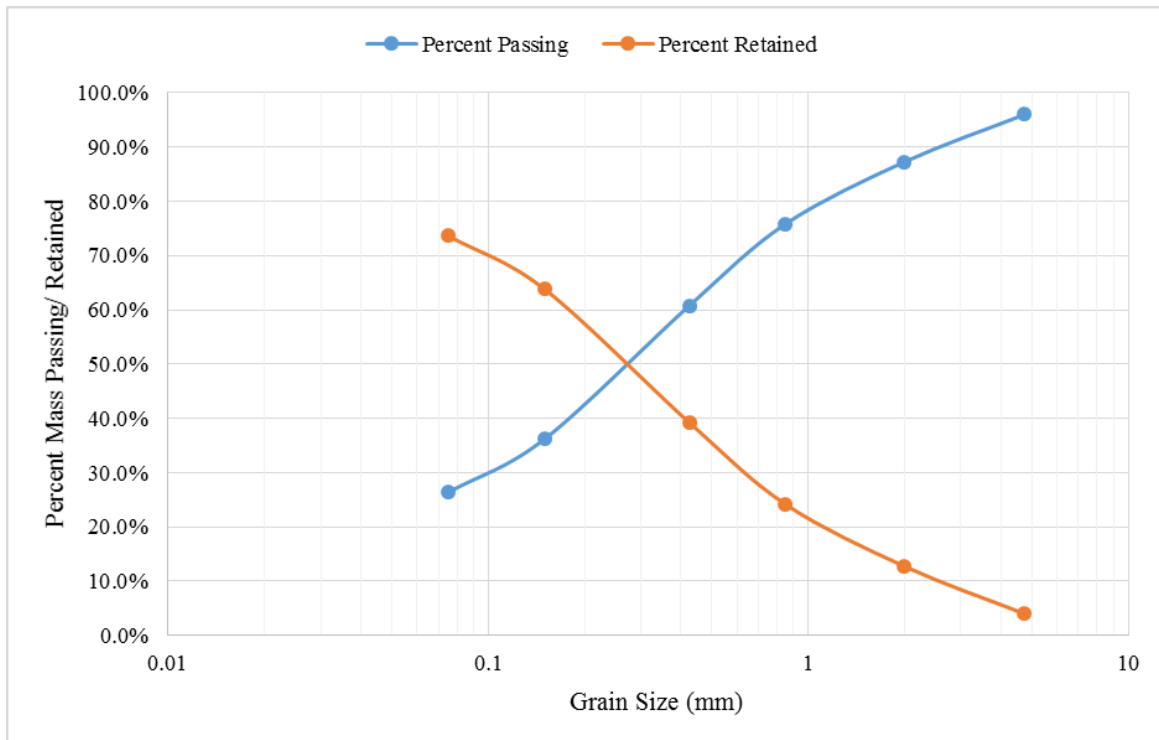


Figure B11: Grain Size Distribution – Swale 2 Mid-Bank, February 2017

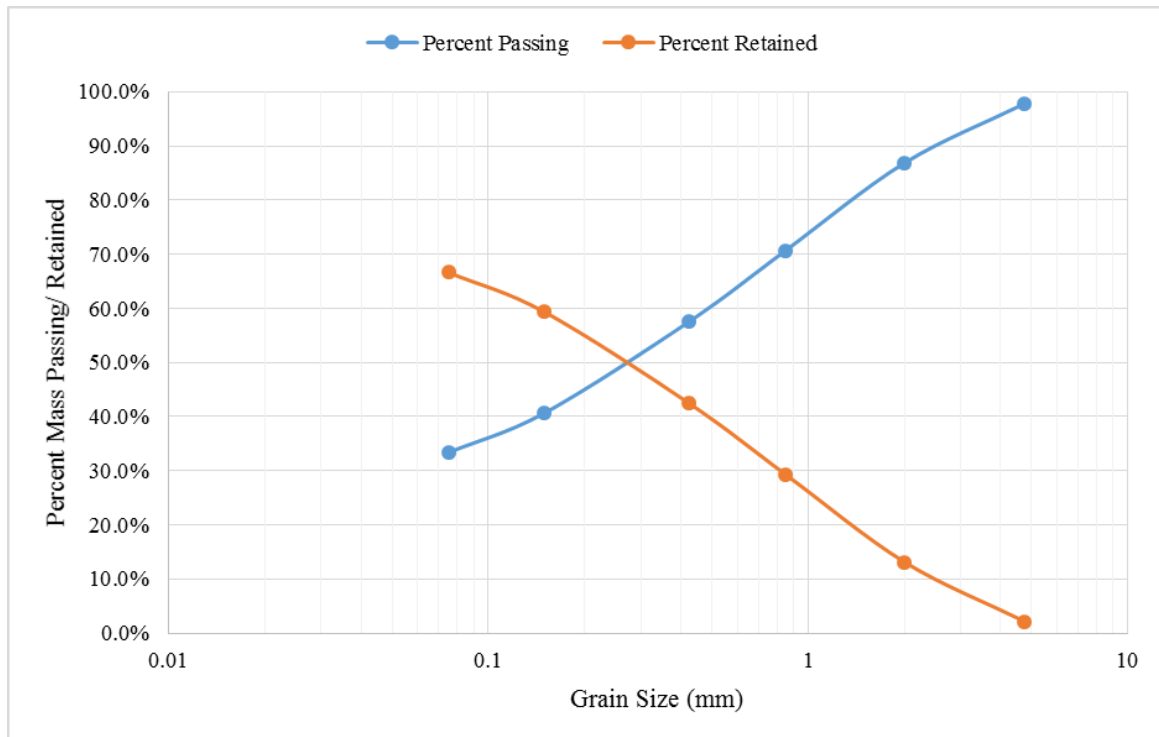


Figure B12: Grain Size Distribution – Swale 2 Mid-Bank, May 2017

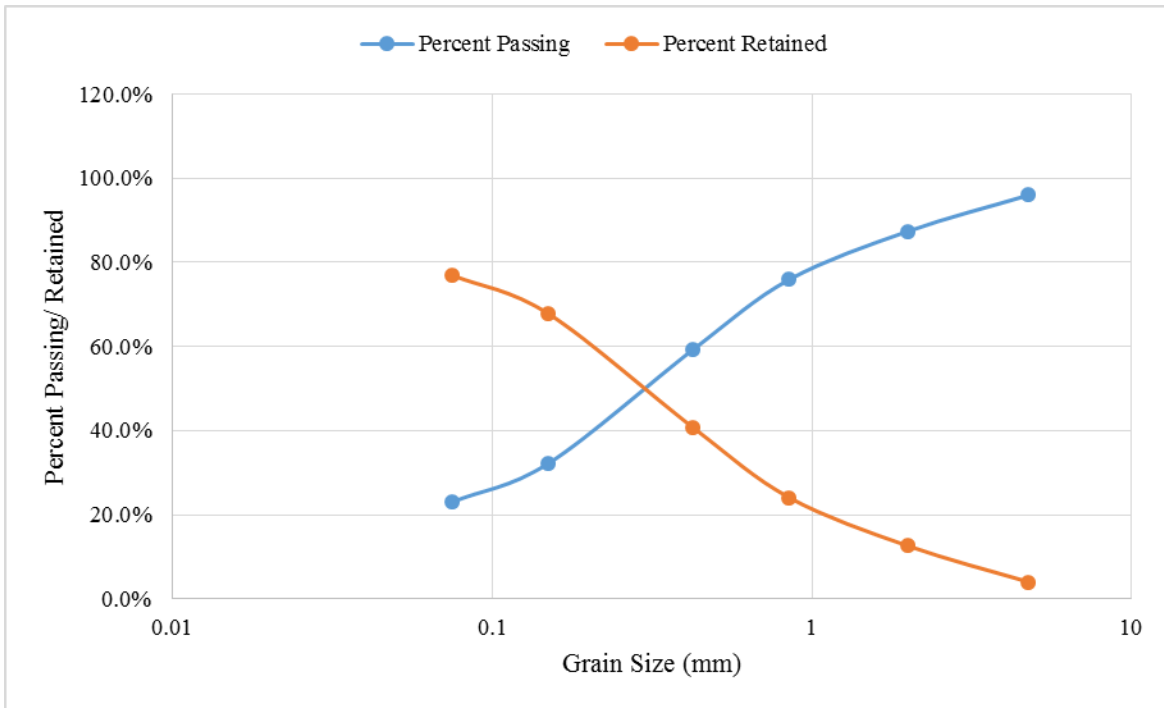


Figure B13: Grain Size Distribution – Swale 2 Deposition, February 2017

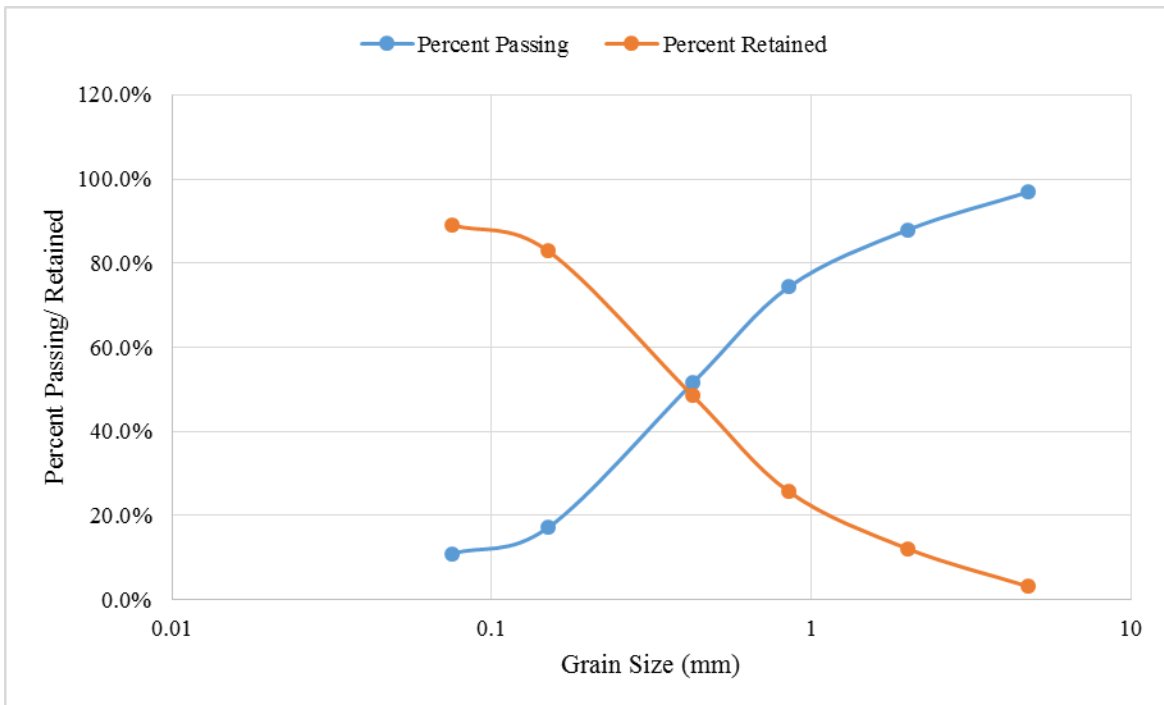


Figure B14: Grain Size Distribution – Swale 2 Deposition, May 2017

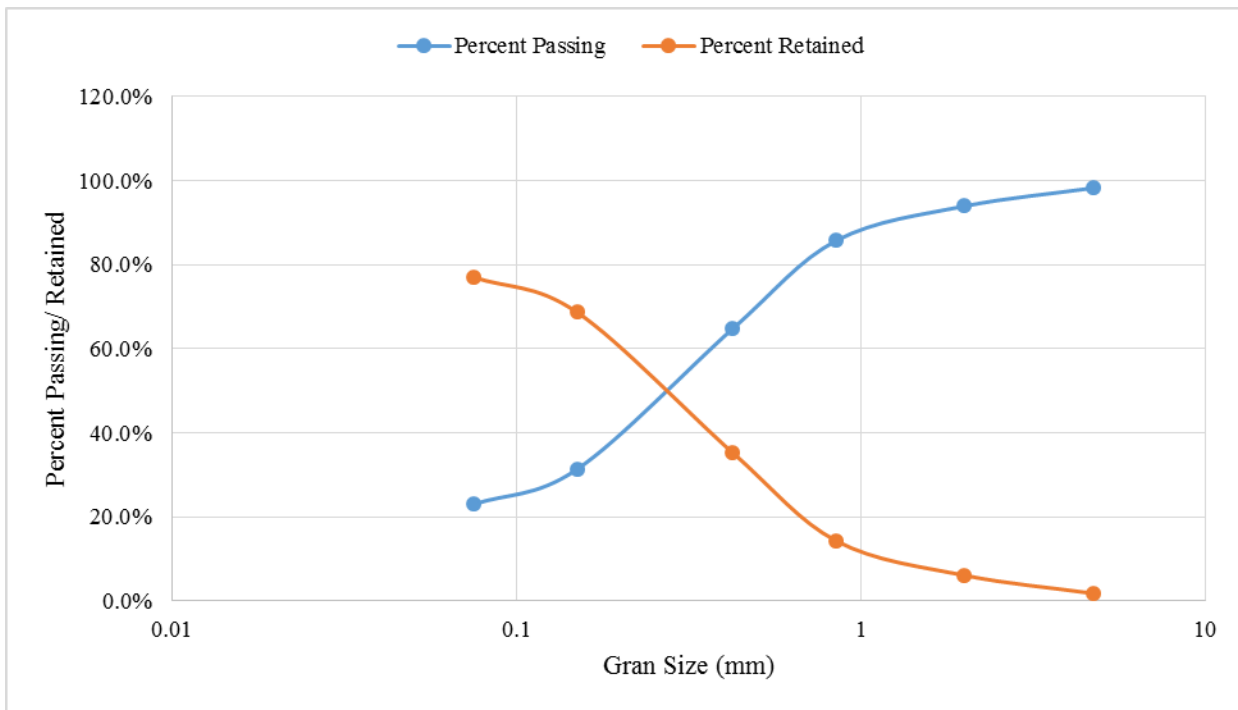


Figure B15: Grain Size Distribution – Rain Garden 1, February 2017

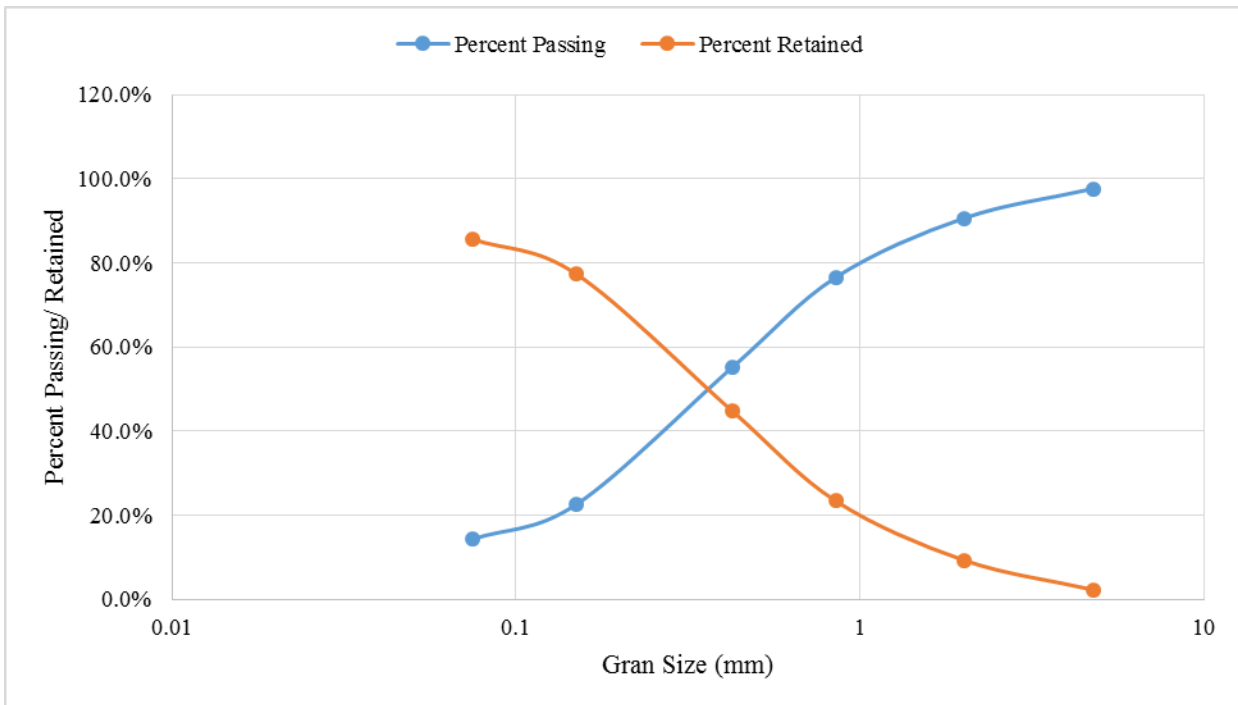


Figure B16: Grain Size Distribution – Rain Garden 1, May 2017

